IL
NUOVO CIMENTO
ORGANO DELLA SOCIETÀ ITALIANA DI FISICA
SOTTO GLI AUSPICI DEL CONSIGLIO NAZIONALE DELLE RICERCHE

VOL. V, N. 2 *Serie decima* 1° Febbraio 1957

On the Properties of Spin 2 Particles.

T. REGGE

Department of Physics, University of Rochester - Rochester, New York (*)

(ricevuto il 3 Ottobre 1956)

Summary. — A theory of spin 2 particles has been worked out. The wave equations are of first order and a symbolic approach which is developed permits easy computation of quantities of physical interest. An interesting application of the sum rules for spin 2 particles is the calculation of the Coulomb scattering in relativistic Born approximation. The theory is also applied to calculate the decay of a spin 2^+ particle into three pseudoscalar particles and into two Dirac particles. The bearing of the decay calculations on the spin 2^+ hypothesis for the K-meson is discussed.

1. – Introduction.

A relativistic theory of spin 2 particles, in many respects similar to Dirac's theory of the electron, is developed in this paper. A spin 2 particle is represented by means of a 30 component wave function obeying a system of equations of the first order in the derivatives. This approach leads in a natural way to the definition of γ_μ matrices strictly analogous to the corresponding ones for the electron. The commutation rules, however, are much more complicated than those for spin $\frac{1}{2}$ particles. Moreover, the wave equation for a spin 2 particle includes the subsidiary conditions which eliminate states with

(*) Now at the Istituto di Fisica of the University of Turin (Italy).

spin lower than 2. This theory is worked out in Sect. **2**. In addition, sum rules and various other computational aids are derived on the basis of a symbolic approach, similar to the algorithm of the Dirac matrices.

On the basis of the formulae in Sect. **2**, it is relatively easy to compute cross-sections of possible physical interest. In Sect. **3**, the unpolarized relativistic Born approximation for the scattering of a spin 2 particle by Coulomb field is calculated. In Sect. 4, the probabilities for the decay of a spin 2 particle into three pseudoscalar particles and into two Dirac particles are calculated. These processes were selected because they are relevant to the spin 2^+ hypothesis for the K-meson [1]. This hypothesis is an attempt to explain the identity of masses and lifetimes of all the K-mesons as due to a single particle with a definite spin and parity, namely 2^+.

2. – Theory of a Spin 2 Particle.

We shall sketch here the essential results of our formulation of the theory for spin 2 particles. The spin 2 particle is conveniently described by two tensors:

$$\varphi_{\mu\nu} = \varphi_{\nu\mu} ; \qquad \varphi_{\mu,\nu\lambda} = -\varphi_{\mu,\lambda\nu} ; \qquad \varphi_{\mu,\nu\lambda} + \varphi_{\nu,\lambda\mu} + \varphi_{\lambda,\mu\nu} = 0 .$$

The Pauli and Fierz equation for these tensors can be written as:

$$(1) \qquad \partial_\lambda \varphi_{\mu\nu} - \partial_\mu \varphi_{\lambda\nu} = m\sqrt{2}\, \varphi_{\nu,\lambda\mu} ; \qquad \partial_\mu \varphi_{\nu,\mu\lambda} + \partial_\mu \varphi_{\lambda,\mu\nu} = m\sqrt{2}\, \varphi_{\nu\lambda} .$$

$$\hbar = c = 1 , \qquad x_4 = ict .$$

And the subsidiary conditions (hereafter referred to as SC) can be written as:

$$(2) \qquad \varphi = \varphi_{\mu\mu} = 0 , \qquad \chi_\nu = \varphi_{\mu,\nu\mu} = 0 .$$

For our purposes, a Lagrangian must be found having Equations (1), (2) as a consequence. The Lagrangian must be varied under the condition $\varphi_{\mu\nu} = \varphi_{\nu\mu}$ and $\varphi_{\mu,\nu\lambda} = -\varphi_{\mu,\lambda\nu} = \varphi_{\lambda,\nu\mu} + \varphi_{\nu,\mu\lambda}$ that is, $\varphi_{\mu\nu}$ and $\varphi_{\mu,\nu\lambda}$ are not different variables from $\varphi_{\nu\mu}$ and $-\varphi_{\mu,\lambda\nu}$ respectively and such a symmetry condition does not have to be derived from the Lagrangian. Particularly convenient is the following change of variables:

$$(3) \qquad \varphi_{\mu\nu} = \psi_{\mu\nu} + \tfrac{1}{4}\delta_{\mu\nu}\varphi ; \qquad \varphi_{\mu,\nu\lambda} = \psi_{\mu,\nu\lambda} + \tfrac{1}{3}(\delta_{\mu\nu}\chi_\lambda - \delta_{\mu\lambda}\chi_\nu) .$$

---

[1] R. E. Marshak and G. Sundarshan: *Proc. of the Sixth Rochester Conference.*

Equation (3) is merely the decomposition of the tensors $\varphi_{\mu\nu}$ and $\varphi_{\mu,\nu\lambda}$ into irreducible parts, which transform under the representation $(\frac{3}{2}, \frac{1}{2})\ \frac{1}{2}, \frac{3}{2})\ (\frac{1}{2}, \frac{1}{2})$; $(1, 1)\ (0, 0)$ of the Lorentz group.

The following Lagrangian is the only one, apart from canonical transformations, which leads to the right set of equations:

$$L = -m[\varphi^*\varphi - \chi_\nu^*\chi_\nu - \psi_{\mu\nu}^*\psi_{\mu\nu} + \psi_{\mu,\nu\lambda}^*\psi_{\mu,\nu\lambda}] +$$

$$+ \frac{1}{\sqrt{2}}(\varphi^*\partial_\mu\chi_\mu - \partial_\mu\varphi^*\cdot\chi_\mu) + \sqrt{\frac{2}{3}}(\chi_\mu^*\partial_\lambda\psi_{\lambda\mu} - \partial_\lambda\chi_\mu^*\cdot\psi_{\lambda\mu}) +$$

$$+ \frac{1}{\sqrt{2}}\cdot[\psi_{\mu\nu}^*\cdot(\delta_\lambda\psi_{\mu,\lambda\nu} + \partial_\lambda\psi_{\nu,\lambda\mu}) - (\partial_\lambda\psi_{\mu\nu}^* - \partial_\nu\psi_{\mu\lambda}^*)\cdot\psi_{\mu,\lambda\nu}] + \text{conj.}\,.$$

The equations derived from this Lagrangian are:

$$\partial_\mu\chi_\mu = -m\sqrt{2}\,\varphi,$$

$$\partial_\mu\varphi - \frac{2}{\sqrt{3}}\partial_\lambda\psi_{\lambda\mu} = -m\sqrt{2}\,\chi_\mu,$$

$$\partial_\lambda\psi_{\mu,\lambda\nu} + \partial_\lambda\psi_{\nu,\lambda\mu} - \frac{1}{\sqrt{3}}\left(\partial_\mu\chi_\nu + \partial_\nu\chi_\mu - \frac{1}{2}\delta_{\mu\nu}\partial_\lambda\chi_\lambda\right) = m\sqrt{2}\,\psi_{\mu\nu}$$

$$-\partial_\lambda\psi_{\mu\nu} + \partial_\nu\psi_{\mu\lambda} + \frac{1}{3}\cdot(\delta_{\mu\lambda}\partial_\sigma\psi_{\sigma\nu} - \delta_{\mu\nu}\partial_\sigma\psi_{\sigma\lambda}) = m\sqrt{2}\psi_{\mu,\lambda\nu}\,.$$

If all the components but φ are eliminated, then it's easily seen that $\varphi = 0$ and $\partial_\nu\chi_\nu = 0$. Similarly $\chi_\nu = 0$, $\partial_\nu\psi_{\mu\nu} = 0$. If an electromagnetic field is introduced, then instead of $\partial/\partial x^l$ we have $\partial/\partial x^l - ie\varphi^l$ and φ and χ_i are no longer zero.

These equations and the Lagrangian can be conveniently written in symbolic form. For this purpose, a 30 dimensional space is defined having the following vectors as a basis:

$$(4) \qquad \begin{cases} |\rangle\,; \quad |\nu\rangle\,; \quad |\mu\nu\rangle = |\nu\mu\rangle\,; \quad |\mu\mu\rangle = 0 \\ |\mu\nu\lambda\rangle = -|\mu\lambda\nu\rangle = |\nu\mu\lambda\rangle + |\lambda\nu\mu\rangle\,. \end{cases}$$

This space is metricized by the relations: $\langle|\rangle = 1$

$$(5) \qquad \langle|\rangle = 1\,, \quad \langle\nu|\mu\rangle = -\delta_{\mu\nu}\,, \quad \langle\nu|\rangle = 0, \quad \langle\mu\lambda|\alpha\beta\gamma\rangle = 0$$

(here μ, ν, λ are vector indices)

$$\langle \mu\lambda|\nu\rangle = 0\,, \qquad \langle \mu\lambda|\nu\varrho\rangle = \tfrac{1}{2}(\tfrac{1}{2}\delta_{\mu\lambda}\delta_{\nu\varrho} - \delta_{\mu\nu}\delta_{\lambda\varrho} - \delta_{\mu\varrho}\delta_{\lambda\nu})$$

$$\langle \mu\nu\lambda|\alpha\beta\gamma\rangle = \tfrac{1}{2}[\delta_{\mu\alpha}\delta_{\nu\beta}\delta_{\lambda\gamma} - \delta_{\mu\alpha}\delta_{\nu\gamma}\delta_{\lambda\beta} - \tfrac{1}{3}\delta_{\mu\nu}\delta_{\alpha\beta}\delta_{\lambda\gamma} + \tfrac{1}{3}\delta_{\alpha\gamma}\delta_{\lambda\beta}\delta_{\mu\nu} + \tfrac{1}{3}\delta_{\mu\lambda}\delta_{\alpha\beta}\delta_{\nu\gamma} -$$
$$- \tfrac{1}{3}\delta_{\alpha\gamma}\delta_{\nu\beta}\delta_{\mu\lambda} - \tfrac{1}{3}\sum_{\text{cicl. }\mu,\nu,\lambda}(\delta_{\mu\alpha}\delta_{\nu\beta}\delta_{\lambda\gamma} - \delta_{\mu\alpha}\delta_{\nu\gamma}\delta_{\lambda\beta})] \text{ and conj.}.$$

We define also:

$$\Psi = \varphi|\rangle + \chi_\nu|\nu\rangle + \psi_{\mu\nu}|\mu\nu\rangle + \psi_{\mu\nu\lambda}|\mu\nu\lambda\rangle$$
$$\overline{\Psi} = \langle|\varphi^* + \langle\nu|\chi^*_\nu + \langle\mu\nu|\psi^*_{\mu\nu} + \langle\mu\nu\lambda|\psi^*_{\mu\nu\lambda}$$

and

$$\gamma_\mu = \frac{1}{\sqrt{2}}\cdot(|\rangle\langle\mu| - |\mu\rangle\langle|) + \sqrt{\frac{2}{3}}\cdot(|\mu\nu\rangle\langle\nu| - |\nu\rangle\langle\mu\nu|) +$$
$$+ \sqrt{2}\cdot(|\beta\nu\rangle\langle\beta\nu\mu| - |\beta\nu\mu\rangle\langle\beta\nu|)\,.$$

With these definitions, the Lagrangian L can be written as:

$$L = -\overline{\Psi}(\delta + m)\Psi$$

and the wave equation as

$$(\delta + m)\Psi = 0\,.$$

In analogy with what has been done in the Dirac algebra, we define also barred operators, as:

$$\mathfrak{Q} = Q_\mu\gamma^\mu\,.$$

Calculation of the powers of $\mathfrak{Q}$ leads to the following table ($|Q\rangle = Q_\mu|\mu\rangle$ etc.):

$$(6)\quad \begin{cases} \mathfrak{Q} = \dfrac{1}{\sqrt{2}}\cdot(|\rangle\langle Q| - |Q\rangle\langle|) + \sqrt{\dfrac{2}{3}}(|Q\nu\rangle\langle\nu| - |\nu\rangle\langle Q\nu|) + \sqrt{2}\cdot(|\mu\nu\rangle\langle\mu\nu Q| - |\mu\nu Q\rangle\langle\mu\nu| \\ \mathfrak{Q}^2 = \dfrac{Q^2}{2}|\rangle\langle| - \dfrac{1}{3}|Q\rangle\langle Q| + \dfrac{1}{3}Q^2|\nu\rangle\langle\nu| + \dfrac{1}{\sqrt{3}}(|\rangle\langle QQ| + |QQ\rangle\langle|) + 2|Q\nu\rangle\langle Q\nu| + \\ \quad + \dfrac{1}{\sqrt{3}}(|\lambda\rangle\langle Q\lambda Q| + |Q\lambda Q\rangle\langle\lambda|) - |\mu\nu\rangle\langle\mu\nu|Q^2 + |\mu\nu Q\rangle\langle\mu\nu Q| + |\mu\nu Q\rangle\langle\nu\mu Q \\ \mathfrak{Q}^3 = \sqrt{2}\cdot[Q^2(|\mu\nu\rangle\langle\mu\nu Q| - |\mu\nu Q\rangle\langle\mu\nu|) + |Q\lambda Q\rangle\langle Q\lambda| - |Q\lambda\rangle\langle Q\lambda Q|]\,, \\ \mathfrak{Q}^4 = Q^2(|\mu\nu Q\rangle\langle\mu\nu Q| + |\mu\nu Q\rangle\langle\nu\mu Q|) - |Q\nu Q\rangle\langle Q\nu Q| - \\ \qquad - |\mu\nu\rangle\langle\mu\nu|Q^4 + 2|\mu Q\rangle\langle\mu Q|Q^2 - \dfrac{2}{3}|QQ\rangle\langle QQ|\,. \\ \mathfrak{Q}^{2J+1} = Q^2\mathfrak{Q}^{2J-1}, \qquad J \geqslant 2. \end{cases}$$

From this table, the SC are easily derived. Clearly, if $(\delta+m)\Psi=0$, then $(\delta^3+m^3)\Psi=0$. From our table and the orthogonality relations (5), we obtain:

$$\langle\,|\,\delta^3=0\,,\qquad \langle\nu\,|\,\delta^3=0\,.$$

The result is therefore:

$$\langle\,|\,m^3\Psi=m^3\varphi=0\,,\qquad \langle\nu\,|\,m^3\Psi=m^3\chi_\nu=0\,.$$

The general solution of the above equations when the total momentum-energy four vector p_μ is fixed has five arbitrary constants; this corresponds to the fact that a spin 2 particle has five spin states. We suppose here that one such set of states has been found satisfying the orthogonality relations. Since we are not interested in any polarization effects, only sums over all these states need be considered. We can say that such a set of states $|v_\sigma^P\rangle$ will satisfy the following relations:

$$(\mathfrak{P}+\mathrm{im})\,|v_\sigma^P\rangle=0\,,\qquad \langle v_\sigma^Q\,|\,v_\tau^P\rangle=\delta_{\sigma\tau}\,,\qquad \langle v_\sigma^P\,|\,(\mathfrak{P}+\mathrm{im})=0\qquad \sigma,\tau\colon\ 1\ldots 5.$$

It is also obvious that:

$$(7)\qquad \begin{cases} \langle v_\sigma^{-P}\,|\,v_\tau^P\rangle=0 \quad \text{if} \quad \sum\limits_\sigma |\,v_\sigma^P\rangle\langle v_\sigma^P\,| = \Xi_P^+ \\ \sum\limits_\sigma |\,v_\sigma^{-P}\rangle\langle v_\sigma^{-P}\,| = \Xi_P^- = \Xi_{-P}^+\,, \qquad \Xi_P^-\,|\,v_\sigma^P\rangle=0 \\ \Xi_P^\pm\,|\,\rangle=\Xi_P^\pm\,|\,\nu\rangle=0\,. \end{cases}$$

The operator Ξ_P^+ satisfies all the formal properties which characterize $(\mathfrak{P}^4=\mathrm{im}\mathfrak{P}^3)/2m^4$ and it is therefore identical with it. Similarly $\Xi_P^-=$ $=(\mathfrak{P}^4+\mathrm{im}\mathfrak{P}^3)/em^4$. $\Xi_P^\pm$ are projection operators which generalize Dyson's $\Lambda_P^\pm$ operators ([2]) to the case of spin 2 particles.

With the help of the above operators, it is possible to evaluate traces over spin states and transition probabilities. One such sum which often occurs is:

$$K=\sum_{\sigma\tau}|\langle v_\sigma^P\,|\,A\,|\,v_\tau^Q\rangle|^2\,,$$

where A is a hermitian operator. The sum is extended over all the spin states σ, τ satisfying:

$$(\mathfrak{P}+\mathrm{im})\,|v_\sigma^P\rangle=0\,,\qquad (\mathfrak{Q}+\mathrm{im})\,|v_\tau^Q\rangle=0\,.$$

We have:

$$K=\mathrm{Tr}\,(\Xi_P^+A\,\Xi_Q^+A)\,.$$

([2]) F. S. Dyson: *Lectures on Advanced Quantum Mechanics.*

From the definition of Ξ_P^- as a projection operator we have the relation:

$$\text{Tr } \Xi_{P_i}^- = 5 . \tag{8}$$

Since the trace of any odd function of the γ_μ matrices is zero, a first consequence of (8) is:

$$\text{Tr } \mathfrak{P}^4 = 10 P^4 .$$

In the following we shall write: $\langle A \rangle = \frac{1}{10} \text{Tr } A$

$$\langle \mathfrak{P}^4 \rangle = P^4 .$$

Direct evaluation from the table (Eq. (6)) gives similarly:

$$\langle \mathfrak{P}^2 \rangle = P^2 \quad \text{and} \quad \langle \mathfrak{P}^{2n} \rangle = P^{2n} . \tag{9}$$

Clearly: $\langle \mathfrak{P}\mathfrak{Q} \rangle = \lambda(PQ)$; putting $P^\nu = Q^\nu$ from (9), we have $\lambda = 1$. Taking into account that traces are invariant under cyclical permutation and reflection of the order of the factors, we can write the following identity:

$$\langle \mathfrak{P}\mathfrak{Q}\mathfrak{R}\mathfrak{S} \rangle = \lambda_1 (PR)(QS) + \frac{\lambda_2}{2} ((PQ)(RS) + (QR)(SP)) .$$

Here $\lambda_1 + \lambda_2 = 1$. Putting $P^\nu = Q^\nu$, $R^\nu = S^\nu$ and averaging over all directions of P^ν and S^ν (here this averaging is possible because, due to the notation $x_4 = ict$, the metric is euclidean), we get the following relation:

$$\langle \Gamma^2 \rangle = 10\lambda_1 + 4\lambda_2 ,$$

where: $\Gamma = \gamma^\mu \gamma^\mu$.

Taking the expression for $\mathfrak{Q}^2$ in our table and averaging over the direction of Q^ν, we get, on the other hand:

$$\Gamma = 2I_0 - I_1 + 2I_2 + \tfrac{3}{2} I_3 ,$$

where

$$I_0 = |\rangle\langle| , \qquad I_1 = -|\nu\rangle\langle\nu| ,$$

$$I_2 = -|\mu\nu\rangle\langle\nu\mu| , \qquad I_3 = |\mu\nu\lambda\rangle\langle\mu\nu\lambda| ,$$

$$I_n I_m = \delta_{nm} I_m , \qquad \sum_n I_n = 1 ,$$

from which we deduce: $\langle \Gamma^2 \rangle = 8$, and $\lambda_1 = \frac{1}{3}$, $\lambda_2 = \frac{2}{3}$ or:

$$\langle \mathfrak{P}\mathfrak{Q}\mathfrak{R}\mathfrak{S} \rangle = \tfrac{1}{3}[(PQ)(RS) + (PS)(RQ) + (PR)(QS)] .$$

A similar calculation yields the result:

$$\langle \mathfrak{ABCPQR} \rangle = \frac{1}{6}[(AB)(CR)(PQ) + (BC)(PA)(RQ) + (CP)(QB)(AR)] +$$

$$+ \frac{1}{12}\cdot[(AB)(CQ)(PR) + (BC)(PR)(AQ) + (CP)(AQ)(BR) +$$

$$+ (PQ)(BR)(AC) + (RQ)(AC)(PB) + (AR)(BP)(QC)] .$$

All these formulae are of no practical interest by themselves. However, they give the clue to the evaluation of traces of particular cases of products of more than six factors which are necessary if we wish to derive the Coulomb scattering cross-section. These particular cases are:

$$\langle \mathfrak{P}^4\mathfrak{E}\mathfrak{Q}^4\mathfrak{E} \rangle , \qquad \langle \mathfrak{P}^3\mathfrak{E}\mathfrak{Q}^3\mathfrak{E} \rangle .$$

To calculate them, it is easier to pass through an intermediate result:

$$\langle \mathfrak{P}^4\mathfrak{Q}^4 \rangle = \frac{17}{180}(PQ)^4 + \frac{29}{45}(PQ)^2P^2Q^2 + \frac{47}{180}P^4Q^4 .$$

This result can be obtained by noting that $\langle \mathfrak{P}^4\mathfrak{Q}^4 \rangle$ is of the form:

$$\langle \mathfrak{P}^4\mathfrak{Q}^4 \rangle = \lambda_1 P^4Q^4 + \lambda_2 P^2Q^2(PQ)^2 + \lambda_3(PQ)^4 .$$

Putting $P_\nu = Q_\nu$, one can readily find that $\lambda_1+\lambda_2+\lambda_3=1$. Furthermore, an average can be performed over the directions of P^ν and Q^ν. Since:

$$\overline{\mathfrak{P}^4} = \left(\frac{5}{9}I_2 + \frac{5}{16}I_3\right)P^4 ,$$

another relation can be derived:

$$\lambda_1 + \frac{\lambda_2}{4} + \frac{\lambda_3}{8} = \frac{625}{1440} .$$

A third relation can be found by calculating λ_3 directly from the table or, as a check, by a different averaging process. A quite similar result follows for:

$$\langle \mathfrak{P}^4\mathfrak{Q}^3\mathfrak{F} \rangle = \frac{73}{180}(PQ)P^2Q^2(PF) + \frac{17}{180}(PQ)^3(PF) + \frac{43}{180}P^2(PQ)^2(QF) +$$

$$+ \frac{47}{180}P^4Q^2(QF) .$$

From this last formula, we finally get:

$$\langle \mathfrak{P}^3 \mathfrak{E} \mathfrak{Q}^3 \mathfrak{E} \rangle = \frac{4}{15} P^2 Q^2 (PQ) E^2 + \frac{13}{18} (PQ)^2 (PE)(QE) - \frac{4}{15} (PQ)^3 E^2 -$$

$$- \frac{11}{45} [P^2 (QE)^2 + Q^2 (PE)^2](PQ) + \frac{47}{90} (PE)(QE) P^2 Q^2 ,$$

$$\langle \mathfrak{P}^4 \mathfrak{E} \mathfrak{Q}^4 \mathfrak{E} \rangle = \frac{7}{60} P^4 Q^4 E^2 - \frac{1}{20} (PQ)^2 Q^2 P^2 E^2 - \frac{1}{15} (PQ)^4 E^2 +$$

$$+ \frac{47}{90} (EP)(EQ) P^2 Q^2 (PQ) + \frac{2}{15} (PQ)^3 (PE)(QE) +$$

$$+ \frac{13}{45} P^2 Q^2 [P^2 (QE)^2 + Q^2 (PE)^2] - \frac{1}{18} (PQ)^2 [P^2 (QE)^2 + Q^2 (PE)^2] .$$

3. – Coulomb Scattering of a Spin 2 Particle.

The treatment of the Coulomb scattering of a spin 2 particle does not differ formally from the corresponding calculation for the electron. The density of current can be written:

$$j_\mu = ie \overline{\Psi} \gamma_\mu \Psi .$$

This expression is valid for both spin 2 and $\frac{1}{2}$ where only the definitions of $\overline{\psi}$ and γ_μ are different. In quantizing the spin 2 field, the same formal identity still exists provided, of course, that we replace plus commutators by minus commutators. For the purpose of calculating the relativistic Born approximation for the Coulomb scattering of spin 2 particle, a straightforward procedure using Feynman's approach can be adopted without trying to justify it from a rigorous point of view. The transition amplitude can be written as:

$$M = ie \int g(x) \mathfrak{A}(x) f(x) \, \mathrm{d}^4 x ,$$

where g, f are the final and initial state wave functions respectively and A_μ is the electromagnetic potential. Substituting in the formula the appropriate expressions, we get:

$$M_{\sigma\tau} = \langle v_\sigma^{P_1} | \mathfrak{E} | v_\tau^{P_2} \rangle$$

P_1, P_2 initial and final momentum
$P_{1,\mu} - P_{2,\mu} = Q_\mu$,
$\mathfrak{E}$ is the Fourier transform of $\mathfrak{A}(x)$

where σ, τ are indices denoting the initial and final spin positions respectively.

Since we are interested only in the unpolarized Coulomb cross-section, we must sum the square of the matrix element over the final states and average it over the initial ones. The transition probabiity w becomes:

$$w = \frac{2\pi}{5} \sum_{\sigma\tau} |M_{\sigma\tau}|^2 \varrho_f .$$

A factor ϱ_f appears because we must take into account the density of final states. Furthermore, on the energy shell, we have the identities:

$$P_i^2 = -m^2 , \qquad P_f^2 = -m^2 , \qquad \boldsymbol{P}_i - \boldsymbol{P}_f = \boldsymbol{Q}$$

$$Q_4 = 0 , \qquad P_{i,4} = P_{f,4} = iE , \qquad Q = |\boldsymbol{Q}| = 2P \sin\theta/2$$

$$\cos\theta = \frac{(\boldsymbol{P}_i \boldsymbol{P}_f)}{|P_i|\,|P_f|} .$$

Once the quantity $\frac{1}{5}\sum_{\sigma\tau} |\langle \nu_\sigma^{P_i} | \mathfrak{E} | \nu_\sigma^{P_f} \rangle|^2$ is evaluated, the procedure does not differ from the already well-known one for the electrons. The quantity under consideration can be written as:

$$2\langle \Xi_{P_i}^+ \mathfrak{E}\, \Xi_{P_f}^+ \mathfrak{E} \rangle = \frac{1}{2m^8} \langle \mathfrak{P}_i^4 \mathfrak{E} \mathfrak{P}_f^4 \mathfrak{E} - m^2 \mathfrak{P}_i^3 \mathfrak{E} \mathfrak{P}_f \mathfrak{E}^3 \rangle .$$

The usefulness of the sum rules we calculated in Sect. 2 now becomes evident. The cross-section is finally given by:

$$A = \left(\frac{Q}{m}\right)^2 ,$$

$$\sigma = \frac{4\pi e^4 Z^2 E^2}{Q^4} \left(1 + \frac{67}{120} A + \frac{71}{360} A^2 + \frac{1}{120} A^3 - \right.$$

$$\left. - \frac{Q^2}{E^2} \left(\frac{11}{120} + \frac{9}{160} A + \frac{1}{60} A^2 + \frac{1}{480} A^3 \right) \right) .$$

This cross-section is to be compared with the Rutherford formula. As is to be expected, the deviations become increasingly important as the energy of the spin 2 particle increases.

4. – Decay of a Spin 2^+ Particle.

A large number of choices is available for the construction of an invariant interaction which can be made responsible for the decay of a spin 2^+ particle

into three pseudoscalar particles. In principle, any invariant constructed out of the field components of a spin 2^+ particle and three pseudoscalar particles should suffice to define an interaction. This is not true whenever the components φ and χ_ν are used because on the energy shell these functions vanish. A second point is that it is impossible to construct an invariant out of $\psi_{\mu\nu}$ or $\psi_{\mu,\nu\lambda}$ and φ_1, φ_2, φ_3 (the pseudoscalar fields) without using gradient operators. These gradient operators are essentially i times the momenta of the fields on which they act. Since there are four fields and the conservation of momentum holds, the problem is to construct an invariant with $\psi_{\mu\nu}$ or $\psi_{\mu,\nu\lambda}$, three pseudoscalars, and any three independent momenta. The simplest interaction H_1 of the proper kind is: ($\varepsilon^{1234} = -\varepsilon^{1324} = 1$, etc.)

$$H_1 = g_1 \psi_{\mu\nu\lambda} \varepsilon^{\nu\lambda\alpha\beta} \partial_\alpha \varphi \partial_\beta \varphi^* \partial_\mu \varphi + \text{conj.} = g_1 \overline{\Psi\varepsilon} \,|\, \alpha\beta\mu\rangle \partial_\alpha \varphi \partial_\beta \varphi^* \partial_\mu \varphi + \text{conj.}\,.$$

For our purposes, two of the fields are supposed to be identical and conjugate to the third since we are considering the reaction $\tau^+ \to \pi^+ + \pi^+ + \pi^-$. The transition probability for this process is given by the expression:

$$w = (2\pi)^4 \delta^4(P_i - P_1 - P_2 - P_3)\,|g_1|^2 \langle \overline{P_1 P_2} P_3 \,|\, \varepsilon \Xi_{P_i} \varepsilon \,|\, \overline{P_1 P_2} P_3 \rangle \varrho_f$$

$$\langle \overline{P_1 P_2} P_3 | = \langle P_1 P_2 P_3 | + \langle P_2 P_1 P_3 |\,.$$

The only point in the above calculation presenting a mathematical difficulty is the evaluation of $\langle \overline{P_1 P_2} P_3 \,|\, \varepsilon \mathfrak{P} : \varepsilon \,|\, \overline{P_1 P_2} P_3 \rangle$. We have used the identities:

$$\frac{\varepsilon \mathfrak{P}_i^4 \varepsilon}{m^4} = \frac{1}{2} \| ts \rangle \langle st \| \qquad (\boldsymbol{P}_i = 0 \quad P_{i,4} = \text{im})$$

where

$$\| ts \rangle = |tqr\rangle \varepsilon^{qrs} + |sqr\rangle \varepsilon^{qrt} \qquad q, r, s, t: 1 \ldots 3,$$

$$\varepsilon^{qrs} = \varepsilon^{rsq} = -\varepsilon^{rqs}; \qquad \varepsilon^{123} = 1\,.$$

The decay probability is then given by:

$$w_1 = \frac{1}{4\pi^3} |g|^2 \cdot \mathrm{d}E_1 \, \mathrm{d}E_2 \cdot \frac{|\boldsymbol{P}_1 - \boldsymbol{P}_2|^2 \cdot |\boldsymbol{P}_1 \wedge \boldsymbol{P}_2|^2}{2}\,.$$

This is Fabri's distribution for $L = 2$, $l = 1$ [3] corresponding to the simplest centrifugal barrier arguments and is in disagreement with experiment. It is

[3] E. Fabri: *Nuovo Cimento*, **11**, 479 (1954).

beyond the aim of this paper to investigate in detail other interactions of higher degree in the gradient operators. However, there is no a priori reason why such interactions should not reproduce Marshak and Sundarshan's distribution (1).

The other process which we are going to discuss is the decay of a spin 2^+ particle into two Dirac particles. The application we have in mind is to the decay reactions $K \to \mu + \nu$ and $K \to e + \nu$. It is known from experiment that electron decays are much more seldom observed (if at all) than muon decays. A similar situation arises in the corresponding decay modes of the pion. It would be interesting to explain this behaviour in terms of a single type of interaction with the same coupling constant, the difference in mass between muon and electron being alone responsible for the branching ratio. The analogy with the pion decay is here instructive because it is well-known that pseudovector coupling gives a branching ratio: $(\pi \to e + \nu)/(\pi \to \mu + \nu) \approx 1/4 \cdot 10^4$, which is consistent with experiment.

We have calculated several electron to muon ratios for different types of interaction in the case of the $K \to e + \nu$ and $K \to \mu + \nu$ decays. The following choices, the simplest types of interaction predict ratios very close to 1:

$$H_2 = g_2 \psi^*_{\mu\nu}(\overline{\chi}\gamma^\mu \partial^\nu \zeta) + \text{conj.} \qquad \chi \text{ neutrino field}$$

$$H_3 = g_3 \psi^*_{\mu\nu}(\overline{\chi}\partial^\mu \partial^\nu \zeta) + \text{conj.} \qquad \zeta \text{ e or } \mu \text{ fields.}$$

However, an interaction of the type:

$$H_4 = g_4 \partial_\lambda \psi^*_{\mu\nu}(\overline{\chi}\gamma^\lambda \partial^\mu \partial^\nu \zeta) + \text{conj.}$$

yields a ratio of the right order of magnitude. We can easily see this by remembering that H_4 is an interaction density and that it has to be integrated over space and time. If the first order approximation only is retained, the fields χ, ζ can be assumed to have energy and momenta on the energy shell. If an integration by parts is performed, then we have:

$$H_4 \approx -g_4 \psi^*_{\mu\nu}(\partial^\lambda \overline{\chi}\gamma^\lambda \partial^\mu \partial^\nu \zeta) - g_4 \psi^*_{\mu\nu}(\overline{\chi}\gamma^\lambda \partial^\lambda \partial^\mu \partial^\nu \zeta) + \text{conj.} \approx$$

$$\approx -\mu g_4 \psi^*_{\mu\nu} \overline{\chi} \partial^\mu \partial^\nu \zeta + \text{conj.}$$

We see, therefore, that H_4 behaves like $-\mu H_3$. Since H_3 alone, as pointed out, gives a ratio $(K \to e + \nu)/(K \to \mu + \nu)$ close to unity, the branching ratio for H_4 must be of the order of m_e^2/m_μ^2, which is consistent with experiment.

* * *

This work was supported in part by the U.S. Atomic Energy Commission.

The author wishes to thank Dr. R. E. MARSHAK for his constant help, kind encouragement and warm hospitality.

RIASSUNTO

La teoria delle particelle di spin 2 viene messa sotto forma più elegante per mezzo di un metodo simbolico simile a quello di Dirac per l'elettrone. Si esaminano e si discutono alcuni processi, tra cui lo scattering su di un potenziale di Coulomb e se ne calcolano le sezioni d'urto.

Spurious Scattering in Nuclear Emulsions.

A. J. Apostolakis, J. O. Clarke and J. V. Major (*)

Department of Physics, The Durham Colleges in the University of Durham, Durham, England

(ricevuto il 15 Ottobre 1956)

Summary. — Spurious scattering has been determined in two emulsion stacks, one exposed to 4.2 GeV π^--mesons from the Berkeley Bevatron and the other to cosmic rays at sea-level. In both stacks the mean modulus of the second differences of spurious scattering ($\bar{d}$) varies with cell-length (t) as $\bar{d} = at^b$ where b is approximately equal to unity and the constant a is different in the two stacks. In the first stack the spurious scattering is relatively small, and reliable measurements of $p\beta$ have been made at 4.3 GeV/c. In the second stack, spurious scattering is larger than in the π-meson stack and uncorrected measurements of $p\beta$ are reliable only up to about 2.5 GeV/c. The apparent value of $p\beta$ corresponding to the spurious scattering in this stack is about 5 GeV/c. The error on the value of $p\beta$ determined in the presence of spurious scattering is given.

1. – Introduction.

The measured scattering of a charged particle in nuclear emulsions is made up of the true multiple scattering of the particle and the apparent scattering or « noise », which, prior to the work of Biswas *et al.* [1], was attributed to reading errors, distribution of the grains of a track about the trajectory of the particle, and the lateral movements of the microscope stage during measurement. These authors demonstrated the existence of other forms of noise, the most important component arising from small movements of the emulsions. This noise has been termed « spurious scattering » and its existence has been

(*) Communicated by Professor G. D. Rochester.

(1) S. Biswas, B. Peters and Rama: *Proc. Ind. Acad.*, A **41**, 156 (1955).

confirmed by FAY [2], LOHRMANN and TEUCHER [3] and BRISBOUT *et al.* [4]. The magnitude of spurious scattering varies considerably from stack to stack; the mean modulus of the second differences of spurious scattering is approximately proportional to cell size. Then at large cell-sizes spurious scattering becomes the most important source of noise and limits the value of $p\beta$ which can be accurately measured. The results of LOHRMANN and TEUCHER indicated that accurate determinations of $p\beta$ are only possible below 2.5 GeV/c, whereas in one stack considered by BRISBOUT *et al.* accurate determinations were made at about 5 GeV/c.

One of the two stacks considered in this paper (the π-stack) and one stack of BRISBOUT *et al.* were exposed together to the π^--meson beam of the Berkeley Bevatron. The processing was carried out independently, and the measurements were made by different techniques. In both stacks spurious scattering effects are smaller than found previously.

In the second stack considered in this paper (the μ-stack) the spurious scattering was measured by use of a new technique for the determination of the momenta of high energy particles (APOSTOLAKIS and MACPHERSON [5]). In this technique, the trajectories of cosmic-ray particles (chiefly μ-mesons) deflected in a strong magnetic field, were traced through layers of emulsion separated by gaps. The device has been termed the « Normal Incidence Stack » and with it momenta up to 100 GeV/c have been measured. A Normal Incidence Stack with a solid block of emulsion layers underneath was exposed to the cosmic rays at sea-level and μ-mesons were traced through the stack and into the block. The momenta of the particles were measured in the top stack and the value of $p\beta$ determined by scattering measurements in the block below.

From the measurements on the π-stack it is shown that the usual formulae for estimating errors on the mean modulus of the second differences of multiple scattering give reasonable values from which the accuracy of the true multiple scattering measured in the presence of spurious scattering has been determined.

2. – Measurements on the 4.2 GeV π^--Meson Tracks.

Scattering measurements on the tracks of particles of energy equal to 4.2 GeV will contain contributions from the true multiple scattering, grain, reading and stage noises, and spurious scattering. The method devised for isolating the spurious scattering was to make scattering measurements on

---

[2] H. FAY: *Zeits. f. Naturfor.*, **10***a*, 572 (1955).

[3] E. LOHRMANN and M. TEUCHER: *Nuovo Cimento*, **3**, 59 (1956).

[4] F. A. BRISBOUT, C. DAHANAYAKE, A. ENGLER, P. H. FOWLER and P. B. JONES: *Nuovo Cimento*, **3**, 1400 (1956).

[5] A. J. APOSTOLAKIS and I. MACPHERSON: In the press.

pairs of tracks less than 50 μm apart and having similar angles of dip in the emulsion. Each track was aligned separately on the microscope stage and scattering measurements were made at points of the tracks which corresponded to within 5 μm over exactly the same part of the stage. The measured second differences D_{1i} and D_{2i} at corresponding points in both tracks will be made up of a random component δ_{1i}, δ_{2i} due to multiple scattering and grain, reading and random stage noises, and a common component, d_i, due to spurious scattering, distortion and systematic stage noise. Thus at corresponding points, the observed second differences are given by,

$$D_{1i} = \delta_{1i} + d_i \qquad \text{and} \qquad D_{2i} = \delta_{2i} + d_i \,.$$

Here it is assumed that the tracks are sufficiently close for the effects of spurious scattering and distortion to be the same in both tracks. If the random component δ_i has a mean deviation $\bar{\delta}$, then the distributions of $(\delta_{1i} - \delta_{2i})$ or $(\delta_{1i} + \delta_{2i})$ have mean deviation $2^{\frac{1}{2}}\bar{\delta}$. By subtracting or adding second differences at corresponding points,

$$(D_{1i} - D_{2i}) = (\delta_{1i} - \delta_{2i})$$

and

$$(D_{1i} + D_{2i}) = (\delta_{1i} + \delta_{2i} + 2d_i)$$

are obtained. The distribution of these will have mean deviations given by

$$M_- = 2^{\frac{1}{2}}\bar{\delta} \qquad \text{and} \qquad M_+ = (2\bar{\delta}^2 + 4\bar{d}^2)^{\frac{1}{2}} \,,$$

respectively where $\bar{d}$ is the mean deviation for spurious scattering, distortion and systematic stage noise. Thus

$$\bar{d} = \tfrac{1}{2}(M_+^2 - M_-^2)^{\frac{1}{2}} \,. \tag{1}$$

Twenty pairs of tracks were measured, at a cell-length of 500 μm, over 2.5 cm of each track. The spurious scattering was estimated at three cell-lengths, 500, 1000 and 2000 μm. The plates were 400 μm thick and had been processed at a hot stage temperature of 18.5 °C. The magnitude of distortion was about 20 μm and contributed little to the second differences.

3. – Measurements on Cosmic Ray Tracks.

Twenty-three particles were traced from the Normal Incidence Stack into the block of stripped emulsions. The momentum of each particle was determined by measuring the sagitta of deflection in the magnetic field by means

of the Normal Incidence Stack. For values of momenta of about 25 GeV/c or less, the standard error on the determination of momentum is about 7% increasing to about 40% at 100 GeV/c. In the block below, estimates of the value of $p\beta$ for each particle were made from scattering measurements. The emulsion layers in the block were each 600 μm thick and were processed at a hot stage temperature of 23 °C. The tracks of the particles selected were greater than 2 cm in each emulsion. Scattering measurements were made at cell-lengths so as to give a signal to noise ratio about 6:1. The noise was the combined stage, grain and reading noises. The value of $p\beta$ was estimated for each particle from measurements on the total length of track with $4D$ cut-off. The standard error was estimated from the number of independent cells.

For five particles of momenta greater than 12 GeV/c the multiple scattering must have been negligible and therefore the observed signal must have been due to noise and spurious scattering. The tracks of these particles were measured at cell lengths of 500 and 1000 μm and the spurious scattering estimated by correcting the observed D for distortion, stage, grain and reading noises, a procedure similar to previous determinations of spurious scattering ([1-4]).

All the measurements, on the tracks of π-mesons and cosmic ray particles, were made on Cooke M 4000 microscopes. Temperature noise was minimized by making measurements at regular intervals of time. All tracks selected were at least 1 cm from the emulsion edge.

4. – Results.

The results from the π- and μ-stacks are shown in Fig. 1 where the mean deviation of spurious scattering ($\bar{d}$) is plotted against cell-length (t). The broken line represents the expected variation of Coulomb scattering with t for π-mesons of $p\beta = 4.3$ GeV/c.

In the π-stack the variation of the spurious scattering with cell-length can be expressed as $\bar{d} \simeq 2.6 \cdot 10^{-4} t$ μm. Similarly in the μ-stack $\bar{d} \simeq 4.2 \cdot 10^{-4} t$ μm. Most results can be expressed in this form i.e. $\bar{d} = at^b$ and in Table I, the constants a and b are shown for all published results.

TABLE I.

	Biswas *et al.*	Fay	Lohrmann and Teucher	Brisbout *et al.*	Apostolakis *et al.*
$a\ 10^{-4}$ μm =	0.2 ÷2.0	3.7÷4.3	∼4	2÷4; 20	2÷4
b =	1.57 ; 1.1	∼1	∼1	1 ; 0.7	∼1

In practice the $p\beta$ for a single track is estimated from the mean modulus $\bar{D}_i$ of the second differences after all second differences $D_i > 4\bar{D}_i$ have been eliminated. It is necessary to find a value of the spurious scattering appropriate

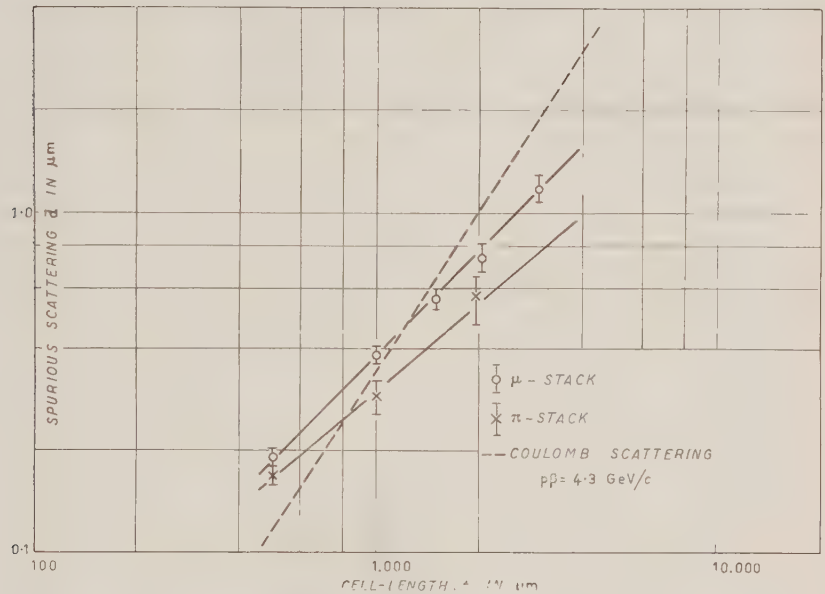

Fig. 1. – The variation of spurious scattering, $\bar{d}$, with cell-length t.

to this cut-off procedure. In the π-stack this was carried out for the 20 pairs on the 2000 μm cell only where the effect of noise is small. The mean modulus of the second differences was $\bar{D}$ and for all $D_i > 4\bar{D}$ the corresponding $(D_{1i} - D_{2i})$ or $(D_{1i} + D_{2i})$ were rejected. This led to a value of $\bar{D}_{co} = (1.15 \pm .04)$ μm and $\bar{d}_{co} = (.46 \pm .12)$ μm. Hence the mean deviation of the multiple scattering contribution to the second differences, $\bar{\delta}_{co}$ was found from

$$\bar{\delta}_{co} = (\bar{D}_{co}^2 - \bar{d}_{co}^2)^{\frac{1}{2}} = (1.05 \pm .09) \text{ μm} .$$

Assuming the scattering constant given by VOYVODIC and PICKUP [6] this corresponds to a value of $p\beta = (4.2 \pm .4)$ GeV/c. However the value of $p\beta$ found from scattering measurements on 100 tracks, each 2.5 cm long was $p\beta = (4.0 \pm .1)$ GeVc. These should be compared with the determination of

[6] L. VOYVODIC and E. PICKUP: *Phys. Rev.*, **85**, 91 (1952).

(4.2 ± .3) GeV for the energy of the beam made at Berkeley (7) with a cloud chamber. It is concluded that in this stack, reliable determination of $p\beta$ can be made at this energy. Also, within the accuracy of the experiment, the movements of the emulsion responsible for spurious scattering are constant over distances equal to the separations of the tracks in the pairs i.e. 50 μm.

In the μ-stack it is possible to compare the values of the $p\beta$ determined there with the momenta of the particles found from the Normal Incidence Stack. This is shown in Fig. 2. For μ-mesons of these energies the momentum

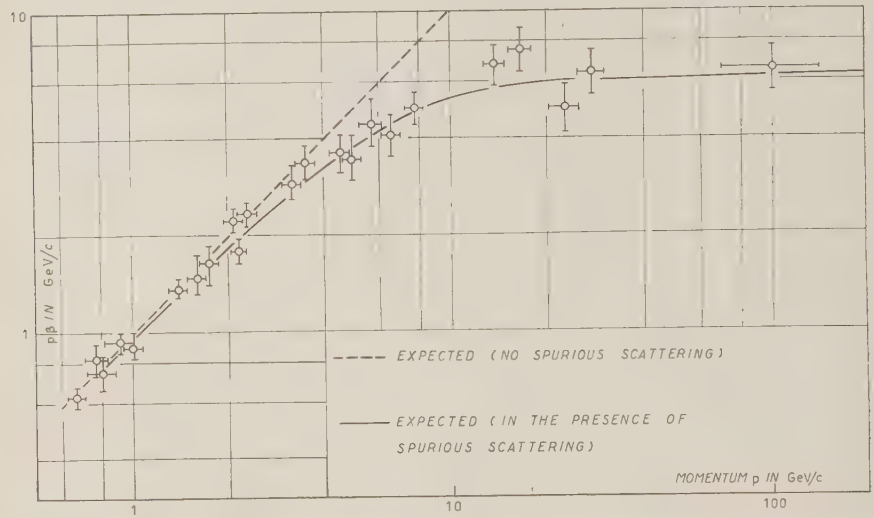

Fig. 2. - The effect of spurious scattering on the determination of $p\beta$ in emulsions.

and $p\beta$ of a particle are expected to be equal; this relation is shown by the broken line. However for $p\beta$ determined in the presence of spurious scattering similar in magnitude to that of Fay (2), the continuous line is the expected relation between $p\beta$ and momentum. It is seen that values of $p\beta$ uncorrected for spurious scattering are reliable for $p\beta$ less than or equal to about 2.5 GeV/c, thereby confirming the results of Lohrmann and Teucher (3).

5. The Estimation of the Error of the Mean Deviation of Multiple Scattering Measured in the Presence of Spurious Scattering.

Whereas the multiple scattering may be estimated in single tracks in an emulsion, it is the average value of spurious scattering over the emulsion which

(7) W. H. Barkas: Private communication.

can be determined with any accuracy. Thus in practice the multiple scattering, or $p\beta^2$, can be corrected for spurious scattering only approximately. In this section, the accuracy of the multiple scattering corrected in this way is considered. The error on the mean deviation of the measured scattering, $\bar{D}$, is considered firstly, the spurious scattering, $\bar{d}$, secondly, and finally the multiple scattering, $\bar{\delta}$.

To obtain a large sample, the scattering in 200 tracks in the π-stack was measured on a 1000 μm cell. Each track was 2.5 cm long.

5·1. *The Error of the Measured Estimate of Scattering.* – For each of the 200 tracks the $1\bar{D}_j$ cut-off procedure was applied. The distribution of the remaining second differences was found by the χ^2 test to be approximately Gaussian. The mean deviation and standard deviation after cut-off were $D_\infty = 1.16$ μm and $\sigma = 1.43$ μm respectively.

In Fig. 3 is shown the histogram of the mean deviations $\bar{D}_j$ after cut-off was applied. The distribution was tested with $a = M/m_2$ and the moment ratio $b_1^{\frac{1}{2}} = m_3/m_2^{\frac{3}{2}}$, where M, m_2 and m_3 are the mean deviation and the second and third moments of the distribution respectively. A negligible departure from normality was found. The standard deviation of the distribution was found to be $S = (.287 \pm .014)$ μm. The expected standard deviation (8) is $S' = (\sigma/n^{\frac{1}{2}})(1 - (2/\pi))^{\frac{1}{2}}$, where σ is the standard deviation of the distribution of second differences and n is the number of statistically independent readings in any one track (9). This expected value is derived by using the estimated value of σ whence $S' = (.274 \pm .014)$ μm and

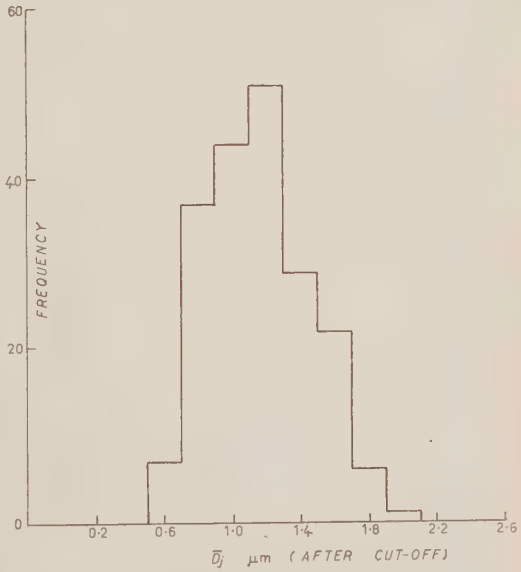

Fig. 3. – The distribution of the $\bar{D}_j$ values after cut-off.

(8) M. G. KENDALL: *The Advanced Theory of Statistics*, p. 215 (1952).
(9) C. O'CEALLAIGH and O. ROCHAT: *Phil. Mag.*, **42**, 1232 (1951).

is in good agreement with the observed value. On substituting $\sigma = (\pi/2)^{\frac{1}{2}}\bar{D}$, a good estimate of the error on the mean deviations $\bar{D}_j$ is $\mathcal{S} = (0.75/n^{\frac{1}{2}})\bar{D}_j$.

5·2. *The Error of the Mean Deviation of Spurious Scattering.* – The error on the mean deviation of spurious scattering can be estimated from equation (1) and is,

$$\sigma_{\bar{d}} = (M_+^2\sigma_+^2 + M_-^2\sigma_-^2)^{\frac{1}{2}}/4\bar{d}\,,$$

where σ_+ and σ_-, are the standard errors on the values of M_+ and M_-. The values of σ_+ and σ_-, are easily found from the r.m.s. residuals of M_+ and M_-. On the 2000 μm cell these yield the value $\sigma_{\bar{d}} = (.14 \pm .03)$ μm. However, taking $\sigma_\pm = (0.75/n^{\frac{1}{2}})M_\pm$, then

$$\sigma_{\bar{d}} = (0.75/4\bar{d}n^{\frac{1}{2}})(M_+^4 + M_-^4)^{\frac{1}{2}}\,,$$

yielding a value $\sigma_{\bar{d}} = (.19 \pm .03)$ μm. Thus this latter expression, which is more convenient to use, gives a reasonable estimate of the error on $\bar{d}$.

5·3. *The Error of the Corrected Multiple Scattering.* – In a track of considerable length, where a large number of second differences is obtainable, the observed mean deviation of the second differences is given by

$$\bar{D}_j = (\bar{d}_j^2 + \bar{\delta}_j^2)^{\frac{1}{2}}\,, \tag{4}$$

in the j-th track, where $\bar{\delta}_j$ is the mean deviation of the true multiple scattering, at least at the longer cells where noise is negligible, and $\bar{d}_j$ is the mean deviation of spurious scattering. In practice $\bar{d}_j$ is not known for each track, but $\bar{d}$, the mean value is known with considerable accuracy. Thus it is not possible to find the true multiple scattering from equation (4) but to estimate it from,

$$\bar{\beta}_j = (\bar{D}_j^2 - \bar{d}^2)^{\frac{1}{2}} \simeq \bar{\delta}_j\,. \tag{5}$$

Fig. 4. – The distribution of the $\bar{\beta}_j$ values. The theoretical curve is a Gaussian distribution of the same standard deviation and mean value.

If the error on $\bar{d}$ is taken to be the standard deviation of the $\bar{d}_j$ distribution, rather than the error on the mean value $\bar{d}$, this should allow for substituting $\bar{d}_j$ by $\bar{d}$. That this is true, is shown in Fig. 4 where the observed histogram of $\bar{\beta}_j$ is shown together with a Gaussian distribution the standard deviation of which was calculated as indicated above. In fact, 61 % of the values of $\bar{\beta}_j$ lie within one standard deviation of the mean value. Thus $\bar{\beta}_j$ is a reasonable estimate of $\bar{\delta}_j$.

6. – Conclusions.

Spurious scattering has been demonstrated in two emulsion stacks. Its magnitude increases with cell-length as $\bar{d} = at^b$, where b is approximately unity and a depends upon the stack. In the π-stack the spurious scattering is relatively small and the technique of measurement indicates that the emulsion movements responsible for spurious scattering are constant over regions extending up to 50 μm. The π- and μ-stacks were processed under similar conditions except that the hot stage temperatures were different. The 400 μm thick plates were processed for 80 minutes at 18.5 °C whereas the 600 μm thick plates were processed for 60 minutes at 23 °C. There is no definite evidence to indicate whether spurious scattering is connected with different temperatures of development or the thicknesses of the emulsions.

If the spurious scattering is determined in a region of a plate, then for tracks in the same region, the true multiple scattering can be estimated from equation (5). The effect of the spurious scattering is to limit the highest value of $p\beta$ which can be reliably measured in the emulsion. LOHRMANN and TEUCHER [3] put this limit at about 2.5 GeV/c and suggested that star size distributions as a function of primary energy, determined from cosmic ray data may be in error. This result has been confirmed for the μ-stack described in this paper. However, reliable measurements of $p\beta$ were made at 4.3 GeV/c in the π-stack, the error introduced by neglecting spurious scattering being about 7 %. The results of BISWAS *et al.* [1] show that the spurious scattering was, in general, smaller for glass-backed emulsions than for stripped emulsions and similar in magnitude to that of the π-stack. In the glass-backed emulsions reliable determinations of $p\beta$ at 5 GeV/c would have been possible. If this is generally true for glass-backed plates, previous results from cosmic ray data on star sizes may not be seriously in error.

* * *

We should like to thank Professor G. D. ROCHESTER for providing the facilities for this work and Dr. E. S. PAGE, Dr. E. RÖSSLE and Dr. A. W.

WOLFENDALE for several useful discussions. One of us (J.O.C.) would like to thank the D.S.I.R. for a Maintenance Allowance.

RIASSUNTO (*)

In due pacchi di emulsioni, uno esposto ai mesoni π^- di 4.2 GeV del bevatrone di Berkeley e l'altro ai raggi cosmici al livello del mare, si è determinato lo scattering spurio. Nei due pacchi il modulo medio delle differenze seconde dello scattering spurio ($\bar{d}$) varia con la lunghezza della cella (t) come $d = a^b l$, dove b è circa uguale all'unità e la costante a è differente pei due pacchi. Nel primo pacco lo scattering spurio è relativamente piccolo e misure attendibili di $p\beta$ sono state eseguite a 4.3 GeV/c. Nel secondo pacco lo scattering spurio è maggiore che nel pacco esposto ai mesoni π^- e misure non corrette di $p\beta$ sono attendibili solo fino a circa 2.5 GeV/c. Il valore apparente di $p\beta$ corrispondente allo scattering spurio in questo pacco è circa 5 GeV/c. Si dà l'errore nel valore di $p\beta$ determinato in presenza di scattering spurio.

(*) *Traduzione a cura della Redazione.*

Remarks on the Fixed Extended Source Pion Theory.

H. Fukutome and Y. Nogami (*)

Department of Physics, Kyoto University - Kyoto, Japan
(*) *Department of Physics, University of Osaka Prefecture - Sakai, Japan*

(ricevuto il 22 Ottobre 1956)

Summary. — Cini and Fubini's analysis on the possibility whether the fixed extended source pion theory can reproduce the low energy experimental p-wave pion-nucleon scattering cross-sections is reinvestigated in the light of the restrictions: (i) The requirement that the probability can not be negative imposes some restrictions on the expectation values of the operators τ_α, σ_l and $\tau_\alpha\sigma_l$, and (ii) there is a geometrical limitation on the scattering cross-section. It becomes clear that, as far as the contribution to Cini and Fubini's sum rules from the high energy region (above cut-off) is small, the theory can not reproduce the experimental scattering cross-sections, even for the low energy region (pion kinetic energy $\lesssim$ 300 MeV). However, there is no reason to consider that the high energy contribution be small. On the other hand, it is almost certain that the theory can reproduce the experimental p-wave pion nucleon scattering cross-section for the low energy region. This implies that the high energy contribution to Cini and Fubini's sum rules is important and should not be neglected.

1. – Introduction.

Chew and Low's analysis (1) on the fixed extended source pion theory (*) has made a definite development in explaining the nature of the low energy p-wave pion nucleon interaction. For the low energy p-wave pion nucleon scattering an effective range treatment has been presented. The scattering length, which is obtained exactly, gives the renormalized coupling constant $f^2 = 0.08$. This value of the renormalized coupling constant is in good agreement with that determined from the low energy limit of the s-wave photo-pion production cross-section (2), and that determined from the analysis

(*) Hereafter, the fixed extended source pion theory is briefly called « cut-off theory ».
(1) G. F. Chew and F. E. Low: *Phys. Rev.*, **101**, 1570, 1579 (1956).
(2) G. Bernardini and E. L. Goldwasser: *Phys. Rev.*, **95**, 857 (1954) (L.).

of the nuclear forces (3). Furthermore, CHEW and LOW have shown that, if the effective range is appropriately adjusted, the experimental phase shift in 33-state is reproduced fairly well up to about the resonance energy.

SALZMAN (4) has solved Low's equation numerically in the one-meson approximation with a cut-off energy $\approx 7\mu$. In the 33-state, the low energy part ($\omega \lesssim 2\mu$) of his solution agrees rather closely with the effective range analysis of CHEW and LOW. The low energy part of the phase shifts in the 11-, 13- and 31-states are fairly suppressed compared with that in the 33-state. We can thus rightly consider that the theory has been almost established for the low energy p-wave pion-nucleon interaction. However, for the behaviour of the exact solution of the cut-off theory in the higher energy region, there have been no convincing arguments.

Recently CINI and FUBINI (5) have reinvestigated the cut-off theory using some exact sum rules which connect the expectation values of the operators $\tau_\alpha \cdot \sigma_i$ and $\tau_\alpha \sigma_i$ to the scattering cross-sections. They have found a rather unexpected result. Namely, putting in the sum rules $g_1 = g_2 = 0$ (*), and introducing for g_3 the effective range formula of Chew and Low, they obtained $f^2 - 0.013$ in strong disagreement with the experimental value. Hereafter we use the following terminology for the energy regions:

$$\begin{aligned} &0 < \omega \lesssim 2\mu && \text{region I,} \\ &2\mu \lesssim \omega \lesssim \omega_{\max} && \text{region II,} \\ &\omega_{\max} \lesssim \omega && \text{region III.} \end{aligned}$$

Their result shows that agreement between theory and experiment in the region I requires contributions to the sum rules from the regions II and III to be large. They have further investigated these situations and reached the conclusion: The possibility that the contribution from the region III is large is ruled out. The contribution from the region II must be, therefore, very large.

However, it should be noted here that, on the p-wave pion-nucleon scattering cross-section (including the inelastic one), there exists a geometrical limitation (6)

$$\sigma_i \leqslant \sigma_{\max} = 12\pi/k^2 \,. \tag{1.1}$$

(3) J. IWADARE S. OTSUKI, R. TAMAGAKI and W. VATARI: *Prog. Theor. Phys.*, **15**, 86 (1956) (L.).

(4) G. SALZMAN: *Proceedings of the Sixth Rochester Conference on High Energy Nuclear Physics* (1956).

(5) M. CINI and S. FUBINI: *Nuovo Cimento*, **3**, 764 (1956); *Phys. Rev.*, **102**, 1687 (1956) (L.). We cite these as C.F.

(*) In this paper we adopt the notation used by CINI and FUBINI (5).

(6) See, e.g., J. M. BLATT and V. F. WEISSKOPF: *Theoretical Nuclear Physics* (1952), p. 317.

Taking account of this limitation, it will be shown that, as far as the contribution to the sum rules from the region III is small, the theory and experiment can not agree at all even in the region I. While, in C. F.'s analysis rather misleading interpretations are pointed out and the contribution from the region III turns out to be not ruled out. Then, considering that the theory is almost well established for the region I, we have the conclusion: *It is not correct to neglect the contribution to the sum rules from the region III.* Consequently it also turns out that the unrenormalized coupling constant or the expectation value of τ_α, σ_l and $\tau_\alpha\sigma_l$, obtained by replacing the cross-sections in the sum rules by the experimental ones, is not trustworthy.

2. – General Relations.

In this section we present exact formulas in the cut-off theory. We p.ı

$$\text{(2.1)} \qquad \begin{cases} \dfrac{(\Psi_r, \tau_\alpha \Psi_{r'})}{\langle r | \tau_\alpha | r' \rangle} = \dfrac{(\Psi_r, \sigma_l \Psi_{r'})}{\langle r | \sigma_l | r' \rangle} = \alpha \,, \\ \dfrac{(\Psi_r, \tau_\alpha \sigma_l \Psi_{r'})}{\langle r | \tau_\alpha \sigma_l | r' \rangle} = \beta \,. \end{cases}$$

Here Ψ_r and $|r\rangle$ are the state vectors of the clothed and bare nucleons, respectively. α and β are C. F.'s $1/\varrho_1$ and $1/\varrho_2$, and $f = \beta f^{(0)}$. f is the renormalized, $f^{(0)}$ is the unrenormalized coupling constant.

The probability that the angular momentum of the pion cloud, in the charge space and the ordinary space, are found to be T(0 or 1) and L(0 or 1) is denoted by P_{TL}:

$$\text{(2.2)} \qquad P_{00} + P_{10} + P_{01} + P_{11} = 1 \,.$$

As is well known, $P_{10} = P_{01}$. Further, from the meaning of probability and (2.2),

$$\text{(2.3)} \qquad 1 \geqslant P_{00} \geqslant 0 \,, \qquad \tfrac{1}{2} \geqslant P_{10} \geqslant 0 \,, \qquad 1 \geqslant P_{11} \geqslant 0 \,.$$

P_{TL} can be expressed in terms of α and β; then we have

$$\text{(2.4)} \qquad \begin{cases} \tfrac{16}{3} \geqslant \tfrac{16}{3} P_{00} = \tfrac{1}{3} + 2\alpha + 3\beta \geqslant 0 \,, \\ \tfrac{8}{3} \geqslant \tfrac{16}{3} P_{10} = 1 + 2\alpha - 3\beta \geqslant 0 \,, \\ \tfrac{16}{9} \geqslant \tfrac{16}{9} P_{11} = 1 - 2\alpha + \beta \geqslant 0 \,. \end{cases}$$

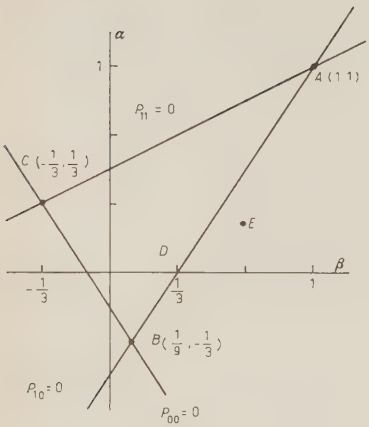

Fig. 1.

The physically allowed region in the α-β-plane is limited in the triangle ABC in Fig. 1, wherein evidently holds

$$\alpha \geq -\frac{1}{3}. \tag{2.5}$$

The limits of weak and strong coupling correspond to the points A and D, respectively.

Next, we put

$$x^{\pm} = \frac{\mu^2}{8\pi^2}\int_{\mu}^{\infty}\frac{\sigma^{\pm}(k)}{k\,v(k)^2}\,\mathrm{d}w_k\,. \tag{2.6}$$

$\sigma^{\pm}$ are the $\pi^{\pm}$-proton scattering cross-sections, respectively. The sum rules which connect f^2, α, β to $x^{\pm}$ are [5,7]

$$\begin{cases} x^{+}-x^{-} = f^2\left(\dfrac{1}{\mu^2}-1\right), \\ x^{+}+x^{-} = f^2\left(1-\dfrac{\alpha}{\mu^2}\right). \end{cases} \tag{2.7}$$

Combining (2.5) and (2.7), we obtain a lower bound for f^2:

$$f^2 \geq \tfrac{1}{2}(x^{+}-2x^{-}). \tag{2.8}$$

Similarly, from the combination of the 2-nd formula of (2.4) and (2.7) follows an upper bound for f^2:

$$f^2 \leqslant \frac{(x^{+}-3x^{-})^2}{3(5x^{-}-3x^{-})}. \tag{2.9}$$

Furthermore, (2.8) and (2.9) give an inequality

$$\frac{x^{+}}{x^{-}} \leqslant \frac{27}{13}. \tag{2.10}$$

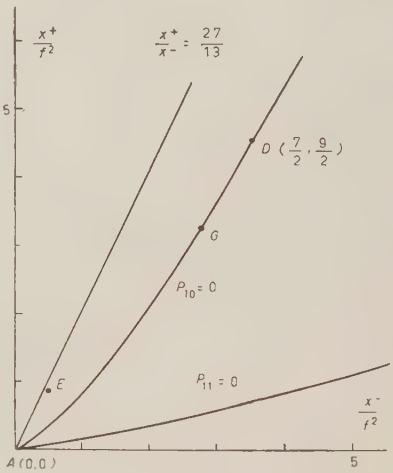

Fig. 2.

(7) H. MIYAZAWA: *Phys. Rev.*, **101**, 1564 (1956).

To see the relations between f^2, α, β and $x^{\pm}$, it is convenients to use the graph shown in Fig. 2, where $x^{\pm}/f^2$ are read on the ordinate and the abscissa, respectively. The physically allowed region is between the curves $P_{11}=0$ and $P_{10}=0$. Points A and D correspond to the limits of weak and strong couplings. The point $B(\alpha=-\frac{1}{3},\ \beta=\frac{1}{9})$ is, though it is too far from A to show in Fig. 2, on the straight line $x^+/x^-=\frac{27}{13}$.

C. F. have used three sum rules, including (2.7), which are expressed in terms of the decomposed partial wave cross-sections, σ_i $(i=1, 2, 3)$. However, since the phase-shift analysis has not yet been performed for pion kinetic energy $\gtrsim 300$ MeV ([8]), σ_i can not be compared directly with the experimental data. Therefore, it is preferable to observe only the experimentally well known cross-sections $\sigma^{\pm}$.

3. – Comparison with the Experiments.

In this section comparison of the theory with the experiment is made under the assumption that the contributions to the sum rules from the region III can be neglected. As experimental datum, we employ the curve presented by Lindenbaum and Yuan ([9]). $x^{\pm}$, which are estimated by replacing $\sigma^{\pm}$ in (2.6) with the experimental values, are denoted by $x^{\pm}_{\text{exp}}$. x_{exp} obtained by the square cut-off are shown in Table I. As is seen from this table, predominant contribution to the integral (2.6) comes from the region $k\lesssim 3\mu$.

Table I.

$k_{\max}/\mu$	2	3	4	5	6	7	8
$10^3\cdot x^+_{\text{exp}}$	53	64	67	70	73	74	79
$10^3\cdot x^-_{\text{exp}}$	18	24	30	35	38	41	44

The point $(x^-_{\text{exp}}/f^2,\ x^+_{\text{exp}}/f^2)$ with $f^2=0.08$ and $k_{\max}=6\mu$ is shown in Fig. 1, 2 by the point E, which is far outside the allowed region. This discrepancy can not be remedied by adjusting $k_{\max}$. If we change the value of f^2, the point E in Fig. 2 moves on the straight line AE. If f^2 becomes small so as to satisfy (2.9), then the point E enters into the allowed region. The critical

([8]) J. Orear: *Phys. Rev.*, **100**, 288 (1955).
([9]) S. J. Lindenbaum and L. C. L. Yuan: *Phys. Rev.*, **100**, 306 (1955).

value of f^2 is given by substitution of $x^{\pm}_{\text{exp}}$ for $x^{\pm}$ in (2.9):

$$f^2 \lesssim 0.0036 \,. \tag{3.1}$$

This evidently disagrees with experiment (*).

Next, yielding a step, we let $x^{\pm}$ fit the experiment only in the region I ($k < 2\mu$). In the region II ($2\mu < k < 6\mu$), we decompose $x^{\pm}$ into the partial wave cross-sections as

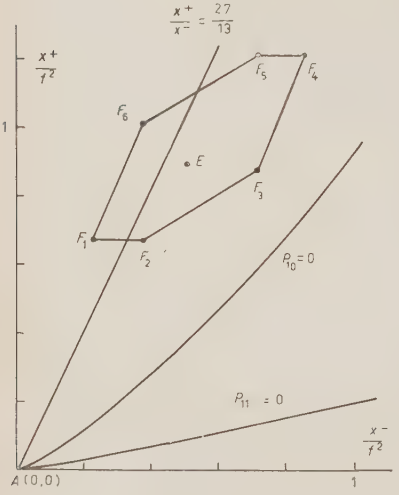

Fig. 3.

$$\begin{cases} x^+ = \tfrac{1}{3}(x_2 + 2x_3) \,, \\ x^- = \tfrac{1}{9}(2x_1 + 5x_2 + 2x_3) \end{cases} \tag{3.2}$$

with

$$x_i = \frac{\mu^2}{8\pi^2} \int_{\mu}^{\infty} \frac{\sigma_i(k)}{k\, v(k)^2} \, \mathrm{d}\omega_k \,, \tag{3.3}$$

and vary x_i as parameters within the scope of (1.1). Then the region of possible $(x^-/f^2,\ x^+/f^2)$ is given by the region in the sexangle $F_1 \ldots F_6$ in Fig. 3. This lies still outside the allowed region. At each vertex of the sexangle, $\sigma_i/\sigma_{\text{max}}$ in the region II takes the value shown in Table II. The point F_1 corresponds to the case where $k_{\text{max}} = 2\mu$. At the point F_3, which is the closest to the allowed region,

$$x^+ = 0.070 \,, \qquad x^- = 0.057 \,. \tag{3.4}$$

Table II.

F_n, $n =$		1	2	3	4	5	6
$\sigma_i/\sigma_{\text{max}}$	1	0	1	1	1	0	0
$i =$	2	0	0	1	1	1	0
	3	0	0	0	1	1	1

(*) This discrepant situation is described in alternative ways.

If we let $x^{\pm}$ and f^2 fit the experiment, (2.7) gives for $k_{\text{max}} = 6\mu$, $\alpha \approx \frac{1}{4}$, $\beta \approx \frac{2}{3}$. The corresponding point in the α-β-plane lies far outside the allowed region, the triangle ABC in Fig. 1. Or, it is the same situation, if we let x^+/x^- and f^2 fit the experiment, x^+ and x^- become enormously large.

If we let $(x^+ + x^-)$ and f^2 fit the experiment, (2.7) gives for $k_{\text{max}} = 6\mu$, $\beta \approx \frac{2}{3}$. Then,

For this point F_3, the critical value for f^2 to enter the allowed region is

$$f^2 \lesssim 0.0019\,. \tag{3.5}$$

This is still much smaller than the experimental value $f^2 = 0.08$. Therefore, $x^{\pm}$ can not fit the experiment even in the region I, as far as the contribution from the region III is neglected.

4. – Conclusion and Discussion.

As is mentioned in the introduction, it is almost sure that agreement between theory and experiment is obtained in the region I. Then we can conclude that, to the sum rules of the type (2.7), the contribution from the region III can not be small. From discrepancies, which result by neglect of the contribution to the sum rules (2.7) from the region III, we can not draw any inference about the reliability of the cut-off theory. We can not calculate the expectation values of τ_3, σ_t and $\tau_3\sigma_t$ from the experimental cross-sections, using the sum rules (2.7).

Our conclusion differs from C.F.'s one, according to which the contribution from the region III should be ruled out. Now we give some critical comments on C.F.'s analysis. C.F. assumed that the cross-section $\sigma(k)$ is proportional to $v(k)^4$. But this is true only for the elastic part of $\sigma(k)$. The inelastic part is proportional to $v(k)^2$. Though it can be shown that $\sigma(k)$ damps proportionally to $v(k)^4$ for infinitely large k and, therefore, the integral of the type (2.6) converges in the cut-off theory, there is no knowing about the behaviour of $\sigma(k)/v(k)^2$ for $k \gtrsim k_{\max}$.

C.F. further inferred that there is an upper bound of $k_{\max}$. Namely, since the integral in the sum rule

$$\alpha = 1 - \frac{1}{\pi}\int_0^{\infty} \mathrm{d}k\, \frac{v(k)^2k^4}{\omega_k}\left(\frac{f^2}{\omega_k^2} - \frac{\mu^2}{8\pi^2}\int_{\mu}^{\infty}\mathrm{d}\omega_p\, \frac{\sigma^+(p) - \sigma^-(p)}{v(p)^2p(\omega_p + \omega_k)^2}\right) \tag{4.1}$$

increases with increasing $k_{\max}$, the restriction $\alpha \geqslant -\frac{1}{3}$ (2.5) is violated for $k_{\max} \gtrsim 5.5\,\mu$. However, this inference can not be accepted because of their

as is seen from Fig. 1, $\alpha \gtrsim \frac{1}{2}$. Introducing these values into the formula

$$x^+/x^- = (1 - \alpha)/(1 + \alpha - 2\beta^2)\,,$$

which is given by (2.7), we have $x^+/x^- \lesssim \frac{9}{11}$. This is less than one half of the experimental value $\approx \frac{7}{4}$.

improper treatment for $\sigma(p)/v(p)^2$. These circumstances are seen in the following way. The expression in the bracket of the right hand side of (4.1) is

$$(4.2)\qquad \frac{f^2}{\omega_k^2} - \frac{\mu^2}{8\pi^2}\int_\mu^\infty \mathrm{d}\omega_p \frac{\sigma^+(p)-\sigma^-(p)}{v(p)^2 p(\omega_p - \omega_k)^2} = \frac{f^2}{\omega_k^2} - \frac{\mu^2}{8\pi^2}\frac{1}{\omega_k^2}\int_\mu^\infty \mathrm{d}\omega_p \frac{\sigma^+(p)-\sigma^-(p)}{v(p)^2 p} +$$

$$+ \frac{\mu^2}{8\pi^2}\int_\mu^\infty \mathrm{d}\omega_p \frac{\sigma^+(p)-\sigma^-(p)}{v(p)^2 p}\left(\frac{1}{\omega_k^2} - \frac{1}{(\omega_p+\omega_k)^2}\right) =$$

$$= \frac{f^2\alpha}{\beta^2}\frac{1}{\omega_k^2} + \frac{\mu^2}{8\pi^2}\int_\mu^\infty \mathrm{d}\omega_p \frac{\sigma^+(p)-\sigma^-(p)}{v(p)^2 p}\cdot\frac{\omega_p(\omega_p+2\omega_k)}{\omega_k^2(\omega_p+\omega_k)^2}\,.$$

Here the 2-nd formula of (2.7) has been used. From (4.1) and (4.2) we have

$$(4.3)\ (*)\qquad \alpha = \frac{1}{1 - \dfrac{\mu^2}{2\pi^3}\displaystyle\int_0^\infty \mathrm{d}k \frac{v(k)^2k^4}{\omega_k^3}\int_0^\infty \mathrm{d}p \frac{\sigma^+(p)-\sigma^-(p)}{v(p)^2}\cdot\frac{\omega_p+2\omega_k}{(\omega_p+\omega_k)^2}} \Big/ \left(1 - \frac{4}{\pi}\frac{f^2}{\beta^2}\int_0^\infty \mathrm{d}k \frac{v(k)^2k^4}{\omega_k^3}\right).$$

For large $k_{\max}$, the integral in the denominator is of the order of $k_{\max}^2$, while the integral in the numerator is of the order of $k_{\max}$. Therefore, (4.3) will not give any restrictions on $k_{\max}$.

If (4.3) should gives some restrictions on $k_{\max}$, still it gives no information about the behaviour of the integrand $\sigma(k)/kv(k)^2$ in (2.7). Thus our aforementioned conclusion will not be upset by such a kind of argument.

At present, we have no reliable means, in the Chew-Low frame, to estimate the extent of the contribution to the sum rules (2.7) from the region III. On this point, however, some information is obtained in the light of the intermediate coupling theory which atacks the eigenvalue problem for the pion cloud in a straightforeward way. The intermediate coupling calculation performed by FRIEDMAN *et al.* ([10]) has given excellent agreement with experiment of p-wave pion nucleon scattering in the region I, and has given

$$(4.4)\qquad \alpha = 0.073\,, \qquad \beta = 0.381\,.$$

The corresponding point is shown by the point G in Fig. 2 (+). This point G

(*) By the way, we notice that (4.3) implies $\alpha \to 0$ for $k_{\max} \to \infty$.

([10]) M. H. FRIEDMAN, T. D. LEE and R. CHRISTIAN: *Phys. Rev.*, **100**, 1494 (1955).

(+) In the intermediate coupling theory, $P_{10} = 0$, i.e. $1+2\alpha-3\beta = 0$.

is rather close to the strong coupling limit D and far from the point E. This implies that the contribution to the sum rules from the region III is considerably large. This suggests that reconsideration would be necessary on the conventional view point, from which the low energy phenomena can be explained irrespectively of the region III, in the cut-off theory.

* * *

We wish to express our thanks to Prof. C. HAYASHI, Dr. Y. MUNAKATA and other many members of the Yukawa Laboratory of Kyoto University for their discussions. One of us (Y. N.) is also grateful to Prof. Z. SHIROGANE of University of Osaka Prefecture for his continual encouragement.

RIASSUNTO (*)

Si riesamina l'analisi fatta da Cini e Fubini della possibilità per la teoria della sorgente di pioni estesa di riprodurre le sezioni d'urto sperimentali dello scattering pione-nucleone per onda p di bassa energia al lume delle seguenti restrizioni: (i) La condizione che la probabilità non possa essere negativa impone alcune restrizioni ai valori probabili degli operatori ξ_α, σ_i e $\xi_\alpha\sigma_i$. (ii) Esiste una limitazione geometrica della sezione d'urto di scattering. È chiaro che finchè il contributo dato alle regole di somma di Cini e Fubini dalla regione di alta energia (sopra al cut-off) è piccolo, la teoria non può riprodurre le sezioni d'urto di scattering sperimentali, neanche per la regione di bassa energia (energia cinetica dei pioni $\lesssim 300$ MeV). Tuttavia non esiste alcuna ragione per ritenere che il contributo della regione di alta energia sia piccolo. D'altro canto è quasi certo che la teoria possa riprodurre la sezione d'urto dello scattering pione-nucleone per onda p di bassa energia. Ciò implica che il contributo della regione di alta energia alle regole di sommazione di Cini e Fubini è importante e non deve essere trascurato.

(*) *Traduzione a cura della Redazione.*

Directional Correlation of the 0.845 and 1.24 MeV γ-Rays of ^{56}Fe.

G. Bertolini, E. Lazzarini and M. Mandelli Bettoni

Istituto di Fisica Sperimentale del Politecnico - Milano

(ricevuto il 26 Ottobre 1956)

Summary. — The directional correlation of the 0.845÷1.24 MeV γ-γ cascade of the ^{56}Fe in coincidence with the β^+ spectrum of 1.5 MeV maximum energy has been studied. The observed correlation function, after correction for the finite angular resolution of the detectors, is given by $W(\theta)=1+(0.102\,3\pm0.002\,7)P_2(\cos\theta)+(0.001\,5\pm0.003\,5)P_4(\cos\theta)$ according to a spin and multipolarity assignment 4(2)2(2)0.

1. – Introduction.

^{56}Co with a half life of $\sim 77d$ decays on ^{56}Fe by positron emission and electron capture. Many excited states of ^{56}Fe are formed and the energies of the γ-rays resulting from their decay have been studied. The results obtained are summarized in the decay scheme shown in Fig. 1 taken from « Nuclear Level Schemes » ([1]), to which volume the reader is referred for a complete bibliography up to June 1955.

In this scheme, the 0.845 MeV level has spin 2 and parity plus, and the 2.08 MeV level spin 4 and parity plus. The assignment of the spins is supported by an alignment experiment of Gallaher *et al.* ([2]) and by an angular correlation measurement of Hurley *et al.* ([3]). Moreover a mean life of the first excited level, estimated to exceed $8\cdot10^{-12}$ s ([4]) does not conflict with an

---

([1]) *Nuclear Level Scheme TID* 5300 (Washington, 1955), p. 54.

([2]) L. J. Gallaher, C. Whittle, J. A. Beun, A. N. Diddens, C. J. Gorter and M. J. Steenland: *Physica*, **21**, 117 (1955); O. J. Poppema, J. G. Siekman and R. van Wageningen: *Physica*, **21**, 223 (1955).

([3]) J. P. Hurley, S. W. Riedman and P. S. Jastram: *Phys. Rev.*, **98**, 1187A (1955).

([4]) K. Jlakovac: *Proc. Phys. Soc.*, A **67**, 601 (1954).

$E2$ character of the 0.845 MeV transition. The parities are supported by a polarization directional correlation of WOOD and JASTRAM ([5]).

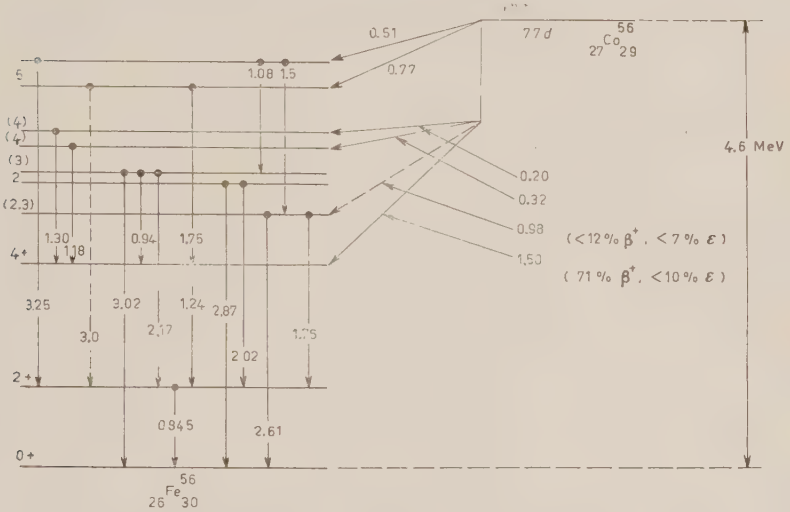

Fig. 1. – Decay scheme of ^{56}Co taken from Nuclear Level Schemes ([1]).

In the measurement of angular correlation reported before ([3]), coincidences with γ-rays of energy higher than 1.24 MeV were not completely excluded and the correlation function was not reported. It seemed therefore worthwile to re-measure the directional correlation in order to define the correlation function using an experimental method to eliminate the coincidences with high energy γ-rays: triple coincidences were taken between two γ-rays of ^{56}Fe and positrons belonging to the 1.50 MeV maximum energy spectrum. Indeed the 2.08 MeV level is known to arise from this decay.

2. – Instrumentation.

The γ spectrum has been investigated with a scintillation spectrometer using NaI(Tl) cylindrical detector 1 in. × 1 in. and employing a conventional channel of amplification and analysis.

The β^+ spectrum has been studied with a high transmission intermediate image β spectrometer ([6]).

([5]) T. WOOD and P. S. JASTRAM: *Phys. Rev.*, **98**, 1187A (1955).
([6]) G. BOLLA, S. TERRANI and L. ZAPPA: *Nuovo Cimento*, **12**, 875 (1954).

The β^+-γ coincidences have been analyzed with a scintillation spectrometer employing an NaI(Tl) cylindrical crystal 1 in. $\times$ 1 in. as γ detector and a cylindrical anthracene crystal of 1 in. diameter and ~ 7 mm thick as β^+ detector. The γ spectrum in coincidence with the positrons was sent in a ten channel analyser (7).

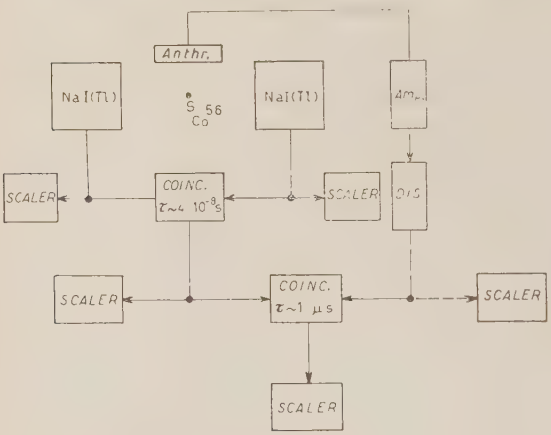

Fig. 2. – Block diagram of the experimental apparatus.

The block diagram for the directional correlation measurement is shown in Fig. 2. The experimental arrangement consisted of two scintillation detectors with NaI(Tl) crystals mounted on an EMI (6262) photomultiplier. The pulses collected at the anode were sent in a limiter stage and then in a coincidence circuit C1 (resolving power $6.6 \cdot 10^{-8}$ s). In the course of the measurement the resolving power was constant within 1%.

The β^- detector, consisting of an anthracene crystal in optical joint with a RCA type 5819 photomultiplier, was placed orthogonally to the plane of the axis of the two γ detectors. ~ 4 μm Al foil covered the anthracene crystal. The output signals from the coincidence circuit C1 and the β^- detector were fed into a second coincidence circuit C2 with resolving power of ~ 1 μs.

Lead collimators were used to protect the NaI(Tl) crystals from scattered radiation and to define the solid angles, which had half-angles of 25°.

3. – Sources.

^{56}Co was prepared in the cyclotron of Amsterdam with specific activity of 50 C/g. The impurities contained in the sample, about 25% of ^{57}Co and a negligible amount of ^{58}Co, did not disturb the measurement of correlation. Actually ^{57}Co decays by electron capture on the 220 keV energy level of ^{57}Fe and in our experimental arrangement the γ-rays arising from this decay were cut-off in the coincidence circuit. ^{58}Co decays by positron emission and by

(7) G. GATTI: *Nuovo Cimento*, **11**, 153 (1954).

electron capture on the 805 keV level of ^{58}Fe; a single γ-ray is known to proceed from this level.

For directional correlation measurement a dry source of $CoCl_2$ was prepared in an aluminium foil 5 μm thick mounted on an aluminium cylinder of 0.2 mm thickness and 10 mm inner diameter.

4. – Experimental Measurement and Results.

a) β^+ spectrum. Two β^+ decays were observed of $E_{max} \sim 440$ keV and $E_{max} \sim 1\,500$ keV, according to M. SAKAI *et al.* [8]. No β^+ spectrum of 990 keV maximum energy, reported in « Nuclear Level Schemes » (Fig. 1) was found. This decay has been observed by CHENG *et al.* [9] but not confirmed subsequently [8].

b) γ *spectrum.* The γ spectrum was found to be similar to that given by SAKAY *et al.* [8] and by GALLAHER *et al.* [2]. It is shown in Fig. 3.

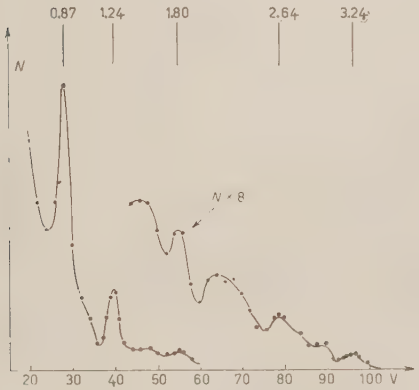

Fig. 3. – γ spectrum of ^{56}Co.

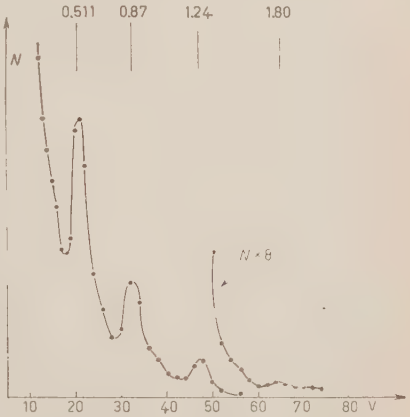

Fig. 4. – γ spectrum in coincidence with positrons of energy higher than 750 keV.

c) β^+-γ *coincidences.* Fig. 4 shows the γ spectrum in coincidence with positrons of energy higher than 750 keV. According to SAKAY *et al.* [8] only 0.845 MeV and 1.24 MeV γ-rays have been found in coincidence with the β^+ decay of 1.50 MeV maximum energy.

---

[8] M. SAKAY, J. L. DICK, W. S. ANDERSON and J. D. KURBATOV: *Phys. Rev.*, **95**, 101 (1954).

[9] L. S. CHENG, J. L. DICK, and J. D. KURBATOV: *Phys. Rev.*, **88**, 887 (1952).

d) 0.845 ÷ 1.24 MeV *γ-rays directional correlation.* The discriminator coupled to the anthracene crystal allowed only the detection of positrons of energy higher than 600 keV. In a first measurement run, γ-γ coincidences were taken for angles between the counter axis, of 90°, 120°, 135°, 145° and their simmetric angles with respect to 180°. In this run only pulses corresponding to energies higher than 350 keV were accepted in the C1 coincidence. An independent measurement of the directional correlation of annihilation radiation, obtained with a ^{22}Na source, verified that for these angles and these operating conditions the annihilation radiation does not affect our measurements. The anisotropy was measured in a successive run, triggering the C1 coincidence with pulses corresponding to energy higher than 650 keV in order to eliminate the contribution of the annihilation radiation. The correct value of the bias has been verified from the absence of genuine coincidences with a ^{22}Na source.

In order to evaluate the random coincidences the single counts of three detectors were taken by means of three indipendent scalers simultaneously with the coincidences C1 and C2. From the measured data the coincidence ratio $W_s(\theta) \quad C(\theta)/N_1N_2N_3$ between genuine coincidences and single counts was then formed and successively the normalized values to 90° $W_s(\theta) - W_s(\theta)/W_s(90°)$ were obtained. A total of 150 000 genuine triple coincidence counts were collected in our experiment.

In order to obtain the 0.845 ÷ 1.24 MeV γ-rays correlation it is necessary to eliminate the spurious correlation between two γ-rays detected by the NaI(Tl) crystals in coincidence with a γ-ray detected by the anthracene crystal. This correlation was measured by covering the anthracene crystal with a polythene absorber 6 mm thick. In such way only coincidences between three γ-rays were taken. The investigated correlation was calculated from the total correlation, taking away the correlation between three γ-rays, and evaluated proportionally to the ratio between the counts of the anthracene crystal when covered and not covered with polythene absorber.

The data of 0.845 ÷ 1.24 MeV γ-rays correlation, obtained in such way, were fitted by least squares to the correlation function $1 + \alpha_2 P_2(\cos\theta) + \alpha_4 P_4(\cos\theta)$ and the correction for the angular resolution was applied as suggested by FRANKEL ([10]). The corrected normalized experimental correlation is described by the equation

$$W(\theta)_{exp} = 1 + (0.1023 \pm 0.0027)P_2(\cos\theta) + (0.0015 \pm 0.0035)P_4(\cos\theta) \tag{11}$$

which, for a transition of the type 4(2)2(2)0 compares well, within the exper-

---

([10]) S. FRANKEL: *Phys. Rev.*, **83**. 673 (1951).

imental accuracy, with the theoretical function

$$W(\theta)_{\text{theor}} = 1 + 0.1020\,P_2(\cos\theta) + 0.0091\,P_4(\cos\theta)\,.$$

From the experimental function $W(\theta)_{\text{exp}}$ the anisotropy has been obtained

$$A = \frac{W(180°)_{\text{exp}}}{W(90°)_{\text{exp}}} = 1.163 \pm 0.005\,.$$

The experimental points (with their statistical errors), the experimental function (dotted line) and the theoretical correlation function (full line) are shown in Fig. 5.

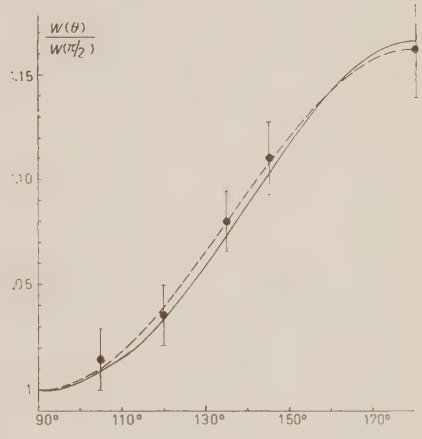

Fig. 5. – Directional correlation function of the 0.845÷1.24 MeV γ-γ cascade. The points represent the experimental results, the dotted line represents the least square fit to the experimental points and the full line the theoretical function for the sequence 4(2)2(2)0.

5. – Conclusions.

In the complex decay of ^{56}Co only a partial decay can be assumed as known. This decay consists in a positrons emission of $E_{\text{max}} \sim 1.5$ MeV followed by 1.24 MeV and 0.845 MeV γ-rays. This rays arise from the decay of the 2.08 and 0.845 MeV excited levels of ^{56}Fe. Our experimental results suggest a spin sequence of 0, 2, 4 for the ground state and the excited levels of 0.845 and 1.08 MeV. There was not evidence for the β^+ decay of 990 keV maximum energy.

The ambiguity of the spin of the ground state of ^{56}Co reported in Fig. 1 has been eliminated from a paramagnetic resonance measurement of JONES *et al.* ([12]), who found spin 4. The allowed shape of the β^- spectrum of 1.5 MeV maximum energy ([8]) and the isotropic correlation β^--γ found by STEVENSON

([11]) The experimental errors were computed according to M. E. ROSE: *Phys. Rev.*, **91**, 611 (1953).

([12]) R. V. JONES, W. DOBROWOLSKI and C. D. JEFFRIES: *Phys. Rev.*, **102**, 738 (1956).

and DEUTSCH ([13]), suggest a parity plus of the ground state of ^{56}Co in agreement with the nuclear shell theory.

* * *

We wish to thank Prof. BOLLA, Director of the Institute, for his kind interest and Dr. RIVA for her collaboration in the experimental measurements.

([13]) D. T. STEVENSON and M. DEUTSCH: *Phys. Rev.*, **83**, 1202 (1951).

RIASSUNTO

È stata misurata la correlazione angolare fra i raggi γ in cascata del ^{56}Fe di energia pari a 0.845 MeV e 1.24 MeV, in coincidenza con i positroni appartenenti al decadimento di $E_{max} = 1.5$ MeV. La funzione di correlazione è data da: $W(\theta) = I + (0.0102\,3 \pm 0.0027)\,P_2(\cos\theta) + 0.0015 \pm 0.0035)\,P_4(\cos\theta)$. Essa è in accordo con un carattere di quadrupolo elettrico e con dei valori degli spin dei livelli involti nel decadimento tali da dare una sequenza (4.2)2(2)0.

IL NUOVO CIMENTO Vol. V, N. 2 1° Febbraio 1957

On the Relation between Blob-Density and Velocity of a Singly Charged Particle in G-5 Emulsion.

G. Alexander and R. H. W. Johnston

Dublin Institute for Advanced Studies

(ricevuto il 3 Novembre 1956)

Summary. — A calibrated curve is presented expressing grain density as a function of $p\beta c$ for π- and μ-mesons, and is found to be in good agreement with the Bethe-Bloch formula for « restricted ionization loss ». The 2-body decays of K-particles were used as monocromatic sources of π- and μ-mesons. Blob-density measurements were reduced to grain-density by means of the O'Ceallaigh theory. A « least squares fit » of the experimental points to the Bethe-Bloch formula, together with the experimental « plateau » point, yielded for the mean ionization potential in AgBr the value (530 ± 100) eV, and for the maximum energy transfer the value $(2.9 \pm 0.5) \cdot 10^4$ eV.

1. – Introduction.

1·1. *Statement of the problem.* – In spite of the use of large emulsion block detectors for studying K-particle decay processes, the number of secondary tracks which are capable of being traced to rest remains severely limited by geometrical and other factors. It remains important therefore to be able to carry out identifications of secondary tracks by the ionization-scattering method. This renders necessary a rather precise knowledge of the ionization-velocity curve in the region $0.79 < \beta < 0.94$ and of the relation between this part of the curve and the « plateau » value of ionization.

In addition, the range-energy relation at high energies is dependent on the value assumed for the term « mean ionization potential » in the theoretical expression for rate of energy loss [1]. This term is related to the corresponding

[1] H. A. Bethe: *Zeits. f. Phys.*, **76**, 293 (1932).

term in the « restricted energy loss » expression for AgBr which determines the grain-density of a charged particle track in emulsion. A direct determination of the latter, by a study of the form of the grain-density/velocity curve, may throw some light on the behaviour of the former in the corresponding velocity range.

Finally, work in large emulsion blocks has been somewhat hampered by a lack of knowledge as to what reliance may be placed on grain or blob-density measurements carried out over a wide area of any given plate. Also, opinions have varied as to how much subjectivity is present in ionization measurements, especially when people without a general training in physics have taken part in the measurements.

1·2. *Scope of the present experiment.* – An experiment is in progress [2] of which the main purpose is to resolve completely the 3-body K-particle decay processes from the 2-body ($K_{\pi 2}$ and $K_{\mu 2}$) background. Scattering and blob-density measurements are being made on both the first and fourth centimetre of secondary track, measured from the point of decay. This enables a nearly complete separation to be obtained: the few percent of tracks the identification of which is subject to any uncertainty are measured in greater detail. This work will be described in full in another paper [3]. In the course of this work we have amassed a considerable quantity of information in the form of measured blob-densities of fast electrons and of π- and μ-mesons of precisely known energy. We have used this information to construct a calibrated theoretical restricted energy loss curve for AgBr in the range $0.79 < \beta < 0.94$ the accuracy of which at any given point is rather better than $\pm 1\%$. The relation of this part of the curve to the plateau value for electrons has been established with similar accuracy. This curve is only weakly dependent on the range-energy relation (see Appendix I) and is based on information from sources of π- and μ-mesons of very precisely defined energy.

Since the positions of the various tracks of which blob-density has been measured were distributed over plates of dimensions 10 cm × 15 cm, we have made an analysis of results according to area which appears to show the existence of variations in emulsion sensitivity (or in degree of development).

We have also made an experimental sampling distribution of the blob-densities in order to find the inherent uncertainty of the measurements as a function of number of blobs counted. We find, despite the fact that the measurements were made by seven different observers of whom only three were physicists, that the spread of the distribution is reasonably consistent with that expected.

(2) G. ALEXANDER, R. H. W. JOHNSTON and C. O'CEALLAIGH: *Proc. VI Rochester Conference* (1956), p. 31.

(3) G. ALEXANDER, R. H. W. JOHNSTON and C. O'CEALLAIGH: to be published.

We have used experimental values of standard deviations to estimate the statistical weights of the points on the ionization cuvre. These take account of the effects of the local variations.

2. – Theory.

2·1. *Bethe-Bloch formula.* – STERNHEIMER [4] gives the following modification of the Bethe-Bloch formula for the rate of energy loss at high energies for singly charged particles in a condensed material

$$\left(\frac{\mathrm{d}E}{\mathrm{d}x}\right)_{T_0} = \frac{A}{\beta^2}\left[\ln\frac{2mT_0}{I^2(z)} + \ln\frac{\beta^2}{1-\beta^2} - \beta^2 - \delta\right], \tag{1}$$

where A is a constant, $I(z)$ is the mean ionization potential in the material traversed and δ is a « density effect » term negligible except when $\beta \to 1$ where it tends to cancel the divergence of the logarithmic term in β.

T_0 is the upper limit of energy transfer defined by the condition of measurement (i.e. δ-rays being excluded). The expression therefore takes into account distant collisions only.

The position of the minimum (the « trough ») is given by the value of β for which

$$Q = 1 + \frac{\beta^2}{1-\beta^2} - \ln\frac{\beta^2}{1-\beta^2}, \tag{2}$$

where Q is the term $\ln(2mT_0/I^2(z))$ in the expression (1).

The value of the term Q is dependent on the ratio of the quantities T_0 and $I^2(z)$. These are given different values by various authors.

If a value of Q were determinable from a close study of the form of the normalized ionization curve for $\beta < .95$, this ratio would be known experimentally. An independent determination of T_0, if possible, would then permit an experimental estimate of the quantity $I(z)$ for AgBr.

2·2. *Polarization effect* [5-9]. – When $\beta \to 1$ it is necessary to consider in detail the behaviour of the term δ. STERNHEIMER [5] gives for the limit $\beta = 1$

$$\delta = \ln\left(\frac{\beta^2}{1-\beta^2}\right) - \ln\left(\frac{\nu_m'^2}{\nu_p^2}\right) - 1, \tag{3}$$

[4] R. M. STERNHEIMER: *Phys. Rev.*, **91**, 256 (1953).
[5] R. M. STERNHEIMER: *Phys. Rev.*, **83**, 851 (1951).
[6] O. HALPERN and H. HALL: *Phys. Rev.*, **57**, 459 (1940).
[7] O. HALPERN and H. HALL: *Phys. Rev.*, **73**, 477 (1948).
[8] G. C. WICK: *Nuovo Cimento*, **9**, 302 (1943).
[9] E. FERMI: *Phys. Rev.*, **57**, 445 (1949).

where the first term cancels the logarithmic increase, where $\nu'_m = I(z)/h$ is the mean effective frequency of the excited levels and $\nu_p = (ne^2/\pi m)^{\frac{1}{2}}$ is the plasma frequency, n being the number of electrons per cm^3 in AgBr. Substituting δ we have

$$\left(\frac{\mathrm{d}E}{\mathrm{d}x}\right)_{\text{plateau}} = A\left[\ln 2mT_0 - 2\ln h\nu_p\right]. \tag{4}$$

We have therefore the possibility of determining T_0 from the plateau/trough ratio, assuming the experimental value of Q already determined for the part of the curve where δ is negligible. Thus it is possible in principle to obtain from experiment a value of $I(z)$ which is a measure of the energy expended in grain formation. Although the logarithmic dependence renders the determination rather imprecise, it is felt that the increased experimental accuracy available in this work enables us to obtain a meaningful result.

2·3. *Ionization in emulsion.* – It is generally assumed that the number of developed grains per unit length of track (grain density) is proportional to the rate of loss of energy of the particle. The experimental procedure, however, is now generally to measure either blob-density (a blob being defined as a cluster containing one or more grains) or else the mean gap length between blobs ([11,12]). Both these experimental methods are relatively free from subjective errors, while direct measurement of grain-density requires a continuous series of decisions by the observer as to how many grains are in each observed blob.

Unfortunately however, if measurements are to be compared with the theory, the use of mean gap length $\bar{G}$ or blob density b imposes the necessity of assuming a model to describe the process of track formation.

A number of such models has been discussed, ranging from the lattice model of HERZ and DAVIS ([13]) to the exponential distribution of silver halide crystals assumed by O'CEALLAIGH ([10-12]). Since the only detectable difference among the models occurs at high grain densities it is felt that the correction from grains to blobs near the minimum ionization may be made using the O'CEALLAIGH model, whether it is exactly true or not.

The relationship between the quantities defined above on this model is given by

$$b = g\exp\left[-K/\bar{G}\right], \tag{5}$$

where K is a « physical development constant » which depends on the mean

([10]) C. O'CEALLAIGH: typescript (unpublished).
([11]) C. O'CEALLAIGH: *Proc. Bagnères Conf.*, 1953, p. 73.
([12]) C. O'CEALLAIGH: *CERN Standardization Publication B.S.* 11 (1954).
([13]) A. J. HERZ and G. DAVIS: *Austral. Journ. Phys.*, **8**, 129 (1955).

crystal size α and the mean grain diameter a:

$$K = a - \alpha + \varepsilon_0 ,$$

ε_0 being an optical constant. A relationship also exists for the mean gap length:

$$\overline{G} = \frac{1}{g} - \alpha ,$$

which indicates that $\overline{G}$ is independent of the quantity K and consequently, in this sense, it is less development-dependent than any other parameter for measuring ionization ([14]).

It is possible to determine K for a given stack of plates by plotting blob-density against range from rest up to say 1 cm or so. The experimental values may be fitted to one of a series of curves ([14]) of varying K for the given mean plateau blob-density, thus determining K.

A more direct method is to measure blob-density and mean gap length simultaneously on a track of constant ionization and to make use of the above relations.

K generally appears to be weakly correlated with the plateau blob-density.

The correction term to convert normalized blob-density to grain-densites in a stack of standard blob-density b_0 (i.e. plataeu, minimum or other arbitrary (*) value) is easily seen from (5) to be given by

$$(6) \qquad \begin{cases} b^* = b/b_0 = g^* \exp\left[-K(g - g_0)\right] \\ \qquad\qquad \sim g^* \exp\left[-K(b - b_0)\right] \end{cases}$$

to a first approximation which is adequate up to about twice minimum. Successive approximations may always be obtained by replacing b values on the right by the first approximation g values.

It is possible to convert normalized blob-densities from one stack of development constant and standard blob-density K_1, b_1^0 to another of K_2, b_2^0. It is not difficult to show that the conversion factor is

$$(7) \qquad \begin{cases} b_1^* = b_2^* \exp\left[K_2(b_2 - b_2^0) - K_1(b_1 - b_1^0)\right] \\ \qquad \sim b_2^* \exp\left[(K_2 b_2^0 - K_1 b_1^0)(b_2^* - 1)\right] \end{cases}$$

to a first approximation.

([14]) C. O'Ceallaigh: *Suppl. Nuovo Cimento*, **12**, 412 (1954).

(*) (Note that we are here broadening the usual definition of b^* or g^*. Finally we normalize to the minimum, this being a better defined point, in our experiment, than the plateau.)

We make use of these relations in relating some ionization values established in earlier work to the new ionization curve, as well as for small corrections from blobs to grains in the minimum region.

3. – Experimental Procedure.

3·1. *Conditions of exposure, processing and scanning.* – A block of G5 emulsion of dimensions $20 \times 25 \times 18$ cm^3 containing 300 strips was exposed to the Bevatron 90° K^+ beam. This stack, known as the « K_2 stack » is the second of a series exposed at the Bevatron for the use of the European laboratories of the G-stack collaboration. Fifty half plates (nos. 101-150) were allotted to the Dublin Institute for Advanced Studies. The momentum of the particles in the median plate (no. 127) was determined from the mean proton range 2.23 cm in that plate. Its value was found to be 409 MeV/c. Corresponding to this momentum, the mean range of the K-particles was 9.8 cm

The processing was carried out at Bristol University by the temperature process. The mean blob-density in the plates used in this experiment was found to be $\sim 15.5/100$ μm for beam π tracks ($1.01 \times$ min).

The plates were scanned by experienced scanners for K^+ decay events. The effect of the scanning process used on the nature of the experimental results will be discussed in the main paper ([3]). Any effects of selection bias which may occur do not affect this work, since it is based on identified $K_{\pi 2}$, $K_{\mu 2}$ and K_β tracks only. Only secondaries in good geometry were considered; the dip in the processed emulsion was required to be $< 6°$.

3·2. *Calibration of plates.* – Initial calibration work was performed using beam π-meson tracks near the end of the proton beam. About 3000 blobs were counted in each plate. These blob-densities were used for the preliminary identification of the first hundred K-secondary tracks. Information from identified tracks in each plate was then used to improve the ionization calibration in the K-decay area of the plate. This procedure was adopted as preferable to the alternative one of calibration using beam π's in the K-decay area, in spite of the uncertainty arising from local variations in sensitivity. Clearly, the effect of scattering (elastic and inelastic) is to give rise to fluctuations in energy as well as inferior collimation of the π-beam, besides an unwanted background of electrons produced in charge-exchange and knock-on processes.

Study of the depth-variation of blob densities of beam tracks indicated a linear development gradient of 23% between the top and bottom of each emulsion. This is an extrapolated value and neglects the etching effect at the surface. Measurements were restricted to distance from the surface and

glass of more than 20 μm (processed) so that a linear depth correction could be assumed. As far as possible, the correction was kept small by using the central portion of the track only.

3·3. *Treatment of the basic data.* – The results of the present work are based on blob-measurements on 150 $K_{\mu 2}$, 65 $K_{\pi 2}$ and 14 K_{β} secondaries distributed over 40 plates in each of which a beam π-meson calibration has been performed. The details of the scattering and blob-measurements and the selection criteria adopted will be described in a later publication and it is thought sufficient to state that contamination of the basic sample by cases of $K_{\mu 3}$-decay is considered to be negligible.

In order to eliminate the effect of difference between plates, we first reduced the data for each separate plate. With each determination of the blob-density (reduced to the median plane of the emulsion by depth-correction) is associated a weight counted in units of 100 blobs and a mean length from decay L depending on the geometry of the particular track. Each plate may contain six categories of blob-densities: $K_{\mu 2}$ 1-st and 4-th cm, $K_{\pi 2}$ 1-st and 4-th cm, beam π and K_{β}. Weighted mean blob-densities were determined for each of the six categories, together with mean values of L for the first four. Any one of these weighted mean values may be chosen as standard and used as a divisor for the remaining five which are thereby raised to the status of normalized blob-densities and are no longer dependent on the particular plate. Weights were attributed to the ratios according to the relation $w = (1/w_1 + 1/w_2)^{-1}$ which can be shown to be valid for ratios of order unity, provided $1/w_1$ and $1/w_2$ are both small. As a preliminary measure the blob-densities were normalized to « $K_{\mu 2}$ 1-st section ». Values were subsequently re-normalized to $b_{\min}$ (as in Table I), after the value of Q (which determines the values of $b_{\min}$) had been found.

The mean values of the normalized blob-densities were then averaged (*) over all the plates, taking into account the weights. The $K_{\mu 2}$ and $K_{\pi 2}$ values then refer to the overall weighted mean lengths from decay.

We now have a set of five blob-density ratios, each with effective weight expressed in units of 100 blobs. It is necessary to determine in some way how this effective weight is related to the actual standard deviation to be attributed to each ratio. This problem has been treated in detail in Appendix II. It is sufficient to state here that the experimental error is related to the weight in a way which appears to depend on the area over which the measurements extend.

(*) Strictly speaking we should correct every blob-density to the overall mean $\bar{L}$ before averaging. However, the error introduced by inverting the averaging and correcting procedures has been found to be negligible.

TAB

Point No.	Description	Length L from decay	β^2	$p\beta^2_\pi$
1	Beam π	—	0.8839	360.6
2	$K_{\mu 2}$ I	0.603	0.8281	278.6
3	$K_{\mu 2}$ II	3.31	0.8046	253.9
4	$K_{\pi 2}$ I	0.654	0.6740	164.7
5	$K_{\pi 2}$ II	3.23	0.6217	141.0
6	π's traced from rest	—	0.4591	87.0
7	π and p mean gap length	—	0.2389	38.2
8	minimum	—	0.93106	494.7
9	plateau	—	1.0000	—

4. – Experimental Results.

4·1. *Least squares fit.* – We have computed the rate of loss of energy in AgBr for values of β ranging from 0.24 to 0.93. The results are presented in Table I. As has been mentioned in Sect. 2·3 the theoretical normalized grain-density g^* is taken to be given by $(\mathrm{d}E/\mathrm{d}x)/(\mathrm{d}E/\mathrm{d}x)_{\mathrm{min}}$. The value of normalized theoretical blob-density b^* is obtained for all points but 6 and 7 (see plates I and II, Table I) by multiplying g^* by the factor $\exp[K(b_0 - b_1)]$ (see Sect. 2·3 (6)).

The experimental values of b^*, their weight w, standard deviations σ and their deviations from the theoretical are also shown. A «least squares fit» was performed using a first approximation value of $Q = 11.2$ [19]. A correction term $q = -0.7$ was found, so that the final theoretical values were computed for $Q = 11.9$.

Points 1, 3 and 4 only were used in the «least squares» calculation. Point 2 was regarded as fixed. Point 5 was rejected on grounds that it might contain a bias towards high ionization due to undetected interactions. Point 6, although not formally included in the least squares determination since it came from a different experiment (see Sect. 4·2 below) was checked for goodness of fit. It was found that the «best-fit» value of Q changed only to 12.2. Point 8 is the calculated minimum for $S = 11.9$. The relation of this point to the others is dependent on the theory. Since the lowest experimental point is for $b^* = 1.01$ and since the fit of the experimental points is good, there can be little uncertainty about the position and relative value of the minimum point.

Theoretical ($Q = 11.9$)			Experimental		
g^*	$\exp[k(b_1 - b_0)]$	b^*	b^*	Effective weight w (+)	Deviation
1.0125	1.0009	1.0116	1.0154	286	+ .0037
1.0475	1.0036	1.0438	1.0438	—	—
1.0679	1.00435	1.0633	1.0604	712	— .0029
1.2166	1.0130	1.2010	1.2025	546	+ .0015
1.2991	1.0204	1.2731	1.2800	355	+ .0069
1.6847	1.0464	1.6100	1.6158	210	+ .0058
3.0161	—	—	(2.92) (×)	—	—
1.0000	1.0000	1.0000	—	—	—
(1.328) (*)	1.0088	—	1.1221	215	—

(*) Experimental value. (+) As determined in Appendix II. (×) g^*, not b^*.

Judged by the standard of the χ^2 test, the fit of the theory to the experimental points is «good» ($P = 0.9$ for «best fit», P still as high as 0.5 for Q as widely varying as 11.5 and 13.0). This reflects, as may be expected, the insensitivity of the curve to the value of Q. It is difficult to attach meaningful fiducial limits to the best estimate of Q. A change in an experimental ionization of one standard deviation ($\sim 0.6\%$) at $b^* \sim 1.3$ would cause a change of 0.4 in the best estimate of Q. This gives an order of magnitude estimate of the experimental error, if we take into account the good fit of point 5.

4·2. *Relation to earlier work.* – Point 6 and 7 are included in the table in order to provide an independent check based on earlier work.

Point 6 is derived from π-mesons traced back from rest in the Sardinian stack S_{30}. A curve based on this work has been given in connection with the confirmatory K_β identification ([15]). The effective weight of this point is derived from the observed spread of the points about the line. Conversion from b^* in stack S_{30} to b^* in stack K_2 was performed using the results of Sect. 2·3.

Point 7 is derived from the mean of two mean gap-length calibrations of protons and π-mesons traced from rest. The calibrations are due to Fowler and Perkins ([16]) and Johnston and O'Ceallaigh ([15,17]). The former contains about twice the experimental material and is given double weight. The

([15]) R. H. W. Johnston and C. O'Ceallaigh: *Phil. Mag.*, **46**, 393 (1955).
([16]) P. H. Fowler and D. H. Perkins: *Phil. Mag.*, **46**, 587 (1955).
([17]) R. H. W. Johnston and C. O'Ceallaigh: *Phil. Mag.*, **45**, 424 (1954).

basic result $\overline{G} = (1/g) - \alpha$ (Sect. 2·3) was used to reduce the $\overline{G}^*$ value to normalized grain-density. If is therefore to be compared with the grain-density curve; all the other experimental points are based on blob-densities.

The good fit of points 6 and 7 provides evidence of the soundness at low grain density of the expressions proposed by O'CEALLAIGH. It also provides support for the contention that ionization data from different emulsions and by different techniques may be compared by relatively simple means.

4·3. *Corrections terms.* – The value of the correction term (grain → blobs) is seen to be small ($\sim 2\%$ at most) for ionization up to 1.28 min. Thus a possible 5% uncertainty in the value of K is of little importance.

The value of the correction term in the worst case (mean gap length → grains point 7) is $(1 - \alpha g_0)/(1 - \alpha g) \sim 1.09$ for $g_0 = 14.1/100$ μm and 1.17 for $g_0 = 25/100$ μm. For point 6, conversion of blobs from a stack with development constants $(K, b_0) = (0.44, 14.1)$ to a stack (0.49, 17.1) (b_0 here refers to plateau ionization) involves a factor of only 1.2%. Conversion from grains to blobs of this value of b^* (in the K_2 stack) involves a factor 1.04.

4·4. *Mean ionization potential.* – Referring again to Table I it is seen that the experimental value of $b_{\text{pl}}/b_{\text{min}}$ is 1.122 ± 0.008.

Using the theoretical expression of Sect. 2·2 with the quantity $h\nu_p$ (plasma energy) taken as 53.3 eV (3.55 Ry) [4] and using the value $Q = 11.9$ to calculate $(\partial E/\partial x)_{\text{min}}$ it is possible to estimate the quantity T_0.

Reducing normalized plateau blob-density to grain (factor 1.0088) we get a value

$$1.133 \quad \frac{g_{\text{pl}}}{g_{\text{min}}} = \frac{\ln [2mT_0/(h\nu_p)^2]}{(1/\beta^2)[Q + \ln \beta_1^2/(1-\beta_1^2) - \beta_1^2]},$$

where β_1 is given by $11.9 = Q = 1 + (\beta_1^2/(1-\beta_1^2)) - \ln(\beta_1^2/(1-\beta_1^2))$, whence $T_0 = (2.9 \pm 0.5) \cdot 10^4$ eV. The experimental error is entirely from the plateau blob-density.

T_0 so far appears to be a rather arbitrary quantity. For example STERNHEIMER [4,5] estimates T_0 as $10^4 \div 10^5$ eV, SHAPIRO and STILLER [18] take $5 \cdot 10^3$ eV, while JAUNEAU and TREMBLEY [19] take 10^4 eV.

Now inserting T_0 in the expression $Q = \ln 2mT_0/I^2(z) = 11.9$ we get an estimate of $I(z) = 527$ eV $= 12.9\overline{Z}$ ($\overline{Z} = 41$ for AgBr). Assuming an experimental error in Q of ± 0.4 and taking into account the error on T_0, we get and estimated experimental error for $I(z)$ of ± 100 eV.

BLOCH [20] gives a value $I(z) = 13.5\overline{Z}$. An experimental determination by

---

[18] M. M. SHAPIRO and B. STILLER: *Phys. Rev.*, **87**, 682 (1952).

[19] L. JAUNEAU and J. TREMBLEY: *Suppl. Nuovo Cimento*, **1**, 230 (1955).

[20] F. BLOCH, *Zeits. f. Phys.*, **81**, 363 (1933).

BAKKER and SEGRÈ [21] using 350 MeV protons stopped in various elements gives a result $I(Z) = 9.4\overline{Z}$ for heavy elements. VIGNERON [22] however gives reasons for regarding the latter as too low and suggests a value $I(Z) = 11.6\overline{Z}$. This latter value has been used by BARONI *et al.* [23] in their range energy calculations.

Although the precision of our determination is poor it represents a direct determination at a higher velocity than heretofore ($\beta \sim 0.86$).

It is necessary to point out however that there exists a point of difference between our experiment and stopping-power experiments. In the latter case, total energy loss is involved, while in our case a mechanism specific to grain formation [24] enters. For example, the cross-section for latent image formation may vary with electron energy [25]. A more detailed theoretical model would then be required [26].

4·5. *Curve.* – The relation between grain-density, blob density in the K_2 stack and $p\beta c$ for π- and μ-mesons is shown graphically in Plates 1 and 2.

Plate 1 gives an overall picture of the curve and includes the points 6 and 7 based on earlier work. The agreement between the theoretical curve for $Q = 11.9$ and the experimental points is seen to be satisfactory.

Plate 2 displays the region $1.0 < b^* < 1.6$ in greater detail, enabling relationship between b^* and $p\beta c$ to be read off to within less than 1% which is justified by the accuracy of the experiment.

For use in emulsion with different values of K, the grain-density curve should be taken as fundamental and correction factors established for blob-density, or else all measurements should be made by the mean gap length or equivalent method [12-16] which can therefore be reduced to grain density without a knowledge of K.

4·6. *Conclusion.* – It has been found possible to make an estimate of the mean ionization potential (effective for development centre formation) in ABgr for $\beta \sim 0.86$ and to establish the experimental form of the $p\beta c$–g^* curve in the region $1 < g^* < 3$. Monochromatic sources of fast π- and μ-mesons were used (i.e. 2-body K-particle decays).

A curve has been constructed which is expected to be of use to experimenters

---

[21] C. J. BAKKER and E. SEGRÈ: *Phys. Rev.*, **81**, 489 (1951).

[22] L. VIGNERON: *Journ. Phys. Rad.*, **14**, 145 (1953).

[23] G. BARONI, C. CASTAGNOLI, G. CORTINI, C. FRANZINETTI and A. MANFREDINI: *Ric. Scient.*, **26**, 1718 (1956).

[24] G. P. S. OCCHIALINI: *Suppl. Nuovo Cimento*, **6**, 377 (1949).

[25] M. HUYBRECHTS and M. SCHÖNBERG: *Nuovo Cimento*, **9**, 9, 764 (1952).

[26] P. BUDINI and L. TAFFARA: *Nuovo Cimento*, **4**, 23 (1956). Computations are in progress.

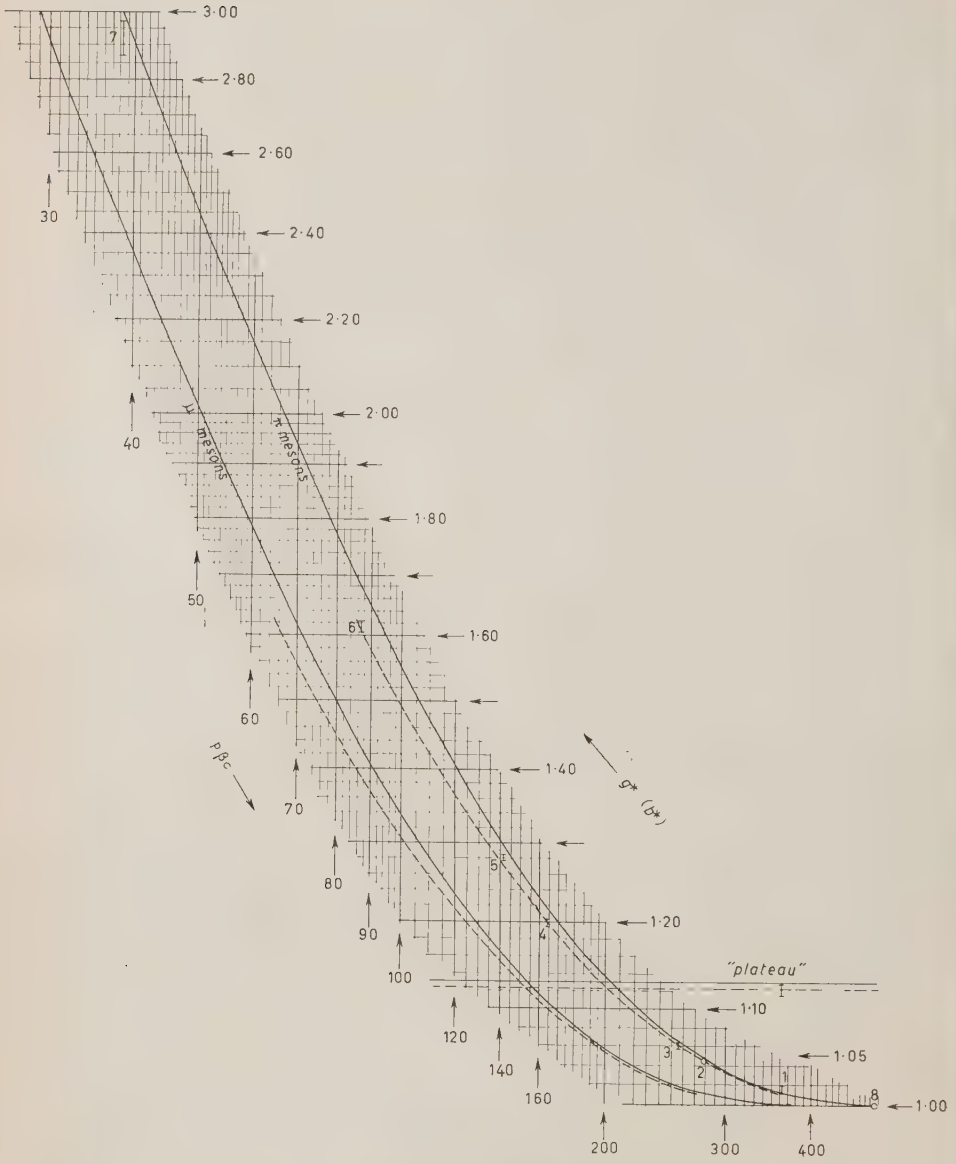
3·00
2·80
2·60
2·40
2·20
2·00
1·80
1·60
1·40
1·20
1·10
1·05
1·00
30
40
50
60
70
80
90
100
120
140
160
200
300
400
μ mesons
π mesons
pβc
σ* (δ*)
"plateau"
7
6
5
4
3
2
1
8

Plate 1.

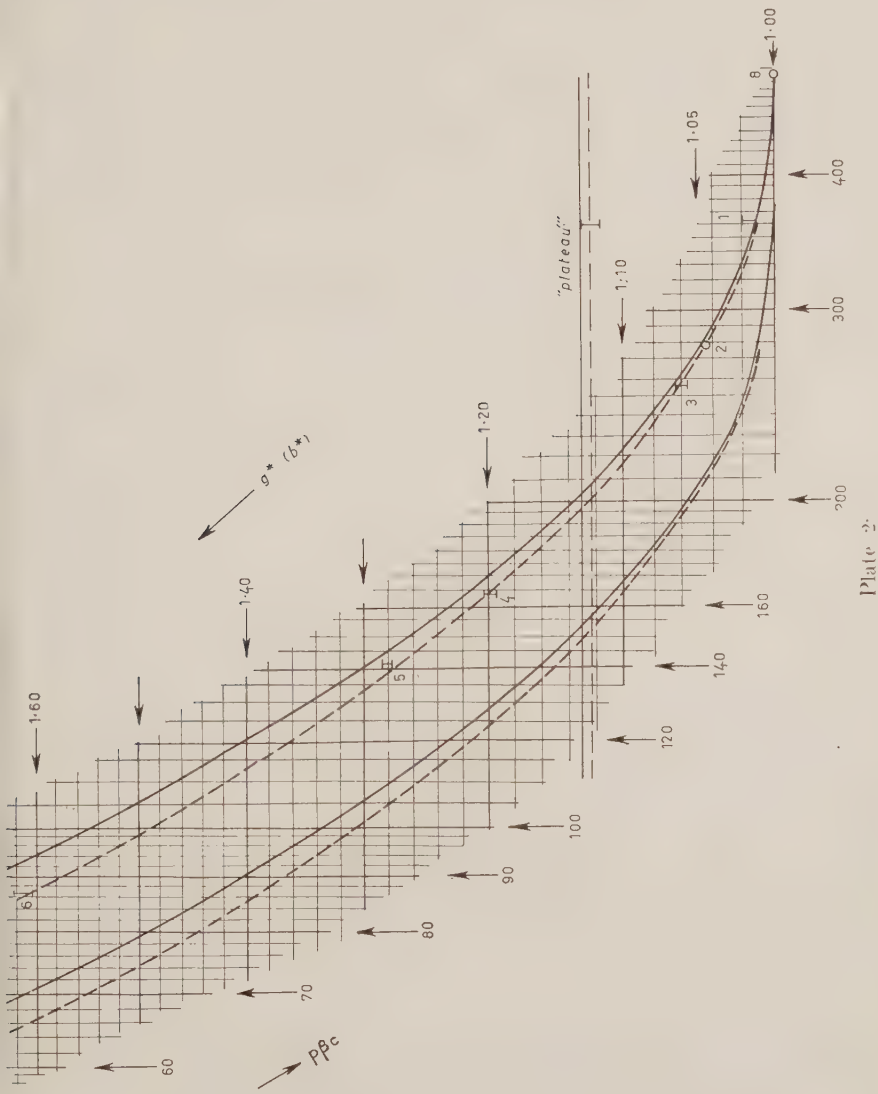
1·00
1·05
1·10
1·20
1·40
1·60
"plateau"
400
300
200
160
140
120
100
90
80
70
60
ρ* (b*)
ρ̄c

Plate 2.

in identifying tracks of fast charged particles for $\beta < .95$, and in distinguishing them from electrons of « plateau » ionization.

* * *

The authors wish to thank Professor C. O'CEALLAIGH for his constant interest and encouragement and Dr. D. KEEFE for helpful discussion. They also wish to acknowledge the skill of the scanners at the Institute (Mrs. M. JOHNSTON, Mrs. J. KEEFE, Miss. M. O'BRIEN and Miss P. LEAHY) whose assistance with the basic measurements was of great value, and also to thank Miss E. SMITH for help with the computation work and Miss R. RYAN (Geophysical Section) for the production of the curve.

The authors are indebted to the Dublin Institute for Advanced Studies for a studentship (R.H.W.J.) and a scholarship (G.A.).

APPENDIX I

Masses and Kinetic Energies Used.

We have assumed meson masses as follows

π^+	π^0	μ	K
139.5	134.6	105.6	494 (MeV).

Substituting in the relation $E = Q((m_2 + Q/2)/m_0)$ ($m_0^+ \rightarrow m_1^+ + m_2^0$ decay scheme) we obtain values for the kinetic energy T at decay

$K_{\pi 2}$	109.1 MeV,
$K_{\mu 2}$	152.7 MeV.

These values are corrected to the mean distances from decay $\bar{L}$ by making use of the (differentiated) Rome range-energy relation (23). The corrections are as follows

$K_{\mu 2}$			$K_{\pi 2}$		
$\bar{L}$ (cm)	ΔT	T	$\bar{L}$ (cm)	ΔT	T
0.603	3.4	149.3	0.646	4.3	104.8
3.31	19.3	133.4	3.24	21.5	87.6

The value of $p\beta$ adopted for the various distances from decay depend on the range-energy relation only *a*) through the correction term ΔT and *b*) in

so far as the τ-meson mass (assumed = K-meson) depends on the range-energy relation. They are consequently independent (to a first approximation) of the absolute value of the range energy relation for $\beta > 0.66$.

Appendix II

1 – Determination of the intrinsic Uncertainty of a Blob Measurement.

The most convenient way to determine this quantity is by means of an experimental sampling distribution.

Blob-densities of individual tracks of $K_{\mu 2}$ secondaries near their point of origin were normalized to the mean $K_{\mu 2}$ decay value in each plate. All values were corrected back to the point of decay. Weights were attributed to the normalized blob-densities according to the expression given in Sect. 3·3. w_1 in this case being the weight of the individual determination and w_2 being the total weight of first section $K_{\mu 2}$ track in the particular plate. (We here neglect correlations between individual track values and the plate mean values). Taking them into account would cause a correction of $\sim 10\,\%$ in w_2 where $1/w_2$ is small compared to $1/w_1$). 187 samples of mean weight $w = 6.89$ (689 blobs) were obtained, distributed about unity with standard deviation a few percent. The value of the standard deviation was then estimated by determining the weighted root mean square deviation from the mean of the distribution. This quantity should correspond to the theoretical value $\sigma_0/\sqrt{w}$, where σ_0 is the intrinsic uncertainty of the distribution. This question has also been considered by O'Ceallaigh [10]. From the O'Ceallaigh model of track formation it is possible to show that for large (say $\gtrsim 1000$ blobs) w the distribution is approximately normal and $\sigma_0 \sim 0.80$. This value has been in common use by experimentalists. Experimentally we find $\sigma_0 = 0.88$, which includes (in this determination) errors due to 1) development gradient determination; 2) local variations over the decay area; 3) possible subjective difference between the seven observers.

We take this value $\sigma_0 = 0.88$ as a measure of the intrinsic uncertainty appropriate to our experimental conditions of blob-density determination.

2. – Determination of the Experimental Errors on the Mean Normalized Blob-Densities.

Each of the five normalized blob-densities has been determined as a weighted mean of normalized values in about thirty plates. By determining the weighted root mean square deviation of these values it is possible to estimate their standard deviations σ appropriate to the mean sample weight.

This quantity σ may be assumed to be composed of parts:

$$\sigma^2 = \sigma_1^2 + \sigma_2^2 + \sigma_3^2 ,$$

where σ_1 is the « intrinsic » standard deviation calculated using the formula $\sigma_0/\sqrt{w}$ with $\sigma_0 = 0.88$; σ_2 is the standard deviation in ionization due to the $\overline{L}$ distribution; σ_3 is the standard deviation due to possible local variations. The following table (Table II) shows the experimental values of σ etc., for the various categories.

TABLE II.

Sample	Mean sample wt. (100 blobs)	Exp. σ %	Calc. $\sigma_1 = 0.88/\sqrt{w}$ %	$\overline{L}$ σ_2 %	$\sigma_3 = \sqrt{\sigma^2 - \sigma_1^2 - \sigma_2^2 \overline{L}}$ %	(Cm)	f
b_1/b_π	21.15	3.0	1.93	0.065	2.3	6.5 (*)	0.41
b_2/b_1	21.80	2.15	1.91	0.18	0.96	3.3	0.79
b_3/b_1	16.55	2.26	2.18	0.93	0	0.6	1.00
b_4/b_1	13.65	2.7	2.38	1.1	0.6	3.2	0.94
b_1 (internal)	6.89	3.36	—	0	0 (+)	0.6	1.00
b_{pl}/b_1	10.50	3.2	2.73	0	—	—	0.73

(*) Distance from decay area to beam π calibration area.
(+) By definition equal to zero.

The quantities b_π and b_{pl} are the blob-densities of beam π-mesons and electrons, while b_1, b_2, b_3 and b_4 refer to $K_{\mu 2}$ 1-st and 4-th cm, $K_{\pi 2}$ 1st and 4-th cm respectively. Only ratios of these quantities appear.

The quantity f is given by the expression $f = \sigma_1^2/(\sigma^2 - \sigma_2^2) = w'/w$ and is a conversion factor for converting the « weight » of each point on the ionization curve to an « effective weight » related to the experimental standard deviation. w and w' are the original and corrected weights respectively. Note that the variance σ_2^2 due to the L distribution has been subtracted out from the experimental variance σ^2 (see Sect. 3·3, footnote).

Since the values of f appropriate to b_2/b_1 and b_4/b_1 are equivalent, it is egitimate to average them and take a mean conversion factor 0.84 for the 4-th cm from decay.

3. – Evidence for Local Variations.

Examination of the σ_3 column in Table II appears to indicate that local variations exist. If they are of a random character, one expects the variance due to them to be in some way proportional to the distance. The figures appear to indicate some kind of increase with distance, but it is not easy to determine the law of increase with the information available. In all cases but the first the figures refer to lengths in all directions, in fact to increasing areas, while for the first point $\overline{L}$ is a distance between the K-decay area and the beam π calibration area. Further, the K-decay area itself is extended over about 10 cm² so that the difficulties are obvious. However, it is considered worthwhile to draw attention to the existence of the effect.

It is worth noting that the value of σ_3 for $K_{\pi 2}$ 1-st section (b_3/b_1) is experimentally zero. This means that the local variations are no greater than for $K_{\mu 2}$ 1-st section, where they are included in the experimental standard deviation $\sigma_0 = 0.88$. Since the decay area for $K_{\mu 2}$ and $K_{\pi 2}$ is the same, this is as expected.

RIASSUNTO (*)

Si presenta una curva calibrata rappresentante la densità granulare in funzione di $p\beta c$ per mesoni π e μ e la si trova in buon accordo con la formula di Bethe-Bloch per la « perdita di ionizzazione ristretta ». Come sorgenti monocromatiche dei mesoni π e μ si sono usati i decadimenti in 2 corpi di particelle K. Le misure di densità di blobs si sono ridotte a densità granulare per mezzo della teoria di O'Ceallaigh. Un adattamento dei punti sperimentali alla formula di Bethe-Bloch col calcolo dei minimi quadrati assieme al plateau sperimentale ha dato per il potenziale di ionizzazione medio in AgBr il valore (530 ± 100) eV e per il massimo trasferimento d'energia il valore $(2.9 \pm 0.5) \cdot 10^4$ eV.

(*) *Traduzione a cura della Redazione.*

Caratteristiche delle disintegrazioni nucleari prodotte da protoni di 140 ± 6 MeV.

II. - Nuclei pesanti.

S. Jannelli e F. Mezzanares

Istituto di Fisica dell'Università - Messina

(ricevuto il 3 Novembre 1956)

Riassunto. — Si studiano le disintegrazioni prodotte da protoni di 140 ± 6 MeV negli elementi pesanti (Ag e Br) delle emulsioni Ilford G5 da 600 μm. Sono state prese in considerazione 634 stelle (delle quali 530 cercate sistematicamente « per area »). I risultati dedotti dall'analisi degli eventi confermano quanto trovato da altri autori nel senso che il processo della disintegrazione può dividersi in due fasi distinte: quella della cascata nucleonica e quella evaporativa. Si ha inoltre una conferma sperimentale dell'esistenza dei protoni di bassa energia attribuibili ai processi di diseccitazione del nucleo dopo l'evaporazione. Dai dati sperimentali ricavati e da quelli di altri autori si ricavano i valori più attendibili di alcune grandezze caratteristiche del processo di disintegrazione preso in esame.

Il problema delle disintegrazioni nucleari prodotte da particelle di alta energia ($T \sim 100$ MeV) è stato largamente studiato sia dal punto di vista sperimentale ([1-19]) che teorico ([20,21]).

Come è noto il processo viene abitualmente descritto in due fasi succes-

([1]) E. Gardner e V. Peterson: *Phys. Rev.*, **75**, 364 (1949).
([2]) W. Harding e L. Baumhoff: *Phys. Rev.*, **75**, 370 (1949).
([3]) E. Gardner: *Phys. Rev.*, **75**, 379 (1949).
([4]) E. W. Titterton: *Phil. Mag.*, **42**, 109 (1951).
([5]) L. S. Germain: *Phys. Rev.*, **82**, 596 (1951).
([6]) J. F. Miller: *Phys. Rev.*, **83**, 1261 (1951).
([7]) G. Bernardini, E. T. Booth e S. G. Lindenbaum: *Phys. Rev.*, **85**, 826 (1952); **88**, 1017 (1952).

sive: la cascata nucleonica e l'evaporazione nucleare; ad esse segue la completa diseccitazione del nucleo residuo (emissione γ, decadimento β). (*).

I lavori sperimentali sono stati condotti dapprima su eventi prodotti dalla radiazione cosmica e successivamente mediante emulsioni esposte a particelle accelerate artificialmente e di energia ben definita.

Le statistiche finora ottenute alle diverse energie sono relativamente povere; pertanto ci è parso opportuno studiare le stelle prodotte in emulsioni Ilford G5 da 600 μm utilizzando un campione più vasto di quelli studiati finora, in modo da ridurre gli errori statistici e poter eseguire un confronto più dettagliato con i risultati teorici (+).

1. – Procedimento sperimentale.

L'osservazione è stata condotta dapprima per area con obbiettivo 55 Koristka e con questo metodo sono state trovate 634 stelle (delle quali 530 in elementi pesanti).

Nella prima parte ([18]), dedicata allo studio delle sezioni d'urto, sono già stati esposti i criteri per l'accettazione degli eventi 1r (stelle ad un ramo) e per la definizione di rinculo.

([8]) H. Fishman e A. M. Perry: *Phys. Rev.*, **86**, 167 (1952).

([9]) C. F. Lees, G. C. Morrison, H. Muirhead a W. G. V. Rosser: *Phil. Mag.*, **44**, 304 (1953).

([10]) G. C. Morrison, H. Muirhead e W. G. V. Rosser: *Phil. Mag.*, **44**, 1326 (1953).

([11]) M. Grilli e B. Vitlae: *Nuovo Cimento*, **10**, 1047 (1953).

([12]) M. Grilli, P. E. Hodgson, M. Ladu e B. Vitale: *Nuovo Cimento*, **12**, 889 (1954); **1**, 314 (1955).

([13]) P. E. Hodgson: *Phil. Mag.*, **44**, 1113 (1953); **45**, 190 (1954).

([14]) W. O. Lock, P. V. March, H. Muirhead e W. G. V. Rosser: *Proc. Roy. Soc.*, A **230**, 215 (1955).

([15]) W. O. Lock, P. V. March: *Proc. Roy. Soc.*, A **230**, 222 (1955).

([16]) W. O. Lock, R. McKeague e P. V. March: *Proc. Roy. Soc.*, A **231**, 368 (1955).

([17]) H. Muirhead e W. G. V. Rosser: *Phil. Mag.*, **46**, 652 (1955).

([18]) S. Jannelli e F. Mezzanares: *Suppl. Nuovo Cimento* (Atti del Congresso di Pisa) in corso di pubblicazione.

([19]) J. Combe: *Journ. Phys. Rad.*, **16**, 455 (1955); *Suppl. Nuovo Cimento*, **2**, 182 (1956).

([20]) M. L. Goldberger: *Phys. Rev.*, **74**, 1269 (1948).

([21]) K. I. Le Couteur: *Proc. Phys. Soc.*, A **63**, 259 (1950); **65**, 712 (1952).

(*) Un'ampia trattazione dell'argomento si trova in P. Morrison: *A Survey of Nuclear Interactions*, in *Experimental Nuclear Physics*, II, pag. 141 e segg. (New York, 1953).

(+) Ringraziamo vivamente i ch.mi proff. A. Rostagni e N. Dallaporta dell'Istituto di Fisica di Padova che ci hanno cortesemente fornito le emulsioni esposte a protoni di 140 MeV del ciclotrone di Harwell ed il dr. M. Grilli per l'aiuto gentilmente prestatoci.

Successivamente, allo scopo di accrescere la statistica, in vista dello studio delle distribuzioni angolari ed energetiche dei rami, sono state cercate a caso altre 220 stelle a 3 o più rami portando così il numero degli eventi che formano oggetto del presente lavoro a 854 (dei quali 634 in elementi pesanti).

Abbiamo constatato che tale aggiunta non altera nè la distribuzione angolare nè quella energetica e che le grandezze che le caratterizzano restano immutate nei limiti degli errori sperimentali.

Per la separazione degli eventi in stelle da elementi leggeri (C, N, O), e stelle da elementi pesanti (Ag, Br) è stato seguito il criterio generalmente adottato secondo cui le stelle che presentano tracce di particelle $\alpha \leqslant 50$ μm (energia ~ 9 Me) provengono da elementi leggeri.

Combe [19] più recentemente ha proposto di considerare come stelle da elementi leggeri anche quelle che presentano tracce di protoni $\leqslant 120$ μm (energia $\leqslant 4$ MeV).

I valori considerati come minimi per l'energia delle particelle emesse rappresentano rispettivamente, per i protoni e le α, le altezze V' della barriera di potenziale dei nuclei pesanti dell'emulsione ($A \sim 100$), tenuto conto degli effetti di penetrazione ($V' = 0.7\ V_{coul}$).

Il criterio adottato da Combe, a nostro parere, non può essere totalmente accolto. In effetti esso non tiene conto dei cosidetti « protoni di diseccitazione ». Questi vengono emessi dai nuclei pesanti alla fine del processo evaporativo, allorchè la emissione di un protone compete con quella di un neutrone (nonostante la barriera di potenziale), a causa dell'alterazione del rapporto tra neutroni e protoni. Secondo Le Couteur [21], se l'energia di eccitazione del nucleo residuo, dopo l'emissione della penultima particella è compresa fra 7 e 10 MeV, l'emissione di un protone è probabile.

Per questi motivi abbiamo adottato il criterio di Combe solo per le stelle aventi un elevato numero n di rami ($n \geqslant 3$): infatti le stelle con $n \leqslant 3$ sono quasi esclusivamente prodotte in nuclei pesanti, come risulta da tutti i lavori in cui la separazione è stata eseguita.

L'adozione di tale criterio ci ha forse condotto a sottovalutare il numero dei protoni di diseccitazione, ma non altera le altre caratteristiche, a causa del piccolo numero di eventi di tal tipo (20 su 634).

2. – Definizioni.

Nel presente lavoro facciamo uso delle definizioni seguenti:

Rami grigi (G) *e neri* (N): distinti dalla conta delle lacune. Un ramo è stato considerato « grigio » se la sua ionizzazione corrisponde a quella di un protone con energia > 30 MeV. Tale energia limite fra le due classi può considerarsi la massima delle particelle evaporative.

« *Protoni* » (p) *e* « *particelle* α » (α): termini usati per brevità per distinguere, tra le tracce terminanti in emulsione, le particelle con $Z = 1$ (compresi ^2H e ^3H) da quella con $Z = 2$ (compreso ^3He). Il valore di Z (1 o 2) è stato determinato con la conta delle lacune alla fine del percorso.

ζ: angolo formato nello spazio dalla traccia con la direzione del primario, misurato nel sistema del laboratorio. Il passaggio al sistema del baricentro non è necessario perchè porta a differenze irrilevanti e comunque dell'ordine degli errori sperimentali.

F_G: rapporto tra il numero dei rami grigi emessi in avanti ($\zeta \leqslant 90°$) e il numero totale dei rami G. Analoghe definizioni per F_N, F_p ed F_χ. Per i rinculi viene usato il simbolo F_R.

Π_p: rapporto fra il numero di protoni ed il numero totale di rami. Π_α analogo rapporto per le particelle α: $\Pi_p + \Pi_\alpha = 1$.

P_{ep}, P_{ep}: frazioni di protoni aventi origine, rispettivamente dalla cascata e dall'evaporazione: $P_{cp} + P_{ep} = 1$. $P_{c\alpha}$, $P_{e\alpha}$: analoghi rapporti per le particelle α: $P_{c\alpha} + P_{e\alpha} = 1$.

Gli istogrammi ad area tratteggiata si riferiscono sempre alle stelle con rinculo visibile.

3. - Distribuzione angolare dei rami.

Le fig. 1 e 2 danno le distribuzioni angolari dei rami G (442) e N (926). Nella fig. 2 è riportata, per confronto, la distribuzione isotropa (istogramma a contorno tratteggiato).

La Tabella I dà i valori di F_G e F_N e dell'angolo medio $\overline{\varphi}$ confrontati con i dati di altri autori: l'accordo è buono, mentre i nostri errori statistici sono notevolmente minori.

Si può ritenere che i rami G, fortemente collimati in avanti, abbiano tutti origine dalla cascata nucleonica. D'altra parte i rami N, la cui distribuzione angolare differisce sensibilmente da quella isotropa, solo in parte possono attribuirsi alla evaporazione.

Dalle Fig. 1 e 2 e dalla Tabella I si constata che, per le stelle con rinculo visibile, la distribuzione an-

Fig. 1. – Distribuzione angolare dei rami grigi. ▨ la stessa nelle stelle con rinculo.

Tabella I. – *Frazione in avanti F ed angolo medio $\bar{\zeta}$ per le tracce grige e nere.*

		F_G	F_N	$\bar{\zeta}_G$	$\bar{\zeta}_N$
Grilli	con rinc.	0.81 ± 0.05	0.60 ± 0.03	—	—
	totale	0.87 ± 0.03	0.63 ± 0.02	—	—
Lees	—	—	—	43°	—
Lock	—	—	—	50°	80°
Nostri	con rinc.	0.77 ± 0.04	$0,48 \pm 0.02$	—	—
	senza rinc.	0.92 ± 0.015	0.59 ± 0.02	—	—
	totale	0.88 ± 0.015	0.63 ± 0.016	$50° \pm 1.5°$	$79° \pm 1.3°$

golare ed il rapporto F risultano modificati: alla minore collimazione in avanti dei rami corrisponde peraltro una forte collimazione dei rinculi. Precisamente, per i rinculi si ha:

$$F_R = 0.74 \pm 0.03$$

in accordo con altri dati sperimentali [12].

La correlazione fra F_G, F_N ed F_R è conforme ad ovvie considerazioni di bilancio generale dell'impulso.

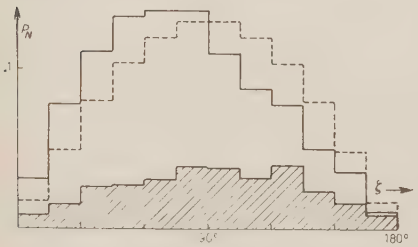

Fig. 2. – Distribuzione angolare dei rami neri. ▨ la stessa nelle stelle con rinculo visibile; ⁻⁻⁻ distribuzione angolare isotropa.

4. – Distribuzione angolare dei protoni e delle particelle α.

La distinzione fra protoni e particelle α, di cui si è detto, è resa possibile nelle nostre lastre da un conveniente sottosviluppo ed è sufficientemente sicura per tracce con percorso > 50 μm.

Al disotto di tale limite la distinzione è spesso incerta e nei casi dubbi la traccia è stata attribuita ad una particella α (cosicchè la stella è stata considerata come prodotta in nucleo leggero).

Il criterio adottato è giustificato dalla esigua percentuale di tracce di protoni con percorso $\leqslant 50$ μm.

La distinzione, necessariamente limitata dall'inclinazione della traccia, è stata eseguita entro un angolo di « dip » $\leqslant 25°$: si è preso così il 42% dell'angolo solido totale.

Nelle Fig. 3 e 4 e nella Tabella II sono riportate le distribuzioni angolari ed i valori di F_p e F_α. Per ottenere tali distribuzioni in ζ è stato necessario

TABELLA II. – *Frazione in avanti F per i protoni e le particelle α.*

		F_p	F_α
GRILLI		0.64 ± 0,10	0.68 ± 0.17
HODGSON		0.63 ± 0.03	0.66 ± 0.06
LOCK		—	0.6 ± 0,05
MORRISON		0.6 ± 0.03	—
Nostri	con rinculo	0.46 ± 0.06	0.48 ± 0.12
	senza rinculo	0.66 ± 0.03	0.66 ± 0.08
	totale	0.6 ± 0.03	0.6 ± 0.05

apportare un'opportuna correzione geometrica, per tenere conto che i protoni e le particelle α erano stati identificati solo per angolo di dip $\geq 25°$. Tale cor-

Fig. 3. – Distribuzione angolare dei protoni. ▨ la stessa nelle stelle con rinculo visibile.

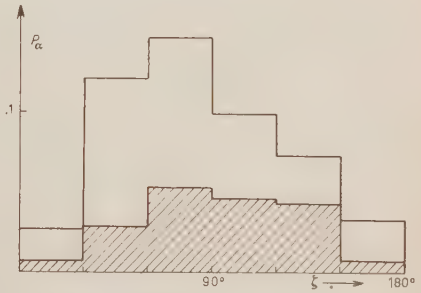

Fig. 4. – Distribuzione angolare delle particelle α. ▨ la stessa nelle stelle con rinculo visibile.

rezione ha effetto trascurabile su F_p ed F_α. La somma delle due distribuzioni corrette riproduce la distribuzione dei rami neri, come ci si deve attendere.

Partendo dai dati ora considerati, si può cercare di dedurre la percentuale di rami di origine evaporativa, sia fra i protoni che fra le particelle α.

Infatti, si può ragionevolmente ammettere che i rami G appartengano tutti alla cascata, e, d'altra parte, che i rami neri della cascata abbiano la stessa distribuzione angolare dei rami G: la frazione in avanti dei rami neri della cascata risulta uguale ad F_G, mentre quella dei rami evaporativi è 0.5 (distribuzione isotropa). Pertanto si può scrivere (cfr. Sez. **2**):

$$(1) \qquad F_p = F_G P_{cp} + 0.5\, P_{ep} = F_G + (0.5 - F_G) P_{ep} .$$

Dalla (1) si ricava P_{ep} mentre dall'analoga equazione relativa alle particelle α si ottiene $P_{e\alpha}$. Dai nostri dati si deduce

$$P_{ep} = 0.74 \pm 0.1 , \qquad P_{e\alpha} = 0.74 \pm 0.13 .$$

Conformemente a quanto trovato da altri autori ([10,13]) i protoni e le particelle α evaporativi costituirebbero dunque il 74 % di tutti i protoni (o di tutte le particelle α) con $T \leqslant 30$ MeV.

Un altro dato significativo è il valore di Π_α (cfr. Sez. 2). I valori ottenuti per esso da altri autori e da noi sono indicati nella Tabella III.

TABELLA III. – *Rapporto Π_α delle particelle α a tutte le particelle cariche emesse.*

GRILLI	avanti	0.26 ± 0.05
	indietro	0.22 ± 0.06
	totale	0.24 ± 0.04
HODGSON		0.22 ± 0.02
LOCK		0.26 ± 0.02
MORRISON		0.16 ± 0.02
Nostri	avanti	0.19 ± 0.03
	indietro	0.20 ± 0.04
	totale	0.20 ± 0.02

Da Π_α si può dedurre il rapporto tra le α e i protoni *emessi nel processo evaporativo*:

$$\frac{\Pi_\alpha P_{e\alpha}}{\Pi_p P_{ep}} = \frac{\Pi_\alpha P_{e\alpha}}{(1 - \Pi_\alpha) P_{ep}} = 0.25 \pm 0.04 . \tag{2}$$

Esso risulta in ottimo accordo con l'analogo rapporto delle probabilità di emissione deducibile dalla teoria di Le Couteur ([21]).

5. – Distribuzione energetica dei protoni e delle particelle α.

Dalla teoria di Le Couteur è possibile ricavare la probabilità $P(T)\,\mathrm{d}T$ che una particella evaporativa sia emessa con energia cinetica compresa fra T e $T+\mathrm{d}T$. Essa è esprimibile mediante la ben nota formula già data da Weisskopf:

$$P(T)\,\mathrm{d}T = (T - V')/\tau^2 \exp\left[-(T - V')/\tau\right] \mathrm{d}T . \tag{3}$$

La temperatura nucleare è deducibile, secondo LE COUTEUR dalla

$$\tau = \sqrt{\frac{12.4\ W}{A}}\ \text{MeV}$$

e l'energia di eccitazione W del nucleo che evapora si può ricavare da ovvie considerazioni di bilancio energetico:

$$W' = W + \sum_1^n T_i + \varkappa(n-1)\ \text{MeV} \tag{4}$$

Nella (4) si è indicato con:

W' l'energia cinetica della particella incidente;

T_i l'energia cinetica della i-esima particella della cascata;

$\varkappa$ l'energia cinetica delle particelle emesse nella cascata, considerata $n-1$ volte poichè il nucleone incidente non è legato ($\varkappa = 8$ MeV).

Prendendo con MORRISON [10] $W = 44$ MeV e mediando A sugli elementi pesanti (Ag e Br) dell'emulsione, si ha:

$$\tau = 2.4 \pm 0.15\ \text{MeV}\,.$$

Dalla (3) si ricavano facilmente l'energia media

$$T = 2\tau + V' \tag{5}$$

e l'energia del massimo della distribuzione

$$T_{max} = \tau - V'\,. \tag{6}$$

Noti i valori

$$V'_p = 4.2\ \text{MeV} \qquad \text{e} \qquad V'_\alpha = 9.6\ \text{MeV}\,,$$

la funzione (3) risulta completamente definita sia per i protoni che per le α. Essa è rappresentata in ciascuna delle Fig. 5 e 6, per i due valori 0.74 (curva a) ed 1 (curva b) della costante di normalizzazione (area racchiusa). Nelle stesse figure, gli istogrammi a contorno intero rappresentano i rispettivi integrali della (3), presi tra opportuni limiti di energia. Sono questi istogrammi che vanno confrontati con quelli desunti dall'esperienza.

Questi ultimi sono stati ottenuti partendo dalla misura del percorso delle tracce già identificate come protoni o α. La distribuzione in percorso desunta

direttamente dall'esperienza è alterata dalla circostanza che tracce aventi differenti percorsi residui hanno diverse probabilità di finire in emulsione ed è perciò necessario apportare una correzione geometrica, la quale, com'è ovvio, cresce d'importanza al crescere dell'energia delle particelle. La correzione è stata calcolata per una distribuzione isotropa, ma si dimostra facilmente che essa risulta valida anche in casi più generali, nei quali rientrano molto bene le nostre distribuzioni angolari sperimentali. Nel corso del calcolo si è tenuto conto che le stelle il cui centro era compreso entro 60 μm dalle superficie estreme dell'emulsione erano state escluse dalla statistica ([18]). Quest'ultima circostanza ha reso praticamente superflua la correzione per le particelle α.

Fig. 5. – Distribuzione energetica dei protoni □ teorica sperimentale ▨ in stelle con rinculo visibile (sper.). *a*) distribuzione teorica normalizzata ad 1; *b*) la stessa normalizzata a 0.74.

Le distribuzioni in percorso così corrette sono state trasformate in distribuzioni energetiche tramite le ben note relazioni percorso-energia. Esse sono riportate (istogrammi a contorno tratteggiato) nelle Fig. 5 e 6. L'area compresa è normalizzata a 1. L'accordo nella zona del massimo, e fino a ~ 12 MeV è soddisfacente, soprattutto per le curve *a*; ciò rappresenta una conferma della stima ([1]) di P_{ep} e $P_{e\alpha}$. Ad energia > 12 MeV le differenze tra i valori sperimentali e le curve di evaporazione divengono apprezzabili, e vanno attribuite al contributo delle particelle della cascata.

Anche alle basse energie si manifesta una divergenza tra i dati sperimentali e la formula di Weisskopf ([3]). Nello spettro sperimentale infatti sono presenti i « protoni di diseccitazione » emessi dopo la fine della fase evaporativa e perciò non previsti dalla formula di Weisskopf (cfr. Sez. 1). Il confronto quantitativo con la teoria di Le Couteur non è soddisfacente: infatti Le Couteur ([21]) prevede che il numero medio per stella, D, dei protoni di diseccitazione (protoni emessi nell'intervallo $0.5 \div 3$ MeV) sia $D \sim 0.2$. Nel nostro campione statistico

di 634 stelle dovrebbero dunque esservi 127 protoni di diseccitazione, contro i 21 che risultano dalle nostre osservazioni. La differenza è molto maggiore di quella che potrebbe essere attribuita ad un erroneo criterio di identificazione delle stelle da elementi pesanti (Sez. **1**).

D'altra parte occorre notare che i calcoli di Le Couteur riguardano stelle di 12 rami e quindi energie di eccitazione molto maggiori della nostra. Resta comunque il fatto che anche i confronti eseguiti da altri autori ([22]) e da Le Couteur ([21]) su questo punto non sono molto significativi. Pertanto il problema dei protoni di diseccitazione richiede ulteriori chiarimenti.

La posizione del massimo dello spettro energetico è in buon accordo con quella prevista dalla (6), pur presentando com'è ovvio, limiti di incertezza piuttosto ampi (cfr. Tabella V, ultime 2 colonne).

Fig. 6. - Distribuzione energetica delle particelle α □ teorica sperimentale ▨ in stelle con rinculo visibile (sper.). *a*) distribuzione teorica normalizzata ad 1; *b*) la stessa normalizzata a 0.74.

I valori medi T_p (ev.) e T_α (ev.) dell'energia delle particelle (p e α) *evaporative* vanno confrontati con quelli deducibili dalla (5).

Essi differiscono dai valori medi $\overline{T}_p(30)$ e $\overline{T}_\alpha(30)$ ottenuti considerando nella loro interezza gli spettri sperimentali fino a 30 MeV, in quanto a questi ultimi contribuiscono anche particelle della cascata. D'altra parte l'eliminazione del contributo della cascata può farsi solo per confronto fra gli istogrammi teorici e sperimentali delle Fig. 5 e 6. Ciò equivale a identificare l'andamento sperimentale con la curva teorica di evaporazione nell'intervallo tra 12 e 30 MeV e rende il confronto tra i valori medi teorici e sperimentali solo parzialmente significativo. Tuttavia tale procedimento trova una buona giustificazione nel fatto già rilevato che le considerazioni relative alla distribuzione angolare

([22]) J. Harding, S. Lattimore e D. Perkins: *Proc. Roy. Soc.*, A **196**, 325 (1949).

conducono ai valori (2) di P_{sp} e $P_{s\alpha}$, i quali meglio si prestano a far concordare le distribuzioni energetiche nella zona del massimo, e fino a 12 MeV.

La Tabella IV fornisce i valori di $T_p(30)$ e $T_\alpha(30)$ per varie classi di stelle e di particelle, confrontate con valori analoghi $T_p(20)$ e $T_\alpha(10)$ ottenuti da altri autori ([12]). L'accordo è soddisfacente.

TABELLA IV. – *Energia media* $\bar{T}(30)$ *dei protoni e delle particelle* α.

		Avanti	Indietro	Totale
GRILLI	protoni	9.4	9	9.2
	particelle α . . .	17	15.9	16.6
Nostri	protoni	11.7 ± 0.5	11.6 ± 0.7	11.6 ± 0.4
	protoni con rinc.	11 ± 1	9.7 ± 0.9	11.3 ± 0.7
	particelle α . . .	16 ± 0.8	14.3 ± 0.5	15.3 ± 0.5
	part. α con rinc.	15.2 ± 1.6	15.2 ± 0.8	15.2 ± 0.8

La Tabella V fornisce il confronto dei valori globali di $T_p(30)$ e $T_\alpha(30)$ con quelli di T_p(ev.) e T_α(ev.) ricavati come sopra indicato e con quelli dedotti dalla (5).

TABELLA V. – *Energia media* $\bar{T}$ (ev) *e moda* T_{max} *dei protoni e delle particelle* α *confrontate con i valori teoricamente previsti.*

	$\bar{T}$			Moda	
	Sperimentale	Sperimentale corretto	Teorico	Sperimentale	Teorico
Protoni	11.6 ± 0.4	8.7 ± 0.2	9 ± 0.3	$6 \div 8$	6.4 ± 0.4
Alfa	15.3 ± 0.5	14.2 ± 0.5	14.4 ± 0.3	$12 \div 14$	12 ± 0.8

6. – Protoni e particelle α della cascata.

Per quanto riguarda le particelle della cascata, la situazione è ancora scarsamente chiarita sia sul terreno sperimentale che su quello delle previsioni teoriche (metodo di Montecarlo). COMBE ([19]) prevede che al crescere dell'energia il numero dei protoni della cascata vada crescendo fino a raggiungere un massimo, mentre MORRISON e coll. ([10]) prevedono che nell'intervallo $6 \div 30$ MeV il numero dei protoni della cascata vada decrescendo al crescere dell'energia. I dati sperimentali sinora pubblicati sono poco numerosi e spesso

discordi. Se si accetta la separazione delle particelle evaporative sopra indicata (Sez. **5**), i nostri dati sembrano indicare che le particelle della cascata fino a 30 MeV vadano crescendo in numero al crescere dell'energia. Ciò confermerebbe le conclusioni di COMBE. Tuttavia tale risultato va preso con cautela, data la ristrettissima statistica su cui si basa. A tal proposito si tenga presente che alle energie più elevate la correzione geometrica diviene molto grande raggiungendo, per 30 MeV, il valore di 4.1.

I valori medi dell'energia delle particelle della cascata, sino a 30 MeV risultano di 22.2 MeV e di 18.6 MeV, rispettivamente per i protoni e per le particelle α.

7. – Conclusioni.

I dati sperimentali esposti confermano i risultati già noti relativi al processo di formazione delle « stelle », e pertanto risultano in accordo con il modello che descrive tale fenomeno come la successione di una cascata nucleonica e di un processo evaporativo.

La statistica notevolmente elevata permette di fornire valori più significativi per alcuni parametri caratteristici che intervengono in tale modello. La Tabella VI raccoglie i più importanti di tali parametri, quali si desumono dal presente lavoro e risultano dalla media ponderale dei dati nostri e di altri autori.

TABELLA VI. – *Parametri caratteristici delle stelle prodotte in nuclei pesanti da protoni di* 140 MeV.

	Presente lavoro	Media ponderale
F_G	0.88 ± 0.015	0.88 ± 0.01
F_N	0.63 ± 0.016	0.62 ± 0.01
F_p	0.6 ± 0.03	0.61 ± 0.02
F_α	0.6 ± 0.05	0.62 ± 0.03
Π_α	0.20 ± 0.02	0.21 ± 0.01
P_{ep}	0.74 ± 0.1	0.71 ± 0.05
$P_{e\alpha}$	0.74 ± 0.13	0.68 ± 0.07
D	0.033 ± 0.007	–

L'ultima riga indica il numero medio per stelle D dei protoni di diseccitazione. Come già rilevato, il valore di D è troppo basso, rispetto alle previsioni teoriche. Il chiarimento di questa discordanza richiede ulteriori indagini teoriche e sperimentali.

* * *

Ringraziamo vivamente il ch.mo prof. V. POLARA per il suo interessamento ed incoraggiamento, il prof. G. CORTINI per l'aiuto prestatoci e le utili discussioni.

SUMMARY

The nuclear disintegrations produced in the heavy elements of Ilford G5 600 μm emulsions by 140 MeV protons have been studied. 634 stars were examined. The results of their analysis are in agreement with the conclusions reached by other workers about the possibility of describing the production of stars according to the well known model of nuclear cascade followed by a nuclear evaporation. The existence of low energy protons emitted sometimes from the nuclei in the de-excitation process, following the evaporation, is confirmed. From the experimental data obtained by us and by other authors are deduced the best values of some parameters which are relevant in the process of production of stars.

IL NUOVO CIMENTO Vol. V. N. 2 1° Febbraio 1957

Nucleon-Nucleus Interaction From the Statistical Model.

W. E. Frahn

Nuclear Physics Division on the National Physical Research Laboratory, C.S.I.R., Pretoria

(ricevuto l'8 Novembre 1956)

Summary. — The statistical nuclear model with exchange forces leads to a non-local interaction between a nucleon and its neighbours in nuclear matter (« Van Vleck-potential »). The implications of this interaction with regard to the modification of nuclear motion and to the energy dependence of the real parts of the optical model parameters are examined. Finally, a derivation of Van Vleck's potential is given from Brueckner's coherent model.

1. – Introduction.

In a previous paper [1] it has been shown, that generally a velocity dependence of the nucleon-nucleus interaction can account for: (i) the modified propagation character of nucleons in nuclear matter and (ii) the energy dependence of the real part of both the optical potential and the nuclear refractive index. The special form of this interaction, which is of a non-local type in co-ordinate space, has been chosen with a simple Gaussian kernel function, in order to give a qualitative description of the observed energy dependence of the real optical model parameters. A physical significance can be ascribed only to the general behaviour and not to the detailed form of the kernel assumed. Furthermore, no derivation has been given in terms of a nuclear model or from special assumptions on the nature of the elementary nucleon-nucleon interaction.

[1] W. E. Frahn: *Nuovo Cimento*, **4**, 313 (1956), referred to as I.

Apart from the fact, that energy dependent effective potentials follow from the coherent nuclear model of BRUECKNER *et al.* ([2-6]) it has been well known for a long time ([7-9]) that the forces exerted on a nucleon by its neighbours in nuclear matter cannot be described by an ordinary static potential. The interaction derived from the statistical nuclear model with exchange forces between the nucleons, turns out to be of a non-local type known as the « Van Vleck-potential » ([10]). In the present paper we reconsider this type of interaction and analyse its implications with regard to the effects discussed qualitatively in I. Finally, this potential will be derived from Brueckner's coherent model

2. – Van Vleck's Potential.

The motion of a nucleon interacting with a heavy nucleus, the constituents of which are treated statistically (disregarding Coulomb effects), is described ([7]) by the Schrödinger equation

$$\frac{\hbar^2}{2M}\Delta\psi(\boldsymbol{r}) + E\psi(\boldsymbol{r}) = \begin{cases} \int K(\boldsymbol{r}-\boldsymbol{r}')\,\psi(\boldsymbol{r}')\,\mathrm{d}\boldsymbol{r}' & (r<R) \\ 0 & (r>R) \end{cases} \tag{1}$$

($R =$ nuclear radius), with

$$K(\boldsymbol{r}-\boldsymbol{r}') = \frac{k_F^3}{3\pi^2}\,J(|\boldsymbol{r}-\boldsymbol{r}'|)\,D(k_F|\boldsymbol{r}-\boldsymbol{r}'|)\,. \tag{2}$$

$J(r)$ denotes the spatial part of the nucleon-nucleon interaction and $(k^3/3\pi^2)D(k_F|\boldsymbol{r}-\boldsymbol{r}'|)$ with $D(x) \equiv (3/x^3)(\sin x - x\cos x)$ is the mixed density function in the statistical approximation, corresponding to a cut-off in momentum space at the Fermi momentum, $\hbar k_F$.

The Schrödinger equation (1) is equivalent to a dispersion relation in nuclear

([2]) K. A. BRUECKNER, C. A. LEVINSON and H. M. MAHMOUD: *Phys. Rev.*, **95**, 217 (1954).
([3]) K. A. BRUECKNER: *Phys. Rev.*, **96**, 508 (1954).
([4]) K. A. BRUECKNER: *Phys. Rev.*, **97**, 1353 (1955).
([5]) K. A. BRUECKNER, R. J. EDEN and N. C. FRANCIS: *Phys. Rev.*, **100**, 891 (1955).
([6]) K. A. BRUECKNER: *Phys. Rev.*, **103**, 172 (1956).
([7]) J. H. VAN VLECK: *Phys. Rev.*, **48**, 367 (1935).
([8]) C. FAY: *Phys. Rev.*, **50**, 560 (1936).
([9]) J. BARDEEN: *Phys. Rev.*, **51**, 799 (1937).
([10]) H. A. BETHE and R. F. BACHER: *Rev. Mod. Phys.*, **8**, 82 (1936).

matter of the form

$$E = \frac{\hbar^2 k^2}{2M} + V(k)\,, \tag{3}$$

where $V(k)$ is the Fourier-transform of the interaction kernel $K(\boldsymbol{r} - \boldsymbol{r}')$.

The special assumption of a Gauss function for the nucleon-nucleon potential

$$J(r) = -V_0 \exp\left[-\frac{r^2}{a}\right] \tag{4}$$

yields the well-known expression

$$V(k) = -V_0 \left| \Phi(x+y) + \Phi(x-y) + \right.$$
$$\left. + \frac{1}{\sqrt{\pi}\, y} \left(\exp\left[-(x+y)^2\right] - \exp\left[-(x-y)^2\right]\right) \right|, \tag{5}$$

with $x = \frac{1}{2} k_F a$, $y = \frac{1}{2} k a$. Φ denotes the error function.

Fig. 1 shows $V(k)/V_0$ as a function of y for the value $x = 1.18$, corresponding to the range parameter $a = 2.17 \cdot 10^{13}$ cm.

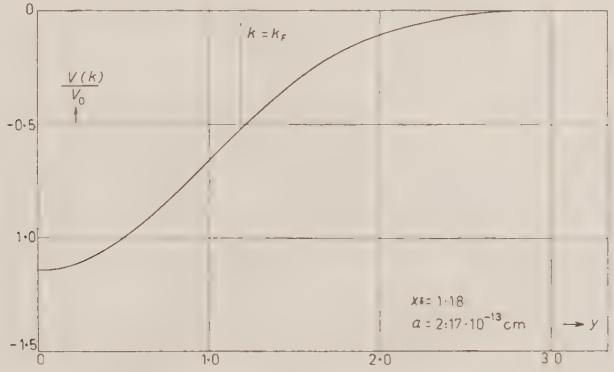

Fig. 1. – $V(k)/V_0$ as a function of y.

It is seen that $V(k)$ shows the behaviour qualitatively described by the phenomenological interaction assumed in I, i.e. the decrease of the effective well depth with nucleon velocity. The asymptotic expression of $V(k)$ for $y \gg 1$ is given by

$$V(k) \approx -\frac{V_0 x}{\sqrt{\pi}} \frac{\exp[-y^2]}{y^2} = -\frac{2}{\sqrt{\pi}} V_0 \frac{k_F}{a k^2} \exp\left[-\frac{a^2}{4} k^2\right]. \tag{6}$$

3. – Effective Mass of the Nucleon.

The development of $V(k)$ for small values of y gives

$$V(k) \approx -\alpha + \beta \frac{k^2}{k_F^2} \tag{7}$$

with

$$\alpha = 2V_0 \left[\Phi(x) - \frac{2x}{\sqrt{\pi}} \exp[-x^2] \right], \tag{8}$$

$$\beta = \frac{8}{3\sqrt{\pi}} V_0 x^5 \exp[-x^2]. \tag{9}$$

In this approximation the influence of the effective potential can be described by a modification of the nucleon mass given by

$$\frac{M}{M^*} = 1 + \frac{\beta}{E_F}, \tag{10}$$

with $E_F = \hbar^2 k_F^2 / 2M$. The effective mass M^* is a function of x and thus of the range parameter a. The functions $\alpha(x)/V_0$ and $\beta(x)/V_0$ are shown in Figs. 2 and 3, respectively.

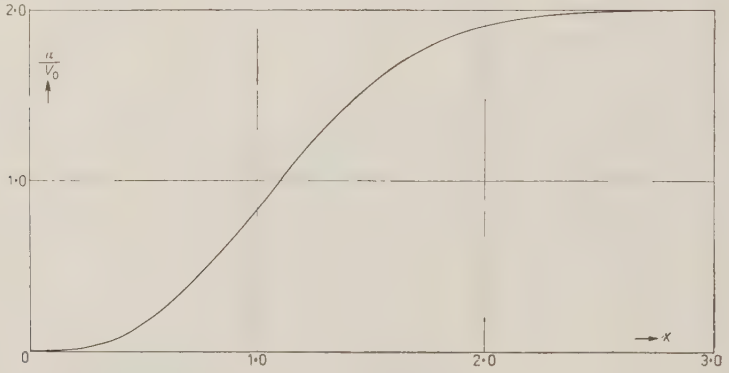

Fig. 2. – α/V_0 as a function of x.

With the values

$$\begin{cases} V_0 = 31 \text{ MeV} \\ a = 2.17 \cdot 10^{-13} \text{ cm} \end{cases} \tag{11}$$

obtained by FEENBERG (11) from the binding energies of light nuclei we get

$$\beta = 26.7 \text{ MeV} \quad \text{and} \quad \frac{M^*}{M} = 0.48 . \tag{12}$$

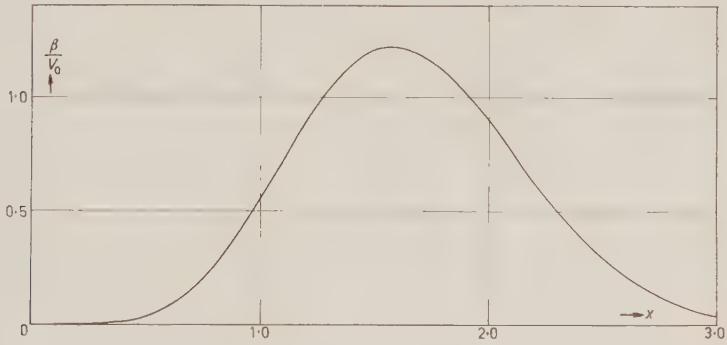

Fig. 3. – β/V_0 as a function of x.

Thus the nucleon mass reduction following from the statistical model is consistent with the value $M^*/M \approx 0.5 \div 0.6$ resulting from other arguments (1,12) and in accordance with experiment (13).

4. – Real Parts of the Optical Parameters.

The energy dependence of the real part of the optical potential is obtained from the dispersion relation (3) by evaluating k as a function of E and inserting into $V(k)$. With Feenberg's value $V_0 = 31$ MeV the resulting function $V(E)$ starts at $V(0) \approx 19$ MeV and decreases rapidly with increasing energy.

A comparison (Fig. 4) with the values of the effective potential obtained from the optical model analysis (14,15) ($V(0) = 42$ MeV (11) and the dotted line in Fig. 4 (15,16)) shows that the potential values derived from the statis-

(11) E. FEENBERG and J. K. KNIPP: *Phys. Rev.*, **48**, 906 (1935).
(12) M. E. JOHNSON and E. TELLER: *Phys. Rev.*, **98**, 783 (1955).
(13) M. A. MELKANOFF, S. A. MOSZKOWSKI, J. NODVIK and D. S. SAXON: *Phys. Rev.*, **101**, 507 (1956).
(14) H. FESHBACH, C. E. PORTER and V. F. WEISSKOPF: *Phys. Rev.*, **96**, 448 (1954).
(15) T. B. TAYLOR: *Phys. Rev.*, **92**, 831 (1953).
(16) A. KIND and L. JESS: *Nuovo Cimento*, **4**, 595 (1956).

tical theory are much too small. In an attempt to fit the statistical expression to the empirical values, we can adjust the nucleon-nucleon parameters, V_0

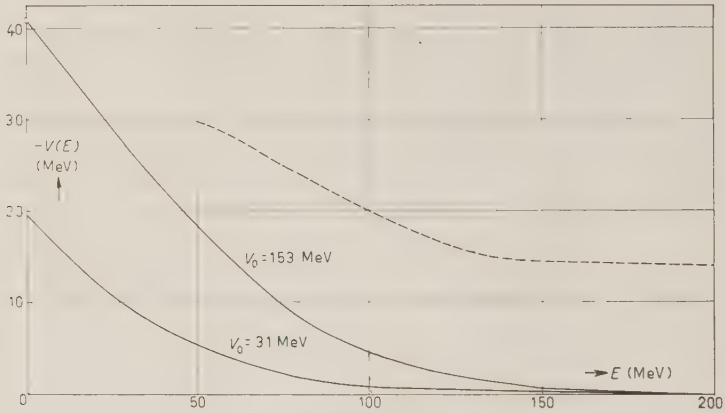

Fig. 4. – Effective nuclear potential as a function of energy.

and a. Adjusting V_0 so as to give the correct value of $V(0)$ and using the same range parameters as before, we obtain $V_0 = 153$ MeV. Then, however, the slope of $V(E)$ for small energies becomes too large. When we try to correct this by taking a smaller value of the range parameter, α will be reduced (cf. Fig. 2), and again a too small value of $V(0)$ is obtained. Thus it is not possible to reproduce the optical model data.

The real part of the nuclear refractive index, $n = k_i/k_e$, obtained from

$$k_i^2 + \frac{2M}{\hbar^2} V(k_i) = k_e^2 \tag{13}$$

or

$$n^2 = 1 - \frac{V(E)}{E} \tag{14}$$

shows a similar disagreement with the values required by experiment.

5. – Derivation from the Coherent Model.

We will now show, that the Van Vleck potential can be derived from the coherent nuclear model of BRUECKNER *et al.* [2-6]. In Brueckner's treatment,

the effective potential acting on a nucleon with wave number k, is given by [2]

$$V(k) = -\frac{\hbar^2}{4\pi M k}\int_{(k-k_F)/2}^{(k+k_F)/2} f(k')[k_F^2 - (k-2k')^2]k'\,\mathrm{d}k' , \tag{15}$$

$f(k')$ being the statistically weighted sum of the nucleon-nucleon scattering amplitudes in forward direction.

On the assumption of a non-local nucleon-nucleon interaction with the kernel

$$G(\boldsymbol{r}-\boldsymbol{r}') = \frac{1}{(4\pi)^{\frac{3}{2}}a^3}\exp\left[-\left(\frac{\boldsymbol{r}-\boldsymbol{r}'}{a}\right)^2\right] \tag{16}$$

acting within a potential well of depth V_0 and radius d, we obtain in Born-approximation

$$f(k) = 2MV_0d^3\exp\left[-\tfrac{1}{4}a^2k^2\right] . \tag{17}$$

This expression follows from the general relation

$$f_{NL}(\theta) = g(k)f_L(\theta) \tag{18}$$

between the scattering amplitudes for the non-local potential $K(\boldsymbol{r},\boldsymbol{r}') = V(r)G(|\boldsymbol{r}-\boldsymbol{r}'|)$ and the local potential $V(r)$, respectively; $g(k)$ being the Fourier-transform of $G(|\boldsymbol{r}-\boldsymbol{r}'|)$.

Inserting (17) into (15) yields

$$V(k) = -\frac{1}{2\sqrt{\pi}}\left(\frac{d}{a}\right)^3 V_0\left[\Phi(x+y)+\Phi(x-y)+\right. \tag{19}$$
$$\left.+\frac{1}{\sqrt{\pi}y}\left(\exp\left[-(x+y)^2\right]-\exp\left[-(x-y)^2\right]\right)\right] .$$

Thus the Van Vleck potential follows from the coherent model under the assumption of non-local nucleon-nucleon forces, treated in Born-approximation. This somewhat surprising result is due to the fact that a non-local nucleon-nucleon interaction introduces the mixed densities into the energy expressions of the statistical theory in place of the normal densities [17].

A similar result can be obtained for the binding energies. A more detailed

[17] J. A. Wheeler: *Phys. Rev.*, **50**, 643 (1936).

treatment of these relationships, especially in connection with the saturation problem, will be given in a subsequent paper.

6. – Discussion.

The reinvestigation of the nucleon-nucleus potential following from the statistical nuclear model, shows some of the features of this model which are familiar from binding energy calculations. The general qualitative behaviour of some collective nuclear properties, viz. the decrease, with increasing momentum, of the effective potential acting on a nucleon and the low energy structure of the dispersion relation in nuclear matter, are fairly well represented by the statistical theory. Quantitatively, however, the predictions of the model are insufficient. Although the modified propagation properties of nucleons described by a reduced nucleon mass, are correctly represented, the real parts of the optical parameters, calculated with the same values of depth and range of the elementary nucleon-nucleon interaction, turn out too small. Especially in the intermediate and high energy regions the decrease of the potential with increasing nucleon energy is much too rapid. Furthermore, the predictions of the model become worse the smaller the range of the nucleon-nucleon forces: a smaller value of the range parameter will give insufficient mass reduction and still further reduce the effective potential values. When we try to adapt the statistical formulae to the empirical data, we obtain values for the depth and range of the nucleon-nucleon potential inconsistent with the properties of the two-nucleon system. These results reflect the fact, well known from the saturation problem ([10]), that the statistical model sets an upper limit to the elementary nucleon-nucleon interaction.

A more detailed analysis of the statistical model should take into account the correlation between the motions of the nucleons, which also gives rise to energy dependent interaction potentials decreasing with increasing nucleon velocity ([18]).

It is to be expected that the predictions of the statistical theory can be considerably improved by imposing a self-consistency requirement in the sense of BRUECKNER ([4,19]).

* * *

The author is indebted to Dr. S. J. DU TOIT, head of the nuclear physics division, for his interest in this work; to Dr. I. J. VAN HEERDEN for useful

([18]) W. J. SWIATECKI: *Phys. Rev.*, **101**, 1321 (1956).
([19]) K. A. BRUECKNER and C. A. LEVINSON: *Phys. Rev.*, **97**, 1344 (1955).

discussions, and to the South African Council for Scientific and Industrial Research for permission of publication.

RIASSUNTO (*)

Il modello nucleare statistico con forze di scambio conduce a un'interazione non locale tra un nucleone e i suoi contigui nella materia nucleare (« potenziale di Van Vleck »). Si esaminano le conseguenze di questa interazione con riguardo alla modificazione del moto del nucleo e alla dipendenza dell'energia delle parti reali dei parametri del modello ottico. Finalmente si dà una derivazione del potenziale di Van Vleck a partire dal modello coerente di Brueckner.

(*) *Traduzione a cura della Redazione.*

Interactions of K^+-Mesons with Emulsion Nuclei Between 40 and 160 MeV (*).

M. Baldo Ceolin, M. Cresti, N. Dallaporta, M. Grilli, L. Guerriero, M. Merlin, G. A. Salandin and G. Zago

Istituto di Fisica dell'Università - Padova
Istituto Nazionale di Fisica Nucleare - Sezione di Padova

(ricevuto il 13 Novembre 1956)

Summary. — 110 meters of K^+ tracks have been followed in the energy interval from 40 to 160 MeV. The events observed have been classified *a*) 5 K-H collisions; *b*) 170 elastic and 91 inelastic scatterings; *c*) 10 charge exchanges; *d*) 56 decays in flight. The discrimination between elastic and inelastic scatterings has been made with a statistical method discussed in Sect. **3**. We have divided also the events in two energy intervals ($40 \div 90$ MeV) and ($90 \div 160$ MeV) in order to study the variation of the cross-section for elastic and inelastic events with the energy (see Table III). From the analysis of the elastic events we have found the existence of a repulsive nuclear potential of about 15 MeV. This result is in agreement with other features relative to inelastic events. From the analysis of the inelastic events we have tried to obtain some information about the elementary K-nucleon cross-section and at present our data seem to indicate that in the energy interval studied, the isotopic state $T = 1$ is predominant, probably as an S wave. In the higher energy interval there is probably a little contribution of a $T = 0$ state as a P wave.

Introduction.

The increasing importance that the study of the properties of heavy mesons is acquiring in physics, makes it desirable to try to gather any kind of new information about the nature of these particles. In this sense it can reasonably

(*) Presented at the Turin Conference, September 1956.

be hoped that the study of the interaction of K -particles with nuclei may provide us with results capable of shedding some light on the K^+-nucleon forces. Of course, to achieve this aim the direct study of K^+-proton interactions would probably be preferable. However before the results with techniques appropriate to such kinds of measurements will be available, we may hope to obtain interesting data from the interactions of K^+ with the nuclei of emulsions, as it appears that in this case, the conditions are such that the optical model for nuclei may be applied with some confidence, and we can deduce from it information on the elementary K^+-nucleon cross sections. Moreover, even when direct K^+-proton data will be available by scattering experiments in pure hydrogen, the emulsion data will still provide an important source of information for K^+-neutron interactions.

Already different investigations ([1,2]) have been made on nuclear interactions produced by K^+-mesons in emulsions: the aim of the present work is to extend the results so far obtained on this subject in this laboratory.

We have used two stacks of nuclear emulsions (Ilford G5) exposed to the K^+ beam of the Bevatron at Berkeley and divided between several European laboratories. In Part I we will give the experimental information concerning the exposures, the selection, the analysis of events, and finally the results obtained; in Part II we will give their interpretation according to the optical model of the nucleus, and we will discuss what conclusions can be drawn from these data concerning the elementary K^+ nucleon cross sections.

Part. I. – Experimental data

1. – Scanning Procedure.

The two stacks referred to in the following as the K_I and K_{II} stack respectively, have been exposed to K -meson beams ([3]) of different energies:

([1]) J. Lanutti, W. Chupp, G. Goldhaber, S. Goldhaber, E. Helmy, E. Iloff, A. Pevsner and D. Ritson: *Phys. Rev.*, **101**, 1617 (1956).

([2]) Communications of S. Goldhaber and N. Dallaporta (results for several European laboratories), Part VI *Proceedings of the Sixth Rochester Conference*, 1956. Communications of the plate groups of Bologna, Bristol, Dublin, Göttingen and Padua laboratories, Turin Conference, September 1956.

([3]) L. T. Kerth, D. H. Stork, R. W. Birge, R. P. Haddock and M. N. Whitehead: *Bull. Am. Phys., Soc.* **30**, No. 3 (1955).

their characteristics are as follows:

	K_I	K_{II}
Energy of the primary beam of protons	6.2 GeV	6.2 GeV
Nature of target	Copper	Copper
Time of flight between the target and the stacks	$\sim 1.3 \cdot 10^{-8}$ s	$\sim 1.3 \cdot 10^{-8}$ s
Momentum of the particles focussed in the stack	340 ÷ 370 MeV/c	280 ÷ 460 MeV/c
Dimensions	$(27 \times 39 \times 7.2)$ cm^3	$(20 \times 25 \times 18)$ cm^3
No. of plates at Padua (600 μm thick)	40	100
Energy interval analyzed	40 ÷ 80 MeV	40 ÷ 160 MeV

The beam of particles focussed in the stacks was composed of protons which stopped after few centimeters of emulsion, π-mesons which crossed the whole plates as slightly ionizing particles, and K-mesons which appeared, soon after the proton endings, as grey tracks. The scanning of events to be studied was made by picking up soon after the proton endings, those tracks which lay in a given ionization range and in given geometrical conditions defined by

	K_I	K_{II}
Angle between the track and the mean direction of beam	$\leqslant 10°$	$\leqslant 5°$
Path per plate	$\geqslant 3$ mm	$\geqslant 4$ mm

and following them until they ended in the stack or went out of it.

For these tracks followed to their ends, the presence of a decay secondary allowed us to identify the particle as a K.

When a secondary was not visible an identification was generally possible by means of range-ionization measurements. It was thus possible to determine the percentage of spurious tracks (almost all protons) amongst those selected

at the barrier, and also to verify the loss of decay secondaries due to the low minimum of ionization in the plates, which was about 7 grains/50 μm. This average loss for the two stacks was 15%.

A knowledge of the percentage of spurious tracks permits us to define statistically the length of K tracks which have not been followed up to their end either because they left the stack, or because of difficulties during the following through.

Moreover, in order to increase the statistics in the high energy range, the following in the K_{II} stack was interrupted at a distance of about 5 cm from the point at which the tracks were picked up. In this case, the determination of the percentage of spurious tracks was made with the following method in addition to those already described:

During the track scanning, a certain number of interactions which were recognized to be due to protons or to π-mesons have been found; referring to the mean free paths of these two types of particles, we have calculated the length which corresponded to the number of interactions found and therefore the length of observed track which was not due to K-mesons and which was then to be subtracted from the total length of track followed.

The total length of K-meson tracks observed in both stacks thus turns out to be

53 ± 2.5 m in the energy interval from 40 to 90 MeV
57 ± 2.5 m in the energy interval from 90 to 160 MeV

110 ± 4 m Total.

2. – Selection of the Events.

Events were recorded during the track scanning:

a) if the track showed a sharp scattering of at least 12° in the plane of emulsion;

b) if in following the track a « star » with one or more prongs was found;

c) if the track clearly disappeared in the emulsion;

d) if a sudden decrease of ionization was observed.

The events so selected were then analyzed as follows:

All the tracks emerging from each interaction have been followed to their ends when they came to rest in the stacks, and carefully observed in order to see whether there was a decay secondary. If one was not visible, the mass

of the primary particle was determined by measurements of $\bar{\alpha}$ and g/g_0 or $\Delta g/\Delta R$ (see Appendix I). If it was a K, the masses of the particles emerging from the interaction were determined in order to see whether there was a K among them. In the majority of cases a decision was possible about the nature of these particles. For some cases although the prongs ended in the emulsion, a direct identification was not possible owing to their unfavorable geometrical features. In these cases however an identification was possible by applying a statistical criterion which will be described in the following (see Sect. 3). This was not possible for 12 cases in which the tracks emerging from the interactions left the stack and this together with their unfavorable geometrical conditions did not allow measurements of any kind.

Apart from these 12 cases, to which we shall refer as « not analyzable events », our events have been provisionally classified as follows:

K-H Interaction of a K with an Hydrogen nucleus.

K_0 Scattering of a K with no additional prong longer than 5 μm.

K_n Interaction from which emerge a K and n prongs longer than 5 μm.

A.C.E. [Apparent Charge Exchange] Interaction of an identified K, from which no identificable K emerges.

Stop Sudden disappearance of an identified K.

D.F. Decay in flight of a K.

The events divided according to this first rough classification are listed in Table I below, and will be analyzed in greater detail later. In the table the events are also divided in two energy intervals from 40 to 90 MeV, and from 90 to 160 MeV.

TABLE I.

	K-H	K_0	K_n	A.C.E.	Stops	D.F.	Not analysable Events
40÷ 90 MeV	2	140	12	4	7	—	12
90÷160 MeV	3	73	36	4	6	—	—
Total	5	213	48	8	13	46	12

3. – Analysis of the Events.

K-H. – Amongst all interactions of type K_1 (one visible prong in addition to the outgoing K), six events have been observed which were coplanar; be-

cause of the good energy and momentum balance they have been interpreted as collisions with a free proton. One of these six events occurred at an energy of 14.5 MeV and has not been included in the general statistics. The characteristics of the events are:

E_1 (MeV)	14.5	67	85	91	126	136
θ lab.	72°	39°	67°	86°	86°	33°
θ c.m.	102°	58°	96°	118°	118°	49°.

The interaction path in nuclear emulsion for K-P encounters is thus (22 ± 10) m ($\sigma = (14 \pm 6)$ mb) in the energy region from 40 to 160 MeV for interactions with an angle of scattering $\geqslant 15°$ in the laboratory system. This angular limit was imposed in order that the energy transferred to the proton even for the lowest energy (40 MeV) of the interacting K might permit a clear test of coplanarity and the balance of the transverse momenta.

K_0 *and* K_n. – For events of type K_0, a correction factor has been applied which takes into account the geometrical loss due to the fact that these events were recorded only when the projected angle in the plane of the emulsion was $\geqslant 12°$. This factor, for the various angular intervals is:

12°-14°	14°-16°	16°-18°	18°-20°	20°-30°	30°-40°	40°-50°	50°-60°	60°-70°	70°-80
4.0	2.5	2.0	1.7	1.37	1.20	1.12	1.08	1.05	1.03

For each event of type K_0 and K_n the angle of scattering was measured. We have also determined the energies E_1 and E_2 of the K before and after the interaction; the methods used will be described and examined in Appendix I.

All K_0 and K_n events have been analyzed in order to separate elastic events from inelastic ones, taking as an elastic event one in which the K does not loose any energy in the center of mass system.

Events of type K_n have all been considered as inelastic.

For each event of the type K_0 the fractional energy loss z_s and its standard deviation σ_z have been determined; z_s is defined as $z_s = (E_1 - E_2)/E_1$, when E_1 and E_2 are the energy of the K before and after the interaction.

Because of the experimental errors, we cannot decide whether an event is elastic or inelastic from z_s alone. We have therefore made a statistical division of the events, determining for each of them the probability of its being elastic or inelastic, (i.e.) $P(E)$ or $P(I) = 1 - P(E)$, by a method of successive approximations.

These probabilities do not depend only on the values of z_s but also on the value z_0, of the fractional energy loss in the laboratory system for an

elastic collision, on the value σ_z of the experimental error and on the value $N(E)/N(I)$ of the ratio of elastic events to inelastic ones.

The first approximation may then be obtained as follows: since presumably $N(E)/N(I)$ depends on the energy and scattering angle of the K, we have first considered separatly events in the two energy intervals, from 40 to 90 MeV and from 90 to 160 MeV. In Fig. 1 *a* and *b* are reported the point

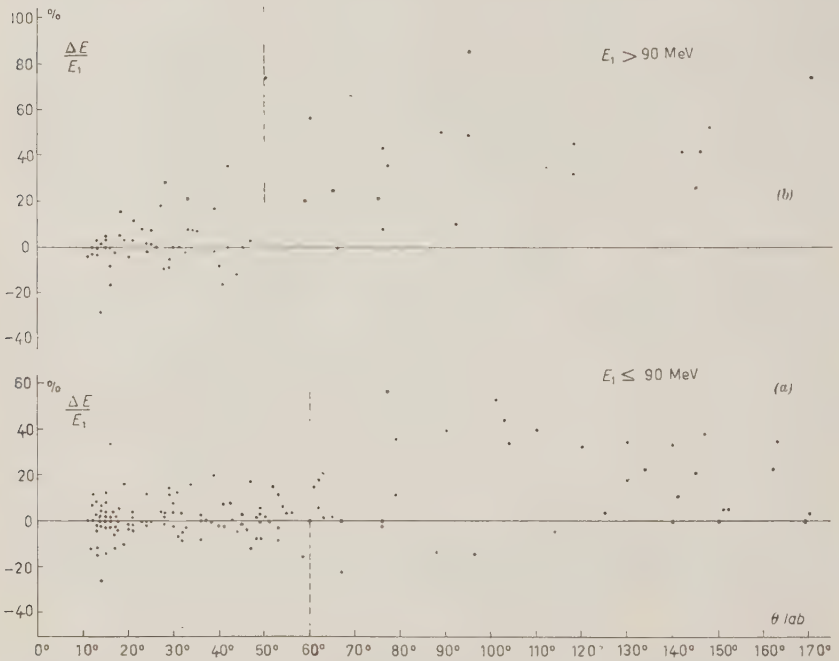

Fig. 1 *a, b.* – Plot of relative energy loss ($\Delta E/E_1$) vs. angle of scattering for two energy intervals.

diagrams of the distribution of z_s versus angle of scattering, for the two energy intervals considered. We see, in both cases, that for small angles the values of z_s are distributed around a value near zero, which corresponds to a preponderance of elastic events while for larger angles positive values of z_s are predominant; these two groups are best divided if we choose as division angles 60° for the lower energy interval and 50° for the higher one.

The distribution of z_s obtained taking into account the broadening due to experimental errors, are reported in Figs. 2 *a, b, c, d*, for the resulting four groups of events.

For each histogram the number of elastic and inelastic events has then been evaluated in the following way: as the first approximation we have considered all events whose z_s was negative as being elastic, attributing the

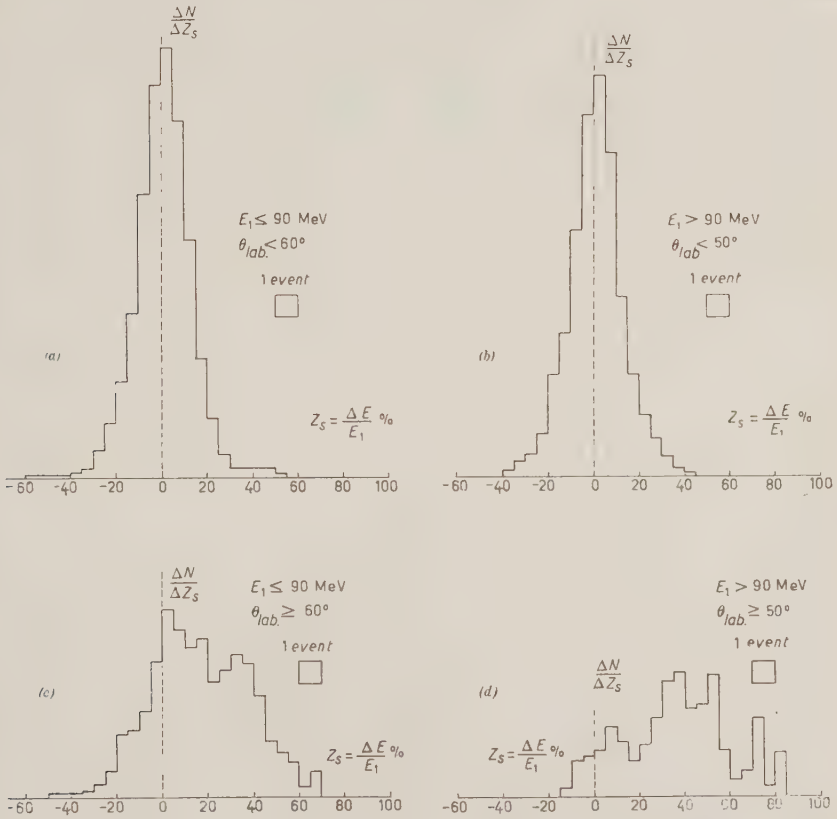

Fig. 2 *a*, *b*, *c*, *d*. – Distribution of relative energy loss for $\bar{K}_0$ events, grouped in energetic and angular intervals.

apparent increase of the energy of the emerging K to experimental errors in measurements. Since appreciable systematic errors can be excluded (see Appendix I) an equal number of elastic events with $z_s < 0$ and with the same distribution is to be expected, and the number of inelastic events can be obtained by subtracting from the distributing of all the $z_s > 0$ the distribution $z_s < 0$ reflected about the zero.

In such a way one obtains, as the first approximation, the value of $N(E)/N(I)$ and the normalized distributions $f(z)$ of z_s for inelastic events.

If the fractional energy loss is $z_s \pm \sigma_z$, the probability for an event to be elastic is proportional to

$$N(E) \cdot G_\sigma(z_s - z_0) ,$$

where z_0 is the value of the fractional energy loss in the laboratory system in the case of an elastic collision which corresponds to the observed angle, and $G_\sigma(z_s - z_0)$ the height of the Gaussian of half-width σ_z taken at the point $z_s - z_0$.

Analogously, the probability for an event to be inelastic, is proportional to

$$N(I) \sim \int_0^1 f(z) \cdot G_\sigma(z - z_s)\, \mathrm{d}z .$$

So, for each event we have

$$\frac{P(E)}{P(I)} = \frac{N(E)}{N(I)} \frac{G_\sigma(z_s - z_0)}{\int_0^1 f(z) G_\sigma(z - z_s)\, \mathrm{d}z} .$$

Now, from the so obtained values of $P(E)$ and $P(I)$, one can calculate a second approximation value for $N(E)/N(I)$ and for $f(z)$, and then repeat the procedure. In our case the values of $P(E)$ and $P(I)$ do not vary appreciably already from the second approximation.

After this analysis, most of the events were seen to be unambiguously elastic or inelastic; only for 23 events of a total of 213 the method led to fractional values of the probabilities; these events weighted according to these respective probabilities were added to the total numbers of both elastic and inelastic events, and to the corresponding angular distributions.

It is worthy of mention that, in the energy interval from 40 to 90 MeV, and for angles $\leqslant 60°$ (Fig. 2*a*) all events result to be elastic, since the hystogram is symmetrical about the value z_0 which would correspond to the mean fractional energy loss for the observed distribution if all the scatterings had been elastic. Apart from two or three events, the same can be said for the hystogram in Fig. 2*b*.

The result of this analysis of elastic and inelastic events is reported in Table II.

Apparent Charge Exchanges. – In order to decide whether the 8 events in Table I represent true charge exchange interactions, the following procedure has been adopted. A plot of the ranges of all the identified particles emerging

from the interactions has been made and is given in Fig. 3, in which are also included the tracks emerging from the « apparent charge exchange » interactions.

As one can see, no identified K has a range shorter than 1 mm after having interacted, and a negligible fraction of the particles with range longer than 1 cm are not K's. Four of our 8 events had all emerging tracks shorter than 1 mm, and these have then been considered as true charge exchange interactions. Furthermore, for each of the secondary tracks of the other 4 interactions, we have taken as the probability of it being a K, the ratio between the number of secondary particles identified as K's and the number of particles identified as not K's in the same range interval. So the estimated number of charge exchange interactions becomes 6.

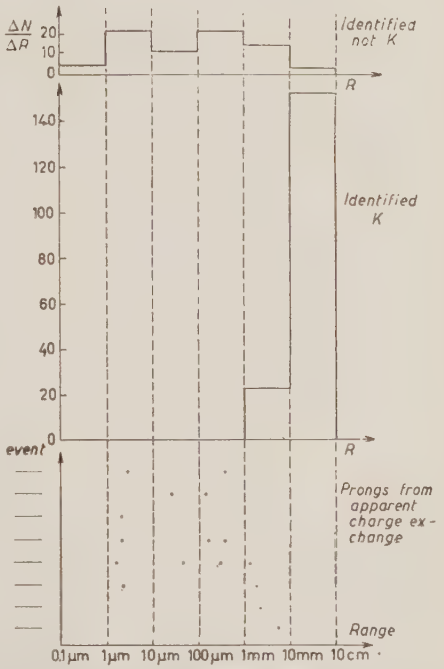

Fig. 3. – Range distribution for identified tracks emerging from K-interactions and for all tracks emerging from apparent charge exchanges.

D.F. *and Stops.* – With regard to the « Stops », two possibilities are present: a stop can be a charge exchange interaction with emission of neutral particles only, as well as a decay in flight of a K with a non-visible secondary.

To divide the stops into charge exchanges and decays in flight, two independent methods have been used: one based on the visibility factor of the decay secondaries in our emulsions, and the other on the assumption that the differential cross-sections for scattering with charge exchange and for simple scattering are not very different. These methods which are fully described and discussed in [4] have led us to divide our 13 stops into 4 charge exchanges and 9 decays in flight for primary energies

---

[4] Plate groups of Bristol, Copenhagen, Dublin, Göttingen and Padua (to be published in the *Nuovo Cimento*).

10 MeV. The total number of charge exchanges resulting from this analysis is given in Table II.

TABLE II. – *Summary of Events.*

	K-H	Elastic	Inelastic			Charge exch.			Not anal.	Total
			a (*)	*b* (*)	Total	*a* (*)	*b* (*)	Total		
40÷ 90 MeV	2	119	21	12	33	—	3	—	12	169
90÷160 MeV	3	51	22	36	58	—	3	—	—	115
Total	5	170	43	48	91	4	6	10	12	284+4

(*) *a* = Events with no prongs.
b = Events with prongs.

We can note here that in those interactions from which the K-meson is not seen to emerge no case of an energy release greater than the kinetic energy of the incident K has yet been observed, i.e. no case which should be interpreted as an absorption of a K^+-meson has been found [1], which is in agreement with the Gell-Mann and Nishijima [5] rules.

4. – Small Angle Scatterings.

In order to determine some characteristics of the nuclear potential between K and nuclei we have moreover observed the scattering also for angles smaller than the previous limits of 12°.

For this purpose we have examined a sample of K tracks having a visible decay secondary, and recorded all scattering with projected angle $\geqslant 5°$.

On a total of 10 m of tracks followed in the energy interval from 40 to 100 MeV we have observed 32 scatterings between 7° and 13°. The results are reported in Table IV.

5. – Experimental Results.

From Table II we can now immediately deduce the interaction lengths for different kinds of events and the relative cross-sections. The results are presented in Table III.

[5] M. GELL-MANN: *Phys. Rev.*, **92**, 833 (1953); K. NISHIJIMA: *Prog. Theor. Phys.*, **12**, 107 (1954); M. GELL-MANN and A. PAIS: *Proceedings of the Glasgow Conference on Nuclear and Meson Physics* (London, 1955).

TABLE III. – *Interaction lengths and cross-sections.*

		Elastic Scattering	Coulomb (+) Scattering	Inelastic Scattering	Charge Exchange	Inelastic (*) cross-section per nucleon
40÷90 MeV	λ (m)	0.25±0.02	—	1.60±0.29	—	—
	σ (mb)	848±78	330	135±22	—	27±0.4
90÷160 MeV	λ (m)	0.58±0.08	—	0.99±0.12	—	—
	σ (mb)	366±51	105	215±29	—	43±0.6
40÷160 MeV	λ (m)	0.36±0.03	—	1.22±0.12	11±3.5	—
	σ (mb)	600±46	210	174±18	20±6	3.9±0.4

(+) These values for Coulomb scattering have been calculated assuming a point charge for the nucleus. (With an extended charge for the nucleus we have that Coulomb scattering = 200 mb for 40÷90 MeV). The r.m.s. of Z is 21,15.

(*) Including the charge exchanges.

The interaction length and cross-section for charge exchanges are given only as a mean value for the whole energy interval, owing to the fact that a number of them have been obtained only as a result of a statistical division of the « Stops ». The 12 non analyzed events which are all in the low energy interval, have been statistically divided into 7 elastic and 5 inelastic.

Concerning τ-mesons, the ratio of interacting τ's to the other interacting K's, is $16/288 = (5.6 - 1.4)\%$. This figure is very similar to the value of about 5% of the ratio τ/K in a beam of K-particles, and this indicates in the limits of the present statistics a m.f.p. for the τ of the same order as that for K's in general (6).

We may observe that elastic scatterings are much more numerous than should be expected for Coulomb scattering only, which reveals a rather important nuclear elastic scattering; the decrease of the elastic scattering cross-section with energy may however be chiefly due to the Coulomb scattering.

The inelastic cross-section appears instead to increase markedly with energy; in order to analyze this effect in a more detailed way, smaller energy intervals

(6) M. WIDGOFF, A. SHAPIRO, R. SCHLUTER, D. RITSON, A. PEVSNER and V. HENRI: preprint and *Proceedings Sixth Rochester Conference*, Part. VI (1956); N. BISWAS, L. CECCARELLI FABBRICHESI, M. CECCARELLI, K. GOTTSTEIN, N. VARSHNEYA and P. WALOSCHEK: *Nuovo Cimento*, **4**, 631 (1956).

(of 20 or 30 MeV) have been considered and the cross-section separately calculated for each of these. The result is shown in Fig. 4 which gives further confirmation of this increase of the cross-section; not much weight may be

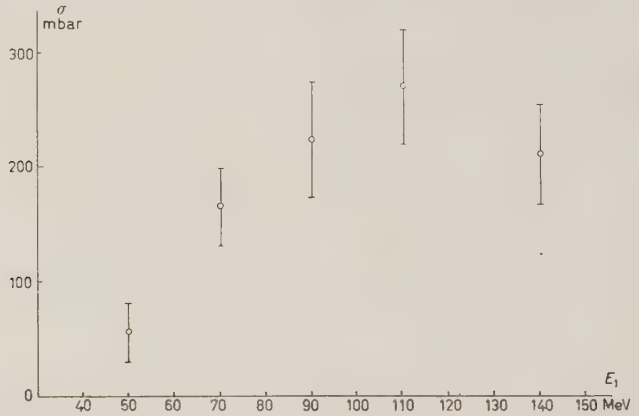

Fig. 4. – Plot of total inelastic cross-section K-nucleus vs. energy of the incoming K.

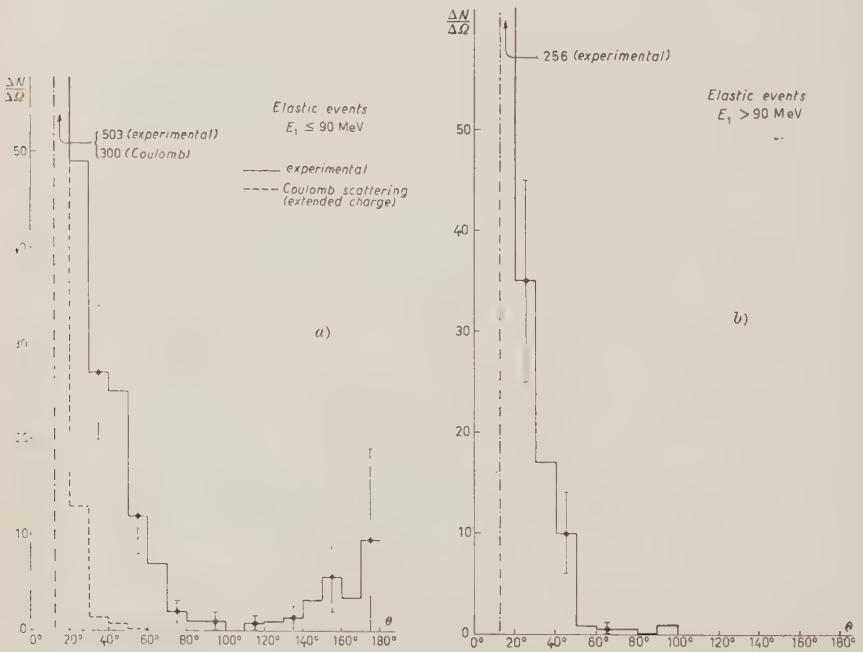

Fig. 5 *a*, *b*. Angular distributions of elastic events for two energy intervals.

given to the higher energy point which has been obtained with a shorter track length.

We may further analyze the behaviour of both elastic and inelastic events as a function of the angle of scattering in the laboratory system. Figs. 5 *a*, *b* give the angular distribution per unit solid angle for elastic events, and Figs. 6 *a*, *b* the same for inelastic events, divided according to the two energy intervals (smaller and greater than 90 MeV). In Fig. 5 *a* the Coulomb distribution for extended charge is drawn for comparison. The nuclear scattering is seen to be large, both for small and large angles, with a minimum around 100°. At higher energies elastic scatterings are seen to decrease rapidly with the angle. Cross-sections for inelastic scatterings on the contrary, do not seem to vary much with the angle and could be accounted for by a nearly isotropic distribution either for the lower or the higher energy intervals.

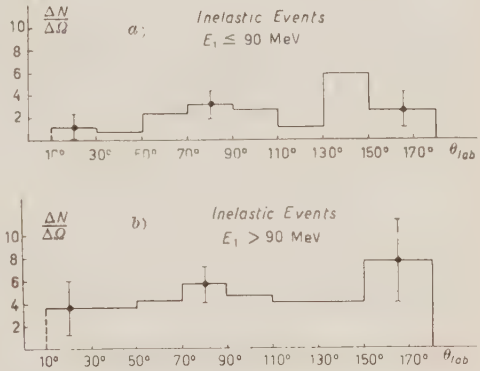

Fig. 6 *a*, *b*. – Angular distributions of inelastic events for two energy intervals.

Part. II. – Interpretation of the Experimental Results

We shall now proceed to interpret the preceeding results in order to see to what extent they will allow us to obtain information about the way in which K-mesons interact with nucleons and nuclei. The most simple way to do this is by assuming an optical model for the nucleus.

It is well known that according to this model the phenomena observed may generally be interpreted as a superposition of a Coulomb scattering and a nuclear scattering due to a complex potential. The real part of this potential gives a coherent contribution to the scattering which should interfere additively or destructively with the Coulomb part according to whether the nuclear potential is repulsive or attractive. The imaginary part contributes to the elastic scattering through shadow scattering, but in this particular case, owing to the fact that the interaction length is so long, it may safely be assumed that shadow scattering is practically absent; thus the imaginary part will

contribute only to the absorption of the K's from the incident wave. Considering that experimentally we have no examples of K absorption, in agreement with the Gell-Mann selection rules, the inelastic events have been interpreted as the incoherent scatterings of K by individual structures inside the nuclei, and as the simplest hypothesis we have assumed that these nuclear structures are single nucleons.

Thus according to this model, elastic and inelastic events are related respectively to the scattering by the whole nucleus or by single nucleons, and are expected to yield information for these two kinds of phenomena. We shall therefore consider them separately.

6. – Elastic Scatterings.

The most important piece of information we have tried to obtain from our elastic scattering data is the value and sign of the real potential of the whole nucleus. We may first consider the value of the total elastic cross-section. According to the calculations of COSTA and PATERGNANI (7), the total elastic cross-section is a function of the kinetic energy of the incident K and of the nuclear potential V_n. If according to the track length followed for each energy interval we calculate from their formulas the average of the cross-section over all our energy interval, we obtain Fig. 7 which gives this average cross-section as a function of the nuclear potential only. It is seen that our experimental value (from 20° on) for the elastic cross-section corresponds to the two possible values of $V_n = +14$ and $V_n = -22$ MeV.

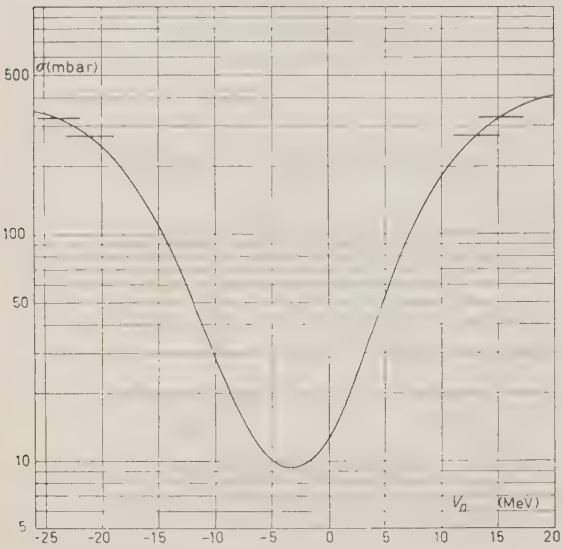

Fig. 7. – Total elastic cross-section (from 20° on) vs. nuclear potential V_n.

(7) G. COSTA and G. PATERGNANI: in the same issue of *Nuovo Cimento*.

In order to decide between them, we must consider the angular distributions; it may be expected that Coulomb scattering will interfere constructively or destructively at small angles with nuclear scattering according to whether the sign of the nuclear potential is the same or opposite to the Coulomb potential. From our data on elastic scattering, it is apparent that scattering between 12° and 20° is in large excess over pure Coulomb scattering, which already gives an indication that the potential V_n is repulsive. The calculations of COSTA and PATERGNANI indicate that the angle for which the interference effect should be most sensitive lies in the region about 10° for the energies considered. Therefore we have extended our analysis to smaller scattering angles (see Sect. **4**). The differential cross-sections to be expected for two values of V_n (+13 and −16 MeV) are given for different values of the primary K energy: weighting these curves according to the energies of the K track lengths effectively observed, the total number of scatterings between 7 and 13° to be expected in both cases have been deduced, and these figures are compared with the experimental values in Table IV.

TABLE IV. – *Number of scatterings (between 7° and 13°) on 10 m track of K of energy between 40 and 100 MeV.*

V_n	Expected	Observed
+ 13	28	
0	19	32
16	7	

The agreement of the observed values with the repulsive potential appears to be rather good, while the discrepancy with the attractive one seems already outside the probable error. The best fit of repulsive potential occurs for a value $V_n = (19 \pm 7)$ MeV somewhat higher than the value obtained from the total cross-section. Therefore there is a strong indication of the presence of a nuclear potential which acts in a repulsive way on the K's (⁸), and we shall see that this evidence is in agreement with other indications coming from inelastic scattering data.

(⁸) We have been informed during the Turin Conference that the Rochester plate group studying also the small angle scattering of K⁺-mesons has obtained results in very good agreement with ours. We would like to thank here the Rochester plate group for this information.

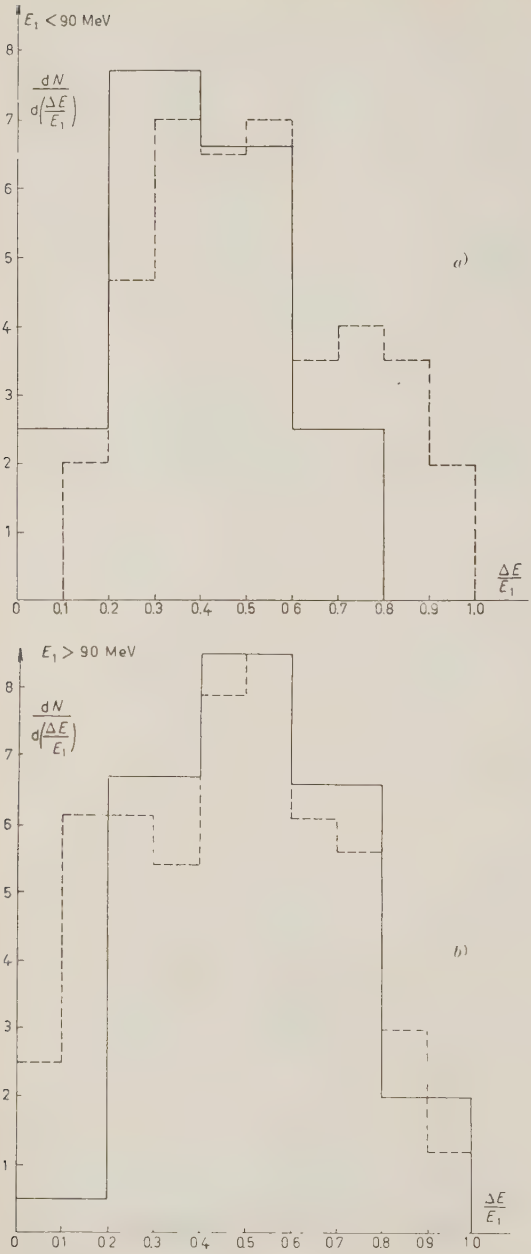

Fig. 8 *a, b*. – Distributions of relative energy loss for inelastic events grouped in two energy intervals.
——— Experimental.
– – – – – Montecarlo.

7. – Inelastic Scattering.

According to our model, the inelastic events will now be interpreted as being due to a single collision of the K with a nucleon of the nucleus. The phenomenon will then be essentially dependent on the elementary K nucleon cross-section, and on the total potential V of the nucleons. We shall now consider what influence these parameters may have on the different results we have observed.

Let us consider first the histograms Fig. 8 *a, b*, which give the distribution of events for a given energy loss. It is expected that the behaviour of at least the curve 8*a* for the low energy interval events will depend in a sensitive way on the value and sign of the nuclear potential V_n. For $V_n = 0$, a Montecarlo calculation [9] has been

[9] G. A. SALANDIN: to be published in *Nuovo Cimento*.

done assuming the observed behaviour of the angular cross-section (Fig. 8 *a*, *b* dotted lines). It is observed that for the higher energy interval, there is a good fit between calculated and experimental distribution: the lack of events with small $z_s = \Delta E/E$ may be due to a possible loss of such kind of events as a consequence of the criteria adopted in our analysis (see Sect. 3). For the low energy interval events (Fig. 8*a*) instead, there appears to be a lack of high energy losses in the observed distribution. This can be considered as a further indication of the presence of a repulsive potential, and in fact, the calculated distribution with a total potential of about + 20 MeV turns out to be much closer to the experimental one. Of course, such an effect of the potential is expected to be much smaller for the high energy interval events, and in fact is not observed (Fig. 8*b*).

Another point of interest is the increasing trend of the z_s with increasing energy as is apparent in Fig. 9 which refers to the mean values of z_s for inelastic events.

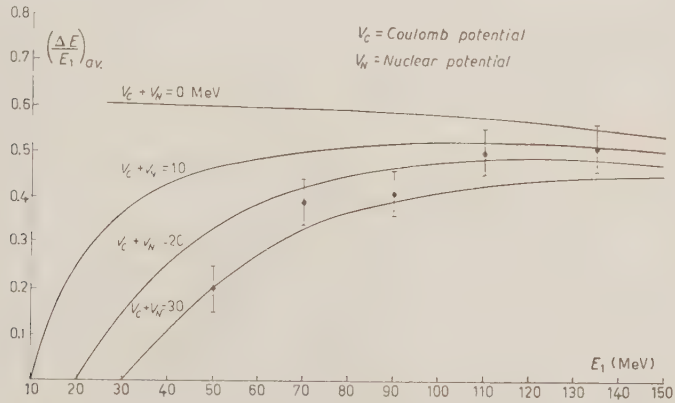

Fig. 9. - Plot of average energy loss for inelastic events vs. energy of the incoming K.

If we now try to fit this behaviour by means of a Montecarlo calculation assuming the experimental angular cross-section and different values of the potential V_n (Fig. 9) we see that only for a repulsive potential we obtain an increase with energy and that in this case the best fit is obtained with a value of $V_n \sim 15$ MeV.

Finally we may also consider the behaviour of z_s as a function of the laboratory scattering angle (Fig. 1*a*, *b*): we observe that for inelastic events in both cases there is no sensible increase of z_s with increasing angle, as one would expect: this effect may be also attributed to the repulsive nuclear potential.

Thus we can conclude from the foregoing discussion that the nuclear repulsive potential, which was introduced in order to explain the small angle elastic scattering, is also necessary to explain many features of the inelastic scattering, so that its existence may now be considered as experimentally well founded. Its value may be considered as lying around 15 MeV, since the different estimates give 14, 19, 15 MeV respectively ([10]).

We may now try to analyze the angular distribution of inelastic events. From Fig. 6 *a*, *b* it is apparent that this distribution is nearly isotropic in the laboratory system. This however has to be interpreted as a complex effect resulting from elementary scatterings due to a K-nucleon cross-section of still an unknown shape in the center of mass system corrected by the action of the Pauli principle in nuclear matter plus the effect of the nuclear repulsive potential. We think that we may as a first approximation disregard the refraction effect of this potential in changing the angles of the K entering and leaving the nucleus ([11]). The potential V_n will then be effective only in diminishing the energy of the K inside the nucleus. According to our model, we may expect that owing to the small total nucleon cross-section, the probability of the same K making two successive collisions will be small, so that practically all inelastic events may be supposed to be due to a single collision ([12]): and in this case the observed angle will be the true scattering angle in the laboratory system.

We may now try to go back from the data in the laboratory system to the angle in the center of mass system, taking into account of course the Fermi motion of the nucleons. The details concerning the way in which it has been done are reported in Appendix II. The result however is that we cannot for a given observed event in the laboratory system give exactly the value of its scattering angle in the center of mass system; but we can assign a determined probability for its having had a given center of mass system angle value. The hystograms corresponding to the total of these probabilities for each center

---

([10]) The only contrasting result to this evidence as far as we know has been obtained by L. OSBORNE (*Phys. Rev.*, **102**, 296 (1956)) who concludes for the evidence of an attractive potential between K and nucleus. As the deductions of OSBORNE are expressed in a very condensed way, we were unable to identify the true reason for the discrepancy.

([11]) This change of angle will be important only for collisions with nucleons on the outside of the nucleus and negligible in other cases; moreover, even in the first case, the changes of the angle value will result either in an increase or a decrease, depending on the position of the nucleon on the surface of the nucleus, and in general will compensate; so from a statistical point of view we may consider that, on the average the angle is not changed by refraction.

([12]) One single event resulted to be dynamically incompatible with this interpretation.

of mass angle are reported in Fig. 10 *a*, *b*, the first one corresponding to the events with primary energy lower than 90 MeV (mean value: 71 MeV), the second to the higher energy interval greater than 90 MeV (mean value: 116 MeV). It is apparent that in both cases we obtain a backward peaked distribution. The ratio of the number of events scattered in the backward hemisphere to those in the forward one is seen to be about $4{,}3 \pm 1{,}5$ in the first case and $5{,}2 \pm 2{,}0$ in the second one.

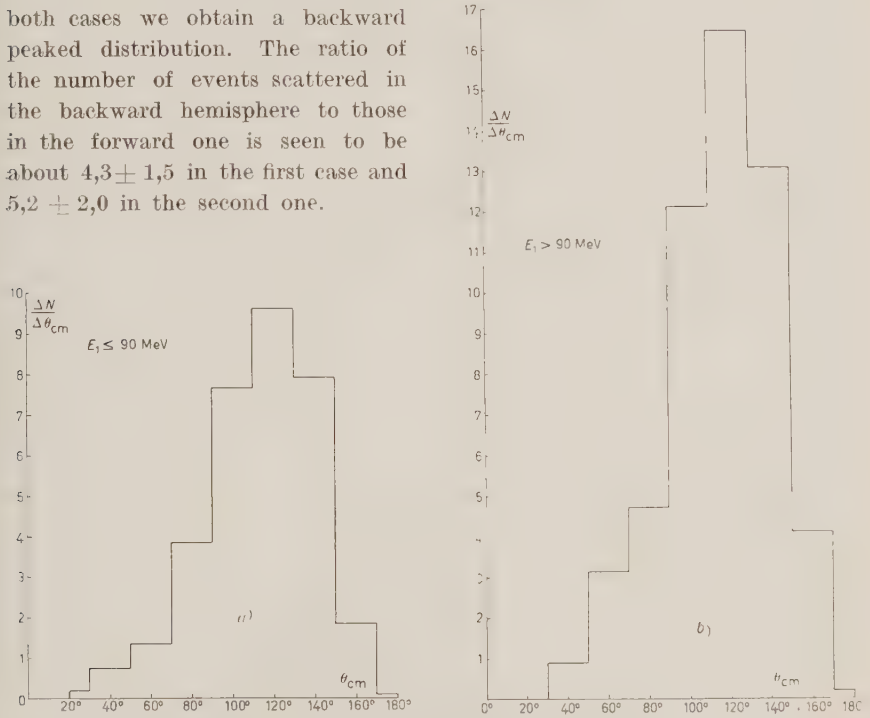

Fig. 10 *a*, *b*. – Angular distributions in the center of mass system of the inelastic events, in two energy intervals.

8. – Discussion of the Elementary K Nucleon Cross-Sections.

We may now try to discuss what evidence may be gathered concerning the elementary K nucleon cross-sections. According to the Gell-Mann scheme, the only reactions to be expected are the following:

$$K^+ + p \to K^+ + p \qquad I$$

$$K^+ + n \to K^+ + n \qquad II$$

$$K^+ + n \to K^0 + p \qquad III\,.$$

If in analogy with pion-nucleon scattering, we also try to interpret K-nucleon scattering according to the idea of charge independence of K-nucleon forces, we obtain the following weights and relative ratios for the reactions I, II, III, for the two possible isotopic spin states $T=0$ and $T=1$.

	I	II	III	(I+II)/III	I/II
$T=0$	0	1	1	1	0
$T=1$	4	1	1	5	4

It may be expected that in the range of energies considered, only the S and P states are responsible for the scattering; if as a first approach, we disregard the distinction between the $P^{\frac{1}{2}}$ and $P^{\frac{3}{2}}$ states and define as a_{00} and a_{01} the amplitudes for the S and P states of $T=0$ and as a_{10} and a_{11} the same amplitudes for $T=1$, then the cross-sections (differential and total) for processes (I, II, III) are given in the center of mass system by ([13]):

$$(1) \qquad \frac{\mathrm{d}\sigma}{\mathrm{d}\Omega} = \lambda^2(\alpha + \beta\cos\theta + \gamma\cos^2\theta)\,, \qquad \sigma = 4\pi\lambda^2\left(\alpha + \frac{1}{3}\gamma\right),$$

where λ is the de Broglie wave length of the K and α, β, γ, are respectively for the three reactions:

$$(2) \qquad \begin{cases} \text{I} & \text{II} & \text{III} \\ \alpha = a_{10}^2 & \alpha = \frac{1}{4}(a_{10} - a_{00})^2 & \alpha = \frac{1}{4}(a_{10} + a_{00})^2 \\ \beta = 6a_{10}a_{11} & \beta = \frac{3}{2}(a_{10} - a_{00})(a_{11} - a_{01}) & \beta = \frac{3}{2}(a_{10} + a_{00})(a_{11} + a_{01}) \\ \gamma = 9a_{11}^2 & \gamma = \frac{9}{4}(a_{11} - a_{01})^2 & \gamma = \frac{9}{4}(a_{11} + a_{01})^2\,. \end{cases}$$

Our aim is now to see if some indication of the relative values of these amplitude coefficients may be obtained from our data.

Direct evidence for the first reaction is of course only provided by the direct K-H interactions. This evidence is particularly important owing to the fact that the K^+-proton scattering may occur only in the $T=1$ state, providing us direct information on this pure T state. However, actually, owing to the very long interaction length, the number of these events is very small.

As far as the total cross-section is concerned, we have already quoted our result of 14 ± 6 mb, based on our five events; in good agreement with the value of 14.6 ± 3.3 mb based on 22 events from various laboratories ([2,14]).

([13]) See S. CEOLIN and L. TAFFARA: in the same issue of *Nuovo Cimento*.

([14]) N. BISWAS, L. CECCARELLI FABBRICHESI, M. CECCARELLI, M. CRESTI, M. GOTTSTEIN, N. VARSHNEYA and P. WELOSCHEK: *Nuovo Cimento*, **3**, 1481 (1956).

In order to obtain information on the angular distribution, the 22 events have been gathered and the histogram of Fig. 11 obtained. These events are

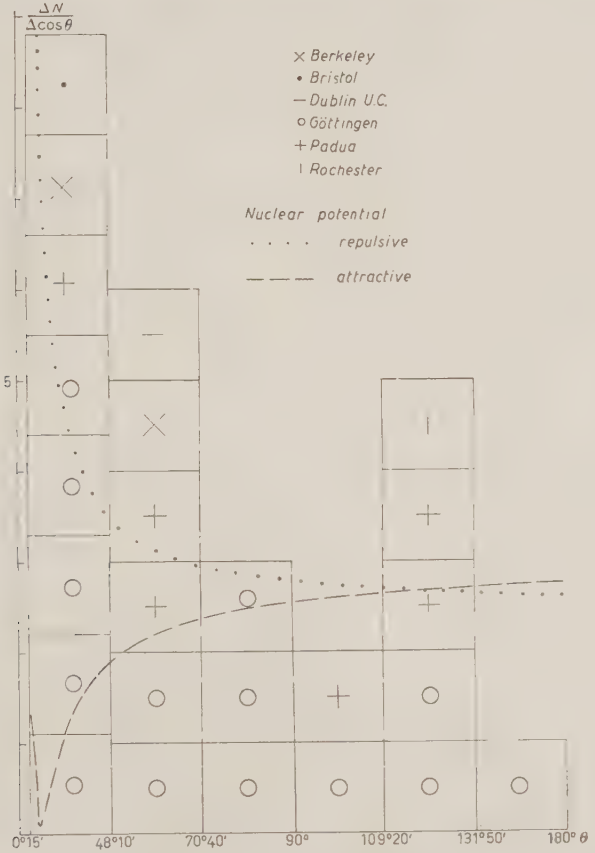

Fig. 11. – Angular distributions in the center of mass system of K-H collisions. The calculated curves are normalized to the number of events with $\theta_{cm} >$ than 90 .

collected from energy intervals ranging from 30 to 140 MeV, so that the resulting angular spectrum has to be considered as an average over different energies; its behaviour may be approximated by a somewhat forward peaked distribution. This forward peak may be interpreted as being due to additive interference of a repulsive Coulomb scattering with a fundamental nuclear repulsive S-state scattering: the expected behaviour of this effect is indicated in the dotted line of Fig. 11 and has been calculated for K⁻-mesons

of 80 MeV, and for a total nuclear cross-section of 10 mb [15]; it is seen that the effect is rather conspicuous and increases the cross-section to the observed value of 14 mb. On the other hand, this assumption is consistent with the total repulsive nuclear potential of the whole nucleus on the K which has already been deduced. Of course we cannot exclude that the nuclear scattering also contains a P wave component in the forward direction.

Let us now see to what extent this rather scarce direct information on scattering in the $T=1$ state may be used to interpret the K-nucleus scattering data.

If we first look at the values of the total cross-sections we are struck by the great difference between the value of 14 mb for the K-proton scattering and the low values around 4 mb for K-nucleon cross-section in nuclear matter defined as

$$\overline{\sigma} = \frac{Z\sigma_p + N\sigma_n}{Z + N}, \tag{3}$$

where σ_p and σ_n are the cross-sections for reactions I and II.

If we disregard the ever present possibility of statistical fluctuations, this difference cannot be explained by assuming only a very low K-neutron cross-section: even in the most favorable case of the absence of state $T=0$ we should have $\sigma_p = 4\sigma_n$ and $\overline{\sigma} \simeq \frac{5}{8}\sigma_p$ which are not compatible with the two experimental values; in order to explain the low value for the average K-nucleon cross-section in the nucleus, we must consider other possible causes: for this purpose it will be useful to consider the differential cross-sections per nucleon in the center of mass system Fig. 12 *a*, *b*, obtained from histograms 11 *a*, *b*.

Both these curves for low and high energy events indicate a strongly backward peaked distribution; in the forward direction for small angles, the absence of events is almost complete. We know however that in the $T=1$ state the forward scattering is important. The low value of the cross-section in nuclear matter may then be attributed essentially to the lack of events with small scattering angles.

As a first cause, it may be possible that owing to the spread of our distribution of z_s (Fig. 2 *a*, *b*) a certain number of events of small inelasticity and scattering angles less than 60° have been according to our assumptions (see Sect. **3**) erroneously considered amongst the elastic ones. We have already

---

[15] The calculation has been done by Drs. COSTA and PATERGNANI, and we wish to thank them here for having given us their result. We are also grateful to the Göttingen plate group for having communicated to us the collected data (published and unpublished) on K-H scattering from the different laboratories.

considered such possible effects in discussing Fig. 8*b*. This number must be small otherwise it would have made the curve skew (Fig. 2 *a*, *b*), which fact was not observed: and therefore its subtraction from the elastic group could not alter appreciably the conclusions drawn from them; however, it would partially fill up the hole observed in Fig. 12 *a*, *b*, as the absolute number of the inelastic events is small compared to the elastic ones.

As a possible second explanation we can consider the intrinsic effect of the Pauli principle in reducing the number of small angle scattering events. We have made a rough estimate of this effect assuming an isotropic cross-section with a total repulsive potential of 25 MeV for the K and according to the Fermi model of the nucleus with two different nucleon distributions: first, the normal one with a maximum energy of 22 MeV for the nucleons; secondly, a more detailed one according to which the protons are concentrated ([16]) in a smaller sphere in the center of the nucleus (radius $1.2 \cdot 10^{-13} A^{\frac{1}{3}}$) which brings their maximum energy to about 34 MeV. The importance of the Pauli re-

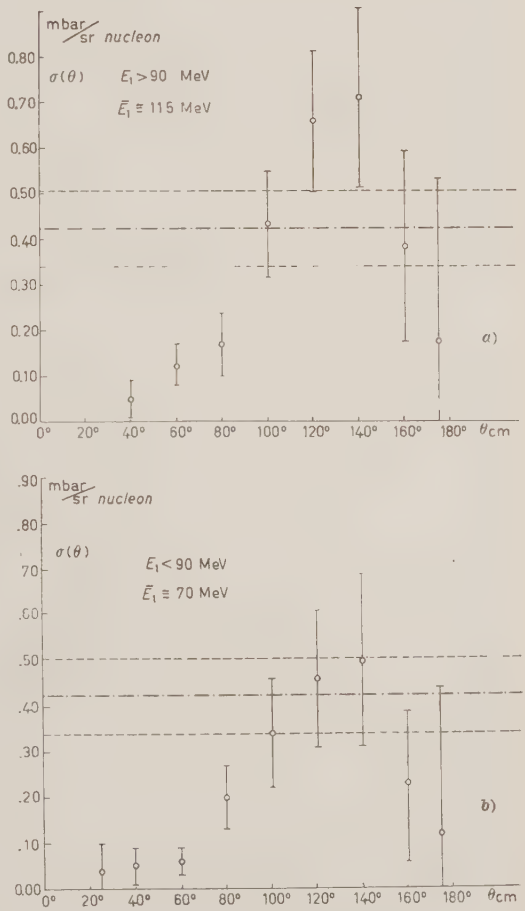

Fig. 12 *a*, *b*. – Angular cross-section (center of mass system) for K-nucleon collisions in nuclear matter. The dotted lines indicate the value (and its error) of the angular cross-section for the K-nucleon collision in $T = 1$ state (S wave) estimated from K-H interactions.

([16]) R. HOFSTAEDTER: *Rev. Mod. Phys.*, **28**, 219 (1956); K. W. FORD and D. L. HILL: *Annual Review of Nuclear Science*, **5**, 25 (1955).

duction factor turns out to be strongly increasing as this maximum energy of the nucleons increases and as the incoming energy of the K decreases; for the mean energy value of our lower energy interval (71 MeV outside and 45 MeV inside the nucleus) the loss factor for the two cases for the total cross-section is 1.6 and 2.5.

We can then try to proceed by making some assumption about the shape of the K-p cross-section in nuclear matter, when corrected for the effect of the Pauli principle. As an example, let us suppose that the pure K-p cross-section is so peaked in the forward direction that the elimination of events due to the Pauli principle operates so as to make it practically isotropic in nuclear matter. Correspondingly the total value of 14 mb will be reduced to a value between 9 and 5.5 mb according to our preceding two estimates of the exclusion principle effect and about half of these values will be the contribution to the mean cross-section in formula (3). We should then subtract a straight strip corresponding to these values from the spectra of Fig. 12 *a*, *b* and this would then indicate the contribution of K-p scattering, the remaining being due to K-n scattering.

However, as the cutting effect of the Pauli principle is difficult to evaluate exactly according to our preceding estimates, and as we do not yet know the exact shape of the K-p cross-section, owing to the fact that our information on it is based only on the events of Fig. 11, we consider that the most reliable procedure we can follow is based on the following assumption: The Pauli principle will chiefly operate so as to make a hole in the forward scattering and leave the backward scattering unchanged. The K-p cross-section will then appear as peaked backwards in nuclear matter, reproducing what is in fact observed. And any comparison between the free K-p cross-section and the same in nuclear matter should be then based only on the backward scattering which should be the same in the two cases.

According to the present view, the backward scattering ($\theta_c > 90°$) will correspond to about $\frac{1}{2}$ of the total K-p cross-section, that is about 5-6 mb; one half of it, that is about 3 mb, will be the proton contribution to the mean nuclear cross-section $\bar{\sigma}$. If we consider the first diagram (Fig. 12 *a*) corresponding to the low energy events, it is seen that this figure covers practically the whole cross-section, so that probably little is left for the possible contribution of the K-n scattering [17]. Of course it is difficult from our data to exclude the presence of a small a_{00} amplitude. If of the same sign relatively to a_{10}, it would contribute to reduce the scattering of the K-n reaction.

---

[17] If we remember that the contribution to the total K^+ proton scattering when corrected for Coulomb scattering is only ~ 10 mb, the corresponding K-n scattering for state $T=1$ contribution should about 1 mb, which is quite compatible with the errors.

A confirmation of this view may be obtained by correcting the forward part for what is lost by the Pauli principle: the hole is practically filled up and the cross-section becomes nearly flat with a value close to the observed one for K-p scattering. For low energies according to these assumptions the general experimental behaviour could then be explained with only the a_{10} K-p scattering.

If we now try to repeat the same analysis for the higher energy interval, we remark from our figure that the loss of events in the forward direction appears to be greater, while on the contrary it should be smaller as the cut-off due to the Pauli principle is already strongly decreased; it appears that in fact the correction is unable to fill all the gap in the forward direction, and that the K-p cross-section is not sufficient to account for all the backward scattering observed. This could be considered as an indication that in this higher energy interval another scattering amplitude has acquired some importance; and owing to its energy dependence it may be expected that it is a P wave. As it should interfere additively with the a_{10} amplitude in the backward direction, it seems more probable that it is the a_{01} amplitude corresponding to the $T=0$ state; although we cannot exclude, if the observed forward scattering in the K-H events is essentially due to the Coulomb interference, that this backward P wave may be also due to the a_{11} amplitude of the $T=1$ state. In the first assumption, the formulas (1) for reaction II will simply reduce to

$$\frac{\mathrm{d}\sigma}{\mathrm{d}\Omega} = \frac{1}{4}\lambda^2(a_{10} - 3a_{01}\cos\theta)^2 \,. \tag{4}$$

In order then to obtain the observed order of magnitude of the effect, the amplitude coefficient a_{01} should be of the same sign and about $\frac{1}{3}$ the magnitude of a_{10}. As it should follow a η^3 law, (η = momentum of the K in center of mass divided by $M_K c$) it would be already reduced enough in the lower energy interval to give a not appreciable contribution.

We therefore think that our present evidence concerning reactions I and II could be interpreted with a most important $T=1$ scattering due chiefly to an S state with the appearance at higher energy of a probable P wave which we have supposed to be due to the $T=0$ state.

It is evident that the preceding discussion modifies the conclusions that one might deduce from the increase of the total nuclear cross-section shown by Fig. 4. First this apparent increase will be moderately reduced by the Coulomb factor $(V-(V_c/E))$ (where V_c is the Coulomb potential on the nuclear radius and E is the energy of the incident K) by which the true cross-section has to be multiplied and which is greater the smaller is the incident energy of the K. Second, according to the true value that should be assumed

for the cut-off of events due to the Pauli principle, this increase will be also strongly reduced or may even disappear; this on the one hand makes us unable to deduce from the apparent increase the relative importance of the P state scattering, but on the other hand gives further support to the evidence that most of the scattering is due to an S state.

As a last step to our analysis we have now to consider also the charge exchange reaction III. It has already been pointed out ([2]) that the experimental ratio III/(I+II) is close to the value $\frac{1}{5}$ and it has been considered as evidence in favour of a predominant $T=1$ scattering. This seems to be in good agreement with our general conclusions, and our experimental data for this ratio are not inconsistent with this assumption. However, we would like to emphasize that the true number of charge exchanges which results from the experimental analysis we have made (see Sect. 3) is difficult to determine with accuracy and so conclusions based on this kind of event have to be considered with caution.

From our evidence on K-n scattering, we could not exclude a contribution of a $T=0$ S-state; however as this possible a_{00} amplitude gives contributions with opposite sign in reactions II and III, a decrease due to its effect for the K-n scattering cross-section would mean a corresponding increase in the charge exchange cross-section and therefore a value of the ratio III/(I+II) sensibly higher than the observed one. Altogether this indicates that if an amplitude a_{00} is present, it must be small in comparison to a_{10}.

The presence of a P scattering amplitude a_{01} which was assumed by us in order to explain the backward peak in the high energy scatterings will of course contribute a forward peak for the charge exchanges of the same energy interval; this effect however should be very difficult to observe, owing to the cutting action of the Pauli principle on the forward scattering, as was first pointed out by the Bologna group: so that we may conclude that the lack of increase of the III/(I+II) ratio with energy should not be considered as contradictory to the existence of the a_{01} amplitude.

9. – Conclusions.

During the analysis of the experimental data concerning the interactions of K^+-mesons with the nuclei of the emulsion we have separated the elastic events from the inelastic ones in order to derive some general conclusions, as we have tried to attribute the two kinds of events to different mechanisms. In fact, we interpret the elastic events as interactions of the K^+ with the whole nucleus, and the inelastic ones as K-nucleon collisions in the nucleus.

A clear distinction between the two types of events is experimentally not possible, but our conclusions are not very sensitive to some mixing between them, especially those concerning the elastic events.

The main results that can be deduced from the analysis of events concern: *a*) the existence of a repulsive nuclear potential and *b*) some probable features of the elementary K-nucleon cross-sections.

a) The existence of a repulsive nuclear potential $V_n \simeq 15$ MeV, was deduced by means of the following data:

— The marked excess of the number of elastic scatterings with respect to the Coulomb scatterings alone.

— The evidence of an additive interference between nuclear and Coulomb scattering for small angles between (7° and 13° and between 12° and 20°).

— The variation of the mean value of z_s, with energy E, for inelastic events.

Some other indications of the existence of a repulsive nuclear potential were obtained from the absence of large values of z_s for the low energy interval events and from the smoothing of the dependence of the mean values of z_s on the angle of scattering.

From all our data, the existence and the order of magnitude of the nuclear potential seems to be well founded.

b) The principal information available to us at present concerning K-nucleon interactions:

$$K^- + p \rightarrow K^- + p \qquad (I)$$

$$K^- + n \rightarrow K^- + n \qquad (II)$$

$$K^- + n \rightarrow K^0 + p \qquad (III)$$

is obtained from the K-H collisions for the pure $T = 1$ state.

Collecting all data at present available (22 events) the cross-section K-p is then (14.6 - 3.3) mb; the angular distribution seems to indicate the existence of a nuclear S-wave which interferes additively with the Coulomb scattering. At present it is obviously not possible to obtain information on the dependence of σ_p on the energy.

Inelastic scattering of K⁻ with nucleons in nuclear matter is characterized by the following data: (1) an apparent total cross-section much lower (about 4 mb) than the K-p cross-section; (2) this cross-section appears to increase with energy; (3) the differential cross-section seems to be strongly peaked backwards in the center of mass system; (4) the cross-section for charge-exchange events III is much smaller than the scattering cross-sections (I - II). These features may be explained by assuming an important effect due to the Pauli principle, which operates in order to cut out most of the forward

scattering in nuclear matter, thus also reducing strongly the value of the total cross-section. Owing to this effect, the increase of the inelastic cross-section may be for the most part only apparent.

The simplest way to interpret our data is the following: in the low energy interval there is a most important contribution of the $T = 1$ state, as an S wave, whereas at higher energies the presence of a P wave, possibly, of the $T = 0$ state, seems probable.

* * *

We are much indebted to the Berkeley staff and particularly to Dr. E. J. Lofgren for the exposure of both stacks to the beam on the Bevatron; to the plate group of Bristol University who obtained and processed the stacks on behalf of all the European laboratories amongst which they were divided; to Drs. D. Greening and B. Sechi-Zorn for their helpful collaboration in the early stage of this research: to the team of observers at this laboratory for their careful scanning of the plates; and finally to the physicists of the plate groups of Bologna, Dublin U.C. and Göttingen, and Prof. G. Cocconi for their general collaboration and many discussions on the problems involved.

We also have pleasure in thanking Prof. A. Rostagni, Director of the Institute, for having given us all necessary facilities for carrying out this work.

Appendix I

During the present experiment, absolute values of the energy of the K's and of the relative losses of energy z_s, used for the analysis of the events, have been obtained from the ionization (g), multiple scattering ($\bar{\varepsilon}$) and effective (R) or estimated range ($\bar{R}$).

The statistical separation of the inelastic from the elastic events depends on the estimated values of z_s and is sensitive to possible systematic errors.

The following considerations will show that the errors in every type of measurements have been correctly estimated and that possible systematic errors are of negligible amount relative to statistical errors.

1) *Ionization Measurements*: For a certain number of events, the evaluation of the energy of the K before its interaction was obtained from the value of the ionization. The measurement was done on at least 1 mm flat track length in the central zone of the emulsion and the value of the corresponding energy was deduced from ionization-range calibration curves, obtained from K-mesons of known range. Each of these curves was pertinent

to a group of plates perfectly homogeneous from the point of view of the developing.

In these measurements the energy of the interacting K was estimated with an error of about 10%.

In other cases, the variation of the ionization of the K just before and after the interaction was directly measured. The knowledge of the range of the outgoing K allowed the evaluation of the energy of the interacting K; for the determination of the errors in this case we must refer to the following considerations.

The outgoing K is generally more dipping than the incoming one; which is generally practically flat. A gradient of the minimum ionization with the depth of the plate introduces an error in the value of Δg and hence of ΔE. Therefore the gradient of the ionization has been determined, and turned out to be $5.3 \pm 5\%$ on 100 μm thickness in the central 300 μm of the plate.

In order to reduce within reasonable limits the error in ΔE depending on the ionization gradient and to allow in any case reliable measurements of the ionization we have not measured Δg if the outgoing K was more dipped than 30°. According then to the mean dip of the incoming K's (0°) and of the outgoing ones (15°) a standard error of $6 \pm 10\%$ is obtained for the z_s that must be added to the purely statistical error. In any case however, the existence of an ionization gradient has not introduced any systematic error, as the outgoing K's were directed with equal frequency towards the glass or the surface in the emulsion.

2) *Scattering measurements*: The value of $\overline{\alpha}$ was determined in the cases for which the identification of the particle was not directly possible owing to the lack of a visibile decay secondary or in the cases of stops in flight. For the elimination of the second order distortions of the emulsion, the method of third differences was applied, and for the elimination of the noise, the different cell-lengths were used; the measurements were done on at least 1 cm track length, in order that the statistical error for the energy should be of the order of 10%.

3) *Range measurements*: The measurement of the energy of the K's coming out from the interactions and which stop in the emulsion without further visible interactions was done by range measurement; the error on the energy deriving from lack of precision in the measurement of the range and from the straggling turned out to be negligible relative to the other estimated errors in the energy measurements.

A further estimation of the energy of the K in the interaction is obtained from the knowledge of the mean range (R) of the not interacting K's and from the track length of the K before the interaction.

Owing to the long interaction length of the K's and to the weak dependence of the cross-section with energy, this procedure does not seem to introduce any systematic error.

The determination of the mean range $\overline{R}$ has been done for a group of 10 consecutive plates, owing to the progressive variation of the mean momentum at entrance of the K's in the stack.

For the K's of stack K_I, owing to the low entrance energy, the lack of precision in the range turns out to be of about 5 mm and from this an error of about 10% for the energy at interaction is deduced.

For the K's of stack K_{II}, the spread about the mean range is 15 mm and therefore the value of $\bar{R}$ was used only to control the absence of systematic errors.

In order to reduce the error in the energy value, this was estimated, whenever possible, in different ways. The mean value was then determined by weighting the single determinations with the relative errors.

Research of systematic errors: In order to verify that the present measurements are not sensibly affected by systematic errors, different independent checks have been made. In a certain number of cases, at least two of the three possible measurements ($\bar{x}$, $\bar{R}$ and g) have been made on the interacting K's.

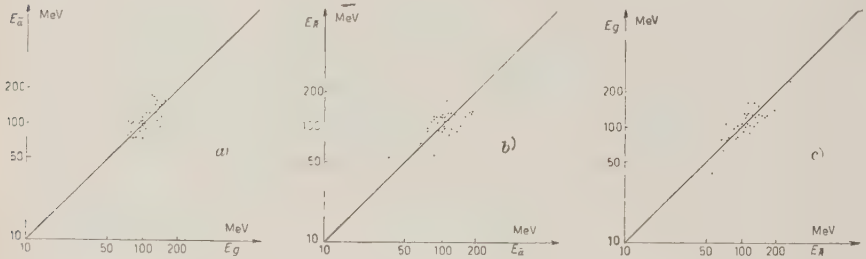

Fig. 13 *a*, *b*, *c*. – Comparison between the energies estimated by different methods.

In Fig. 13 *a*, *b*, *c*, are reported for each of these events the energies obtained from $\bar{x}$, (E_α) as a function of the energy from $\bar{R}$, $(E_{\bar{R}})$, or respectively E_x as a function of E_g, and finally $E_{\bar{R}}$ as a function of E_g: in each of these cases the points obtained show that there are not systematic deviations between any two kinds of estimated energies.

A second check for the absence of systematic errors was obtained by calculating for each event the deviation measured in standard units between the energy from the mean range $E_{\bar{R}}$ and the energy from ionization (and) or scattering (E), where $\sigma_{\bar{R}}$ is the standard error of the measurement of $E_{\bar{R}}$ and $\bar{\sigma}$ is the standard error in the measurement of E.

The values of the deviation measured in standard units thus obtained have been reported in an histogram (Fig. 14) and this results to be symmetrical around the zero

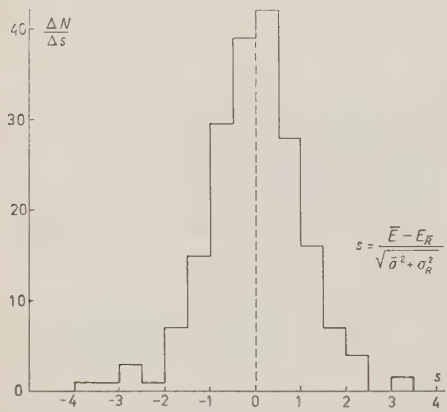

Fig. 14. – Distribution of deviations (in standard units) between the energies from mean range and from ionization (and) or scattering measurements.

and with a behavior very similar to that of a gaussian of unit half breadth. This fact not only checks the absence of systematic errors, but assures us that the errors in the single determinations have been correctly estimated.

A last check of the absence of systematic errors has been obtained by considering those events for which the absence of a visible decay secondary has made necessary the identification of the nature of the particle from measurements of $\bar{\alpha}$ and g. For each pair of values $\bar{\alpha}$ and g relative to the various particles of an uncertain nature the value of the corresponding mass was obtained. The single values turned out to be gathered in two groups clearly separated with the mean values of $975 \pm 50\ m_e$ and $1760 \pm 90\ m_e$. The deviations from the expected values are within statistical fluctuations.

Appendix II

The procedure used to transform the K-nucleon scattering events observed in the laboratory system to the center of mass system runs as follows:

We have first to consider all the possible initial states of the nucleons in the nucleus according to the Fermi distribution and calculate for each of them what should be the angle of scattering θ_c between K and nucleon in the center of mass system which with fixed values of E_1 and E_2 (energies of the incident and outgoing K's) should give the observed angle θ_L in the laboratory system.

Each of these possible θ_c values has then to be weighted according to the following factors: *a*) the weight of the nucleon configuration in the Fermi sphere of momenta; *b*) the factor $(\overline{V} - \overline{V}')/\overline{V}$, where $\overline{V}'$ is the nucleon velocity and $\overline{V}$ is the velocity of the K; *c*) a weight proportional to the value of the total cross-section K-nucleon as a function of energy: this factor has been deduced from the observed increase of the total cross-section K-nucleus (Fig. 4), roughly corrected for the effect of Pauli principle and the Coulomb factor; *d*) finally each value should be weighted also according to the differential angular cross-section K-nucleon: as this is unknown we have assumed an isotropic distribution.

In each case in which the recoiling nucleon in the laboratory system happens to have an energy smaller than the upper limit of the Fermi sphere, a weight 0 is given to the corresponding configuration of the collision, as required by the Pauli principle.

For any experimental event all the weights corresponding to a given center of mass system angle value are then summed together, and normalized to 1; and so to any event corresponds a probability distribution covering a given range of possible θ_c values: the histograms of Fig. 10 *a*, *b*, were made by summing these probabilities for all events.

RIASSUNTO

Sono stati seguiti 110 m di traccia di K^+ nell'intervallo energetico da 40 a 160 MeV. Gli eventi osservati sono stati classificati nel seguente modo: *a*) 5 urti K-H; *b*) 170 scattering elastici e 91 anelastici; *c*) 10 scambi di carica; *d*) 46 decadimenti in volo. La discriminazione tra scattering elastici ed anelastici è stata fatta con un metodo statistico che è discusso in Sez. 3. Abbiamo diviso inoltre gli eventi in due intervalli energetici, da 40 a 90 MeV e da 90 a 160 MeV, al fine di studiare la variazione della sezione d'urto con l'energia per gli eventi elastici e per quelli anelastici (vedi Tabella III e Fig. 4). Dall'analisi degli eventi elastici abbiamo trovato l'esistenza di un potenziale nucleare repulsivo di circa 15 MeV. Questo risultato è in accordo con le caratteristiche relative agli eventi anelastici. Dall'analisi degli eventi anelastici abbiamo cercato di ottenere alcune informazioni intorno alla sezione d'urto elementare K-nucleone, e attualmente i nostri dati sembrano indicare che nell'intervallo energetico studiato, lo stato isotopico $T=1$ è preponderante, probabilmente come onda S. Nell'intervallo energetico più alto è probabile un piccolo contributo di uno stato $T=0$ come onda P.

On the Scattering of K^+-Mesons by Nucleons in Perturbation Theory (*).

C. Ceolin and L. Taffara

Istituto di Fisica dell'Università - Padova
Istituto Nazionale di Fisica Nucleare - Sezione di Padova

(ricevuto il 13 Novembre 1956)

Summary. — Using the method of Feynman and considering both the Λ and Σ-particles as intermediate states, the differential and total cross-sections for the scattering of scalar and pseudoscalar K^+-mesons by nucleons have been calculated in the second order approximation of perturbation theory. As a result, the various values are given which may be assumed by the ratios:

$$R = \frac{\text{process with charge exchange}}{\text{process without charge exchange}} \quad \text{and} \quad R' = \frac{\sigma(K^- N)}{\sigma(K^- P)},$$

as a function of the ratio $s = g_\Lambda^2/g_\Sigma^2$ of the interaction constants for the reactions $N \to K + \Lambda$ and $N \to K + \Sigma$. These results are then discussed in relation to the few experimental data so far available.

1. – Introduction.

The study of the interactions of K^--mesons with nucleons is today of the greatest importance in that one may hope to obtain information which, together with that already obtained from the study of decay process and production regarding spin, parity, isotopic spin, etc., allow us to clarify our ideas about the nature of these particles.

As the interactions of K^+ with hydrogen nuclei are very rare (owing to the long mean free path), the most experimental data so far available are con-

(*) Presented at the Turin Conference, September 1956.

cerned with events in which the K^- interacts with the whole of the nucleus, and from which information about elementary scattering of K^- by nucleons can by obtained indirectly [1]; therefore the experimental results on which one can rely and of which the theory must take account are, at present, rather scarce; and there are very few tests for limiting the choice of a theoretical interpretation.

The success of the Gell-Mann scheme in interpreting, at least qualitatively, some prominent aspects of the phenomenology of the heavy unstable particles has, as is well known [2], suggested some of the principal characteristics of these particles. K-mesons (without distinguishing the possible subgroups) are considered as bosons and isofermions (of isotopic spin $T=\frac{1}{2}$), while the hyperons are fermions and isobosons (of isotopic spin $T=0$ for the Λ, and $T=1$ for the Σ).

With these values assigned, the Gell-Mann selection rules require that, in K^--nucleon scattering, the reactions occur through intermediate states which, when we limit our considerations to the second order process only, can only be those which appear in the scheme:

$$\text{(1)} \qquad K + N \to K + K + Y \to K + N,$$

where Y indicates a hyperon which may be either the Λ or the Σ.

The total isotopic spin of the reaction (1) can obviously assume the value zero or unity. It is now necessary to establish what influence the consideration of the Λ or the Σ as possible intermediate states may have on the scattering amplitudes of the pure T-states, and to calculate explicitly the values of these amplitudes in order to obtain the respective differential and total cross-sections. At present, there are two possible ways which are both simple and natural for the first evaluation of the values of the scattering amplitudes: *a*) one of the few experimental data which may be considered as certain is that the interaction length of K^+-proton collisions is notably greater (and therefore the cross-section notably smaller) than the corresponding geometrical values. This relative weakness of the K^+-nucleon interaction allows one to

(1) J. LANNUTTI, W. CHUPP, G. GOLDHABER, S. GOLDHABER, E. HELMY, E. ILOFF, A. PEVSNER and D. RITSON: *Phys. Rev.*, **101**, 1617 (1956); Communications of S. GOLDHABER and N. DALLAPORTA (results for several european laboratories), Part. VI *Proceedings of the Sixth Rochester Conference* (1956). Communications of the plate groups of Bologna, Bristol, Dublin, Göttingen and Padua laboratories, Turin Conference, September 1956; M. BALDO-CEOLIN, M. CRESTI, N. DALLAPORTA, M. GRILLI, L. GUERRIERO, M. MERLIN, G. A. SALANDIN and G. ZAGO (to be published in *Nuovo Cimento*).

(2) M. GELL-MANN and A. PAIS: *Proceedings of the 1954 Glasgow Conference on Nuclear and Meson Physics* (London), p. 342.

think that a pure perturbation theory of this problem would not be without interest, at least as a first approach. *b*) The perturbation method however would prove inadequate for the treatment of the problem if the experimental evidence should lead to the discovery of resonant states in the scattering processes: in this case, a treatment of the same problem with the Tamm-Dancoff formalism could be more useful. In the present work we propose to deal with point *a*) only, that is to develop a theory of K^+-nucleon scattering by the method of perturbation in the second order approximation.

It is first necessary to make specific assumptions about the values of the spin and parity of the particles concerned. The more simple case (and the most plausible, considering the actual experimental situation [3]) consists in assuming a spin $\frac{1}{2}$ for the hyperons (both Λ and Σ) and spin zero for the K's; for the parity, however, since there are no indications for the hyperons and since that of K is controversial [4], it will be convenient to carry out the calculations both for scalar and pseudoscalar coupling.

In Sect. **2** the relationship between the scattering amplitudes will be obtained for the various intermediate states (Λ and Σ) and for the various values of isotopic spin. In Sect. **3** we will deal with the explicit calculation of the spatial part of the matrix element according to perturbation theory, and the corresponding results will be given for the collision cross-section and for the ratios R and R' (defined in the following Sections) for the various particular cases.

Finally, in Sect. **4**, the results of the preceeding sections will be compared with the few experimental data so far available.

2. – The only process compatible with the Gell-Mann selection rules which contributes to the K^+-nucleon scattering cross-sections in the second order approximation of perturbation theory, is that indicated in (1); its graph is represented in Fig. 1.

We intend, first, to study the dependence of the interaction matrix of this process on the isotopic spin.

We have here to face a somewhat new situation as a consequence of the fact that the graph which appears in Fig. 1, as one can easily see, has, in

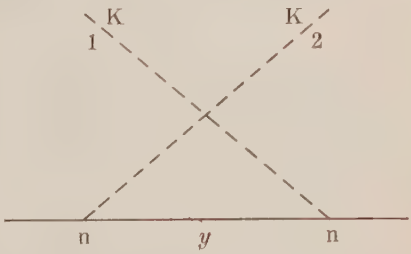

Fig. 1.

(3) M. RUDERMANN and R. KARPLUS: *Phys. Rev.*, **102**, 247 (1956); A. BONETTI, M. BALDO-CEOLIN, D. GREENING, S. LIMENTANI, M. MERLIN and G. VANDERHAEGHE: Turin Conference, September 1956 (in course of publication on *Nuovo Cimento*).

(4) T. D. LEE and C. N. YANG: *Phys. Rev.*, **102**, 290 (1956).

ordinary space only a fermionic line with one boson coming in and the other going out, while from the point of view of isotopic space it has two isofermionic lines connected by only one boson. Since both the K-meson and the nucleon depend in the same way on the isotopic spin, it is clear that, from the point of view of isotopic space, the graph of Fig. 1 is completely equivalent to the interaction diagram of two nucleons interacting by means of one pion.

Indicating with τ_1 and τ_2 the isotopic spins of the first and second isofermionic lines, the factor specifying the dependence of the interaction matrix of process (1) on the charge is then $\boldsymbol{\tau}_1 \cdot \boldsymbol{\tau}_2$ in the case in which the intermediate state is represented by a Σ-particle, and 1 (unit matrix) in the case in which the intermediate state is represented by the Λ-particle.

The interaction matrix results therefore to have the following expression:

$$H = g_\Sigma^2 \cdot \boldsymbol{\tau}_1 \cdot \boldsymbol{\tau}_2 \cdot M(\Sigma) + g_\Lambda^2 \cdot 1 \cdot M(\Lambda) \,, \tag{2}$$

where g_Λ and g_Σ are the interaction constants of the process $\mathrm{N} \rightarrow \mathrm{K} + \Lambda$ and $\mathrm{N} \rightarrow \mathrm{K} + \Sigma$ respectively and $\mathrm{M}(\Lambda)$ and $\mathrm{M}(\Sigma)$ are dependent only on the space co-ordinates and will be evaluated in Sect. **3**.

If we now consider the total isotopic spin, and indicate with H_0 and H_1 the matrix element (having a spatial dependence only) corresponding to the two states $T=0$ and $T=1$, then H can be also written in the following form:

$$H = P_0 \cdot H_0 + P_1 \cdot H_1 \,. \tag{3}$$

where P_0 and P_1 are the projection operators of the states $T=0$ and $T=1$ defined by:

$$P_0 = \frac{1 - \boldsymbol{\tau}_1 \cdot \boldsymbol{\tau}_2}{4} \,, \quad P_1 = \frac{3 + \boldsymbol{\tau}_1 \cdot \boldsymbol{\tau}_2}{4} \,. \tag{4}$$

By comparing (2) and (3) and taking account of (4), we get:

$$\begin{cases} H_1 = g_\Lambda^2 \cdot M(\Lambda) + g_\Sigma^2 \cdot M(\Sigma) \,, \\ H_0 = g_\Lambda^2 \cdot M(\Lambda) - 3 g_\Sigma^2 \cdot M(\Sigma) \,. \end{cases} \tag{5}$$

From the experimental point of view, elementary reactions which may be directly studied are the following:

$$\begin{cases} a) \quad \mathrm{K}^+ + \mathrm{p} \rightarrow \mathrm{K}^+ + \mathrm{p} \\ b) \quad \mathrm{K}^+ + \mathrm{N} \rightarrow \mathrm{K}^+ + \mathrm{N} \\ c) \quad \mathrm{K}^+ + \mathrm{N} \rightarrow \mathrm{K}^0 + \mathrm{p} \end{cases} \tag{6}$$

the first and the second representing the pure scattering, and the third charge exchange scattering. In this way, we are interested only in the matrix elements of matrix (3) corresponding to the reactions *a*), *b*) and *c*).

In evaluating these matrix elements, it is useful to remember the graph of Fig. 1: from this it clearly results that, while τ_1 refers to the isofermionic line (which consists of nucleon-K), τ_2 refers to the isofermionic line 2 (which consists of K-nucleon); therefore, τ_1 operates on the parts pecified by the index 1, and τ_2 operates on the part specified by index 2. In this way, the eigenfunctions of the initial and final states must be chosen in such a way that, if the first is represented by $\eta_K(1)\cdot\eta_N(2)$ the second must be represented by $\eta_N(1)\cdot\eta_K(2)$.

According to this, the matrix elements we have to calculate are:

$$\begin{aligned} H(\mathrm{K^+p}\,|\,\mathrm{K^+p}) &= \langle\eta_p(1)\cdot\eta_{K^+}(2)\,|\,H\,|\,\eta_{K^+}(1)\cdot\eta_p(2)\\ H(\mathrm{K^+N}\,|\,\mathrm{K^+N}) &= \langle\eta_N(1)\cdot\eta_{K^+}(2)\,|\,H\,|\,\eta_{K^+}(1)\cdot\eta_N(2)\rangle\\ H(\mathrm{K^+N}\,|\,\mathrm{K^0p}) &= \langle\eta_N(1)\cdot\eta_{K^+}(2)\,|\,H\,\eta_{K^0}(1)\cdot\eta_p(2)\rangle \end{aligned}$$

and applying (3) and (4) we obtain:

$$(7)\qquad \begin{cases} H(\mathrm{K^+p}\,|\,\mathrm{K^+p}) = H_1\\ H(\mathrm{K^+N}\,|\,\mathrm{K^+N}) = \frac{1}{2}(H_1 - H_0)\\ H(\mathrm{K^+N}\,|\,\mathrm{K^0p}) = \frac{1}{2}(H_1 + H_0) \end{cases}$$

which, taking account of (5) becomes:

$$(8)\qquad \begin{cases} H(\mathrm{K^+p}\,|\,\mathrm{K^+p}) = g_\Lambda^2\cdot M(\Lambda) + g_\Sigma^2\cdot M(\Sigma)\\ H(\mathrm{K^+N}\,|\,\mathrm{K^+N}) = 2\cdot g_\Sigma^2\cdot M(\Sigma)\\ H(\mathrm{K^+N}\;\mathrm{K^0p}) = g_\Lambda^2\cdot M(\Lambda) - g_\Sigma^2\cdot M(\Sigma) \end{cases}$$

3. – The evaluation of the spatial parts $M(\Lambda)$ and $M(\Sigma)$ is carried out with the usual technique of Feynman diagrams. We get:

$$(9)\qquad M(y) = 2\pi\left(\frac{M^2}{W_0\cdot W_1\cdot E_0\cdot E_1}\right)^{\frac{1}{2}} \frac{\overline{u}_1\cdot\Gamma\cdot(\not{p}_0 \quad \not{f}_1 \quad M_\Sigma)\Gamma\cdot u_0}{M^2 + m^2 - M_Y^2 - 2p_0k_1},$$

where the meaning of the symbols is as follows:

M = nucleon mass
M_Y = hyperon mass
m = K-meson mass

$E, \boldsymbol{p}$ = energy momentum four-vector of the nucleon

$W, \boldsymbol{p}$ = energy momentum four-vector of the K-meson

u_0 and u_1 = spinors representing the nucleon in the initial and final state respectively

$$\Gamma = \begin{cases} 1 \text{ for the scalar case} \\ \gamma_5 \text{ for the pseudoscalar case.} \end{cases}$$

All the quantities are measured in units $\hbar = c = 1$. Expression (9) is valid for both the cases of $Y = \Lambda$ and $Y = \Sigma$.

Finally, applying the well known formula:

$$(10) \qquad d\sigma = \frac{1}{(2\pi)^2} |H|^2 \cdot \frac{\frac{1}{8} W_0 W_1 E_1}{(W_0^2 - m^2)} dW_1,$$

and by means of (8) the following expressions for the differential and total cross-section are obtained:

$$(11) \qquad \begin{cases} d\sigma(K^+p \,|\, K^+p) = (g_\Sigma^4 \cdot A_\Sigma^2 + g_\Lambda^4 \cdot A_\Lambda^2 + 2 g_\Sigma^2 \cdot g_\Lambda^2 \cdot A_\Sigma \cdot A_\Lambda) dw_1 \\ d\sigma(K^+N \,|\, K^+N) = 4 g_\Sigma^4 \cdot A_\Sigma^2 \cdot dw_1 \\ d\sigma(K^+N \,|\, K^0p) = (g_\Sigma^4 \cdot A_\Sigma^2 + g_\Lambda^4 \cdot A_\Lambda^2 - 2 g_\Sigma^2 \cdot g_\Lambda^2 \cdot A_\Sigma \cdot A_\Lambda) dw_1 \end{cases}$$

with:

$$(12) \qquad \begin{cases} A_Y^2 = \dfrac{\pi\{2(1 + \mu_Y)^2 + (w_0 - w_1)[(1 + \mu_Y)^2 - \mu^2] - 2(1 + \mu_Y)(w_0 + w_1) - 2w_0 \cdot w_1\}}{M^2(w_0^2 - \mu^2)(1 + \mu^2 - \mu_Y^2 - 2w_1)^2} \\ A_Y \cdot A_{Y'} = \\ - \dfrac{\pi\{(1 + \mu_Y)(1 \pm \mu_{Y'})(2 - w_0 - w_1) + [2w_0 \cdot w_1 - \mu^2(w_0 - w_1)] - (w_0 + w_1)(2 \pm \mu_Y \pm \mu_{Y'})\}}{M^2(w_0^2 - \mu^2)(1 + \mu^2 - \mu_Y^2 - 2w_1)(1 + \mu^2 - \mu_{Y'}^2 - 2w_1)^2} \end{cases}$$

where all the energies are measured in units of M and the two signs (plus and minus) are referred respectively to the scalar and pseudoscalar cases.

In Fig.s 2 and 3 the form of $A_\Sigma^2 \cdot (dw_1/d\vartheta)$, $A_\Lambda^2 \cdot (dw_1/d\vartheta)$ and $A_\Sigma \cdot A_\Lambda \cdot (dw_1/d\vartheta)$ are reported as a function of the scattering angle and for a kinetic energy of the incident meson of 80 MeV (scalar and pseudoscalar case).

In Figs. 4, 5 and 6 are given the shapes of the differential cross-sections for the varios processes of defined charge in the particular case $g_\Sigma^2 = g_\Lambda^2$ both in the laboratory system an in the c.o.m. system.

On integrating (11) we obtain the corresponding total cross sections. The

result is:

$$
(13)\qquad
\begin{cases}
\sigma(\mathrm{K^+p}\,|\,\mathrm{pK^+}) = g_\Sigma^4 B_\Sigma + g_\Lambda^4 \cdot B_\Lambda + 2g_\Lambda^2 \cdot g_\Sigma^2 \cdot B_{\Lambda\Sigma} \\
\sigma(\mathrm{K^+N}\,|\,\mathrm{NK^+}) = 4g_\Sigma^4 \cdot B_\Sigma \\
\sigma(\mathrm{K^+N}\,|\,\mathrm{K^0})\mathrm{N} = g_\Sigma^4 B_\Sigma + g_\Lambda^4 \cdot B_\Lambda - 2g_\Lambda^2 \cdot g_\Sigma^2 B_{\Lambda\Sigma}
\end{cases}
$$

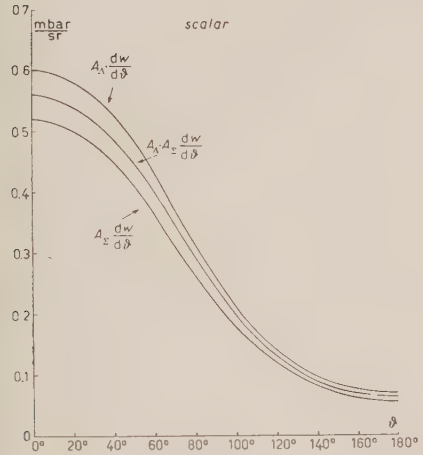

Fig. 2.

Fig. 3.

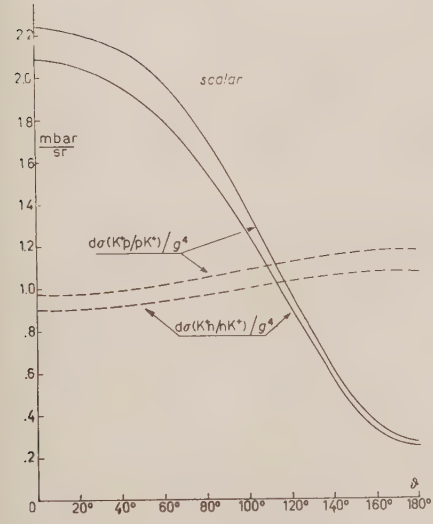

Fig. 4. - – – – differential cross section in c.m. system; —— differential cross section in laboratory system.

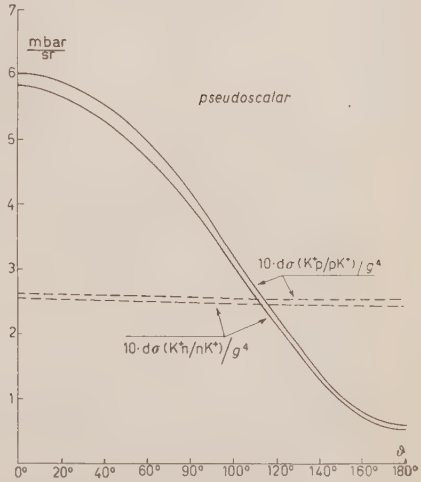

Fig. 5. - – – – differential cross section in c.m. system; — differential cross section in laboratory system.

with

$$
(14)\quad
\begin{cases}
B_{\Upsilon} = \dfrac{\pi}{4M^2(w_0^2-u^2)}\cdot \\
\qquad \cdot\Big\langle \dfrac{2(w_0-\eta)\{4(1\pm\mu_{\Upsilon})^2 \quad (1+\mu^2-\mu_{\Upsilon}^2)[(2\pm\mu_{\Upsilon})^2-(1+\mu^2)]\}}{(1+\mu^2-\mu_{\Upsilon}^2-2w_0)(1+\mu^2-\mu_{\Upsilon}^2-2\eta)} + \\
\qquad -[2w_0-(2\pm\mu_{\Upsilon})^2+(1+\mu^2)]\log_{\Upsilon}\Big\rangle \\
B_{\Upsilon\Upsilon'} = \dfrac{\pi}{M^2(\mu_{\Upsilon}^2-\mu_{\Upsilon'}^2)(w_0^2-\mu^2)}\cdot\langle\{2(1\pm\mu_{\Upsilon})(1\pm\mu_{\Upsilon'})(2+w_0)- \\
\qquad -2w_0(\mu^2+2\pm\mu_{\Upsilon}\pm\mu_{\Upsilon'})-(\mu_{\Upsilon'}^2-\mu^2-1)[2w_0+\mu^2-(1\pm\mu_{\Upsilon})(1\pm\mu_{\Upsilon'})- \\
\qquad -(2\pm\mu_{\Upsilon}\pm\mu_{\Upsilon'})]\}\log_{\Upsilon'}-\{2(1+\mu_{\Upsilon})(1\pm\mu_{\Upsilon'})(2+w_0)- \\
\qquad -2w_0(\mu^2+2\mp\mu_{\Upsilon}\pm\mu_{\Upsilon'}) \quad (\mu_{\Upsilon}^2-\mu^2-1)[2w_0+\mu^2- \\
\qquad -(1\pm\mu_{\Upsilon})(1\pm\mu_{\Upsilon'})-(2\pm\mu_{\Upsilon}\pm\mu_{\Upsilon'})]\}\log_{\Upsilon}\rangle,
\end{cases}
$$

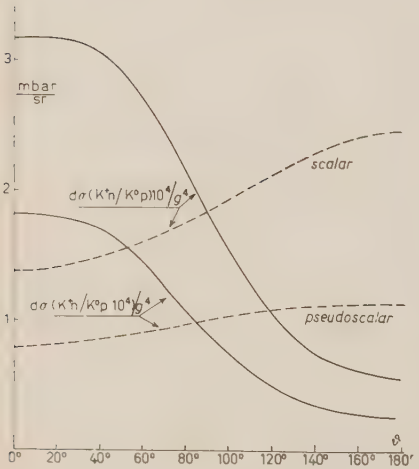

Fig. 6. - ---- differential cross section in c.m. system; differential cross section in laboratory system.

where

$$
(15)\quad
\begin{cases}
\log_{\Upsilon} = \log\dfrac{1+\mu^2-\mu_{\Upsilon}^2-2w_0}{1+\mu^2-\mu_{\Upsilon}^2-2\eta}, \\
\eta = \dfrac{w_0-w_0\mu^2-2\mu^2}{1+2w_0+\mu^2}.
\end{cases}
$$

In Figs. 7 and 8 B_{Σ}, B_{Λ} and $B_{\Lambda\Sigma}$ are given as functions of energy for the scalar and pseudoscalar cases; in Figs. 9, 10 and 11 are represented the total cross-sections for the particular case $g_{\Lambda}^2 = g_{\Sigma}^2$.

For a comparison with experimental data, in addition to the shape of the differential and total cross-section, it is also useful to refer to the values of the ratios:

$$
R = \frac{\text{processes with charge exchange}}{\text{processes without charge exchange}} \quad \text{and} \quad R' = \frac{\sigma(K^+N)}{\sigma(K^+p)},
$$

which, in the approximation used in this work are given by:

$$
(16)\qquad R = \frac{g_{\Sigma}^4\cdot B_{\Sigma} + g_{\Lambda}^4\cdot B_{\Lambda} - 2\cdot g_{\Lambda}^2\cdot g_{\Sigma}^2\cdot B_{\Lambda\Sigma}}{5\cdot g_{\Sigma}^4 B_{\Sigma} + g_{\Lambda}^4\cdot B_{\Lambda} + 2\cdot g_{\Lambda}^2\cdot g_{\Sigma}^2\cdot B_{\Lambda\Sigma}},
$$

$$R' = \frac{4 \cdot g_\Sigma^4 B_\Sigma}{g_\Sigma^4 \cdot B_\Sigma + g_\Lambda^4 \cdot B_\Lambda + 2 \cdot g_\Lambda^2 \cdot g_\Sigma^2 B_{\Lambda\Sigma}} . \tag{17}$$

It is possible to obtain easily a distribution of R and R' as a function of the ratio $s = g_\Lambda^2 / g_\Sigma^2$. By putting, for the sake of semplicity, $B_\Sigma = B_\Lambda = B_{\Lambda\Sigma}$ (which is true to a good approximation, as one can see from Fig. 6, especially for the pseudoscalar case) we get:

$$R = \frac{(1-s)^2}{4 + (1+s)^2} , \qquad R' = \frac{4}{(1+s)^2} . \tag{18}$$

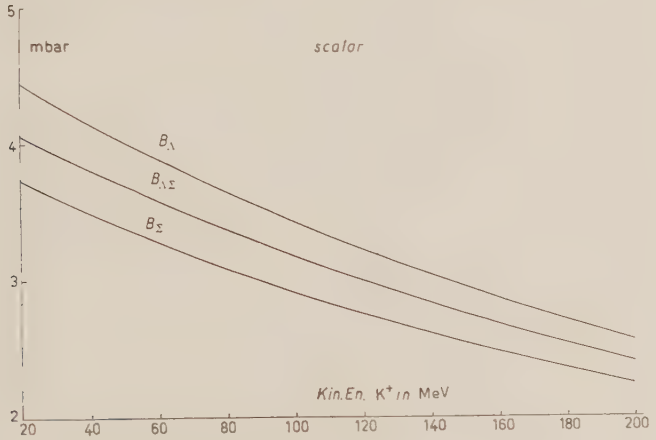

Fig. 7.

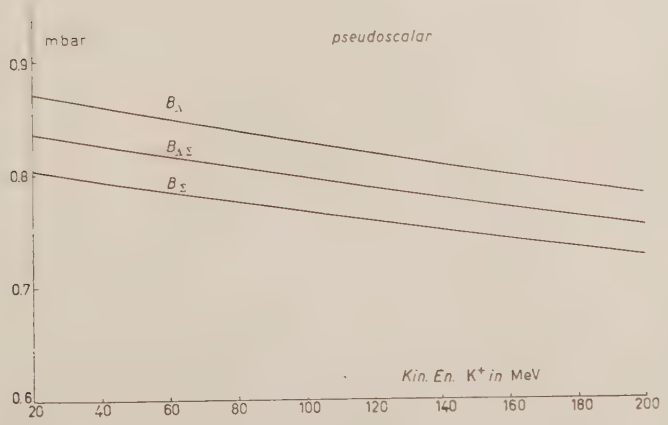

Fig. 8.

In Figs. 12 and 13 R and R' are given as function of s. In these figures a representation is used in which the distances of a point of the axis of the

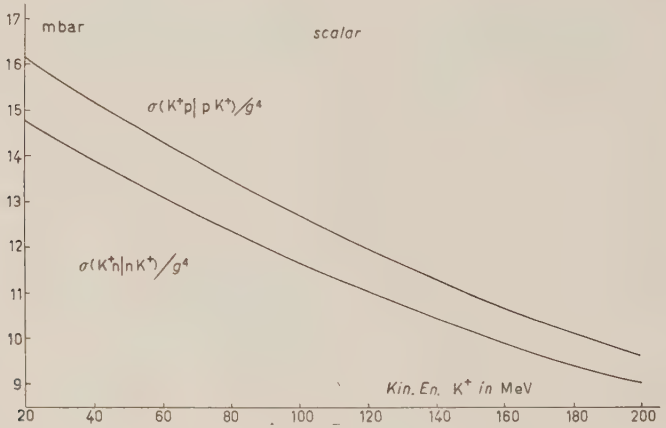

Fig. 9.

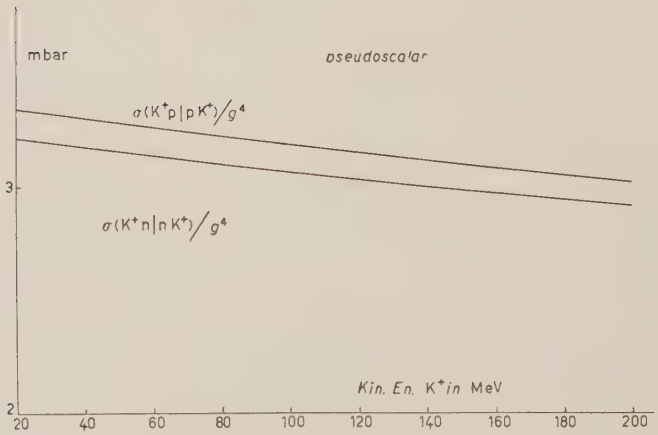

Fig. 10.

abscissae from the points A and D are proportional respectively to g_Λ^2 and g_Σ^2. in this way the ratio of such distances gives directly the values of s. Further we have added points A, B, C and D corresponding to the cases $g_\Lambda^2 = 0$, $g_\Lambda^2 = g_\Sigma^2$, $g_\Lambda^2 = 3g_\Sigma^2$ and $g_\Sigma^2 = 0$. As one case see from (5), in the point C,

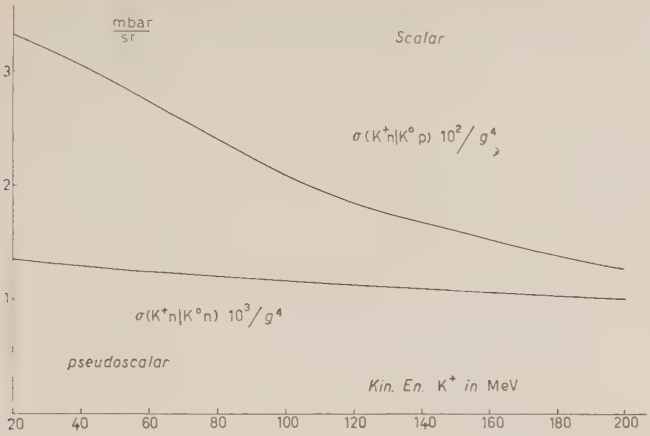

Fig. 11.

corresponding to $s = 3$, the scattering amplitude $T = 0$ vanishes. In this case the most important state in the scattering should be that corresponding to $T = 1$ even without the presence of resonance phenomena.

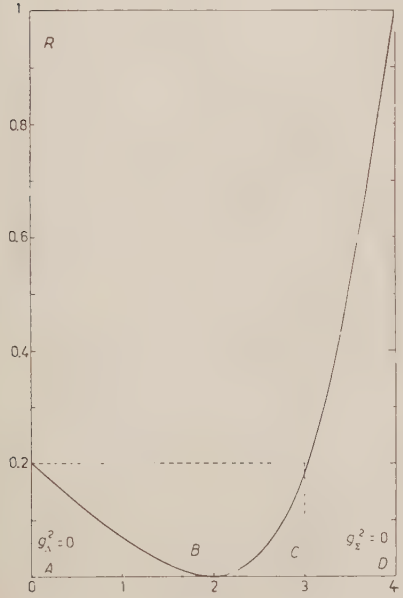

Fig. 12.

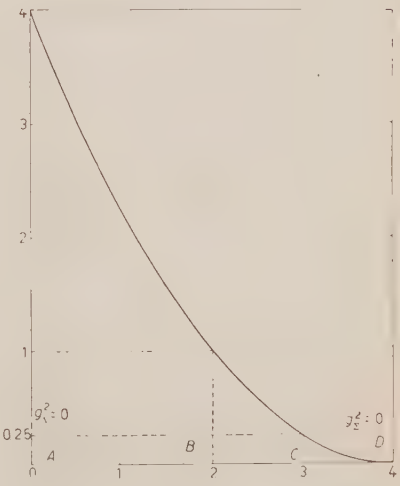

Fig. 13.

4. – As has already been stated in the first Section, the experimental data on the K-nucleon scattering at present available, are not yet sufficent to allow a clear picture of the process as a whole to be drawn. As a result, the comparison of our results with this experimental evidence can have only a limited meaning.

According to the results discussed in their paper by BALDO *et al.* [1] for the energy range of the incoming K of about 70 MeV in the laboratory system, the scattering should be due chiefly to the $T=1$ state. If we assume that the value of about 10 mb for the total cross-section in this case is correct (as deduced from the pure K-hydrogen scattering, when the observed value of 14 mb is corrected for the Coulomb constructive interference), this allows us to determine the value of the interaction constants g_Λ^2 and g_Σ^2; since in our theory state $T=1$ correspond to $g_\Lambda^2 = 3 \cdot g_\Sigma^2$, we get:

$$\text{for the pseudoscalar case} \qquad g_\Sigma^2 \approx 0.9\,, \qquad g_\Lambda^2 \approx 2.7\,,$$

$$\text{for the scalar case} \qquad g_\Sigma^2 \approx 0.4\,, \qquad g_\Lambda^2 \approx 1.2\,.$$

The values thus obtained are less than that for the pions in the pseudoscalar case ($g^2_{\text{pions}} \approx 10$) and greater than that for the pions in the scalar case ($g^2_{\text{pions}} \approx 0.25$).

Nothing definite can be said concerning the behaviour of the cross-sections with the energy, since the apparent increase of the total cross-sections with energy may be due to the decreasing effect of the Pauli principle in forbidding small angle interactions with decreasing energy [1].

Therefore the behaviour obtained in our theory, although not very probable, cannot yet be considered as disproved by the actual data.

If we now consider the angular distribution of the cross-sections, the present evidence based chiefly on the few pure K-proton data, seems to indicate, especially when corrected from the Coulomb interference, a behaviour which is rather flat. This again is in agreement with the behaviour predicted in our theory either for scalar and pseudoscalar couplings.

Therefore we may conclude that, a far as present data are concerned, perturbation theory does not present in the case of K-nucleon scattering so a striking disagreement with observation as for the case of the pion scattering, and this somewhat contributes to strengthen the reasons according to which this calculation was thought to be of some interest.

* * *

We are greatly indebted to Prof. N. DALLAPORTA for useful discussion and advice.

RIASSUNTO

Usando il metodo di Feynman e considerando sia la particella Λ che la particella Σ come possibili stati intermedi, sono state calcolate le sezioni d'urto differenziali e totali, nell'approssimazione del secondo ordine della teoria delle perturbazioni, per lo scattering di mesoni K scalari e pseudoscalari su nucleoni. Sono stati inoltre dati i vari valori che i rapporti:

$$R \quad \frac{\text{processi con scambio carica}}{\text{processi senza scambio carica}} \quad \text{e} \quad R' = \frac{\sigma(K^+N)}{\sigma(K^-p)},$$

possono assumere in funzione del rapporto $s = g_\Lambda^2/g_\Sigma^2$ fra le costanti di interazione riguardanti i processi elementari $N \to K + \Lambda$ e $N \to K + \Sigma$. Alla fine sono stati discussi i risultati ottenuti dalla presente teoria in relazione ai pochi risultati sperimentali finora disponibili.

K^+ Nuclei Interactions According to the Optical Model (*).

G. Costa and G. Patergnani

Istituto di Fisica dell'Università - Padova
Istituto Nazionale di Fisica Nucleare - Sezione di Padova

(ricevuto il 13 Novembre 1956)

Summary. — The optical model has been applied to the scattering of K^+-mesons by nuclei. We have determined the nuclear potential V_n following two different procedures: the first consists in the calculation of the elastic K^+-nucleus cross-sections as functions of V_n; the second connects V_n with the total inelastic K^+-nucleus cross-section through the elementary K^+-nucleon interaction, described by means of a Yukawa potential. The results obtained in the two cases are very similar.

1. – Introduction.

Several investigations of the scattering of K^+ mesons by nuclei of nuclear emulsions are at present in course [1,2]. The experimental conditions generally allow analysis of the events in order to discriminate between elastic and inelastic scattering, in a rather similar way as was done for the scattering of π-mesons by nuclei. As is well known, this phenomenon has been interpreted

(*) Presented at the Turin Conference, September 1956.

[1] J. Lannutti, W. Chupp, G. Goldhaber, S. Goldhaber, E. Helmy, E. Iloff, A. Pevsner and D. Ritson: *Phys. Rev.*, **101**, 1617 (1956); Communications of S. Goldhaber and N. Dallaporta (results for several European laboratories), Part VI *Proceedings of the Sixth Rochester Conference*, 1956; Communications of the plate groups of Bologna, Bristol, Dublin, Göttingen and Padua laboratories, Turin Conference, September 1956; L. T. Kerth, D. H. Stork, R. W. Birge, R. P. Haddock, M. N. Whitehead: *Bull. Am. Phys. Soc..*, **30**, No. 3.

[2] M. Baldo-Ceolin, M. Cresti, N. Dallaporta, M. Grilli, L. Guerriero, M. Merlin, G. Salandin and G. Zago: *Nuovo Cimento*, **5**, 402 (1957).

by different authors by means of the optical model (3); and this coherently describes the various features of the process (1). Therefore, it seemed useful to us to apply now also the general theory of this model to the particular case of K^--mesons.

In the general formulation of the optical model the nucleus is described by means of a complex potential $V_r + i V_i$, so that the nuclear interaction of a particle is reduced to a two-body problem. The real part of the potential directly determines the elastic coherent scattering: for this the imaginary part also contributes through shadow scattering: the imaginary part causes, on the other hand, an attenuation of the intensity of the incoming particle wave. The model does not specify what happens to the particle subtracted from the incident beam: in our case we assume that it is never absorbed, according to the Gell-Mann rules (5), and that it suffers a scattering by a single nucleon, which makes it appear after the process as the result of an inelastic interaction.

It is now known that the mean free path of K^- in nuclear matter is very long ($\lambda \sim 3.5 \cdot 10^{-12}$ cm for kinetic energies of the order of 80 MeV) (2). From this value we can deduce the imaginary part of the potential, by means of the relation (6):

$$\frac{2V_i}{h} = \frac{\beta c}{\lambda} .$$

We obtain for V_i a value of about one MeV: this allows us to say at once that, taking also in account the order of magnitude of the experimental elastic cross-section, the shadow scattering must be negligible. We assume therefore that the coherent scattering of K^-, at least in the energy interval considered, is only due to the real potential: this consists of a Coulomb term V_c, for which we have chosen the expression determined by a uniform spatial distribution of electric charge, and a nuclear term V_n.

(3) General formulation: H. A. Bethe: *Phys. Rev.*, **57**, 1125 (1940); S. Fernbach, R. Serber and T. B. Taylor: *Phys. Rev.*, **75**, 1352 (1949); applications to nucleon scattering: K. M. Gatha and R. J. Riddel: *Phys. Rev.*, **86**, 1035 (1952); H. Feshbach, C. E. Porter and V. F. Weisskopf: *Phys. Rev.*, **90**, 116 (1953); **96**, 448 (1954); applications to π-meson scattering: E. Clementel: *Nuovo Cimento*, **9**, 369 (1952); A. Pevsner and J. Rainwater: *Phys. Rev.*, **100**, 1431 (1955).

(4) A. Minguzzi, G. Puppi and A. Ranzi: *Nuovo Cimento*, **2**, 178 (1955); A. Minguzzi: *Nuovo Cimento*, **12**, 799 (1955).

(5) M. Gell-Mann: *Phys. Rev.*, **92**, 833 (1953); K. Nishijima: *Prog. Theor. Phys.*, **12**, 107 (1954); M. Gell-Mann and A. Pais: *Proceedings of the Glasgow Conference on Nuclear and Meson Physics* (London, 1955); J. Lannutti W. Chupp, G. Goldhaber, S. Goldhaber, E. Helmy, E. Iloff, A. Pevsner and D. Ritson: *Phys. Rev.*, **101**, 1617 (1956).

(6) E. Clementel and C. Villi: *Nuovo Cimento*, **2**, 178 (1955).

Our aim is then to determine the nuclear potential V_n in value and sign: we have tried to do this in two different ways: first, we have considered V_n as a parameter and calculated the elastic scattering cross-section as a function of V_n; we may then obtain the value of V_n by comparison with the data. Secondly, we have tried to obtain V_n starting from the K^+-nucleon interaction. We have supposed that it might be described by means of a Yukawa potential, with a range of the order of the Compton wave length of the K and with a strength g^2 determined from experimental data. With these hypotheses we have calculated the potential V_n and the total inelastic K^+-nucleus cross-section; by comparing the latter with the corresponding experimental value it is possible to deduce g^2 and to obtain indirectly a value for V_n.

2. - Evaluation of the Nuclear Potential from Elastic Scattering.

As far as the elastic scattering of K^+ is concerned, we consider, as stated in the preceding section, only the real part of the potential. Its analitic expression in the inner region of the nucleus is the following:

$$V_r' = \frac{Ze^2}{r}\left[\frac{3}{2} - \frac{1}{2}\left(\frac{r}{R}\right)^2\right] + V_n , \tag{1}$$

that is, the potential due to a uniform distribution of electric charge plus a constant nuclear potential V_n; in the external region V_r reduces to the pure Coulomb potential

$$V_r'' = \frac{Ze^2}{r} . \tag{1'}$$

The radial wave function of the scattered particle is a solution of the equation

$$\frac{\mathrm{d}^2u}{\mathrm{d}r^2} + \left[\frac{2m}{\hbar^2}(E - V_r) - \frac{l(l+1)}{r^2}\right] u = 0 \tag{2}$$

in which the potential defined by (1) appears.

The general theory of the scattering of a particle by a modified coulombian field leads to the following expression for the differential cross-section, when the problem is treated in spherical co-ordinates, with the partial wave method (7).

$$\frac{\mathrm{d}\sigma}{\mathrm{d}\Omega} = \left| \frac{n}{2K \sin^2(\theta/2)} \exp\left[-in \ln \sin^2(\theta/2) + i\pi + 2i\eta_0\right] + \right. \tag{3}$$
$$\left. + \frac{1}{K}\sum_l (2l+1) \exp\left[i(2\eta_l + \delta_l)\right] \sin \delta_l \cdot P_l(\cos\theta) \right|^2$$

(7) L. I. SCHIFF: *Quantum Mechanics* (1949), p. 116, 120.

where

$$n = \frac{Ze^2}{\hbar v} \qquad \text{and} \qquad \eta_l = \arg \Gamma(l + 1 + in) .$$

In (3) the first term is the Rutherford scattering amplitude; the other terms are the scattering amplitudes for the different partial l-waves relative to the total potential in the internal region of the nucleus; the phases η_l represent the distorsion of the plane wave due to the coulombian field, while the phases δ_l indicate the deviation from these Coulomb functions of the wave function of the particle scattered by the field due to the potential (1). To calculate exactly these phases, one should have matched across the nuclear boundary the logarythmic derivatives of the radical wave functions which are solutions of equation (2). We have preferred to calculate the phase shifts by means of the approximation method of W.K.B.J. For the application of this method it is necessary that the relative variations of the potential are small within a distance equal to a wave length of the particle; for this reason we have substituted for a nuclear sharp boundary a gradual variation in an interval of the order of the range of nuclear forces. This is advantageous in comparison with the exact method, for in this way we were able to match continuously the potential of the inner region of the nucleus with the Coulomb one: this seems to us the physically more correct procedure.

We have used the modified formula of LANGER [8], in which instead of the expression $l(l+1)/r^2$ for the centrifugal potential there is the expression $(l - \frac{1}{2})^2/r^2$. In such a way the analitical form of the phase shifts, obtained as differences of the arguments of the asymptotic approximated wave functions with and without the nuclear potential [9], is the following:

$$(4) \qquad \delta_l = \int_{r_0}^{\infty} \sqrt{K^2 - U'_r - (l + \tfrac{1}{2})^2/r^2}\, \mathrm{d}r - \int_{r_1}^{\infty} \sqrt{K^2 - (2nK/r) - (l + \tfrac{1}{2})^2/r^2}\, \mathrm{d}r, \qquad \text{with} \quad U'_r = \frac{2m}{\hbar^2} V'_r ;$$

r_0 and r_1 are the turning points, solutions of the equations obtained by putting the two intergrands equal to zero.

[8] R. E. LANGER: *Phys. Rev.*, **51**, 669 (1937).

[9] P. M. MORSE and H. FESHBACH: *Methods of Theoretical Physics*, Part. II (1953). p. 1101.

With the phases shifts so obtained (*), we have calculated by means of (3) the differential cross-sections for four values of the kinetic energy of the

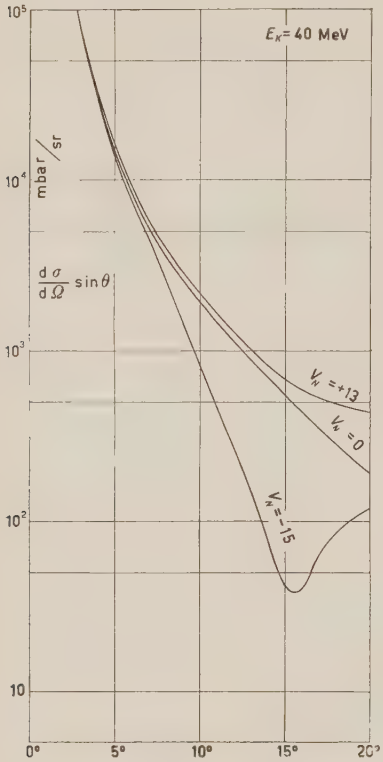

Fig. 1.

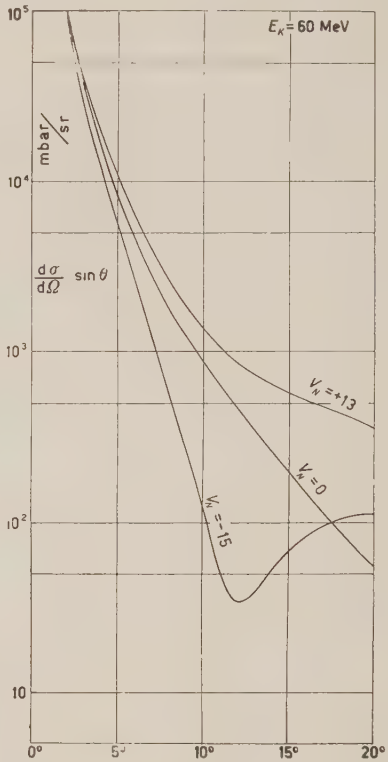

Fig. 2.

Differential cross-sections in the angular interval $2° \div 20°$.

(*) The calculation was partially made graphically. As a check we have also made an analitical calculation by assuming for V_r a constant mean value. With such an approximation, and from (4) follows:

$$(4') \qquad \delta_l = \sqrt{(K^2 - \overline{U}_r')R^2 - (l+\tfrac{1}{2})^2} - (l+\tfrac{1}{2})\cos^{-1}\frac{l+\tfrac{1}{2}}{R\sqrt{K^2-\overline{U}_r'}} -$$

$$- \sqrt{K^2R^2 - 2nKR - (l+\tfrac{1}{2})^2} - (l+\tfrac{1}{2})\sin^{-1}\frac{(l+\tfrac{1}{2})^2 + nKR}{KR\sqrt{(n^2+(l+\tfrac{1}{2})^2}} +$$

$$+ (l+\tfrac{1}{2})\sin^{-1}\frac{(l+\tfrac{1}{2})^2 + nKR}{Kr_1\sqrt{n^2+(l+\tfrac{1}{2})^2}} + n\ln\frac{\sqrt{K^2R^2 - 2nKR - (l+\tfrac{1}{2})^2} + KR - n}{Kr_1 - n}.$$

The values of the phases obtained in this way are very similar to those obtained with the graphical calculation.

K-meson ($E_k = 40$; 60; 80 and 100 MeV) and for different values of the nuclear potential V_n.

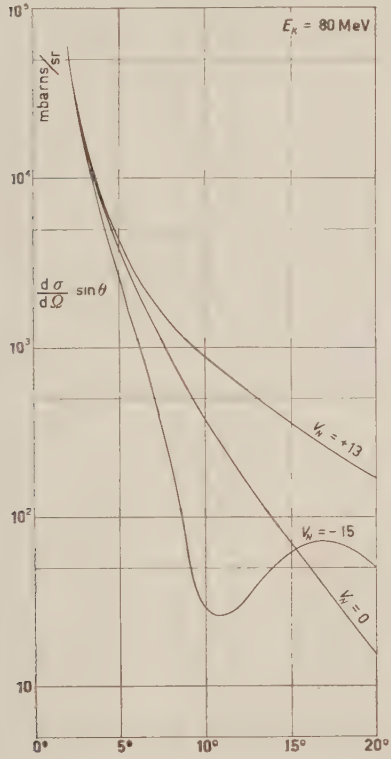

Fig. 3.

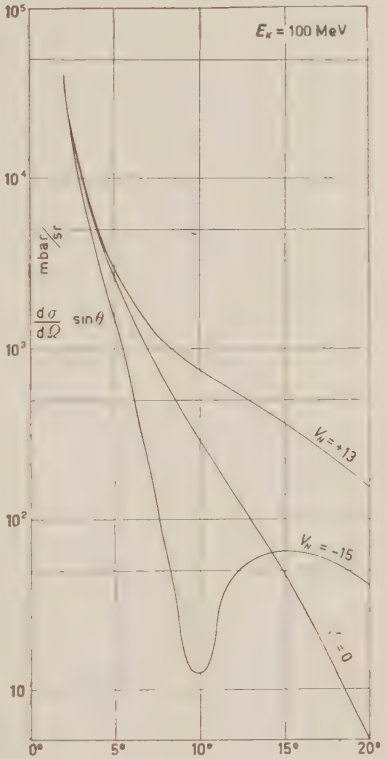

Fig. 4.

Differential cross-sections in the angular interval $2° \div 20°$.

We have considered the nuclei of nuclear emulsions as of two types: 43% heavy nuclei with $A = 95$, $Z = 42$, and 57% light nuclei with $A = 14$, $Z = 7$; as nuclear radius we have assumed $R = A^{\frac{1}{3}} r_0$ with $r_0 = 1.36 \cdot 10^{-13}$ cm. The number of phases required varies with energy and type of nucleus from a minimum of 3 or 4 for $E_k = 40$ MeV and a light nucleus, to a maximum of $9 \div 10$ for $E_k = 100$ MeV and a heavy nucleus.

The detailed shape of the differential cross-section seemed to us significant only for small angles and is given in Fig. 1-4 for the angular interval $2° \div 20°$: in this region the two Coulomb and nuclear potentials interfere strongly, and a by difference appears between the cases of attractive and repulsive V_n.

For larger angles the differential cross-section is strongly variable with

energy, with the value of the potential and with its shape at the nuclear boundary: therefore it cannot be used for comparison with present experimental data.

From these curves we have obtained the cross-sections integrated from 20° to 180°: they are reported in Fig. 5 for the different energies as functions of V_n. It is seen that the same value of the cross-sections may be obtained with two separate values of V_n different in modulus and generally also in sign.

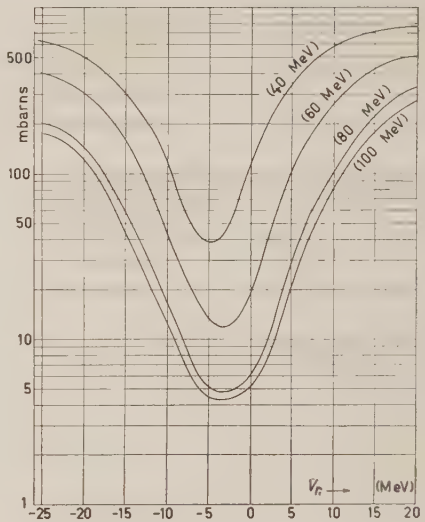

Fig. 5. - Elastic cross-sections integrated from 20° to 180° as functions of V_n.

The preceding results have been used, to calculate the value and sign of the potential V_n as is reported in the preceding paper of BALDO *et al.* [2].

To this purpose we may consider first another diagram (Fig. 6) which gives the cross-sections integrated from 20° to 180° as a function of the kinetic energy of the incoming K for different values of the potential V_n. In the same figure are reported also the experimental values obtained from elastic scattering data between 40 and 120 MeV. It is seen that for V_n we can assume, within the errors, in the whole energy interval, a constant value of about 15 MeV if repulsive, and somewhat greater than 20 MeV if attractive.

One can also calculate the mean value of the cross-section for the effective distribution in energy of the events observed and compare it with the mean cross-section [2]. In this way we obtain for the nuclear potential the two solutions $V_n = -22$ MeV and $V_n = +14$ MeV.

The decision between the two solutions has been obtained by integrating the differential angular cross-sections for small angles between 7° and 13° and comparing again with the observed values. The best agreement is obtained for the repulsive solution for a value of V_n somewhat greater than the preceding one [2]. The difference cannot be considered significant owing to the statistical errors. It is therefore considered that both determinations are consistent with a unique solution of a repulsive nuclear potential V_n of about 16 MeV.

3. – Evaluation of the Nuclear Potential from Inelastic Scattering.

Several attempts have been made to calculate the inelastic cross-sections of particles colliding with nuclei, starting from the interaction with free nucleons ([10,11]).

We have extended these proceedings to the particular case of K^+-mesons. Our aim is to calculate in another way the nuclear potential V_n, connecting it with the total inelastic K^+-nuclei cross-section, and at the same time to ascertain if it is possible to give a self-consistent description for elastic and inelastic scattering.

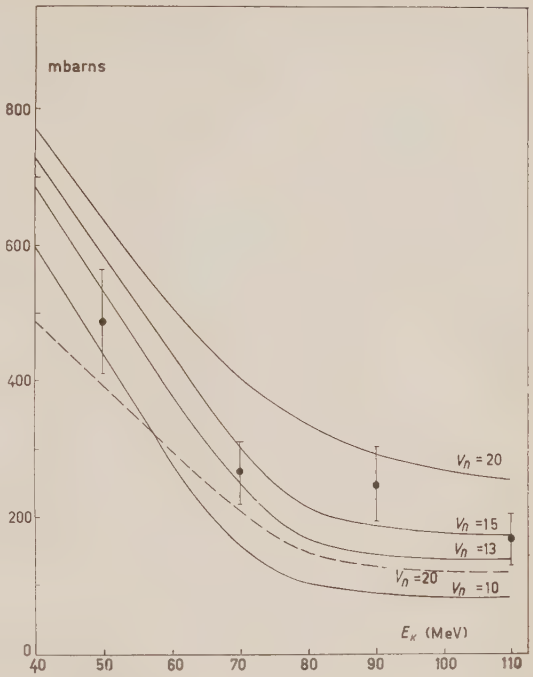

Fig. 6. – Elastic cross-sections integrated from 20° to 180° as functions of the kinetic energy of the incident K^+.

We assume that the K^+-nucleon interaction may be described by means of a Yukawa potential:

$$V(r) = (g^2/r) \exp[-\alpha r], \tag{5}$$

with a range $1/\alpha$ equal to the Compton wave length of K-particles; its strength g^2 is to be obtained from a comparison of the theoretical inelastic cross-section with the corresponding experimental value.

We do not hope to obtain, with such an interaction, correct angular and energy distributions for the K^+'s inelastically scattered by nuclei, except for what concerns the kinematics of interacting particles and their statistics. However, at the present stage of experimental data, this choice, requiring the

([10]) M. Lax: *Rev. Mod. Phys.*, **23**, 287 (1951); *Phys. Rev.*, **85**, 621 (1952); K. Watson: *Phys. Rev.*, **89**, 575 (1953).

([11]) M. Cini and S. Fubini: *Nuovo Cimento*, **2**, 75 (1955).

least number of assumptions seems to us the most reasonable. Further, the shape of the differential K-nucleon cross-section, determined by the type of assumed interaction; influences the total inelastic cross-section essentially with the ratio of forward and backward scattering; which determines the weight of the exclusion principle. In our case $30\,\%$ of the interactions are not allowed: this percentage is only slightly dependent on the range of the potential assumed.

Since the mean free path of K^+-mesons in nuclear matter appeared from experimental data to be long enough (much longer than that of pions) we thought that a first approximation perturbation method might give a likely result. We have used the independent particle model for the nucleus; that is to say we have described the nucleus as a product of antisymmetric eigenfunctions which we consider as plane waves. This should be strictly possible by considering a constant potential in a cubic spatial region; but if the nucleus is large enough with respect to the wavelength in consideration, as in our case, its form does not play an important role; under this assumption we may consider the total momentum to be conserved.

In the initial state we have the K-particle, represented as a plane wave, and the nucleus described as above, with all the lowest levels occupied. In the final state, having adopted a two body interaction, and considering that only one collision takes place in inelastic scattering, the nucleus has one excited level.

With the preceding hypotheses and approximations, the calculation is developed as described below. The inelastic cross-section is expressed by:

$$\sigma = \frac{\Omega_k}{v_k} w \,, \tag{6}$$

where Ω_k is the normalization volume for the incident K^+, v_k its velocity; w is the transition probability for unit time towards any final state in which the nucleus is excited as a consequence of the interaction with the K^+. In the first approximation we have:

$$w = \int \mathrm{d}N \, |\langle \psi_f | \, V \, | \psi_i \rangle|^2 \Delta_E^2(E_i - E_f), \tag{7}$$

where $V = \sum_{n=1}^{n=A} V(\bar{r}_n - \bar{r}_k)$, $E_i - E_f$ is the difference between the energies of the initial and final unperturbed states and

$$\Delta_E^2(E_i - E_f) = \frac{4}{(E_i - E_f)^2 t} \sin^2 \frac{(E_i - E_f)t}{2\hbar} \,.$$

$\mathrm{d}N$ is the number of final states, specified by the expression:

$$\mathrm{d}N = \frac{1}{(2\pi)^9} \Omega_n \Omega_n' \Omega_k' \, \mathrm{d}\bar{k}_n \, \mathrm{d}\bar{k}_n' \, \mathrm{d}\bar{k}_k' \,, \tag{8}$$

where $\bar{k}_n$, $\bar{k}'_n$ and $\bar{k}'_k$ are respectively the wave numbers of the excited nucleons, before and after the collision, and of the emerging K^+: Ω_n, Ω'_n and Ω'_k are the corresponding normalization volumes Ω_n and Ω'_n may be different from each other if the bound nucleon goes into a free state; we assume that it remains in the region of the nuclear potential also in the final state.

The coefficient 4 follows from having considered the two possibilities of spin and charge for nucleons, while for the K^+-particle we assume zero spin. ψ_i, ψ_f are the initial and final unperturbed eigenfunctions: they are different from each other for the substitution of the plane waves of a nucleon and of the incident K^+ in the former:

$$\frac{1}{\sqrt{\Omega_k}} \exp[-i\bar{k}_n \cdot \bar{r}_n] \cdot \frac{1}{\sqrt{\Omega_k}} \exp[-i\bar{k}_k \cdot \bar{r}_k], \tag{9}$$

with the plane waves of the excited nucleon and of the scattered K^+ in the latter

$$\frac{1}{\sqrt{\Omega'_n}} \exp[i\bar{k}'_n \cdot \bar{r}_n] \cdot \frac{1}{\sqrt{\Omega'_k}} \exp[i\bar{k}'_k \cdot \bar{r}_k]. \tag{9'}$$

Taking account of the antisimmetry of the eigenfunctions of nucleons, and of having considered a two body potential, we obtain:

$$\langle \psi_f | V | \psi_i \rangle = (\Omega_n \Omega'_n \Omega_k \Omega'_k)^{-\frac{1}{2}} \int \frac{g^2}{r} \exp[-\alpha r + i\bar{k} \cdot \bar{r} + i\bar{K} \cdot \bar{R}] \, \mathrm{d}\bar{r} \, \mathrm{d}\bar{R}, \tag{10}$$

where

$$r = \bar{r}_k - \bar{r}_n, \qquad \bar{R} = \tfrac{1}{2}(\bar{r}_k + r_n),$$

$$2\bar{k} = \bar{k}'_k - \bar{k}_k - \bar{k}_n - \bar{k}'_n, \qquad K = \bar{k}'_k + \bar{k}'_n - \bar{k}_k - \bar{k}_n.$$

The integrations must be carried out taking into account that the eigenfunctions describing the nucleons go to zero outside the nucleus: we may vary r from zero to infinity, and R only in the inner region of the nucleus; this approximation, which simplifies the calculation, is sufficiently good because the radius of the nucleus is large with respect to the range of the forces considered. Then we have:

$$\langle \psi_f | V | \psi_i \rangle = \frac{1}{\Omega_n \Omega_k} H(\bar{k}) \cdot I_p(K), \tag{11}$$

where

$$H(\bar{k}) = \int_{\Omega \to \infty} \frac{g^2}{r} \exp[-\alpha r + i\bar{k} \cdot \bar{r}] \, \mathrm{d}\bar{r}, \qquad I_p(\bar{K}) = \int_{\Omega_n} \exp[i\bar{K} \cdot \bar{R}] \, \mathrm{d}\bar{R}$$

and w assumes the expression:

$$w = \frac{1}{2^7 \pi^9 \Omega_n^2 \Omega_k^2} \int\int\int\int H^2(\bar{k})\ I_p^2(\bar{K})\ I_E^2(E_f - E_i)\, \mathrm{d}\bar{k}_n\, \mathrm{d}\bar{k}'_n\, \mathrm{d}\bar{k}'_k \,. \tag{12}$$

The calculation has been made conserving energy and momentum, that is we have substituted the functions A_p^2, A_E^2 with δ-functions: with an adequate change of variables and averaging over all the orientations of $\bar{k}_k$, since the final result must be independent of the latter ([11]), we arrived at the following expression for the total inelastic cross section:

$$\sigma_{in} = \frac{32}{3} A r_0^3 \left(\frac{c}{v_k}\right)^2 \left(\frac{g^2}{\hbar c}\right)^2 \int\int\int \frac{k}{(\varkappa^2 - k^2)^2}\, k_n^2\, \mathrm{d}k_n\, \mathrm{d}k\, \mathrm{d}\cos\vartheta \,. \tag{13}$$

where $A^{\frac{1}{3}} r_0$ is the radius of the nucleus, v_k is the velocity of the incident K^+, $\bar{k} = \bar{k}_n - \bar{k}'_n = \bar{k}'_k - \bar{k}_k$ and ϑ is the angle between $\bar{k}$ and $\bar{k}_n$.

The integration of k_n is made over all the values of the Fermi sphere while the other two integrations are made in an adequate region, limited by energy conservation and exclusion principles.

With the same hypotheses and approximations we have also calculated the nuclear potential V_n of the optical model, by averaging the elementary interaction over all the nucleons ([12]). This is easily obtained by considering in the matrix element the final state coincident with the initial one. We get in this way:

$$V_n = \langle \psi_i | V | \psi_i \rangle = \frac{3\hbar c}{r_0^3 \alpha^2} \left(\frac{g^2}{\hbar c}\right). \tag{14}$$

A comparison of the expression (13) with the experimental value for the total inelastic cross-section allows us to obtain a value for « g », and then a value for V_n, by means of (14). A comparison of the latter value with that obtained from the elastic cross-sections, as indicated in the preceding section, will test the validity and consistency of the model used.

The calculation has been made for 80 MeV: that is however the energy of the K^+ inside the nucleus; their energy outside will be, if we assume the repulsive solution for V_n and the Coulomb potential, about 100 MeV. We have then compared the formula (13) with the value of the experimental cross-section obtained around 100 MeV: from this comparison a value of $g^2/\hbar c = 0{,}55$

([12]) N. FRANCIS and K. WATSON: *Phys. Rev.*, **92**, 291 (1953); A. KIND and C. VILLI: *Nuovo Cimento*, **1**, 749 (1955); R. M. FRANK, J. L. GAMMEL and K. M. WATSON: *Phys. Rev.*, **101**, 891 (1956).

is deduced, and from it and from (14) we obtain $V_n = 18$ MeV a value of the same order of magnitude as the value directly obtained from elastic scattering.

The type of interaction between K and nucleon that has been assumed for our calculations in the second part of this work may be considered as being somewhat arbitrary: in fact, the model of the interaction is thus certainly oversimplified, as no difference is supposed to exist, independently from the Coulomb effect (*), between the interaction of the K^+ with proton and neutron, as seems to be the case according to the experimental data [2]. Therefore, no consideration has been given to the angular distribution, for which the type of interaction has much importance. For what concerns instead the total cross-section, it is important to observe that the quantity that determines its value either directly, or through the effect of the Pauli principle is chiefly the range of the potential: we have assumed that this range corresponds to the Compton wave length of the K. It may be observed that the inelastic cross-section and V_n depend in a rather critical way on this value, in such a way that it would not be easy to obtain an agreement for these two quantities with experimental data, when we should even slightly change the assumed value of this range. This seems to be rather independent of the exact shape assumed for the potential and may be considered in agreement with our assumption of considering only two body interactions. On the other hand, this assumption and the first approximation procedure here employed are also justified by the high value of the m.f.p. of the K^+ in nuclear matter observed experimentally. It would remain to be seen to what extent the binding energy of nucleons could be important: we think, referring to the preceding considerations, that it could have and influence chiefly on the kinematic relations and not on the integral values of the cross-sections. If we accept these remarks, we think that the results here obtained may be considered as an indication of the self consistency of the model adopted.

* * *

We are indebted to Prof. N. DALLAPORTA for having suggested this work and for helpful discussions.

(*) We see that we may completely neglect, for the inelastic interactions inside a nucleus, the Coulomb contribution, as our value of $g^2/\hbar c$ of 0.55 is much greater than $e^2/\hbar c = 1/137$.

RIASSUNTO

È stato applicato il modello ottico allo scattering dei mesoni K^- da parte dei nuclei. Si è determinato il potenziale nucleare V_n seguendo due procedimenti diversi: il primo consiste nel calcolo delle sezioni d'urto di scattering elastico K^--nucleo in funzione di V_n; il secondo collega V_n, attraverso l'interazione elementare K^--nucleone, descritta mediante un potenziale di Yukawa, alla sezione d'urto totale anelastica K^+-nucleo. Si ottengono nei due casi risultati molto simili.

The Range in G5 Nuclear Emulsion of Protons with Energies 87, 118 and 146 MeV.

M. W. Friedlander (*), D. Keefe (+) and M. G. K. Menon (−)

H. H. Wills Physical Laboratory, University of Bristol

(ricevuto il 15 Novembre 1956)

Summary. — A comparison was made between the ranges of artificially accelerated protons in Aluminium and in Ilford G5 photographic emulsion. The ranges in emulsion were obtained by direct measurements along the particle tracks, and those in Aluminium by an attenuation method. The ranges of protons of three different energies were 19.31, 13.23 and 7.82 g/cm² in Aluminium, and 22.85, 15.58 and 9.50 g/cm² in emulsion of density 3.791 g/cm³ conditioned to 58% relative humidity. The corresponding energies were 146.5 MeV, 117.9 MeV and 87.4 MeV. Assuming the range-energy relation for protons to be at present better determined for Aluminium than for photographic emulsion, this experiment provides new information concerning the relation between particle range and energy in nuclear emulsion.

1. – Introduction.

One of the great advantages in the use of stacks of photographic emulsion strips is the possibility of using range measurements for the precise determination of particle energies of quite considerable magnitude. Of the several familiar parameters which may be determined by measurements on the track of a particle and used to estimate its energy, the range is that which—under many circumstances—is most easily and accurately measurable. Since the observational errors in the measurement of length can be very small, precision in the estimation of energy from a measured range is normally limited by

(*) Now at Washington University, St. Louis, U.S.A.
(+) Now at University College, Dublin.
( ) Now at Tata Institute for Fundamental Research, Bombay.

the statistical fluctuation in the range (« straggling ») and by uncertainties in the range-energy relation. Clearly, the measurement of a sufficient number of events can affect a reduction in the error of the energy estimate because of straggling but cannot overcome the limitations arising from the second cause. In several recent experiments on the heavy unstable particles produced in high-energy nuclear disintegrations, uncertainties due to lack of information on the range-energy relation in emulsion outweigh in effect those due to statistical causes.

With the exception of three sets of measurements at high energies all experimental observations to date on the range of particles of known energy have been made on particles of velocity less than $0.28c$, corresponding to a proton energy of 40 MeV. Of these calibrations, the most extensive is that by Bradner, Smith, Barkas and Bishop [1], who used protons of known magnetic rigidity as did Panofsky and Fillmore [2]. In all other observations, (Lattes, Fowler and Cuer [3]; Rotblat [4], Catala and Gibson [5]; Gibson, Prowse and Rotblat [6]; Nereson and Reines [7]), the sources of energetic particles have been nuclear reactions involving well-measured energy releases. The measurements of Lattes, Fowler and Cuer were made in Ilford B1 emulsion, most other authors using Ilford C2 emulsion. In addition, a few measurements appear to have been made in Ilford E1, Ilford G5 and Kodak NT-2a emulsion, but have not been reported in any detail (Rotblat [4]). In these experiments neither the chemical composition nor the density at the time of exposure of the particular batch of emulsion used has been stated. In addition, in many cases the treatment of the emulsions prior to exposure was such that it is unlikely that the distribution of water throughout the emulsion was uniform, and the drying procedure adopted varied considerably from one experiment to the next. (cf. Oliver [8]). Furthermore, it has been found in this laboratory, that the densities of different batches of emulsion have differed by as much as 5%, even though they have had similar humidity conditions during manufacture and packing.

Despite these differences in procedure the experimental observations below 40 MeV appear to be well represented by the theoretical curves of Vigneron [9].

[1] H. Bradner, F. M. Smith, W. H. Barkas and A. S. Bishop: *Phys. Rev.*, **77**, 462 (1950).
[2] W. K. H. Panofsky and F. L. Fillmore: *Phys. Rev.*, **79**, 57 (1950).
[3] C. M. G. Lattes, P. Fowler and P. Cuer: *Proc. Phys. Soc.*, **59**, 883 (1947).
[4] J. Rotblat: *Nature*, **165**, 387 (1950); **167**, 550 (1951).
[5] J. Catala and W. Gibson: *Nature*, **167**, 551 (1950).
[6] W. Gibson, D. Prowse and J. Rotblat: *Nature*, **173**, 1180 (1954).
[7] N. Nereson and F. Reines: *Rev. Sci. Instr.*, **21**, 534 (1950).
[8] A. Oliver: *Rev. Sci. Instr.*, **25**, 326 (1954).
[9] L. Vigneron: *Journ. Phys. Rad.*, **14**, 145 (1953).

FAY *et al.* ([10]) have calculated a best fit to the experimental points, and their range-energy curve is close to that of VIGNERON.

Two of the high-energy sets of measurements differ essentially from those at the lower energies. At proton energies of (208 ± 4) MeV (DE CARVALHO and FRIEDMAN ([11])) and 342.5 MeV (HEINZ ([12])) the range of the protons in emulsion has been determined by an attenuation experiment, whereas at the lower energies individual tracks were measured. The energies of the protons used in these calibrations were determined from their ranges in copper, and the range-energy tables of ARON ([13]), the latter relation incorporating the results of MATHER and SEGRE (1951). In both high energy experiments, emulsion sheets of known density and water content were used. In one experiment (DE CARVALHO and FRIEDMAN) G5 emulsion was used, in the other, C2 emulsion. The chemical compositions of these two emulsions are so nearly the same that it is not anticipated that there will be any difference between their stopping powers, on the average.

Since the present work was completed, BARKAS, BARRETT, CUER, HECKMAN, SMITH and TICHO ([14]), have given the results of measurements made on the ranges of four groups of π-mesons, having energies between 29 MeV and 105 MeV and of μ-mesons arising in the decay at rest of the π-mesons The experiment was performed under carefully controlled conditions; the density and humidity of the emulsion and the magnetic rigidity of the π-mesons were all well determined. Each group of π-mesons comprised about 20 tracks. In their preliminary report, BARKAS *et al.* do not discuss the corrections applied because of loss of tracks through scattering out of the stack or because of the effect of inelastic scattering of the π-mesons in making the range distribution skew towards the shorter side.

The calculations of FAY *et al.* are based on a best fit to the experimental data below 40 MeV and take the form of a simple power law for proton ranges greater than 700 μm. Extrapolation of this directly appears to lead to an underestimation of the energy corresponding to long proton ranges. However, the calculated relations of VIGNERON (and its extension by BARKAS) and BARONI *et al.* ([15]) besides fitting the low energy points, also agree well with the high energy points of HEINZ, DE CARVALHO and FRIEDMAN and BARKAS

([10]) H. FAY, K. GOTTSTEIN and K. HAIN: *Suppl. Nuovo Cimento*, **11**, 234 (1954).
([11]) H. G. DE CARVALHO and J. FRIEDMAN: *Rev. Sci. Instr.*, **26**, 261 (1955).
([12]) O. HEINZ: *Phys. Rev.*, **94**, 1728 (1954).
([13]) W. ARON: *U.C.R.L. Report*, 1325 (1951).
([14]) W. H. BARKAS, P. H. BARRETT, P. CUER, H. H. HECKMAN, F. M. SMITH and H. K. TICHO: *U.C.R.L. Report*, 3254 (1956), also *Phys. Rev.*, **102** 583 (1956).
([15]) G. BARONI, C. CASTAGNOLI, G. CORTINI, C. FRANZINETTI and A. MANFREDINI: *C.E.R.N.*, B.S., 9 (1954).

et al. In a recent paper, CALDWELL ([16]) has discussed the range-energy relation, calculated as a function of I_E, the excitation potential, and suggests that I_E may be considerably higher than previously supposed. This might affect the energy determinations of the protons used by HEINZ and by DE CARVALHO and FRIEDMAN.

In the present experiment, the ranges of the protons were determined by direct microscope measurements on the individual tracks in G5 emulsion. Thus, the measurements need no correction for the discrepancy between projected and mean lengths arising from Coulomb scattering, as in the attenuation method.

The comparison ranges in aluminium were measured by the method described in the paper of TAYLOR and WOOD ([17]).

2. – Experimental Details.

Two small stacks of Ilford G5 emulsion each consisting of 15 sheets with dimensions 12 cm × 5 cm × 600 μm were used in the experiment. For some days before packing, the emulsion strips were allowed to come into an equilibrium state in a humidor which maintained the relative humidity at 58%. The stacks were weighed immediately after packing and again following exposure; the change in weight was less than one part in 10^4 and it is safe to conclude that the relative humidity during exposure was indeed 58%. The direct measurement of density (at 58% relative humidity) gave a value 3.791 ± 0.004 g/cm³; the silver halide concentration was (0.8250 ± 0.0005) g/cm of emulsion, implying a density of 3.803 g/cm³ from the knowledge of the emulsion composition. (The authors are grateful to Mr. C. WALLER for carrying out the analysis and density determinations at Ilford Ltd.)

Each stack was packed using a glass backing plate to provide rigidity and surrounded by Duplex paper in such a manner that the topmost surface and the edges of the stack were protected by only one layer of paper. The emulsion sheets were in direct contact with each other and no tissue paper spacers were used. Both stacks were exposed to the 150 MeV external proton beam of the Harwell cyclotron in two ways: (*a*) with the beam entering the paper-covered stack through the surface of the top emulsion sheets, at a glancing angle of about 5°, and (*b*) with the beam entering the edges of the stacks approximately parallel to the emulsion plane. Two further exposures were made at lower energies in manner (*b*) only, with aluminium absorbers interposed between the beam exit aperture and the emulsion to reduce the beam

([16]) D. O. CALDWELL: *Phys. Rev.*, **100**, 291 (1955).
([17]) A. E. TAYLOR and E. WOOD: in course of publication (1956).

energy, the one absorber being 6.0805 g cm² and the other 11.4864 g cm² in thickness. A check was made on the constancy of the proton energy over the exposure period by measuring the range of the beam in aluminium immediately before and after the series of emulsion exposures. Both measurements were in agreement and the mean range found for the uninterrupted beam was 19.31 g cm² of aluminium. The analysis of daily checks on the energy of the beam over a period of several weeks, showed that a variation in range of 0.03 g cm² may occur between successive runs, and this uncertainty has been included in the errors quoted for the ranges in Aluminium.

The ranges of the proton tracks in the developed emulsions were measured using Cooke M4000 microscopes, the stage micrometers being found to be accurate to better than one part in 2000 by calibration against a Leitz etalon. Tracks were selected for measurement close to their points of entry into the stack, and were only accepted for measurement if they were within about 5° of the beam direction in both projection and dip. Each track was then followed through successive emulsion sheets to its end or to its point of exit from the stack. Co-ordinates were recorded at the points of entry and exit in each emulsion strip and also at points where any change in direction of the track took place. This direct method of measuring true path length eliminates the systematic underestimation inherent in the simpler measurement of chord length and obviates the necessity of applying a correction for the scattering of the particle. The true length of each track was then calculated from the measured projected length and the known original emulsion thickness.

To the range as measured in this way there are certain corrections to be applied. The first arises from the energy loss of the protons in traversing the paper packing of the stacks. Direct measurements of the stopping power of the Duplex paper for protons of 130 MeV. showed that the stopping power of one thickness of paper for penetration at normal incidence was equivalent to 0.0139 g cm² of aluminium or about 48 μm path-length in emulsion. A calculation using the density and approximate chemical composition of the paper indicated a value of 45 μm equivalent path length in emulsion. The second correction is necessary to deduce from the range measured in the chosen stacks the appropriate value in an infinite block of emulsion. Since the stacks were of finite size, the probability is slightly greater for a particle to come to rest within the emulsion if it has a range below the mean value rather than if the statistical fluctuations resulted in its having a range longer than the average. Consequently the arithmetical mean of the sample measurements is biassed towards underestimating the true mean value. The correction to the measured value was greatest for the highest energy particles (amounting to a little over a tenth of a percent in range) and was negligible for the other two groups of tracks. The value of this correction was in all cases deduced from

an examination of the distribution of segment length for those particles which escaped from the stack before coming to rest.

It is well known that the estimation of the true length of a track traversing an emulsion sheet is subject to errors arising from deformation of the emulsion during processing. One such effect is the areal distension of the emulsion sheet known to occur under certain processing conditions in a small fraction of cases and this will cause a spurious over-estimation of track lengths. From measurements made upon the separation of fiducial X-ray marks on each plate it was found that one emulsion sheet of the thirty used in the experiment had stretched by about 0.2%; the effect upon the mean range of the protons is about twenty times less and has been neglected. Apart from the dilation or contraction of the emulsion as a whole, length measurements will also be affected by the more familiar type of distortion in which the bottom-most layer of emulsion adhering to the glass is assumed to retain its original shape and the upper layers to be shifted with respect to it. Direct measurements of the distortion vector have shown approximate agreement with the « elastic solid » model of emulsion distortion described by LAL, YASH PAL and PETERS [18] as regards the relation between the first and second order distortion vectors. Since for our tracks, this correction was at most 0.04%, it has been neglected. For those particles which entered through the edge of the emulsion sheets, all measurements in the first plate have assumed that the original position of the emulsion edge is that defined by the bottom-most layer of the processed emulsion sheet.

3. – Results.

All tracks followed were classified under three headings:

(*a*) those which escaped from the stack, produced nuclear interactions or suffered inelastic scattering — as evidenced by an abrupt change in ionization and direction;

(*b*) those which suffered « elastic scattering », i.e. small-angle deflections without any apparent change in ionization, and came to rest within the stack: and

(*c*) those which ended in the emulsion without undergoing any sharp deviations along their path.

Since it is impossible to exclude in any individual case belonging to class (*b*) that the particle in question had not undergone an inelastic scattering involving only a small transfer of energy, the distributions in ranges of the tracks of

[18] D. LAL, YASH PAL and B. PETERS: *Proc. Ind. Acad. Sci.*, **38**, 398 (1953).

classes (*b*) and (*c*) were analyzed separately. In fact, both the respective shapes and means of the distributions were found to be in excellent accord and the distribution in scattering angles of those in class (*b*) were found to be in good agreement with that expected to arise from Coulomb scattering alone. Accordingly, events of classes (*b*) and (*c*) were both included in the calculation of the mean and median values given below.

The range distribution of the protons in emulsion belonging to both classes (*b*) and (*c*) have been combined in Fig. 1 and the mean and median values and the standard deviations of the three energy groups are summarized in Table I.

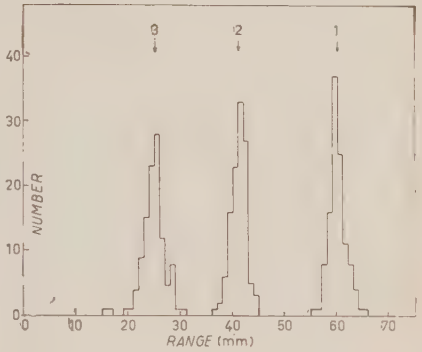

Fig. 1. – A histogram showing the ranges of the protons in the three energy groups; group 1 comprises 114 tracks, group 2, 116 tracks and group 3, 107 tracks.

TABLE I.

Group	1	2	3
Mean Range (mm)	60.27 ± 0.16	41.10 ± 0.14	25.11 ± 0.17
Median Range (mm)	60.13 0.20	41.42 ± 0.17	25.18 0.21
Number of tracks	114	116	107
Standard deviation of distribution (mm)	1.73	1.49	1.78

For protons in this energy region, the range straggling is $\sim 1.2\%$ (BARKAS and YOUNG [19]). From the shape of the observed range distributions, it was concluded that there was no significant departure from a symmetrical distribution in the cyclotron beam energy. It can be seen from Table I that the mean and median values of range, as expected for a symmetrical distribution, do not appear to differ systematically.

Unfortunately, however, the mean and the median of Group 2 are not in very good agreement, the difference between them being just the sum of their

[19] W. H. BARKAS: *U.C.R.L. Report*, 2579 (1954).

respective errors. This discrepancy is not unlikely to have occurred by chance but it is necessary to recall that deductions based on this measurement will vary somewhat depending upon which statistic is used. The considerations of the Appendix would seem to suggest that in this case the median is the closer estimate of the population mean.

In Table II are given the ranges in g/cm² of the three groups of protons in emulsion and in aluminium. In expressing the ranges in g/cm² rather than millimetre units the directly measured emulsion density, (3.791 ± 0.004) g/cm³ was used. The proton energies in the last column are those deduced from the range-energy relation of TAYLOR and WOOD ([17]) and include uncertainties arising from the calibration experiment of BLOEMBERGEN and VAN HEERDEN ([20]) and from the beam fluctuations. The ranges in aluminium do not include any correction to allow for the Coulomb scattering of the beam within the absorbers and refer to the thicknesses interposed to reduce the beam to « half-height ».

TABLE II.

Proton group	Range (g/cm²)		Energy (MeV)
	Emulsion	Aluminium	
1	22.85 ± 0.06	19.31 ± 0.03	146.5 ± 0.1
2	15.58 ± 0.05	13.23 ± 0.03	117.9 ± 0.2
3	9.50 ± 0.06	7.82 ± 0.03	87.4 ± 0.2

4. – Discussion.

Recently FOWLER and SCHARFF ([21]) have drawn attention to the inconvenience of intercomparing various theoretical range-energy relations extending over a large band of energies. The usual method of direct graphical representation of Energy versus Range on log-log graph paper becomes very cumbersome when a precision of reading of less than about 1% is sought for widely different energies. Instead, they have proposed that the energy corresponding to a given range (either experimental or theoretical) be expressed as a *ratio* to that value of energy appropriate to the same range calculated from a standard formula. These authors have shown that the simple relation

$$E = 1.1R + 25\sqrt{R} - 2 ,$$

([20]) N. BLOEMBERGEN and P. J. VAN HEERDEN: *Phys. Rev.*, **83**, 561 (1951).
([21]) P. H. FOWLER and M. SCHARFF: in course of publication (1956).

where E is measured in MeV and R in g/cm², agrees approximately ($\pm 5\%$) with the experimental and theoretical data for protons with ranges between 0.1 g/cm² and 3 000 g/cm². Accordingly any proposed range-energy relation may be written exactly, as follows:

$$E = \varphi(R) \cdot (1.1R + 25\sqrt{R} - 2) ,$$

where φ is close to unity, and affords a convenient measure of the discrepancies between various proposed curves and the experimental values.

In Table III are given the values of φ obtained from the present measurements and the values taken from the calculated curves of BARONI *et al.*, FOWLER and SCHARFF, VIGNERON and BARKAS (private communication). The theoretical figures have all been corrected to an emulsion density of 3.791 g/cm² assuming that $\varphi(R)$ changes by -1% per 6.6% increase in emulsion density (FOWLER and SCHARFF ([21])).

TABLE III.

Values of $\varphi(R)$			
Energy	87 MeV	118 MeV	146 MeV
Present measurements (*)	1.023 ± 0.006	1.036 ± 0.003	1.027 ± 0.002
BARONI *et al.*	1.017	1.016	1.013
FOWLER and SCHARFF (+)	1.039	1.041	1.039
BARKAS-VIGNERON . . .	1.033	1.033	1.027

(*) $\varphi(R)$ calculated using the mean ranges.
(+) Calculated range-energy relation, using varying ionization potential and STERNHEIMER ([22]) density effect corrections.

It is necessary to emphasize that the quoted errors on the experimental values of φ given in Table IV refer to the statistical errors arising in the experiment and are valid only if the range-energy relation used for Aluminium is correct. If further measurements indicate that the relation used needs modification this will require an adjustment of the energy values given. On the other hand the Emulsion-Aluminium comparison figures of Table II are, of course independent of the range-energy relation and the statistical errors given presumably represent the true uncertainties in the result.

([22]) R. STERNHEIMER: *Phys. Rev.*, **88**, 851 (1952).

* * *

We wish to thank Professor C. F. POWELL for the hospitality and facilities of his laboratory and his interest in the work. We also wish to thank Mr. C. WALLER of Ilford Limited, for the careful preparation of these emulsions and for the analysis and density measurements. We are particularly grateful to Drs. A. E. TAYLOR and E. WOOD of the A.E.R.E., Harwell, for their assistance with the exposure of the plates and for their many helpful comments and suggestions, and also to Mr. M. C. CHESHIRE of the cyclotron team. For much useful discussion, we are also grateful to Mr. P. H. FOWLER.

APPENDIX

The Ionization Potential of Emulsion.

The stopping power, S, of the emulsion relative to Aluminium has been calculated for the various energy intervals which are given in Table IV. S is defined by the equation:

$$S = \frac{\Delta R_{\mathrm{E}}}{\Delta R_{\mathrm{Al}}} ,$$

where ΔR_{Al} is the thickness measured in g/cm^2 of aluminium required to reduce the energy of the beam by the same amount as a thickness ΔR_{E} of emulsion. For the purposes of this comparison, the ranges in Aluminium have been increased by the usual correction, $ZR/6440$, to take account of the slightly greater path length actually traversed in the absorbers because of the deviations due to multiple Coulomb scattering.

The experimental values for I_{E}, the mean ionization potential of the emulsion may then be calculated from the formula:

$$\ln I_{\mathrm{E}} = (1 - q)\left\{\ln \frac{2mc^2\beta^2}{1 - \beta^2} - \beta^2\right\} + q \ln I_{\mathrm{Al}} ,$$

where m = mass of the electron, and βc = average particle velocity. The relative stopping power per electron, q, is defined by:

$$q = S(N_{\mathrm{Al}}/N_{\mathrm{E}}) ,$$

where N_{Al} and N_{E} are the number of electrons per cm^3 in Aluminium and Emulsion respectively. For the batch of emulsion used, $N_{\mathrm{E}} = 1.039 \cdot 10^{24}$ cm^{-3}

and the N_{Al} was taken as $7.83 \cdot 10^{23}$ cm^{-3}. The ionization potential of Aluminium I_{Al}, was assumed to have the constant value 168 eV (SACHS and RICHARDSON [23]).

Opinions vary as to whether the ionization potential of emulsion changes appreciably with velocity; in principle, this matter can be decided by measuring S, using thin sheets of absorbers, at different energies. However, as is well known, the exponential dependence of I_E upon the measured stopping power makes it very difficult to determine I_E accurately without absorption experiments of the highest precision. Increased precision may be obtained by the use of greater thicknesses of absorber but then only at the expense of information about the variation of I_E with velocity. Furthermore, in the direct comparison of total ranges, such as for the intervals 0 : 87 MeV, 0 : 118 MeV, 0 : 146 MeV, in Table IV, the simple formula given above is no longer valid and the so-called « shell corrections » must be considered at low energies.

TABLE IV.

Energy Region (MeV)	I_E (eV)	
	Calculated from mean ranges	Calculated from median ranges
0 – 87	375 ± 25	381 ± 31
0 – 118	321 ± 14	336 ± 17
0 – 146	337 ± 11	332 ± 13
87 – 118	241 ± 36	267 ± 45
87 – 146	311 ± 24	293 ± 30
118 – 146	373 ± 48	318 ± 60

From Table IV it can be seen that the experimental values of I_E are very widely scattered and subject to such statistical fluctuations that it is pointless to treat the three measurements independently and look for a systematic variation in I_E. Since any changes in I_E between 87 and 146 MeV are likely to be slight, a comparison of the Ionization Potentials based upon the means and upon the medians suggests that the median range of Group 2 is probably the better estimate of the true population mean. If so, then the internal consistency of the three independent measurements would be improved.

Because of these fluctuations it is difficult to draw any very far-reaching conclusions concerning the value of I_E, though generally the measurements tend to favour a value not very much greater than 300 eV.

[23] D. C. SACHS and J. R. RICHARDSON: *Phys. Rev.*, **89**, 1165 (1953).

RIASSUNTO (*)

Si è fatto un confronto fra i range di protoni artificialmente accelerati in alluminio e in emulsioni fotografiche Ilford G5. I range in emulsione furono ottenuti per misura diretta delle tracce delle particelle, quelli in alluminio con un metodo di attenuazione. I range dei protoni di tre differenti energie furono di 19.31, 13.23 e 7.82 g/cm^2 in alluminio e di 22.85, 15.58 e 9.50 g/cm^2 in emulsione di densità 3.791 g/cm^3 condizionata a 58% di umidità relativa. Le corrispondenti energie erano 146.5 MeV, 117.9 MeV e 87.4 MeV. Assumendo che la relazione range-energia pei protoni sia attualmente meglio determinata per l'alluminio che per l'emulsione fotografica, il presente esperimento fornisce nuovi dati sulla relazione, nelle emulsioni nucleari, tra il range delle particelle e l'energia.

(*) *Traduzione a cura della Redazione.*

IL NUOVO CIMENTO Vol. V, N. 2 1° Febbraio 1957

On the Correlation of the Intensity of μ^-- and μ^+-Mesons with the Pressure at Sea-level, and with the Height of the 100 mb Layer.

U. Fasoli, C. Maroni, I. Modena (*), E. Pohl (+), and J. Pohl-Rüling

Istituto di Fisica dell'Università - Padova
Istituto Nazionale di Fisica Nucleare - Sezione di Padova

(ricevuto il 22 Novembre 1956)

Summary. — The vertical intensities of μ^+- and μ^--mesons have been measured by means of a counter apparatus with magnetic discrimination for the sign of charge. The mean daily counting rates are 5 500 μ^+ and 4 600 μ^- extended over 18 months. The coefficients for correlation between the intensities of the μ^+ and μ^- with the atmospheric pressure at sea-level (α^+ and α^-) and with the height of the 100 mb layer (γ^+ and γ^-) have been obtained. There is a difference between the coefficients for the two types of mesons which is beyond the statistical errors; in fact $|\alpha^-| > |\alpha^+|$ and $|\gamma^+| > |\gamma^-|$. The results have been interpreted by means of a particular integral of the diffusion equation, considering the mesons as being produced by two distinct sources: one due to the collisions between the primary component with the nuclei of the upper atmosphere and the other due to the secondary nucleonic component.

1. – Introduction.

The problems of the origin of cosmic rays and the relative acceleration mechanism, have not yet been satisfactorily resolved. It may be that this is due, at least in part, to a lack of precise information about time variations and the anisotropy of the primary flux.

(*) Now at Servizio nell'Areonautica Militare.

(+) Now at the Abteilung für Radiologie und Isotopenforschung, Physiologisches Institut der Universität Innsbruck, Innsbruck, Austria.

The time variation of the secondary components found by various authors (e.g. [1]) are mainly due to meteorological factors. Correlations have therefore been sought between meteorological factors and the variations of intensity of the components of cosmic rays in order to be able to correct experimental results and thereby detect possible effects not due to meteorological causes. In fact such effects have been found, but some of them are too small to represent evidence for a genuine variation in the primary flux.

To increase our information about the primary flux, a measurement of the variation of the positive excess would seem to be useful, particularly as far as an eventual solar contribution might be concerned [2]. Measurements of this kind have not so far been carried out with an apparatus having such a high counting rate, that the statistical errors become relatively small. If however a variation of the positive excess corresponding to variations of the primary flux exists, this effect would be overlaid by variations of meteorological origin if the μ^+- and μ^--mesons behave differently in the atmosphere. Thus it is necessary to determine the meteorological correlation factors separately for μ^+- and μ^--mesons.

In the present work, the correlation coefficients for μ^+- and μ^--mesons relative to the sea-level pressure and the height of the 100 mb layer have been obtained by means of a counter set of high counting rate, capable of discriminating between the two types of μ-mesons. The results obtained have been interpreted by the application of an approximate integral [3] of the diffusion equation.

2. – The Experimental Layout.

This is substantially the same as that already described in an earlier work on the positive excess underground [4]. Geiger-counters arranged in 16 triple coincidences register the μ^+- and μ^--mesons separately: these are discriminated by an electromagnet having an iron nucleus: the separation is almost total, due to the system of anticoincidences which eliminates events due to showers and which has been fully described in the preceeding works [4,5]. The background, measured without magnetic field, is only 2% of the normal counting rate.

[1] H. ELLIOT: *Progress in Cosmic Ray Physics* (1952), p. 455.

[2] I. FILOSOFO, I. MODENA, E. POHL and J. POHL-RÜLING: *Nuovo Cimento*, **3**, 112 (1956).

[3] G. PUPPI: *Progress in Cosmic Rays* (1956), p. 340.

[4] I. FILOSOFO, E. POHL and J. POHL-RÜLING: *Nuovo Cimento*, 12, 809 (1954).

[5] E. BERETTA, I. FILOSOFO, B. SOMMACAL and G. PUPPI: *Nuovo Cimento*, **10**, 1354 (1953).

The zenithal aperture of the apparatus is 70° in the North-South direction and 22° in the East-West. The energy band of the mesons so gathered is given in Fig. 1 and has been determined by a graphical method. Its centre is at 1.0 GeV and has a half-width of 0.6 GeV.

The electronics is of the traditional type, except for the 16 triple coincidences which follow a circuit described by one of us (6).

The apparatus is fully automatic, data being registered every two hours by photographing the registering instruments. To eliminate possible inequalities due to the geometry of the apparatus or efficiency of the counters or electronic circuits, the direction of the magnetic field has been reversed every 24 hours.

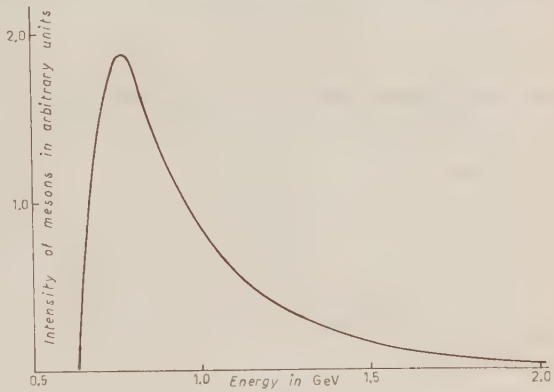

Fig. 1. – Energy band collected by the apparatus.

The mean daily counting rates for μ^+- and μ^--mesons are respectively 5500 and 4600. Measurements have been carried out during the period May 1955 to October 1956 representing a total of 410 working days and about $4.5 \cdot 10^6$ ($\mu^+ + \mu^-$) registered.

The experiment has been carried out at Padua (25 m above sea level long. 11° 53′ E, lat. 45° 24.5′ N) in a temperature controlled enclosure under a thin roof having negligible absorbing properties.

3. – Experimental Results.

The correlations have been made between the daily mean counting rates of the mean values of the local atmospheric pressure (*) and the height of the 100 mb layer, which has been derived from the 03,00 UT curves for the 100 mb-layer, published in the daily bulletin of the « Täglicher Wetterbericht » (+).

(6) E. Pohl: *Nuovo Cimento*, **3**, 642 (1956).

(*) This has been supplied by the Servizio Meteorologico dell'Aeronautica Militare at Padua.

(+) Published by « Deutscher Wetterdienst », Zentralstelle Bad Kissingen (Postfach 50).

The correlation coefficients, defined by the well known expression:

$$n^{\pm}_{\text{corr}} = n^{\pm} - \alpha^{\pm} p'_i - \gamma^{\pm} h'_i \quad (*)$$

have been determined by the normal method of double correlation carried out in 7 partial periods each of two months durations.

TABLE I.

Period of time	α^+ in %	α^- in %	γ^+ in %	γ^- in %	$\overline{P}$ mb	$\overline{h}$ km	$\overline{t}$ °C
I 2.5.–1.8. 1955	−1.70±0.63	−2.21±0.67	− 4.39±1.57	− 2.42±1.67	1012,2	16.44	21.0
II 7.8.–15.10. 1955	−2.92±0.50	−3.05±0.53	− 0.88±1.70	− 3.09±1.82	1012.7	16.39	18.0
III 19.10–31.12. 1955	−1.93+0.32	−2.16±0.34	− 7.88±1.48	− 5.94±1.57	1013.0	16.02	6.9
IV 1.1.–1.3. 1956	−1.51±0.41	−1.33±0.44	−13.36±2.55	−12.24±2.76	1012.2	15.88	0.7
V 3.3.–19.5. 1956	−1.75±0.35	−1.49±0.37	−12.50±1.57	− 9.75±1.65	1011.4	16.06	16.5
VI 31.5.–12.8. 1956	−0.40±0.66	−2.19±0.70	− 5.66±2.58	− 4.61±2.73	1010.9	16.46	21.5
VII 12.8.–12.10. 1956	−1.61±0.48	−2.47±0.53	−10.96±1.72	−10.40±1.82	1012.4	16.40	19.5
Mean values	−1.69±0.17	−2.13±0.18	− 7.95±0.64	− 6.04±0.68			

(*) $n^{\pm}$ = number of the $\mu^{\pm}$ registered;
$P'_i = P_i - \overline{P}$; P_i = pressure at sea level, $\overline{P}$ = mean pressure;
$\alpha^{\pm}$ = coefficient of correlation with the pressure;
$h'_i = h_i - \overline{h}$; h_i = height of the 100 mb layer; $\overline{h}$ = mean height;
$\gamma^{\pm}$ = coefficient of correlation with h.

The coefficients calculated in this way are given in Table I and in Fig. 2, together with h and t (the temperature at sea level (*)).

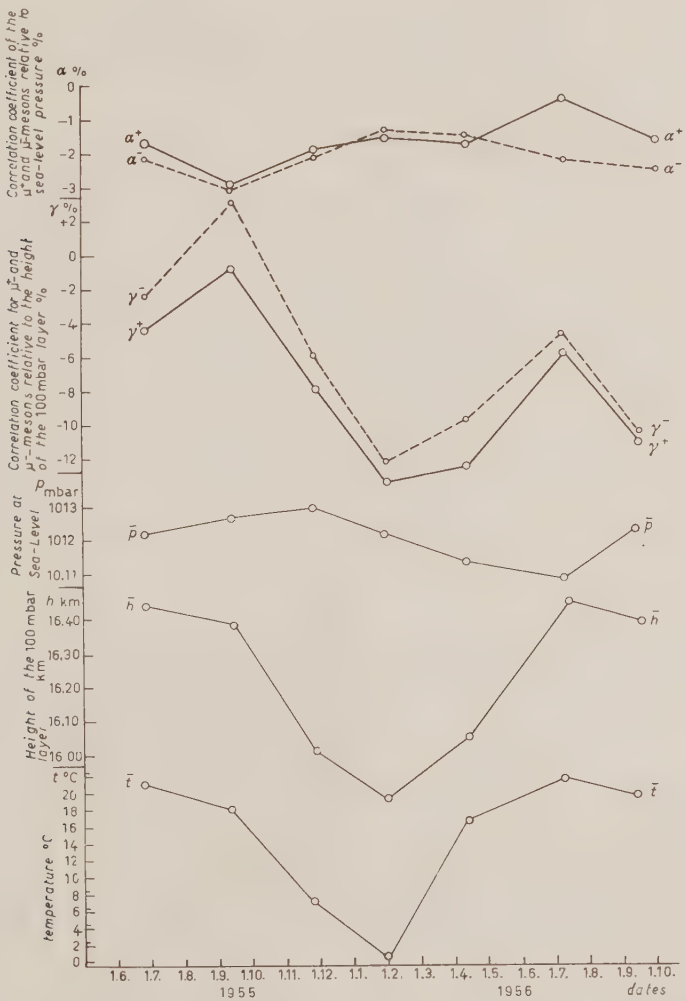

Fig. 2. – Correlation coefficients of the μ^+- and μ^--mesons relative to the height of the 100 mb layer and the sea-level pressure, the mean heights of the 100 mb layer, the mean sea-level pressure and the mean temperatures at sea-level of the various periods as functions of time.

(*) This has been supplied by the Servizio Meteorologico dell'Aeronautica Militare at Padua.

4. – Interpretation of the Results.

The values of the correlation coefficients obtained experimentally may be explained by our present knowledge of the behaviour of the cosmic radiation in the Earth's atmosphere.

To do this the following hypotheses must be made:

1) The production of mesons is multiple.

2) In an inelastic nucleon-nucleon collision, the process of transmission of the charge to the meson field is not less probable than that of the retention of the charge by the nucleons. Both these hypotheses have been amply confirmed by numerous studies with machines and with cosmic rays.

One may now state that: *a*) the mesons responsible for the positive excess are produced in the collisions of the primary particles of the Cosmic Radiation with the nuclei of the upper atmosphere; *b*) the secondary nucleon component in which the number of neutrons equals or exceeds that of the protons, gives rise to a meson component not having an excess, or with a slight negative excess which dilutes the positive excess due to the first collisions.

The attribution of the positive excess substantially to the first collisions suggests a scheme by which the problem of the determination of the values of the coefficients may be attacked. In fact, we consider the meson component produced by two sources: a first source S_1 with positive excess, due to the first collision, and a second S_2 with a slight negative excess produced by the successive collisions.

For the evaluation of the intensity of these sources we make the following hypotheses:

1) The primary nucleonic component is absorbed exponentially in the atmosphere with an absorption length equal to the mean free path for inelastic collisions ($\Lambda = 80$ g/cm^2).

2) The total nucleonic component (primary − secondary) is absorbed exponentially in the atmosphere with an absorption length $R = 125$ g/cm^2.

3) The cross-section for pion production depends only on the E/W ratio of the energies of the emitted pion and of the struck nucleus (the hypothesis is necessary to allow us to affirm that the mesonic secondary component conserves the spectrum of the primary flux).

Under these conditions one may write for the two sources (7)

$$S_1(E, t) = \frac{1}{R} g_\pi(E) \exp\left[-\frac{t}{\Lambda}\right],$$

$$S_2(E, t) = \frac{1}{R} g_\pi(E) \left(\exp\left[-\frac{t}{R}\right] - \exp\left[-\frac{t}{\Lambda}\right]\right),$$

where t is the depth in the atmosphere and $g_\pi(E)$ is the energy spectrum for the production of pions, and which is assumed to have the form:

$$g_\pi(E) = \frac{\gamma A}{E^{\gamma+1}},$$

with $\gamma = 1.75$ and $A = 0.23$.

We may now separate the contribution due to the two signs of mesons. For this, with δ as the positive excess in the first collision, we put

$$g_\pi = \frac{1}{2}[g^+ + g^-], \qquad \frac{\delta}{2} = \frac{g^+ - g^-}{g^+ + g^-}.$$

One then obtains:

$$g^+ = g\left(1 + \frac{\delta}{2}\right), \qquad g^- = g\left(1 - \frac{\delta}{2}\right).$$

For the second source similar expressions may be written by introducing instead of the positive excess a slight negative excess the effect of which may, however, be ignored in a first approximation. Finally one obtains for both signs of mesons produced throughout the atmosphere, for all energies:

$$\mu^\pm = \int_0^\infty \int_0^t \frac{1}{R} g_\pi(E) \left\{\pm\frac{\delta}{2}\exp\left[-\frac{t}{\Lambda}\right] + \exp\left[-\frac{t}{R}\right]\right\} W(E - \beta t;\, t;\, \tau)\, \mathrm{d}E\, \mathrm{d}t,$$

where $w(E - \beta t, t, \tau)$ is the survival probability, τ the mean life for the meson, E the energy of the two signs of pions at production, β the energy loss per unit path.

The complexity of the function $w(E - \beta t, t, \tau)$ renders difficult the analytical integration of the expressions for μ^+ and μ^-. For this reason they are unsuitable for use in this form. The difficulty may be overcome by means

(7) P. Bassi, E. Clementel, I. Filosofo and G. Puppi: *Nuovo Cimento*, **6**, 484 (1949).

of the pair of equations for the diffusion of π and μ having the form:

$$\frac{\partial \pi}{\partial t} = \frac{\partial}{\partial E}(\beta_\pi \pi) - \left(\frac{1}{\Lambda} + \frac{B}{tE}\right)\pi + \frac{1}{R}\exp\left[-\frac{t}{R}\right] g_\pi(E)\,,$$

$$\frac{\partial \mu}{\partial t} = \frac{\partial}{\partial \varepsilon}(\beta_\mu \mu) - \frac{b}{t\varepsilon}\mu + \frac{B}{tK\varepsilon}\pi(K\varepsilon, t)\,.$$

For these equations an approximate integral exists, having the form ([3]):

$$\mu' = \frac{\gamma A}{K^\gamma}\left[\frac{R\varepsilon}{\eta t}\right]^{b/\eta} \frac{B}{B + K\eta}\,\frac{1}{\eta^{\gamma+1}}\,,$$

where

$$\eta = \varepsilon + \beta t\,, \qquad b = \frac{m_\mu c}{\tau_\mu} H\,, \qquad B = \frac{m_\mu c}{\tau_\mu} H\,,$$

K is the ratio between the energies of the π and the μ in the laboratory system, which is 1.27. H is defined by the relation

$$p_h = p_0 \exp\left[-\frac{h}{H}\right].$$

The expression then becomes:

$$\mu^\pm = \frac{1}{2}\,\frac{B}{B + K(\varepsilon + \beta t)}\cdot\frac{1}{(\varepsilon + \beta t)^{\gamma+1}}\,\frac{\gamma A}{K^\gamma}\cdot$$
$$\cdot\left\{\pm\frac{\delta}{2}\left[\frac{\Lambda\varepsilon}{(\varepsilon + \beta t)t}\right]^{b/(\varepsilon+\beta t)}\frac{\Lambda}{R} + \left[\frac{R\varepsilon}{(\varepsilon + \beta t)t}\right]^{b/(\varepsilon+\beta t)}\right\}.$$

Putting

$$D^\pm(\varepsilon) = \pm\frac{\delta}{2}\,\frac{\Lambda}{R}\left(\frac{\Lambda\varepsilon}{\eta t}\right)^{b/\eta} + \left(\frac{R\varepsilon}{\eta t}\right)^{b/\eta},$$

$$E^\pm(\varepsilon) = \pm\frac{\delta}{2}\,\frac{\Lambda}{R}\left(\frac{\Lambda\varepsilon}{\eta t}\right)^{b/\eta}\ln\frac{\Lambda\varepsilon}{\eta t} + \left(\frac{R\varepsilon}{\eta t}\right)^{b/\eta}\ln\frac{R\varepsilon}{\eta t}$$

and recalling the definition of the correlation coefficient:

$$\gamma^\pm = \frac{1}{\mu^\pm}\,\frac{\partial \mu^\pm}{\partial h}\,, \qquad \alpha^\pm = \frac{1}{\mu^\pm}\,\frac{\partial \mu^\pm}{\partial t}\,,$$

one has:

$$\gamma^\pm = \frac{K\eta}{h(B + K\eta)} + \frac{b}{\eta h}\cdot\frac{E^\pm(\varepsilon)}{D^\pm(\varepsilon)}\,,$$

$$\alpha^\pm = -\left[\frac{KB}{B + K\eta} + \frac{\beta(\gamma + 1)}{\eta} + \frac{b}{t}\,\frac{(\eta + \beta t)}{\eta^2}\right] - \frac{b\beta}{\eta^2}\,\frac{E^\pm(\varepsilon)}{D^\pm(\varepsilon)}\,.$$

The numerical value of the coefficients, calculated by means of the above equations is then

$$\alpha^+ = -2.25\%\ \text{per cm Hg} \qquad \gamma^+ = -7{,}06\%\ \text{per km}$$

$$\alpha^- = -2{,}28\% \quad » \qquad \gamma^- = -6.87\% \quad »$$

The agreement between these values and the mean experimental values is good. It is to be noted, however, from Fig. 2 that γ' has a strong seasonal variation which seems to be related to the movement of the 100 mb layer and the ground temperature. In the final formula the dependence of γ' on the height is not sufficient to explain the experimental variations.

To see if this dependance is due to a temperature effect the triple correlations have been carried out introducing the temperature into the expression (*). Despite this, the seasonal effect for γ' has not vanished. In this connection we note that the same behaviour for γ' has been detected with another apparatus for the measurement of the total intensity of cosmic rays, having a cut-off at 10 cm of Pb (+). This completely excludes the possibility that the observed effect is a statistical fluctuation or due to an instability of the circuits. On the other hand, it is also possible that our description of the atmosphere and of the diffusion phenomena therein is too simple.

5. – Conclusion.

This work has revealed the existence of a difference between the correlations with the meteorological factors for the intensity of the mesons of the two signs, especially as far as the correlation with the 100 mb layer is concerned.

It is therefore possible to predict an equally appreciable correlation between the positive excess and the same factors. The knowledge of the behavior of the cosmic rays in the atmosphere justifies, at least qualitatively, the mean experimental values obtained, without succeeding, however, in interpreting the seasonal variation.

(*) For information only, we give the mean value of the coefficients obtained with the triple correlation:

$\alpha^+ = -1.91 \pm 0.17\%\ (\text{cm Hg})^{-1}$ $\beta^+ = -0.11 \pm 0.03\%\ (°\text{C})^{-1}$ $\gamma^+ = -5.00 \pm 0.70\%\ (\text{km})^{-1}$

$\alpha^- = -2.14 \pm 0.18\%$ » $\beta^- = -0.06 \pm 0.03\%$ » $\gamma^- = -3.26 \pm 0.75\%$ »

One should note the appreciable difference between β^+ and β^-, the temperature correlation coefficients.

(+) This will be the subject of a future publication.

From this it becomes obvious that the correction of the experimental data should be made by calculating the coefficients for periods of time which are not too long.

* * *

We are indebted to Prof. G. PUPPI who has been supervising our work. Thanks are also due to the « Servizio Meteorologico dell'Aeronautica Militare » at Padua for supplying the local meteorological data and to G. SALMASO for the execution of the numerical computations.

RIASSUNTO

Con un dispositivo di contatori Geiger sono state misurate le intensità verticali dei mesoni μ^+, μ^- discriminati in segno da un campo magnetico. Le intensità medie registrate sono di 5 500 μ^+ e 4 600 μ^- al giorno e il periodo di misure è di 18 mesi. Si sono ricavati i coefficienti di correlazione delle intensità dei μ^+, μ^- con la pressione atmosferica al livello del mare (α^+ e α) e con l'altezza dello strato di 100 mb (γ^+ e γ^-). I coefficienti trovati sono diversi per i mesoni dei due segni, al di fuori degli errori statistici e precisamente $|\alpha^-| > |\alpha^+|$ e $|\gamma^+| > |\gamma^-|$. I risultati ottenuti sono stati interpretati mediante un particolare integrale dell'equazione di diffusione e considerando i mesoni come prodotti da due sorgenti distinte: una costituita dagli urti della primaria con i nuclei dell'alta atmosfera e l'altra dagli urti della nucleonica secondaria.

Etude du nombre de mésons virtuels sur un modèle simple.

E. Arnous (*)

Institut H. Poincaré et Ecole Normale Supérieure - Paris

(ricevuto il 28 Novembre 1956)

Summary. — A well-known model is studied, where the nucleons are considered as fixed and extended sources interacting with a neutral scalar field. The exact wave function of the ground state is computed and it is shown that the probability distribution of the number of virtual mesons is a Poisson distribution. The mean value of that number is computed as a function of the radius of the sources and of the distance between the nucleons. It is seen that his number of virtual mesons never exceeds one or two, for radii and distances of the order of 10^{-13} cm and values of $g^2/4\pi\hbar c$ of the order one. The above results seem to justify methods of the Tamm-Dancoff type.

— — —

Pauli et Källén (1), Thirring (2), Enz (3), Källén et Glauber (4) et Okabayashi et Sato (5) ont étudié un certain nombre de modèles non-relativistes d'interactions méson-nucléon et photon-électron, qui sont suffisamment simples pour pouvoir être traités sans approximation, mais suffisamment complexes pour refléter les particularités essentielles des modèles relativistes utilisés en théorie des champs quantifiés.

Ils ont pu montrer sur ces modèles, que la renormalisation de la charge et celle de la masse introduisent des états liés à propriétés pathologiques (états « fantomatiques ») dès que les rayons des sources qui représentent les nucléons

(*) Maître de Recherches au Centre National de la Recherche Scientifique, Paris.

(1) W. Pauli et G. Källén: *Det. Kgl. Dansk. Vid. Selskab.*, **30**, Nr. 7 (1955).

(2) W. Thirring: *Helv. Phys. Acta*, **28**, 344 (1955). Voir aussi E. Arnous: *Journ. de Phys.*, **17**, 107, 374 (1956).

(3) C. Enz: *Supplemento al Nuovo Cimento*, **3**, 363 (1956).

(4) G. Källén et R. J. Glauber: à paraître.

(5) T. Okabayashi et S. Sato: *Prog. Theor. Phys.*, à paraitre.

et les électrons sont inférieurs à un rayon critique de l'ordre de $g^2/4\pi Mc^2$ et $e^2/4\pi mc^2$ respectivement.

Dès lors, si l'on applique les méthodes usuelles de renormalisation aux modèles relativistes, où les particules sont ponctuelles, on doit s'attendre à ce qu'elles introduisent aussi des états fantomatiques et il est naturel de penser que ces états doivent, du moins en théorie mésique, fausser les résultats de façon sensible.

La raison profonde de l'apparition de tels états et des difficultés qui en résultent est sans doute qu'un élément essentiel manque actuellement dans nos théories. Nous pouvons l'appeler « structure de la particule » ou « structure de l'espace autour de la particule », à la condition de ne pas attacher un sens trop précis au mot « structure ».

Evidemment, en donnant un certain rayon aux sources qui représentent les nucléons dans les modèles non-relativistes, on introduit déjà une des caractéristiques de la structure du nucléon, qui est son extension et nous savons que, si nous choisissons le rayon suffisamment grand, les pathologies disparaissent.

De même, en introduisant un cut-off dans les théories relativistes (6), on impose artificiellement aux impulsions une limite supérieure, qu'une structure des particules introduirait naturellement, et l'on fait probablement aussi disparaître les pathologies.

Mais il ne suffit pas d'introduire un élément de la structure capable d'éliminer les pathologies. Ceci permet tout au plus d'améliorer les résultats obtenus avec des particules ponctuelles. Si l'on veut que l'accord avec l'expérience devienne quantitatif, l'introduction d'autres éléments de la structure des particules est nécessaire. Or, ces éléments sont actuellement inconnus. Il faut donc attendre que l'expérience les révèle.

Telle est la conclusion à laquelle semble conduire l'examen de la situation présente de la théorie des champs quantifiés. Toutefois, elle n'est justifiée que si l'on est en mesure de montrer que le désaccord entre théorie et expérience ne vient pas, comme on l'a souvent pensé, des méthodes d'approximation utilisées.

C'est ce que nous allons essayer de montrer ici, en utilisant de nouveau un modèle non relativiste que l'on sait traiter sans approximation: celui où les nucléons sont considérés comme des sources fixes et étendues en interaction avec le champ mésique scalaire neutre. On peut, en effet, montrer avec ce modèle, que la loi de probabilité qui donne le nombre de mésons virtuels dans le champ est une loi de Poisson

$$P_n = \frac{\bar{n}^n}{n!} e^{-\bar{n}},$$

(6) W. HEITLER et E. ARNOUS: *Nuovo Cimento*, **2**, 1282 (1955).

et l'on peut tracer les courbes qui donnent le nombre probable c des mésons, en fonction du rayon des nucléons et de leur distance, pour différentes valeurs de la constante de couplage.

Or, il ressort de l'examen de ces courbes que l'effet de la structure des nucléons est de limiter le nombre des mésons virtuels et que ce nombre ne peut guère dépasser un ou deux pour des rayons et des distances de l'ordre de 10^{-13} cm et pour $g^2/4\pi\hbar c \sim 1$.

Par suite, des méthodes du type Tamm-Dancoff, qui sont totalement injustifiées pour des particules ponctuelles, car c est alors infini (cf. (7)), deviennent raisonnables pour de tels rayons, c'est-à-dire encore pour des cut-off de l'ordre de la masse du nucléon.

La conclusion de cette étude est ainsi que la cause du désaccord, qui subsiste entre théorie et expérience, n'est pas l'insuffisance de nos méthodes d'approximations, mais essentiellement l'absence de structure des particules dans nos modèles. Dans quelle mesure les modèles de WENTZEL (2) et de KRAMERS (3) confirment-ils ces conclusions, il serait intéressant de le savoir.

1. – Modèle.

Notre modèle est le modèle bien connu suivant: les nucléons sont considérés comme des sources fixes et étendues. Désignons par $g\varrho(\boldsymbol{x})$ la densité de charge mésique sphérique qui représente un nucléon,

$$\varrho = g \sum_i \varrho(\boldsymbol{x} - \boldsymbol{R}_i)$$

est alors la densité de charge mésique qui représente l'ensemble des nucléons, et l'hamiltonien du système est

$$H_0 = \frac{1}{2}\int \mathrm{d}\boldsymbol{x}\,[\pi^2(\boldsymbol{x}) + (\operatorname{grad}\varphi(\boldsymbol{x}))^2 + \mu^2\varphi^2(\boldsymbol{x})]\,, \tag{1}$$

$$H_1 = g\int \mathrm{d}\boldsymbol{x} \sum_i \varrho(\boldsymbol{x} - \boldsymbol{R}_i)\varphi(\boldsymbol{x})\,, \tag{2}$$

$$H = H_0 + H_1\,,$$

où $\varphi(\boldsymbol{x})$ est le champ mésique, $\pi(\boldsymbol{x})$ le champ canoniquement conjugué et μ la masse du méson ($\hbar = c = 1$).

(7) L. VAN HOVE: *Physica*, **18**, 145 (1952).

Si l'on passe à l'espace des impulsions, on trouve

$$(3) \qquad q(\boldsymbol{x}) = \left(\frac{1}{2\pi}\right)^{\frac{3}{2}} \int \frac{\mathrm{d}\boldsymbol{k}}{\sqrt{2\omega_k}} (\exp[i\boldsymbol{k}\cdot\boldsymbol{x}]a(\boldsymbol{k}) + \exp[-i\boldsymbol{k}\cdot\boldsymbol{x}]a^*(\boldsymbol{k})) ,$$

$$(4) \qquad \pi(\boldsymbol{x}) = \left(\frac{1}{2\pi}\right)^{\frac{3}{2}} \int \mathrm{d}\boldsymbol{k} \sqrt{\frac{\omega_k}{2}}\, i\, (\exp[-i\boldsymbol{k}\cdot\boldsymbol{x}]a^*(\boldsymbol{k}) - \exp[i\boldsymbol{k}\cdot\boldsymbol{x}]a(\boldsymbol{k})) ,$$

$$(5) \qquad \varrho(\boldsymbol{x}) = \left(\frac{1}{2\pi}\right)^{3} \int \mathrm{d}\boldsymbol{k} \exp[i\boldsymbol{k}\cdot\boldsymbol{x}]u(\boldsymbol{k}) ,$$

$$(6) \qquad H_0 = \int \mathrm{d}\boldsymbol{k}\,\omega_k a^*(\boldsymbol{k})a(\boldsymbol{k}) + \frac{1}{2}\int \mathrm{d}\boldsymbol{k}\,\omega_k ,$$

$$(7) \qquad H_1 = \int \mathrm{d}\boldsymbol{k}\,\omega_k[\lambda(\boldsymbol{k})a(\boldsymbol{k}) - \lambda^*(\boldsymbol{k})a^*(\boldsymbol{k})] .$$

$$(8) \qquad \lambda(\boldsymbol{k}) = \left(\frac{1}{2\pi}\right)^{\frac{3}{2}} g\, \frac{u(\boldsymbol{k}) \sum \exp[i\boldsymbol{k}\cdot\boldsymbol{R}_i]}{\omega_k^{\frac{3}{2}}\sqrt{2}} ,$$

$$K = |\boldsymbol{k}| , \qquad \omega_K = \sqrt{K^2 + \mu^2} .$$

a^* et a désignent les opérateurs de création et d'annihilation de mésons d'impulsion $\boldsymbol{k}$.

2. – Diagonalisation de l'hamiltonien.

Comme il est bien connu, on peut diagonaliser l'hamiltonien H, en lui faisant subir la transformation

$$(9) \qquad e^{iG} = \exp\left[\int \mathrm{d}\boldsymbol{k}[\lambda(\boldsymbol{k})a(\boldsymbol{k}) - \lambda^*(\boldsymbol{k})a^*(\boldsymbol{k})]\right] .$$

e^{iG} est, en effet, un opérateur de la forme e^{x+y} et le commutateur de x et y est un « nombre c »:

$$(10) \qquad [x, y] = -\int \mathrm{d}\boldsymbol{k}\,|\lambda(\boldsymbol{k})|^2 = -c .$$

On peut donc l'écrire sous la forme

$$(11) \qquad e^{iG} \equiv e^{x+y} = e^{-c/2}e^{y}e^{x} = e^{c/2}e^{x}e^{y} .$$

On trouve alors ($a = \partial/\partial a^*$ et $a^* = -\partial/\partial a$)

$$(12) \qquad e^{-iG}(H_0 + H_1)e^{iG} = H_0 + V ,$$

où

$$V = -\int \mathrm{d}\boldsymbol{k}\,\omega_k\,|\lambda(\boldsymbol{k})|^2 . \tag{13}$$

3. – Fonction d'onde de l'état fondamental.

On en déduit immédiatement la fonction d'onde ψ de l'état fondamental. En effet, e^{iG} établit une correspondance biunivoque entre les fonctions propres de H_0 et celles de $H_0 + H_1$. Au niveau le plus bas de H_0, c'est-à-dire au vide $|0\rangle$, correspond le niveau le plus bas de $H_0 + H_1$, c'est-à-dire l'état fondamental

$$\psi = e^{iG}\,|0\rangle . \tag{14}$$

Comme $a(\boldsymbol{k})\,|0\rangle = 0$, on a

$$\exp\left[\int \mathrm{d}\boldsymbol{k}\,\lambda(\boldsymbol{k})\,a(\boldsymbol{k})\right]|0\rangle = |0\rangle$$

et, par suite

$$\psi = \exp[\,\cdot\, c/2]\,\exp\left[-\int \mathrm{d}\boldsymbol{k}\,\lambda^*(\boldsymbol{k})\,a^*(\boldsymbol{k})\right]|0\rangle . \tag{15}$$

Or, chaque opérateur a^* crée un méson. Dans l'espace de Fock, ψ est donc du type

$$\psi \left(\begin{array}{c} \psi_0 \\ \psi_1\ (\boldsymbol{p}_1) \\ \psi_2\ (\boldsymbol{p}_1, \boldsymbol{p}_2) \\ \cdot \\ \cdot \end{array} \right),$$

avec

$$\psi_n(\boldsymbol{p}_1, \ldots, \boldsymbol{p}_n) = \exp[-c/2]\,\frac{(-1)^n}{n!}\left[\int \mathrm{d}\boldsymbol{k}\,\lambda^*(\boldsymbol{k})\,a^*(\boldsymbol{k})\right]^n |0\rangle . \tag{16}$$

Explicitons ψ_n. On a successivement

$$a^*(\boldsymbol{k})\,|0\rangle \quad \delta(\boldsymbol{p}_1 - \boldsymbol{k}),$$

donc

$$\int \mathrm{d}\boldsymbol{k}\,\lambda^*(\boldsymbol{k})\,a^*(\boldsymbol{k})\,|0\rangle \quad \lambda^*(\boldsymbol{p}_1).$$

Puis

$$a^*(\boldsymbol{k})\lambda^*(\boldsymbol{p}_1) = \frac{1}{\sqrt{2}}\{\delta(\boldsymbol{p}_1 - \boldsymbol{k})\lambda^*(\boldsymbol{p}_2) + \delta(\boldsymbol{p}_2 - \boldsymbol{k})\lambda^*(\boldsymbol{p}_1)\},$$

donc

$$\frac{1}{2}\int \mathrm{d}\boldsymbol{k}\lambda^*(\boldsymbol{k})a^*(\boldsymbol{k})\lambda^*(\boldsymbol{p}_1) = \frac{1}{\sqrt{2}}\lambda^*(\boldsymbol{p}_1)\lambda^*(\boldsymbol{p}_2)$$

etc... Finalement

$$\psi_n(\boldsymbol{p}_1 \dots \boldsymbol{p}_n) = \exp[-c/2]\frac{(-1)^n}{\sqrt{n!}}\lambda^*(\boldsymbol{p}_1)\dots\lambda^*(\boldsymbol{p}_n)\,. \tag{17}$$

C'est la composante à n mésons de la fonction d'onde de l'état fondamental dans l'espace de Fock. On remarquera qu'elle n'est pas de carré sommable pour des particules ponctuelles ($u = 1$).

4. – Nombre de mésons dans le champ.

On en déduit la probabilité de trouver n mésons dans le champ. C'est en effet

$$\mathcal{P}_n = \langle \Psi_n, \Psi_n \rangle = \int \mathrm{d}\boldsymbol{p}_1 \dots \mathrm{d}\boldsymbol{p}_n |\Psi_n|^2 = \frac{e^{-c}c^n}{n!}\,, \tag{18}$$

où

$$c = \int \mathrm{d}\boldsymbol{k}\,|\lambda(\boldsymbol{k})|^2\,. \tag{10}$$

Elle est donnée par une loi de Poisson [8] de valeur moyenne c.

5. Valeur probable du nombre de mésons en fonction du rayon des sources et de la distance entre les nucléons.

Prenons, par exemple,

$$u^2(\boldsymbol{k}) = \frac{1}{1 + r^2k^2}\,, \tag{19}$$

où r représente le rayon de la source, et supposons $r \leqslant \hbar/\mu c$.

---

[8] Cf. H. Umezawa: *Quantum Field Theory*, p. 217 et bibliographie citée.

a) S'il y a un seul nucléon,

$$c \equiv c_1 = \frac{g^2}{4\pi^2}\int_0^\infty \frac{k^2\,\mathrm{d}k}{(k^2+\mu^2)^{\frac{3}{2}}(1+r^2k^2)} \tag{20}$$

$$= \frac{g^2/4\pi\hbar c}{\pi(1-\mu^2r^2)}\left\{\frac{1}{2\sqrt{1-\mu^2r^2}}\log\frac{1+\sqrt{1-\mu^2r^2}}{1-\sqrt{1-\mu^2r^2}} - 1\right\}.$$

Les courbes suivantes donnent c_1 en fonction de r pour différentes valeurs de $\alpha = g^2/4\pi\hbar c$ comprises entre 1/10 et 10.

b) Pour deux nucléons distants de R, on trouve

$$C \equiv C_2 = \frac{g^2}{4\pi^2}\,\frac{1}{iR}\int_{-\infty}^{\infty}\frac{dk\,k\exp[ikR]}{(k^2+\mu^2)^{\frac{3}{2}}(1+r^2k^2)} + 2C_1\,. \tag{21}$$

Si $r = \hbar/\mu c$, l'intégrale précédente est égale à

$$C_2 = (g^2/4\pi)\,\frac{1}{3}\,\mu R\,\frac{2}{\pi}\,K_1(\mu R) + 2C_1\,. \tag{22}$$

où K_1 est la fonction de Hankel modifiée d'ordre 1.

Si $r < \hbar/\mu c$, on écrit

$$C_2 = \frac{g^2}{4\pi}\,\frac{2}{\pi}\int_0^\infty \frac{k\sin k\,\mathrm{d}k}{(k^2+\mu^2R^2)^{\frac{3}{2}}(1+k^2(\mu^2r^2/\mu^2R^2))} + 2C_1\,, \tag{23}$$

et l'on calcule numériquement l'intégrale. On trouve les courbes suivantes:

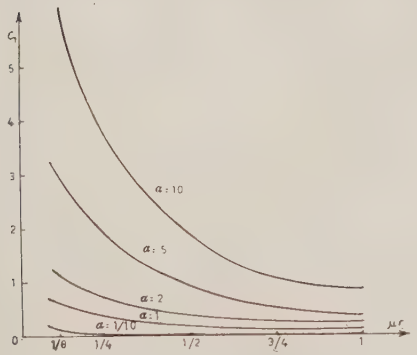

Fig. 1. – Nombre de mésons virtuels en fonction de μr, calculé avec la fonction source $u^2 = 1/(1+K^2r^2)$.

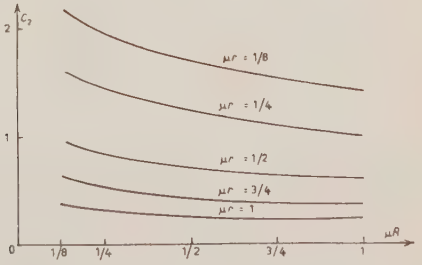

Fig. 2. – Nombre de mésons virtuels en fonction de μR, pour différentes valeurs du rayon r des sources. On prend $g^2/4\pi\hbar c = 1$ et la fonction source $u^2 = 1/(1+k^2r^2)$.

6. – Pour compléter cette étude, donnons encore la self-énergie du nucléon en fonction de r et le potentiel d'interaction entre deux nucléons en fonction de r et R, toujours avec la fonction source $u^2 = 1/(1 + k^2 r^2)$:

$$V \text{ self} = -\frac{g^2/4\pi\hbar c}{2r(1+\mu r)}, \tag{24}$$

$$V(R) = \frac{-g^2/4\pi\hbar c}{R}\,\frac{\exp[-R/\lambda] - \exp[-R/r]}{1 - r^2/\lambda^2}, \tag{25}$$

où $\lambda = \hbar/\mu c$ et $V(0) = 2V$ self.

* * *

En terminant, je remercie M. le Professeur W. HEITLER pour l'intérêt qu'il a pris à ce travail et les fructueuses discussions que nous avons eues à ce sujet.

RIASSUNTO (*)

Si studia un modello ben noto in cui i nucleoni si considerano come sorgenti fisse ed estese in interazione con un campo scalare neutro. Si calcola la funzione d'onda esatta per lo stato fondamentale e si dimostra che la distribuzione di probabilità del numero di mesoni virtuali è una distribuzione poissoniana. Il valor medio di tale numero si calcola in funzione del raggio delle sorgenti e della distanza tra i nucleoni. Si vede che questo numero di mesoni virtuali non supera mai 1 o 2 per raggi e distanze dell'ordine di 10^{-13} cm e valori di $g^2/4\pi\hbar c$ di ordine 1. I risultati di cui sopra appaiono giustificare metodi del tipo di quello di Tamm-Dancoff.

(*) *Traduzione a cura della Redazione.*

Multiple Meson Production and Angular Distribution of Shower Particles Produced in Cosmic Ray «Jets».

L. v. Lindern

Max-Planck-Institut für Physik - Göttingen
Istituto di Fisica dell'Università - Padova
Istituto Nazionale di Fisica Nucleare - Sezione di Padova

(ricevuto il 29 Novembre 1956)

Summary. — In nuclear emulsions exposed to the cosmic radiation, showers have been studied (*) which are produced by singly charged or neutral particles, mainly perhaps nucleons (i.e. «Jets» or mesonic showers; their total, number being 22.) The analysis has been restricted to events whose primary energies are greater than 20 GeV, and the number of visible shower particles of which are equal to or greater than 8. An upper limit of $N_h=3$ for the «heavy» and «grey» prongs has been chosen for each event. (The total number of charged shower particles is 255 and of «grey» or «heavy» prongs is 28.) Such selected showers are interpreted in terms of multiple meson production, and the shower particles are supposed to be mainly mesons produced at one single nucleon-nucleon collision. Within the spread of primary energies observed ($20 \div 500$ GeV) the angular distribution of shower particles shows a significant deviation from isotropic emission in the centre of mass system of the two colliding nucleons.

In a recent paper Schein, Glasser and Haskin [1] reported further details on the so-called «S-star», an event of very high energy ($\sim 10^{13}$ eV) initiated by a singly charged particle of the cosmic radiation. This event is interpreted

---

(*) The data reported in this work are based on a summary of explorations made at Göttingen (Max-Planck-Institut für Physik) and Padua (Istituto di Fisica). I am very much indebted to Dr. G. Salandin who kindly made available his measurements.

(1) M. Schein, R. G. Glasser and D. M. Haskin: *Nuovo Cimento*, **2**, 647 (1955).

by them as an example of multiple π-meson production in a nucleon-nucleon collision. The measured angular distribution shows a strongly peaked anisotropy of particle emission around the collision axis in the center of mass system (CMS) (See note added in proof). This is of particular interest because such an effect is predicted by theories like Heisenberg's [2] or Landau's [3], and also may be compared with the Fermi-model of multiple meson production [4].

In Fermi-theory anisotropy is to be expected only for non-central collisions, in which transverse momentum transfer prevents rotational symmetry with respect to the collision axis, and the distribution of particle emission should be shaped like a Catherine-wheel: an effect which so far has not been observed [5].

The angular distribution predicted by HEISENBERG [2] or LANDAU [3] are generally similar to each other in shape and are both different from that of FERMI [4]: they should be peaked symmetrically around the collision axis, the more so the higher are the energies of the emitted particles. This also applies to central collisions. Especially in the case of Heisenberg-theory, a central point of interest is to know experimentally how strongly the degree of anisotropy is coupled with the energies of the emitted particles, because then it would be possible to test the suppositions upon which the theory is based [5]. (For instance the assumption of strong interaction between the created particles which implies the special shape of their energy spectrum).

Much experimental work has been done on multiple meson production [6] but decisive knowledge is still rare. The effect itself, i.e. the generation of many mesons at one single nucleon-nucleon collision has now been quite well established by work done in the lower energy region using artificially accelerated particles [7]. In this energy region, however, the approximations used in the theories of Heisenberg [2], Fermi [4] and Landau [3] are not valid: complex quantum mechanics must be taken into account there. Thus, so far, and

---

[2] W. HEISENBERG: *Zeits. f. Phys.*, **133**, 65 (1952); *Vorträge über kosmische Strahlung* (Berlin-Göttingen-Heidelberg, 1953).

[3] S. S. BELENKI and L. D. LANDAU: *Uspechi Fiz. Nauk*, **56**, 309 (1955); L. D. LANDAU: *Izv. Akad. Nauk SSSR, Ser. Fiz.*, **17***n*, 51 (1953).

[4] E. FERMI: *Progr. Theor. Phys.*, **5**, 570 (1950); *Phys. Rev.*, **81**, 683 (1951).

[5] It is a pleasure to thank Professor HEISENBERG and Dr. SYMANZIK for many discussions about these points.

[6] See for instance R. E. MARSHAK: *Meson Physics* (New York, 1952), 273 ff.; A. BETHE and F. DE HOFFMANN: *Mesons and Fields*, II (Evanstone, Ill.; White Plains, N. Y., 1955).

[7] W. B. FOWLER, G. MAENCHEN, W. M. POWELL, G. SAPHIR and R. W. WRIGHT: *Phys. Rev.*, **101**, 911 (1956).

probably for some time to come, only the cosmic radiation makes available information in the high energy region which could be compared with present theories of multiple production.

In cosmic ray experiments at high altitudes the problem always arises of having clean conditions of observation. The need for sufficient statistics must be a compromise with the certainty of excluding complex events. Using nuclear emulsions as detectors this means that the higher are the numbers of shower particles initiated by a singly charged or neutral particle, and the smaller are the numbers of low energy tracks in a shower, the higher is the possibility of excluding events in which cascade processes in complex nuclei have had a disturbing influence ([8]).

Previous work ([9]) of this type, together with the « S-star » observation ([1]) shows by energy calculation that Fermi-theory in its original form ([4]) does not fit the data very well. Fermi-theory results in a much higher value of the expected mean energies of the created particles than does the Heisenberg-model. The mean energies $\overline{E}_{0s}$ in the CMS depend on the primary energies as $\overline{E}_{0s} \sim \log E_{\text{prim}}$ for the Heisenberg-model ([2]) (E_{prim} primary energy in the LS), while in the Fermi-model ([4]) they will follow the fourth root of the primary energy; $E_{0s} \sim E_{\text{prim}}^{\frac{1}{4}}$. In addition the shapes of the differential energy distributions are different in both models and correspond to a power spectrum $1/E_{0s}^2$ on the one hand, and on the other to thermodynamical equilibrum. In a previous joint work ([9]) all detailed shower analyses available have been plotted. No experimental evidence was found that the mean energies of the secondaries are correlated with the primary energy in the way suggested by Fermi's and Landau's theories. A logarithmic dependence would be a better fit to the data. Also, in the energy distribution, more low energy particles were found than is predicted by Fermi's or Landau's model. This effect cannot wholly be attributed to bias of the scattering measurements. A power spectrum like Heisenberg's would be a better fit to the data. The theory of Landau to some extent keeps a mean position between the two theories of Fermi and Heisenberg, inasmuch as it gives an energy dependence similar to Fermi's, but an angular distribution similar to Heisenberg's ([5]).

At very high energies strong anisotropy of particle emission can occur in the CMS as is demonstrated by the « S-star » analysis ([1]). Also other workers ([10,11]) have reported to some extent on anisotropic emission (See note added in proof). Poor statistics have not allowed the finding of a definite

([8]) W. Heitler and C. Terreaux: *Proc. Phys. Soc. Lond.*, A **66**, 929 (1953).
([9]) L. v. Lindern: *Zeits. f. Naturf.*, **11***a*, 340 (1956).
([10]) D. Lal, B. Peters and Swami: *Pro. Ind. Acad. Sci.*, A **36**, 75 (1952).
([11]) M. F. Kaplon and D. M. Ritson: *Phys. Rev.*, **88**, 386 (1952); W. E. Hazen, R. E. Heinemann and E. S. Lennox: *Phys. Rev.*, **86**, 198 (1952).

deviation from isotropic emission in the CMS for primary energies spreading from 20 to 1000 GeV ([12,13]).

In principle there should be two ways of obtaining more complete information. One is to measure the energies of the particles to permit exact transformations into the CMS, but the restricted sample of measurable energies demands an extensive calculation which is seriously dependent on the accuracy of scattering measurements. On the other hand one could measure more angular distributions so as to have more complete statistics. Though very tedious this could be done with a considerably higher degree of accuracy than energy measurements allow. As has already been shown in ([9,11]) the angular distributions measured in the laboratory system (LS) are not very sensitive to different assumptions about the production process. Only strong anisotropy at very high energies seriously affects the angular distribution in the LS. Therefore very much material is necessary in order to obtain significant results. For this reason all the data on angular distributions available at Göttingen ([9,15]) and Padua ([16]) has been put together and treated in the same way.

1. – Angular Distribution in the Laboratory-System (LS) and Conditions in the Centre of Mass System (CMS).

a) At higher values of the primary energy, in a first order approximation, one may for the simplicity of the calculations assume the quotient of the velocities of the primareis and secondaries to be equal to unity. $m = \beta_{0s}/\beta_s = 1$ (β_s = velocity of one nucleon in the CMS; β_{0s} = velocity of one shower particle in the CMS, supposing all to be π-mesons. The influence of heavy meson production has not been taken into account in the following). Then, for isotropic emission, one obtains the formula for calculating the primary energy which is often used ([14,17]): $\gamma_s = 1/\mathrm{tg}\,\theta_L(\frac{1}{2}) \approx 1/\theta_L(\frac{1}{2})$. $\theta_L(\frac{1}{2})$ corresponds to the half opening angle of the cone which contains half of the particles of the shower in the LS. $\gamma_s = (1-\beta_s)^{-\frac{1}{2}}$ = primary energy of one nucleon in rest mass units in the CMS. The primary energy in the LS is $E_{\mathrm{prim}} = Mc^2(2\gamma_s^2 - 1)$, $Mc^2 = 938$ MeV. The energies calculated by this formula may be too high by a factor of up to 2 since the suppositions of $m = 1$ and isotropic emission

---

([12]) T. F. Hoang: *Journ. d. Phys. Rad.*, **14**, 395 (1953).

([13]) A. Engler, U. Haber-Schaim and W. Winkler: *Nuovo Cimento*, **12**, 930 (1954).

([14]) C. Castagnoli, G. Cortini, C. Franzinetti, A. Manfredini and D. Moreno: *Nuovo Cimento*, **10**, 1539 (1953).

([15]) K. Gottstein and M. Teucher: *Zeits. f. Naturf.*, **8***a*, 120 (1953).

([16]) G. Salandin: *Thesis Padova*, 1955.

([17]) C. C. Dilworth, S. J. Goldsack, T. F. Hoang and L. Scarsi: *Nuovo Cimento*, **10**, 1261 (1953).

can only be rough approximations ([18]). Calculating the primary energies only from the half-angle is influenced strongly by statistic fluctuations, whereas all information of angular distribution should be used ([14,17]). In this paper the primary energies are calculated as described in a previous work ([9]): the treatment is generally similar to that of CASTAGNOLI *et al.* ([11]).

The integral angular distribution in the LS is obtained under these conditions by using the transformation rules:

$$F_1^* \qquad \gamma_s^2 \sin^2 \vartheta_L \qquad 1 \qquad (\gamma_s^2 \quad 1) \sin^2 \vartheta_L ,$$

ϑ_L: angle of particle emission in the LS with respect to the primary direction.

For higher values of the primary energy the distribution can be approximated best by

$$F_1 = \frac{u^2}{1 \quad u^2} \qquad \text{with} \quad u = \gamma_s \cdot \vartheta_L .$$

To a large extent this distribution is independent of primary energy. In Fig. 1 F_1 is plotted, and the deviations at lower values of the primary energy

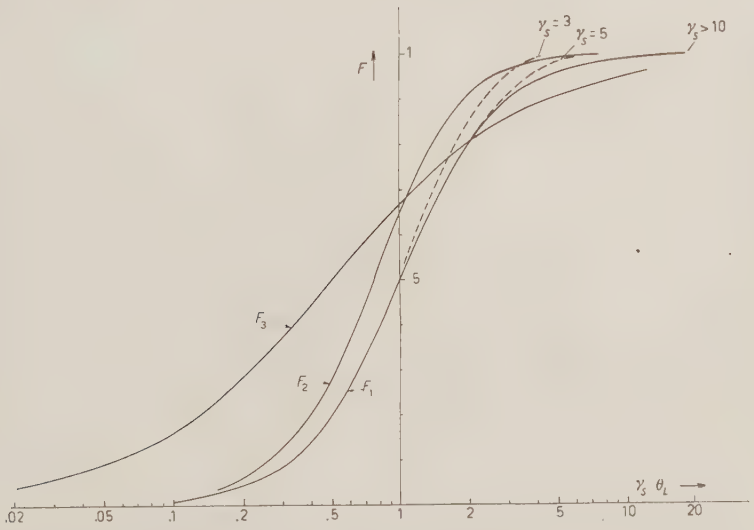

Fig. 1. – Approximately calculated integral distributions of angles in the lab. system for multiple meson production in nucleon-nucleon collisions. F_1: Isotropy and $m=1$, F_2: Isotropy and Heisenberg-spectrum ([2,18]); F_3: strong anisotropy an Heisenberg-spectrum ([18]) (see text).

([18]) K. SYMANZIK: Anhang 7*a*, 563 in W. HEISENBERG: *Vorträge über kosmische Strahlung* (Berlin-Göttingen-Heidelberg, 1953).

are also drawn; a logarithmic scale has been chosen for convenience. Regarding energy conservation, the assumption that $m = 1$ can hardly be maintained if a higher number of particles is produced; in which case m should be smaller than 1. On the other hand the velocities of all shower particles should not be equal.

b) Another curve has therefore been plotted, calculated from formulae given by SYMANZIK ([18]). It approximately represents the angular distribution in the LS if the emission in the CMS is still isotropic, but the particle energies are distributed as $1/E_{0s}^2$ (E_0^s = energy of secondaries in the CMS), a special spectrum proposed by HEISENBERG ([2]), which leads to:

$$1 - F_2 = \frac{1}{(1+u^2)^{\frac{3}{2}}} \qquad \text{with } u = \gamma_s \vartheta_L .$$

Curve F_2 reaches its half-value earlier than does curve F_1. Now there are many particles of lower energy in the CMS; their angles transformed to the LS will be somewhat smaller than in the case of $m = 1$. The primary energy calculated by the half angle must be reduced by a factor of 0.77 in this case. Apart from a constant difference due to the factor 0.77 this curve is only little steeper in slope than is curve F_1. The assumption of other energy spectra such as Fermi's or Landau's should only result in smaller deviations from F_1, because in these the mean energies of the secondaries are higher than in Heisenberg's. The curve for $m = 1$ should give a lower limit to the slope for isotropic emission in the CMS. Although this result is only qualitative it will be of importance later.

c) As an extreme case SYMANZIK ([18]) has calculated a strong anisotropic emission in the CMS which is given by Heisenberg's assumptions ([5]). It results in a maximum difference between the two cones in the LS corresponding to backward and forward emission in the CMS. His approximation can also be written in terms of $\gamma_s \theta_L$ and should be valid if $\gamma_s > 20$.

$$1 - F_3 = \frac{1}{1 + 2u} \qquad \text{with } u = \gamma_s \vartheta_L .$$

(In this case the primary energy calculated by the half-angle must be reduced by a factor of 0.5.) The curve F_3 shows that apart from the constant difference due to the factor 0.5, anisotropy of a type mentioned here reduces the slope of the integral distribution. The collimation of higher energy particles around the collision axis also favours smaller and larger angles. The forward and backward cones of the CMS are separated in the LS to a larger extent. With respect to curve F_1 the anisotropy and the energy spectrum lead to opposite

effects; the slope is steepened by the energy spectrum and lowered by the anisotropy.

2. – Measurements and Discussion.

Leitz and Koristka microscopes have been used at Göttingen and Padua respectively for all measurements reported here. The Ilford G5 emulsions (400 μm and 600 μm) were flown during the Sardinia expeditions (1952 and 53). From the scanned material 22 « Jets » have been selected which satisfy the following selection criteria: 1) The primary must be a singly charged or neutral particle of energy higher than 20 GeV. 2) The number of shower particles visible in each event must be equal to or greater than 8 (tracks with ionization less than 1.4 times minimum). 3) The number of « grey » or « heavy » prongs present must be less than or equal to 3. (« Grey » or « heavy » prongs are mainly due to evaporation or cascade processes of complex nuclei.) As a result of this selection there is a high probability for observing undisturbed multiple processes. The higher number of charged shower particles prevents stronger modification by the emission of neutral particles. The distribution of charged shower particles is taken to be representative of the total distribution. The influence of nucleons remaining from the initial collision is neglected. Thus these selected events may serve for our detailed discussion. The total number of charged shower particles in the selected events is 255, that of « grey » or « heavy » prongs is 28; their mean number per event are 11.6 and 1.3 respectively.

The angles of emission with respect to the primary direction have been calculated from projected and dip angles. The influence of error is regarded as being small for projected angles but somewhat higher for strongly dipping

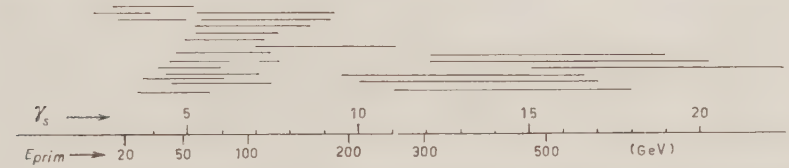

Fig. 2. – Primary energies of the 22 events calculates as described in [9]. The indicated intervals are due to statistical fluctuations.

events, which were therefore also excluded. The influence of multiple scattering could be neglected in this energy region. The primary energies of our events are plotted in Fig. 2. In Fig. 3 the integral distribution of one « jet » is shown, and is compared with an isotropic one in the CMS for $m = 1$ and

primary energy of 340 GeV. As shown above, angular distributions are comparable for different primary energies if the distribution of the product $\gamma_s\theta_L$ is taken into account. Each angle has therefore been multiplied by the energy of its corresponding primary, and the products $\gamma_s\theta_L$ have been plotted for all shower tracks together (Fig. 4). For convenience, points represent the middle of each step in the integral shapes. The mean step-length indicated corresponds to the mean number of shower particles per event, which is 11.6 in this case (see also Fig. 3). Each point is supposed to be of the same weight, because particle numbers do not fluctuate much. The mean error in angular measurement has been calculated from repeated measurements. It is somewhat larger for very low and very high values of the emission angles (for $\theta_L < 1°$ and $\theta_L > 60°$), but this can be neglected because they are rare and the discussion does not depend strongly upon them. A systematic error in calculating the primary energies only results in a constant parallel transposition of all points. The discussion is not affected by this to any great extent. To prevent bias those events are also plotted whose integral shape shows a very steep slope, possibly signifying a strong disturbance by complex nuclei.

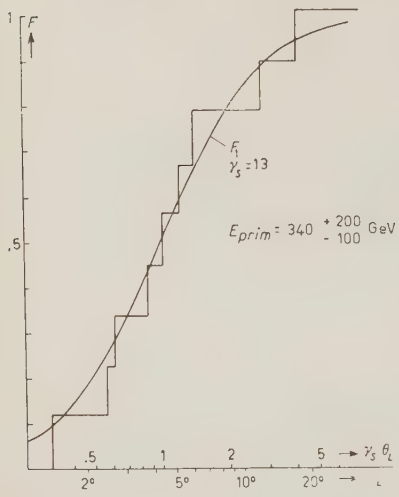

Fig. 3. – Integral angular distribution of one event in the LS. The curve corresponds to an isotropic emission and $m=1$ in the CMS. (F_1) The primary energy is $E_{\text{prim}} = 340^{+200}_{-100}$ GeV.

Completing previous work [9] this summa-

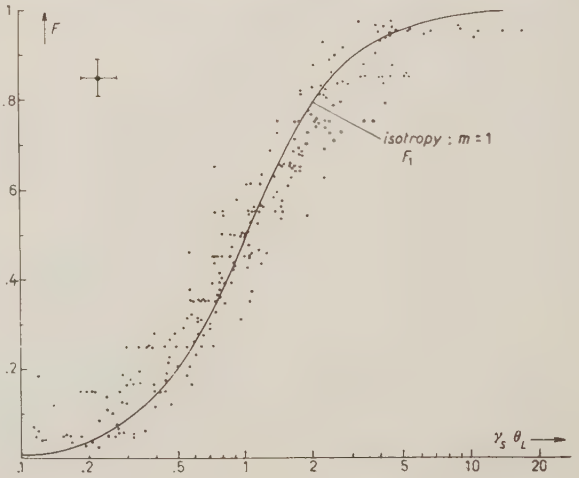

Fig. 4. – Integral distributions of products $\gamma_s\theta_L$ for 22 selected events. The curve represents isotropic emission and $m=1$ in the CMS (F_1) (see text).

rized material allows significant deviation from isotropic emission in the CMS to be detected. This is shown by considering the differential distribution of

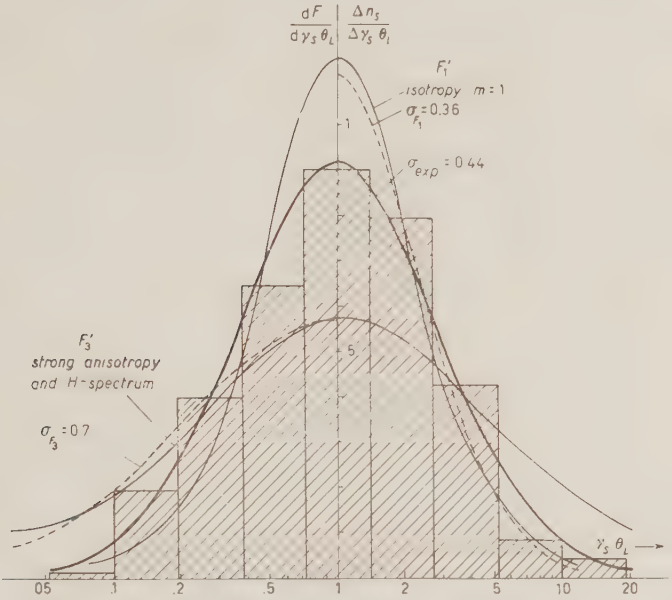

Fig. 5. - Differential distribution of 255 values of $\gamma_s\vartheta_L$ plotted in Fig. 4. The curve F_1' corresponds to an isotropic emission and $m=1$ in the CMS. It is approximated by a Gaussian curve of $\sigma_{F_1}=0.36$. Approximately the curve F_3 represents strong anisotropic emission and Heisenberg-spectrum for very high primary energies ([2,18]). Its Gaussian approximation is of value $\sigma_{F_3}=0.7$. The best fitting Gaussian curve to the data is of value $\sigma_{exp}=0.44$ (see text).

the products $\gamma_s\vartheta_L$ in Fig. 5. For comparison the differential curves for isotropic emission (F_1') and strong anisotropy (F_3') have also been drawn, and have been displaced to make their maximum abscissa coincide. (The curve corresponding to F_2 would only be somewhat more peaked than F_1'). They are well approximated by Gaussian curves whose standard deviations correspond to the shape of the angular distribution in the CMS: $\sigma_{F_1}=0.36$ for an isotropic one of maximum breadth ($m=1$, see above), and $\sigma_{F_3}=0.7$ for a strongly anisotropic one. The best fitting Gaussian curve for the data is $\sigma_{exp}=0.44$. The 95% probability interval ranges from $0.41<\sigma_{exp}<0.46$ as shown by a χ^2-test. If the distribution in the CMS is isotropic, then, bearing in mind statistical fluctuations of the primary energies and errors of measurement ($\sigma_{E\,prim}\sim 0.1$, $\sigma_{meas}<0.1$), σ_{exp} should not exceed 0.39 with a

probability of 95%. Thus the deviation is significant though not very large. This can also been seen in Fig. 6 where the integral distribution of all shower tracks has been plotted as a total.

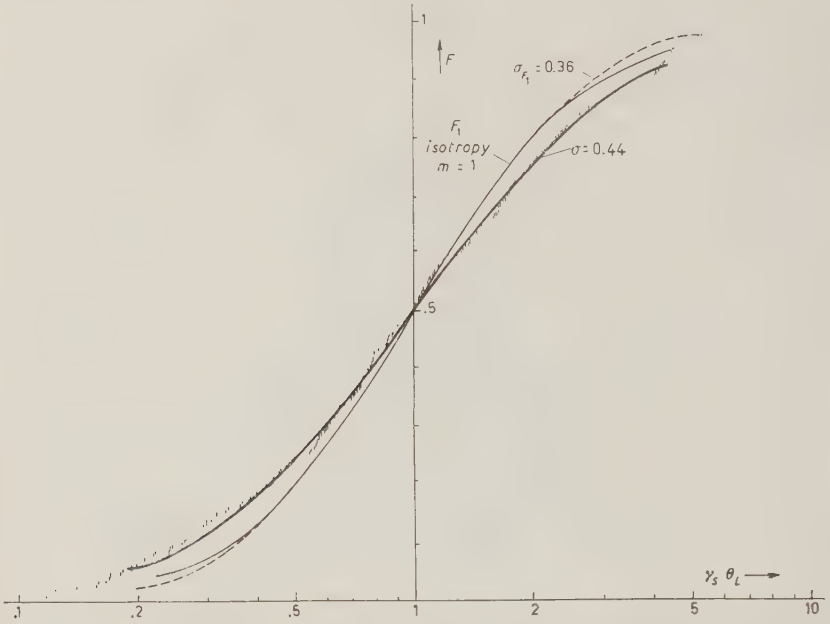

Fig. 6. Integral distribution of all values $\gamma_s \theta_L$ as a total. The meaning of symbols for the curves is given in Fig. 5.

3. – Conclusion.

The deviation reported here can be ascribed to a non-isotropic emission in the CMS, probably of a type corresponding to Heisenberg's or Landau's theory. An explanation in terms of disturbing cascade processes is made very improbably by the selection of events, and is in contrast to the effect which prefers both lower and higher values of the emission angles in the LS. The special degree of anisotropy cannot easily be derived from this material because as yet unexplained opposing effects must be taken into account, such as those due to the energy spectrum and to the disturbance by complex nuclei.

* * *

The author wishes to thank Professor W. Heisenberg for his encouragement, and is also much indebted to Professors A. Rostagni and N. Dalla-

PORTA for their kind interest and for hospitality at Padua. Many thanks are also due to the groups of Göttingen and Padua and in particularly to Professor M. MERLIN and Dr. K. GOTTSTEIN for their invaluable help. Special thanks are due to Dr. G. SALANDIN for the kind attribution of his measurements.

Note added in proof.

For very high energy events anisotropic distribution has recently been reported also by A. DEBENEDETTI, C. M. GARELLI, L. TALLONE and M. VIGONE: *Nuovo Cimento*, **4**, 1142 (1956); E. LOHRMANN: *Zeits. f. Naturfor.*, **11***a*, 561 (1956) and F. D. HÄNNI, C. LANG, M. TEUCHER, W. WINZELER and E. LOHRMANN: *Nuovo Cimento*, **4**, 1473 (1956).

RIASSUNTO

Nelle emulsioni nucleari esposte ai raggi cosmici, sono stati studiati dei getti i quali sono generati da una singola carica o da particelle neutre, probabilmente nucleoni (cioè « jets » o getti mesonici; il loro totale essendo 22). L'analisi è stata limitata agli eventi con energie primarie superiori a 20 GeV e numero di particelle visibile eguale o maggiore di 8. Per ogni evento è stato scelto un massimo limite di $N_h = 3$ per le tracce « nere » e « grige ». (Il numero totale di particelle cariche dei getti è 255 e delle tracce « grige » o « nere » è 28.) Gli stessi getti scelti sono interpretati come produzione multipla di mesoni, e si suppone che le particelle dei getti, siano probabilmente mesoni prodotti da una sola collisione nucleone-nucleone. Nello spazio della energia primaria osservata (20 ÷ 500 GeV) la distribuzione angolare delle particelle dei getti mostra una deviazione significante dalla emissione isotropa nel baricentro dei due nucleoni urtanti.

Comparison between (n, p) and (p, p′) Experiments on Intermediate Energy.

L. Colli
Laboratori CISE - Milano
Istituto Nazionale di Fisica Nucleare - Sezione di Milano

U. Facchini
Laboratori CISE - Milano

S. Micheletti
Istituto di Scienze Fisiche dell'Università - Milano
Istituto Nazionale di Fisica Nucleare - Sezione di Milano

(ricevuto il 15 Gennaio 1957)

Summary. — An analysis of some experimental results giving proton spectra of n, p reactions induced with 14 MeV neutrons on ten elements ranging from Mg to Zr and the spectra of protons emitted in pp′ reactions from eight elements from Al to Au under bombardment of 18 MeV protons has been done. It is evident that such results are not clearly interpreted in the statistical evaporation theory and that level densities of the residual nucleus cannot be derived. Furthermore a relation existing among these spectra is brought to evidence; this relation has been found valid in all comparable cases: the spectra of the protons emitted from n, p and pp′ reactions are the same when the curves are compared versus the energy of the emitted proton. The shape of the spectra, when corrected for the effect of the barrier, does not shown strong variations versus the mass number A of the nucleus.

In this paper we are considering the results of some experiments on n, p and p, p′ reactions, with the aim of obtaining information on the mechanism of the interaction between particles and nuclei at intermediate energies. The n, p measurements have been taken by some of us with neutrons of 14.5 MeV energy for ten elements from Mg to Zr and have been presented in our previous papers [1-3]. The p, p′ measurements have been taken by Gugelot [4]

---

[1] L. Colli and U. Facchini: *Nuovo Cimento*, **4**, 671 (1956).
[2] C. Badoni, L. Colli and U. Facchini: *Nuovo Cimento*, **4**, 1618 (1956).
[3] L. Colli and U. Facchini: *Nuovo Cimento* (in the press).
[4] P. C. Gugelot: *Phys. Rev.*, **93**, 425 (1954).

with protons of 18 MeV energy and for eight elements from Al to Au. Both groups of experiments which have been obtained with incident particles of comparable energy give with good precision the spectra of protons emitted by the reaction considered.

The first step of this discussion will be to find out a possible interpretation of these results in the light of the statistic evaporation theory, as has been developed and presented by BLATT and WEISSKOPF [5].

It is important to point out that, even in the opinion of the authors, the results of the statistic evaporation theory must be considered with some reservation, particularly as far as concerns the energy examined in this paper.

Nevertheless, we feel it is interesting to make this comparison because the statistic evaporation theory is the only one developed to the point of calculating the shape of the spectrum of the emitted particles and also because some experimental results particularly on neutron emission, seem to confirm some of its predictions.

The fundamental hypotheses of the theory we are discussing are that the particle impinging on the target nucleus interacts strongly with the nucleons of the nucleus, and that the energy carrried by the particle is shared immediately among the nucleons, so that all the system formed by the particle and the target nucleus, and called the compound nucleus, reaches thermodynamical equilibrium.

When the excitation of the compound nucleus is high enough as in our case it is possible that nucleons are emitted by evaporation: a particle is emitted from the compound nucleus when, by means of collisions inside the nucleus, it reaches a kinetic energy high enough to permit it to escape from the nuclear field. According to these hypotheses the emission of the particles takes place irrespective of how the compound nucleus was formed and depends only on the kind of the compound nucleus, on its excitation energy and on the total angular momentum.

The escaping particle carries away a given quantity of energy from the system. The remainder of the energy is in such a quantity that the residual nucleus is generally left in one of its excited states. The statistical assumption consists in supposing that any excited state has equal probability of excitation. In these hypothesis the energy spectrum of the proton emitted by an excited nucleus is given by the formula:

$$n(\varepsilon)\,\mathrm{d}\varepsilon \div \varepsilon\sigma(\varepsilon)\omega(\varepsilon_0 - \varepsilon)\,\mathrm{d}\varepsilon\,,$$

where $n(\varepsilon)\,\mathrm{d}\varepsilon$ is the number of protons emitted with energies between ε and $\varepsilon + \mathrm{d}\varepsilon$; $\sigma(\varepsilon)$ is the cross-section of the inverse reaction, i.e. of a proton of

[5] J. M. BLATT and V. F. WEISSKOPF: *Theoretical Nuclear Physics* (New York, 1952).

energy ε against the residual nucleus, and $\omega(\varepsilon_0 - \varepsilon)$ is the level density of the residual nucleus, where the levels have such momentum that the total momentum conservation is verified. $\omega(\varepsilon_0 - \varepsilon)$ corresponds to an excitation of the residual nucleus given by $E = \varepsilon_0 - \varepsilon$; ε_0 being the maximum possible energy of the protons emitted.

The spectrum given by this formula is obviously independent from the kind of reaction, that is from the way by which the nucleus is excited. The term $\varepsilon\sigma(\varepsilon)$ contains practically the barrier transmission and depends only on the energy of the emitted proton. The term $\omega(\varepsilon_0 - \varepsilon)$ which represents the level density of the residual nucleus, is the one in which we are interested. Knowing $n(\varepsilon)$ from the experimental results we can calculate $\omega(E) = \omega(\varepsilon_0 - \varepsilon) = n(\varepsilon)/\varepsilon\sigma(\varepsilon)$. The value of the cross-section $\sigma(\varepsilon)$ we used in the calculation was taken from BLATT and WEISSKOPF [5] and corresponds to the value of the nuclear radius given by $r = 1.5 \cdot 10^{-13} A^{\frac{1}{3}}$. These values are, as known, obtained in the statistical theory of the formation of the compound nucleus.

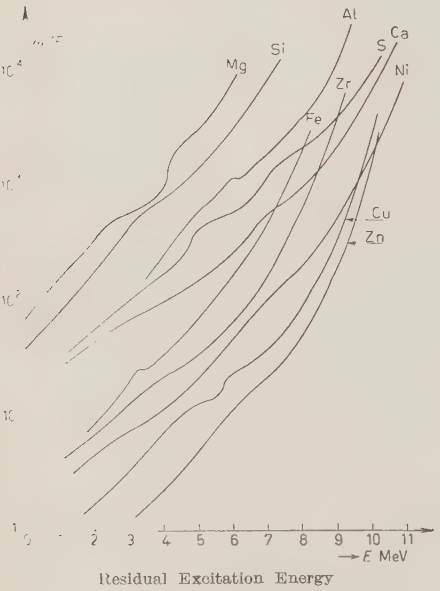

Fig. 1. – Curves giving $\omega(E) = n(\varepsilon)/\varepsilon\sigma(\varepsilon)$ obtained from measurements of proton energy spectra of the n, p reaction for ten elements plotted against residual nucleus excitation energy E. Ordinates are given in arbitrary units on a logarithmic scale.

Fig. 1 shows the curves representing $\omega(E)$ which are obtained from the measurements of energy spectra of protons from the n, p reactions of the ten elements Mg, Al, Si, S, Ca, Fe, Ni, Cu, Zn, Zr.

In this figure the excitation energy of the residual nucleus E in MeV is reported on the abscissa, and the ordinates are given in arbitrary units on a logarithmic scale.

All the curves have a similar shape, showing a concavity facing upward; all are steeper at higher excitation energies.

For comparison in Figs. 2 and 3 are shown the curves $\omega(E)$ obtained from our experiments on n, p reactions and from Gugelot's experiments on p, p′ reactions for the elements Al, Fe, Ni and Cu which are common to the two sets of measurements.

It must be pointed out that the residual nucleus is never the same for the same elements; from the n, p reaction we obtain always a nucleus with one

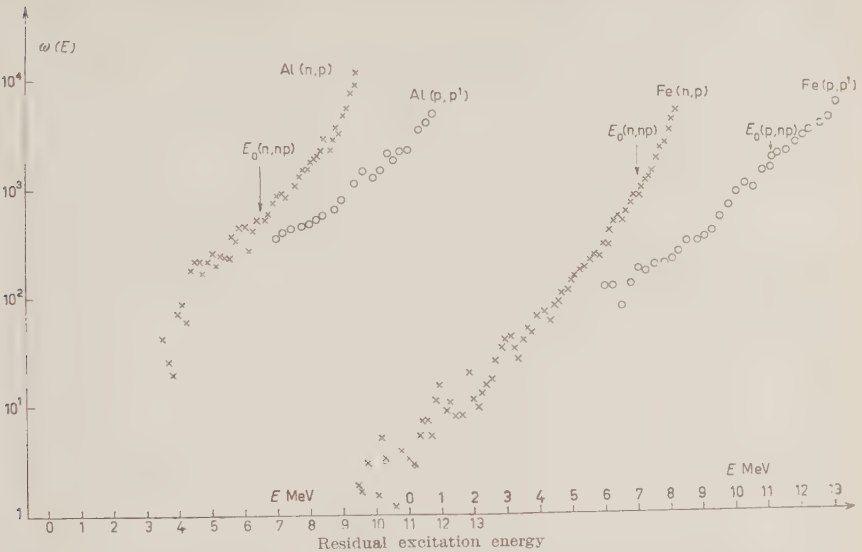

Fig. 2. – Comparison between $\omega(E)$ curves obtained from experimental data on n, p and p, p' reactions of Al and Fe. The curves are normalized in order to make them coincide at lowest excitation energy. The value E_0 corresponding to the threshold energy for n, np and p, np reactions is shown on the curves.

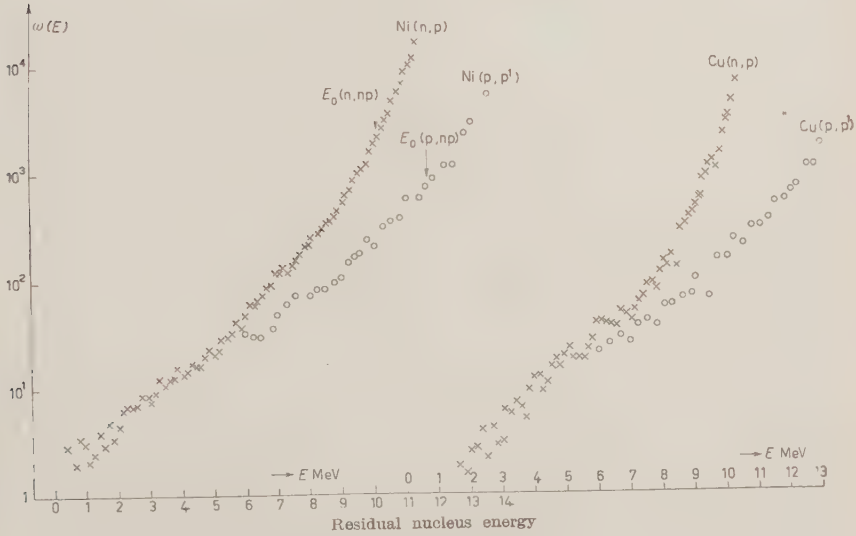

Fig. 3. – Comparison between $\omega(E)$ curves from n, p and p, p' for Ni and Cu. Scales and normalization are the same as in Fig. 2.

neutron more and one proton less that the one obtained from the p, p′ reaction. Yet, from the point of view of the statistic evaporation theory this should not make much difference.

The curves in Figs. 2 and 3 are normalized, in order to make them coincide at the lowest excitation energies.

Let us first consider the shape of the curves of Fig. 1: our knowledge of the level density is mainly theoretical, the experimental data being rather scarce and not sufficient to give a complete outline of level densities for many nuclei and in a large energy interval.

In the Fermi model, in which the nucleons are considered as independent particles in a potential well, the level density is given by

$$\omega(E) \div \exp[2\sqrt{aE}],$$

where a is a constant for each nucleus, the value of which increases with the mass of the nucleus. According to this formula, the curves of Fig. 1 whould show a parabolic shape with concavity facing downward; besides, their slope should increase rapidly with the increase in mass number A. Our curves, as the Gugelot's ones, do not show this behaviour.

If we consider now Figs. 2 and 3 we can see that the $\omega(E)$ curves obtained with the different reactions are in complete disagreement with one another.

All these considerations lead to the conclusion that the curves called here $\omega(E)$ do not represent truly the level density of nuclei.

An interpretation of the p, p′ spectra has been given by HAYAKAWA, KAWAY and KIKUCHI [6]. These authors have made an analysis of the spectrum of protons emitted in the Fe(p, p′) reaction, calculating the probability of the direct emission of a proton by means of a single interaction with the incident particle (knock-out proton) and calculating also the spectrum of protons emitted in the statistic evaporation theory while taking into account the protons emitted by means of the reactions (p, 2p), (p, np), (p, pn). These reactions should be important at the lowest proton energies, corresponding to 3 or 4 MeV, due to the rather high energy threshold for the emission of two particles. On the contrary, the knock-out process contribute protons at rather high proton energies, at the other end of the spectrum, and so the shape of the spectrum is changed at both ends.

Similarly in the case of protons emitted in n, p reactions all these processes may be considered; for many elements studied (n, np) reactions are possible at proton energy lower than 3-6 MeV, depending on the nucleus. Particularly, D. L. ALLAN [7] who obtains spectra from n, p reactions in the same conditions

[6] S. HAYAKAWA, M. KAWAY and K. KIKUCHI: *Prog. Theor. Phys.*, **13**, 415 (1955).
[7] D. L. ALLAN: *Proc. Phys. Soc.* (in the press).

and of the same shape as ours, explains the proton spectra of Al, Fe, Cu, Ni taking into account three different processes of proton emission: evaporation of a proton (n, pγ) or (n, pn), evaporation of a proton after the emission of a neutron (n, np) and proton emission by direct interaction of the impinging neutron with a single proton.

In this way a proton spectrum must be divided into three different parts.

1) The central part of the spectrum is attributed to evaporation of a proton according to the statistical theory of Weisskopf.

2) The low energy part is explained by means of the (n, np) reaction. In few cases ALLAN attributes an important quantity of protons to this reaction, explaining the rather high probability of the n, np reaction by taking into account that in these cases the reaction n, 2n for ε between 3 and 5 MeV cannot take place for reasons of energy conservation and so it is likely that the evaporation of a first neutron be followed by that of a proton (in competition it is possible to have only n, nγ).

3) The high energy part of the spectrum is explained by direct effect. By this is meant a proton emitted by single interaction with the incident neutron. In such scheme, all those protons which are not explained by evaporation processes should be emitted through this direct effect.

Obviously, taking these considerations into account, the curves $n(\varepsilon)'\varepsilon\sigma(\varepsilon)$ no longer represent the level densities, and no longer is an agreement possible between the values obtained from reactions n, p and p, p′.

In the light of the above, it is possible to make the following observations:

1) In the case of Mg and Si the n, np reaction is not possible when proton energies are higher than 3 MeV; yet at low energies ε, i.e. at high values of E, the spectra do not show a behaviour much different from those of other elements.

2) In Figs. 2 and 3 the value of the energy E_0 which corresponds to the threshold for the n, np and p, np reactions is shown on the curves. If we note the curves in these figures, we see that they do not show agreement with one another even at E values lower than E_0. In n, p and p, p′ reactions, therefore it would be necessary to assume a different contribution of the direct process for n, p and p, p′ reactions.

The direct process theory is not yet developed to the point of calculating such a contribution in every case; it is not possible to verify the validity of these conclusions.

However, we would like to report an interesting property of these spectra, that establishes a simple relation between them, which we have verified in all

the cases in which the comparison could be made: the spectra of the protons emitted by an element bombarded by 18 MeV protons or by 14.5 MeV neutrons are equal between each other when compared directly on the scale of the energy ε of the emitted proton. Fig. 4 shows the spectra of protons obtained by Al, Fe, Cu and Ni, with the reactions n, p at 14.5 MeV and p, p′ at 18 MeV, drawn as a function of the emitted proton energy ε and normalized.

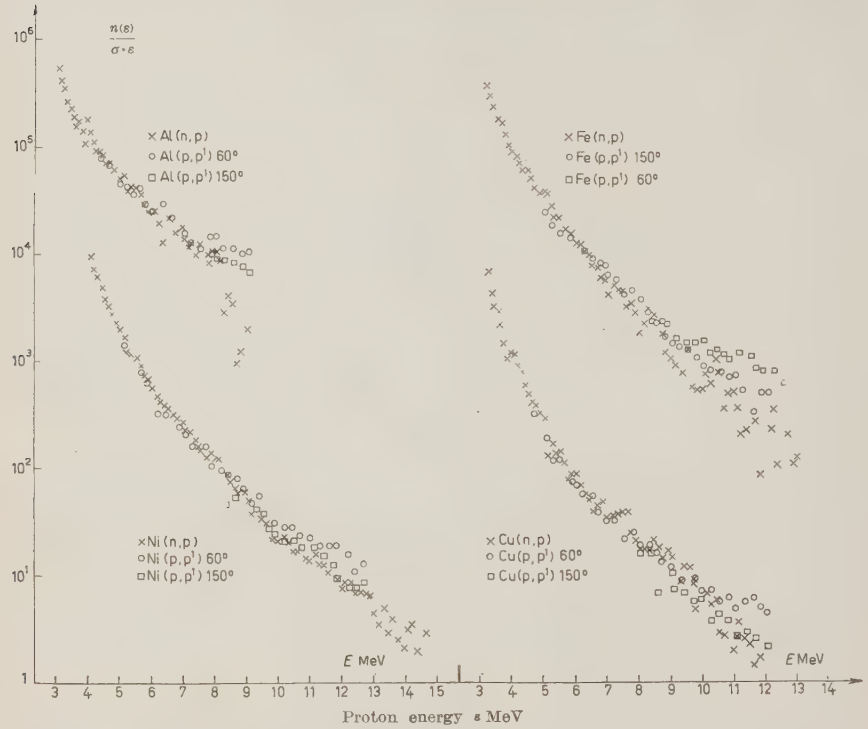

Fig. 4. - Values of the function $n(\varepsilon)/\varepsilon\sigma(\varepsilon)$ calculated from proton spectra emitted in n, p and p, p′ reactions. The curves are drawn as a function of the emitted proton energy ε.

In order to make the comparison easier, we have drawn in this figure also the curves giving $n(\varepsilon)/\varepsilon\sigma(\varepsilon)$. The comparison can be made only for energies higher that $4 \div 5$ MeV, the limit of the measurements obtained by GUGELOT. The agreement is particularly good with protons emitted at 150° in the p, p′ reactions.

A similar result was found by GUGELOT in the case of two proton spectra from Ag, obtained respectively from p, p′ reactions with 18 and 16 MeV

proton energy. Despite the different energies, the spectra of the emitted proton were equal.

Besides it must be pointed out that the curves shown in Fig. 1 have a similar behaviour and particularly so in the part corresponding to high energy protons, i.e. to low values of E on the scale shown in Fig. 1, in spite of the great difference in the values of the mass number A, if we disregard the more or less pronounced bumps shown by many spectra.

We must also point out that when compared in function of the proton energy even few proton spectra from γ, p reactions have the same shape as the ones discussed above as is clearly seen considering for instance the spectra obtained by LEIKIN *et al.* [8] for Cu(γ, p) and Ni(γ, p) with γ-rays of energies of 18, 20 and 24 MeV.

On the contrary, proton spectra from (d, p) and (α, p) reactions do not show a similar behaviour.

At this stage we cannot explain this similarity of proton spectra.

It would be interesting to establish if this equality is accidental or true and if this relationship can be based on taking into account a compound nucleus formation or some other mechanism of emission based for instance on a nucleon cascade or on a single particle excitation.

It must be noted also that many of our proton spectra show rather clearly some deviations from a smooth shape, often in the form of bumps or drops, having a shape similar to the giant reronances shown by the neutron cross-section curves in the region 0 ÷ 3 MeV and explained by the optical model theory.

* * *

We gladly thank Prof. BRUNO FERRETTI for his very interesting discussions.

(8) E. M LEIKIN, R. M. OSOKINA and B. S. RATNER: *Proc. Acad. Sci. USSR*, **102**, 245, 493 (1955).

RIASSUNTO

Un'analisi di alcuni risultati sperimentali che danno gli spettri dei protoni emessi in reazioni n, p con neutroni da 14 MeV da 10 elementi dal Mg allo Zr, e dei protoni emessi in reazioni pp' con protoni da 18 MeV da 8 elementi dall'Al al Au, mostra che tali risultati non sono chiaramente interpretabili sulla base della teoria dell'evaporazione statistica, e che da questi spettri non possono essere ricavate le densità di livelli del nucleo residuo. Viene messa in evidenza inoltre una relazione esistente fra questi spettri, che è stata trovata valida in tutti i casi confrontabili: gli spettri dei protoni emessi per mezzo delle reazioni n, p e pp' sono uguali quando sono confrontati direttamente in funzione dell'energia di emissione del protone. La forma dello spettro stesso, una volta corretto per l'effetto della barriera di potenziale, non varia molto col variare del numero di massa A del nucleo studiato.

NOTE TECNICHE

Camera di ionizzazione per raggi X fino a 31 MeV.

F. Ferrero, R. Malvano e C. Tribuno

Istituto di Fisica dell'Università - Torino
Istituto Nazionale di Fisica Nucleare - Sezione di Torino

(ricevuto il 30 Novembre 1956)

Riassunto. — Si descrive una camera di ionizzazione per raggi X fino a 31 MeV e se ne misura l'efficienza sia in relazione ai valori calcolati, sia in confronto allo standard comunemente usato nello studio delle reazioni fotonucleari.

— — —

Nello studio dei processi fotonucleari con elettroacceleratori, per misurare il flusso di fotoni, si ricorre in genere a camere di ionizzazione disposte in convertitori opportuni. La conoscenza della loro risposta in funzione dell'energia è necessaria per il calcolo delle sezioni d'urto.

In questa nota si è fatto un confronto tra una camera a parete spessa di alluminio (5 cm) da noi costruita e lo standard più comunemente usato finora in questi lavori [1], cioè una camera a ditale Victoreen posta dietro un convertitore di plexiglas dello spessore di 4 cm (4.70 g/cm^2).

In Fig. 1 è riportato il disegno in sezione della camera di ionizzazione. Essa è costituita essenzialmente da 5 piastre di alluminio, ciascuna spessa 1 mm, distanti fra di loro 3 mm e separate da anelli di plexiglas. Le due piastre estreme e la centrale servono da collettori di ioni mentre le due interne sono collegate ad una tensione positiva V di 300 V. Tale tensione è scelta in modo che l'efficienza di raccolta [2] $(1\ u)[\ln(1-u)]$ differisca dall'unità di pochi percento, quando r raggiunge il massimo valore ottenibile dalla nostra macchina acceleratrice (≈ 0.5 u.e.s./cm^3 s). Nel nostro caso di sorgente impulsata a 50 Hz, u vale $21.8\ rd^2/V$ (d è la distanza tra le piastre in centimetri).

Le piastre sono state opportunamente isolate tra loro e la variazione di

[1] J. W. Boag: *Brit. Journ. Radiol.*, **23**. 601 (1950).
[2] L. Katz e A. C. Cameron: *Canad. Journ. Phys.*, **29**, 518 (1951).

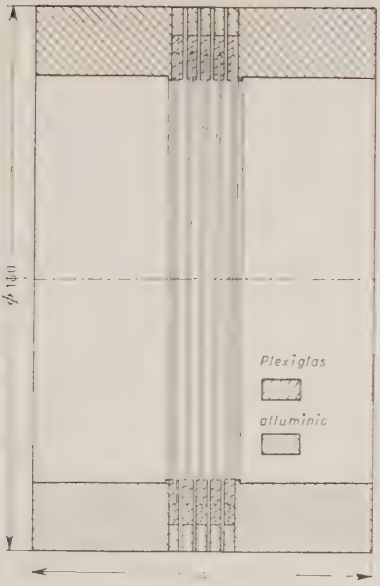

Fig. 1.

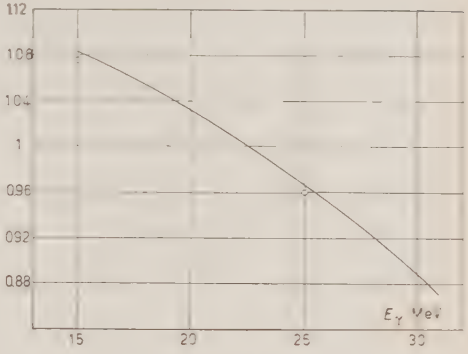

Fig. 2.

tensione è misurata con un elettrometro a campo ausiliario, la cui sensibilità è facilmente controllabile con una pila campione. Davanti e dietro alla camera è possibile inserire un convertitore dello spessore voluto.

Per confrontare la risposta della nostra camera di ionizzazione con convertitore di alluminio, con lo standard utilizzato da KATZ e CAMERON si è proceduto nel modo seguente. Sul fascio, opportunamente collimato, di raggi X del betatrone si è posta una camera di ionizzazione Victoreen da 25 r in aria (monitor) ed alternativamente la nostra camera e lo standard di Katz. Le misure sono state eseguite ad energie di bremsstrahlung variabili tra 15 e 31 MeV. Il rapporto tra la risposta dello standard di Katz ed il nostro in funzione di E_γ è rappresentato in Fig. 2. Sulle ascisse è riportato il rapporto tra i due valori di $\bar{S}_{\text{plex}}$ ed $\bar{S}_{\text{Al}}$, dove

$$\bar{S}_{\text{plex}} = \frac{\int \Phi(W) S_{\text{plex}}(W)\, dW}{\int \Phi(W)\, dW} \qquad \bar{S}_{\text{Al}} = \frac{\int \Phi(W) S_{\text{Al}}(W)\, dW}{\int \Phi(W)\, dW},$$

[$S(W)$ rappresenta il rapporto tra la densità di ionizzazione prodotta ed il flusso di energia per ogni valore di $W = h\nu$; $\Phi(W)$ è lo spettro di bremsstrahlung].

I valori di $\bar{S}_{\text{Al}}$ sono stati ricavati da FLOWERS *et al.* [3], mentre i valori di $\bar{S}_{\text{plex}}$ si deducono dal lavoro di JOHNS *et al.* [4].

Nella Fig. 2 la curva rappresenta il valore sperimentale del rapporto $\bar{S}_{\text{plex}}/\bar{S}_{\text{Al}}$: i singoli punti sperimentali non sono riportati, tuttavia la media

---

[3] B. H. FLOWERS, J. O. LAWSON e E. B. FOSSEY: *Proc. Phys. Soc.*, B **65**, 286 (1952).

[4] H. E. JOHNS, L. KATZ, R. A. DOUGLAS e R. N. H. HASLAM: *Phys. Rev.*, **80**, 1062 (1950).

dei valori delle singole misurazioni è affetta da un errore non superiore allo 0.5%. I due circoletti a 15 e 25 MeV rappresentano il valore del rapporto teorico; l'accordo sembra eccellente.

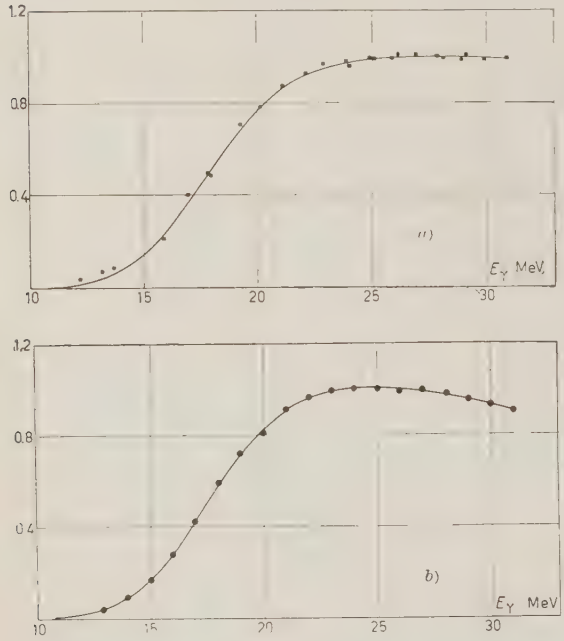

Fig. 3.

Come applicazione e verifica di questa taratura si sono misurate le curve di attivazione del rame nella reazione di fotodisintegrazione $^{63}Cu(\gamma, n)^{62}Cu$, misurando il flusso di fotoni con gli standard di plexiglas ed alluminio.

Per ottenere punti sperimentali confrontabili, si è reso necessario sia mantenere costante l'energia della macchina entro almeno lo 0.5%, sia conoscerne con sufficiente precisione il valore assoluto. A tal fine, mediante un semplice dispositivo atto a variare finemente il momento di espansione degli elettroni, si è riusciti a mantenere l'indice dello strumento misuratore dell'energia (megavoltmetro Brown-Boveri) in posizione fissa durante tutto il periodo di irradiazione: la taratura in energia di tale strumento è stata ottenuta misurando alcune soglie fotonucleari ben conosciute. I punti sperimentali sono riportati nelle Fig. 3 *a*, *b*. La curva nella Fig. 3 *a* è dedotta dal lavoro di KATZ mentre la curva di Fig. 3*b* rappresenta il prodotto della curva suaccennata per il rapporto delle risposte dei due standard (le curve sono normalizzate a 25 MeV). I punti sperimentali ben descrivono entro gli errori le curve di attivazione.

* * *

Ringraziamo il prof. A. O. HANSON e l'ing. L. GONELLA per la collaborazione portata nel presente lavoro.

SUMMARY

An ionization chamber for X-rays up to 31 MeV is described and its efficiency is compared to some calculations and to the standard often used in the study of photonuclear reactions.

(La responsabilità scientifica degli scritti inseriti in questa rubrica è completamente lasciata dalla Direzione del periodico ai singoli autori)

Investigation of an Electromagnetic Cascade of Very High Energy in the First Stage of its Development.

M. Mięsowicz, O. Stanisz and W. Wolter

Institute of Nuclear Physics, Department of Cosmic Rays - Krakow

(ricevuto il 17 Settembre 1956)

Some examples of high energy showers of electron pairs have recently been published. The development of some of these showers seems to show that they may be initiated by several photons ([1-5]). At the same time the range of the energy in which electron showers initiated by a single photon have been found and investigated in emulsions is extended to above 10^{11} eV ([4,6,7]).

One of the anomalies found in the high energy showers is the deficiency of low energy pairs as compared with the number of high energy pairs. This effect has been reported for showers assumed to be initiated by several photons by Debenedetti *et al.* ([2]) and for a shower initiated probably by a single photon by the authors of the present letter ([6]). It was suggested by Wataghin ([8]) that these anomalies have a general character for all electronic showers of high energy ($\simeq 10^{12}$ eV). Dyson ([9]) suggested that this anomaly might be explained on the basis of the theories of Ter Mikaelian ([10]) and Landau and Pomerančuk ([11]). It is very important for these suggestions whether the anomaly mentioned above does really exist in the showers initiated by a single photon of very high energy. It therefore seems very desirable to carry out investigations on cascades

([1]) M. Schein, D. M. Haskin and R. G. Glasser: *Phys. Rev.*, **95**, 855 (1954).

([2]) A. Debenedetti, C. M. Garelli, L. Tallone, M. Vigone and G. Wataghin: *Nuovo Cimento*, **12**, 954 (1954); **2**, 220 (1955); **3**, 226 (1956).

([3]) A. Milone: *Pisa Conference*, June 1955.

([4]) M. Koshiba and M. F. Kaplon: *Phys. Rev.*, **100**, 327 (1955).

([5]) L. Barbanti Silva, C. Bonacini, C. Depietri, I. Iori, G. Lovera and R. Perilli Federi and A. Roveri: *Nuovo Cimento*, **3**, 1465 (1956).

([6]) M. Mięsowicz, W. Wolter and O. Stanisz: *Pisa Conference*, June 1955; A. Jurak, M. Mięsowicz, O. Stanisz and W. Wolter: *Bull. Acad. Pol., Cl. III*, 369 (1955).

([7]) K. Pinkau: *Nuovo Cimento*, **3**, 1285 (1956).

([8]) G. Wataghin: *Proc. of the Sixth Rochester Conference*, **9**, 24 (1956).

([9]) F. I. Dyson: *Proc. of the Sixth Rochester Conference*, **9**, 29 (1956).

([10]) M. L. Ter-Mikaelian: *Izv. Akad. Nauk SSSR, Ser. Fiz.*, **19**, 657 (1955).

([11]) L. D. Landau and I. Pomerančuk: *Dokl Akad. Nauk SSSR*, **92**, 535, 735 (1953). (See also: E. L. Feinberg and I. Pomerančuk: *Suppl. Nuovo Cimento*, **3**, 652 (1956)).

TABLE I.

Pair	Distance from the point of origin of the first pair (μ)	E_1 (eV)	E_2 (eV)	$E_1 + E_2$ (eV)	The most probable parent pair	Radial distance from the nearest electron track (μ)
1	0	—	—	$7.0 \cdot 10^{11}$	—	—
2	9400	$2.0 \cdot 10^8$	$1.0 \cdot 10^8$	$3.0 \cdot 10^8$	$1(l)$ or $1(r)$ (*)	$< 0.5_0$
3	16400	$1.3 \cdot 10^8$	$1.0 \cdot 10^7$	$1.4 \cdot 10^8$	$1(r)$	$< 0.4_5$
4	17500	$6.0 \cdot 10^8$	$\geqslant 7.0 \cdot 10^8$	$\geqslant 1.3 \cdot 10^9$	$1(l)$	$< 0.2_8$
5	23800	$1.3 \cdot 10^8$	$8.0 \cdot 10^7$	$2.1 \cdot 10^8$	$1(r)$	1.0_8
6	27800	$\geqslant 1.0 \cdot 10^9$	$7.5 \cdot 10^8$	$\geqslant 1.8 \cdot 10^9$	$1(l)$	$< 0.2_3$
7	30000	$< 6.0 \cdot 10^7$	$6.0 \cdot 10^7$	$< 1.2 \cdot 10^8$	?	12.6
8	30600	—	—	$> 1.3 \cdot 10^{10}$ (a)	$1(l)$	$< 0.4_5$
9	34900	—	—	$5.2 \cdot 10^9$ (b)	$1(l)$ or 8	$< 0.2_3$
10	38700	$1.0 \cdot 10^7$	$6.8 \cdot 10^6$	$1.7 \cdot 10^7$	6	$< 0.4_5$
11	40900	—	—	$> 1.0 \cdot 10^{10}$ (c)	$1(r)$	1.3_1
12	41600	—	—	$> 3.9 \cdot 10^{10}$ (a)	$1(l)$	$< 0.8_4$
13	42800	—	—	$> 2.6 \cdot 10^{10}$ (a)	$1(l)$ or 12	$< 1.3_3$
14	43500	$\geqslant 2.7 \cdot 10^8$	$1.0 \cdot 10^8$	$\geqslant 3.7 \cdot 10^8$	8	0.9_5

(*) (l) or (r) means left or right track of the pair.

(a) The lower limit of energy estimated from the opening angle of the core containing several tracks using the formula of Borsellino. It is highly probable that this value is underestimated, since the influence of multiple scattering is neglected.

(b) From relative scattering measurements on the assumption of equipartition of energy.

(c) as (a) measurements are taken between the tracks of this pair.

deriving from single photons of the highest energies at their beginning. At greater depths these anomalies should disappear because of the decrease in the energy of the electrons of the cascade.

Hitherto there have been known in the literature only 2 cascades generated by single photons of energies of $\simeq 10^{12}$ eV. These were recently analysed by PINKAU [7].

This letter is intended to give an account of an analysis of a cascade generated probably by a single photon of an energy approaching the value of 10^{12} eV

with a particular consideration of the beginning of the development of the cascade where we could expect to find the above-mentioned anomaly. Preliminary results of the measurements of this cascade have already been published ([6]).

The shower consists of high energy pairs, 14 of which are generated within 1.55 rad length from the origin of the first pair. Most of these pairs are included within a very narrow cone of an angle of about 10^{-4} rad. The length of the cascade in one emulsion is about 4.2 mm. The data on the observed pairs are given in Table I. Most of the pairs are apparent tridents, as can be seen from column 7 of Table I.

The evaluation of energy of the primary photon initiating the cascade was carried out with the energy spectrum of electrons at a depth of 2.5 rad length. The scattering measurements were made on the tracks contained within a circle of a radius of 250 μm from the core. The number of tracks of electrons with energies higher than $5 \cdot 10^8$ eV within the circle of a radius of 200 μm was 34. The calculations of the full number of electrons in this energy interval at this depth on the basis of the lateral distribution of particles were carried out by a method described by PINKAU ([7]). Then, using the tables of JANOSSY and MESSEL ([12]), the energy E_0 of the primary photon could be found if we assumed the equipartition of energy for particles of the first pair. From these measurements we go t $E_0 = (7.0^{+3.4}_{-2.6}) \cdot 10^{11}$ eV. The limits of error of the value of E_0 were found, taking Janossy's ([13]) standard deviations for a given number of tracks and finding the values of energy corresponding to the extreme number of electrons of energies greater than $5 \cdot 10^8$ eV. From the value of E_0 the numbers of electrons of different energies for different radii have been obtained and they are in agreement with the observed values within Janossy's standard deviations.

We obtained information on the energy of the primary pair independently in another way, from measurements of ionization on the first part of the unresolved track of the first pair. From these measurements ([14-16]) it was possible with the use of the formula given by ČUDAKOV ([14]) to estimate the opening angle of the first pair. We obtained the value $\omega = 3 \cdot 10^{-6}$ rad, and hence from the formula $E = 4mc^2/\omega$ we got for E_0 the value $\sim 10^{12}$ eV. We consider these measurements as only approximate, since in the formula from which we evaluate the angle there are constants which are not accurately known.

We have now investigated the spec-

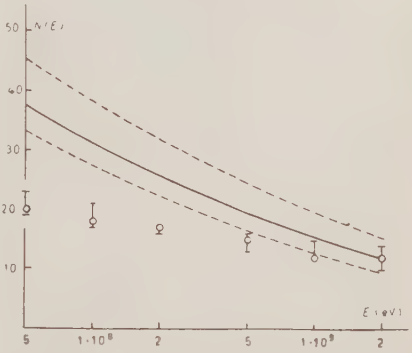

Fig. 1. – The integral energy spectrum of electrons at the depth of 1.55 rad length.
Circles: the observed numbers of electrons. Full-line: the spectrum calculated from cascade theory for the primary photon energy $E_0 = 7.0 \cdot 10^{11}$ eV. Dotted lines: the spectra for energies of the primary photon corresponding to the limits of error.

([12]) L. JÁNOSSY and H. MESSEL: *Proc. Roy. Irish Acad.*, **54** (A), 217 (1951).

([13]) L. JÁNOSSY: *Acta Phys. Hung.*, **2**, 289 (1952)

([14]) A. E ČUDAKOV: *Izv. Akad Nauk SSSR, Ser. Fiz.*, **19**, 651 (1955).

([15]) D. H. PERKINS: *Phil. Mag.*, **46**, 1146 (1955)

([16]) W. WOLTER and M. MIĘSOWICZ: *Nuovo Cimento*, **4**, 648 (1956).

trum of electrons at a depth of 1.55 rad length. In Fig. 1 the integral energy spectrum of electrons observed at this depth is shown. This spectrum is obtained directly from the figures given in Table I, taking into account the energy losses of electrons by « bremsstrahlung » and ionization. The circles show the numbers of electrons with energy greater than the given value. The vertical lines give the uncertainty of energy determination. The full line shows the spectrum of electrons calculated from the cascade theory (Approximation B) ([12]) on the assumption that the energy of the primary photon is $E_0 = 7 \cdot 10^{11}$ eV as mentioned above. The dotted lines represent the spectra calculated for energies giving the limits of error of he primary photon energy (4.4 resp. $10.4 \cdot 10^{11}$ eV).

We can see from Fig. 1 a deficiency in the number of electrons of energy lower than $5 \cdot 10^8$ eV as compared with the prediction of the cascade theory.

Qualitatively it is possible to explain this effect according to the suggestions of DYSON ([9]) on the basis of the theory of TER-MIKAELIAN ([10]) and LANDAU and POMERANČUK ([11]). According to these theories if an electron moves through photographic emulsion with energy E greater than $\simeq 10^{10}$ eV the spectrum of « bremsstrahlung » photons radiated by this electron, for photon energies lower than a critical energy k_c, is strongly cut down for low photon energies. For photographic emulsions $k_c \simeq 8 \cdot 10^{-15} E^2$. This means that for the two electrons of our first pair this energy of photons below which we might expect a lack of photons is $k_c \simeq 10^9$ eV. As at the depth $t = 1.55$ rad length the observed energy spectrum of electrons is strongly influenced by the spectrum of the photons radiated by the first pair, it is possible to explain the observed deficiency of electrons of energies $\simeq 10^8$ eV and lower by the lack of photons of these energies in the radiation emitted by the first two electrons. This explanation is supported by direct observation of pairs generated on the tracks of the first pair. It can be seen (Table I) that no photons of energy smaller than 10^9 eV were converted on the left track, whereas some pairs with energies $\simeq 10^8$ are seen only on the right track. That might be explained by assuming an assymetry of energies in the two electrons of the first pair. In consequence of the $k_c \sim E^2$ dependence, k_c may differ for both electrons of the first pair by one order of magnitude.

It seems that the observed deficiency of low energy electrons at the depth $t = 1.55$ rad length is outside the limits of the probable fluctuations. Nevertheless it is not possible to conclude quantitatively from this example whether it is in accordance with the mentioned theory.

* * *

The authors are very greateful to Miss A. JURAK for the work done in the course of scanning for pairs and in the scattering measurements.

Nuclear Disintegration Cascades by Heavy Primaries.

S. Tokunaga and T. Ishii

Department of Physics, Saikyo University - Kyoto, Japan

K. Nishikawa

Department of Physics, Wakayama University - Wakayama, Japan

(ricevuto il 12 Novembre 1956)

In the stack of 48 4 inch by 6 inch Ilford G5 600 μm pellicles which was flown with the emulsion surfaces vertical for 6 hours up to the maximum altitude of 8 mb by a polyethylene balloon at Kobe in Japan in 1955, two events of nuclear disintegration cascades by heavy primaries were found. With the stack developed cascade showers were searched for in the lower part of the stack, and electron cascades were traced back to their origin when they were found. On these occasion some events different from purely electronic showers were also found. Thus, the events here described were discovered.

One is shown in Figs. 1, 2, 3 and 4 (the event I). The heavy primary having charge $Z=11$, entering the stack with 37 degrees of zenith angle, produced a

Fig. 1. - Projection D drawing on a nuclear cascade disintegration (the event I).

thin track at A and continued to B, there causing a star $8+44_{Na}$, from which a helium nucleus and a lithium nucleus were emitted as a result of the fragmentation of the primary sodium nucleus. The helium nucleus interacted with a nucleus of the emulsion at C, producing a star $19+9_{He}$, and the lithium nucleus at D, a star $17+120_{Li}$. As the helium nucleus continues after the event C with nearly the same direction as before, the event is considered the stripping process of ^{4}He into ^{3}He. The ^{3}He fragment leaved the stack after running 30.6 mm without causing any interactions. The angle between the direction before and after the interaction C was obtained by measuring the relative distance between the lithium and helium track at several points after the interaction C, and was found to be about $1\cdot10^{-4}$ radian. The probability, that the event is not caused by the helium, but caused by a neutron emitted in the event B and juxtaposed with the helium track at C by chance, is estimated $5\cdot10^{-4}$. These facts confirm our consideration.

All the interactions in the event I were summarized in Table I, together with the distance between them.

By means of two methods the energy of the primary particle is estimated to be 500 GeV per nucleon, one is from the opening angle between the fragmentation products, a helium and lithium nucleus, and the other from the median angle of the shower particles. The results of the analysis on the meson showers of each event will be reported elsewhere [1].

The collision mean free path of the event is 3.1 g/cm^2, if all events are regarded as nuclear events, and 4.1 g/cm^2, if event A is not taken into consideration, as the thin track from A may be a high energy knock-on electron. It is very remarkable that the mean free path of these interactions is very small, that is about more than ten times smaller than normal. The probability that we would have such small mean free path for the events A, B, C and D would be $1.4\cdot10^{-5}$, assuming the cascade reaction should arise from the superposition of abnormal fluctuation of the mean free path, and $2\cdot10^{-4}$ for the events B, C and D.

TABLE I.

Interaction A	$0+1_{Na}$	Distance from the entering point to A	0.785 cm
Interaction B	$8+44_{Na}$	from A to B	0.654 cm
Interaction C	$19+9_{He}$	from B to C	0.521 cm
Interaction D	$17+120_{Li}$	from B to D	1.204 cm

The second event is shown in Fig. 5. The heavy primary having charge $Z=12+1$ entering the stack, interacted with the nucleus of the emulsion at A, producing a star $5+6_{heavy}$, from which a particle with charge $Z=8$ and two particles with charge $Z=2$ are emitted, and two of them caused interactions. In this case the mean free path is 4.86 cm.

Some nuclear disintegration cascades have been reported so far by A. MILONE [2] and H. YAGODA [3]. Milone's

[1] S. TOKUNAGA: *Journ. Phys. Soc. Japan* (in press).

[2] A. MILONE: *Suppl. Nuovo Cimento*, **12**, 354 (1954).

[3] H. YAGODA: *Bull. Am. Phys. Soc.*, Series II, 64 (1956).

Fig. 2. – Microphotograph of the interaction *B* of the event I. The Na nucleus causes $8+44_{Na}$ star from which a He and a Li nucleus emerge in the same direction as the incident primary.

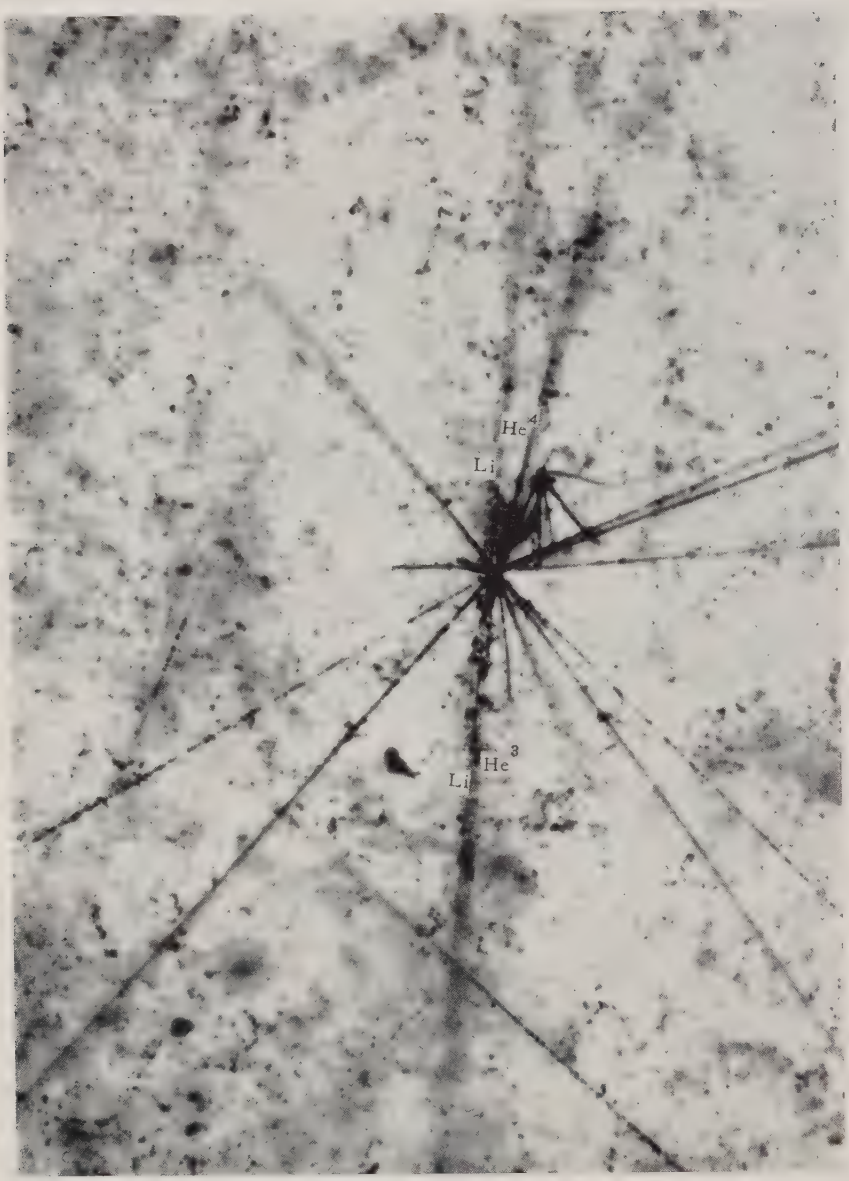

Fig. 3. $-\frac{1}{1}$ Microphotograph of the interaction C of the event I. The He nucleus emerging from the interaction B produces the interaction C $19+9_{He}$. In this event the He nucleus passes through without any loss of its charge. It is taken to be the stripping process of ^{4}He to ^{3}He.

Fig. 4. – Microphotograph of the interaction *D*. The Li nucleus which emerged from the interaction *B* caused a large shower $17+129_{Li}$ after traversing 12.0 mm from *B*.

event has a mean free path of 7.3 g/cm², and Yagoda's 2.66 g/cm². Yagoda's is similar to our first event, having nearly the same mean free path. The fact that several examples of such nuclear disintegration cascade events have been found suggests that there may be something unknown about heavy primary cosmic rays.

YAGODA suggests that there may be heavy primaries consisting of antiparticles.

But the cross-section of antiproton thus far found being only about twice as large as ordinary nucleons [4], it would be difficult to give an immediate conclusion. However, there being also experimental results [5,6] about east-west asymmetry at high altitude which suggest the possible existence of negative charged primaries, it cannot be wholly denied.

* * *

The authors wish to express their hearty gratitude to Prof. O. MINAKAWA for his sustained interest throughout the course of the work. Also, our sincere appreciation and thanks go to the members of the Kansai Balloon Group for making possible the balloon flight.

This work was financially supported by a Grant of Scientific Research from the Ministry of Education for the 1955 fiscal year.

Fig. 5. - Projection drawing of a nuclear cascade disintegration (the event II).

(4) O. CHAMBERLAIN, D. V. KELLER, H. M. STEINER, C. WIEGAND and T. YPSILANTIS: *Phys. Rev.*, **102**, 1637 (1956).

(5) M. I. FRADKIN: *Soviet Physics JETP*, **2**, 87 (1956).

(6) B. BHOWMIK: *Phys. Rev.*, **89**, 327 (1953).

On Lehmann's Method of Renormalization.

N. Nakanishi

Kyoto University - Kyoto, Japan

(ricevuto il 15 Novembre 1956)

As is well known, Lehmann [1] has given some general properties of propagators in the quantized field theory, but the reason why he has obtained automatically the renormalized propagators only is not clear at first sight. On this point, Nambu [2] has taken the rather optimistic standpoint that the renormalization procedures are generally carried out by taking the imaginary parts, while Hiida and Sawamura [3] have asserted that it is due to the substantial difference between renormalized propagators and unrenormalized ones. But it seems that both arguments are duobtful. Therefore we shall demonstrate that Dyson's prescription [4] of renormalization is actually obtained by Lehmann's method. As recently the renormalizations for unstable particles [5] are proposed, we shall treat the unstable case, too.

For simplicity, we consider only a scalar one-body propagator. As is well known the integral equation

$$\Delta'_F = \Delta_F + \Delta_F \Sigma^* \Delta'_F \,, \tag{1}$$

holds for the propagator Δ'_F, where Σ^* is the proper self-energy. If we introduce a propagator

$$\Delta^*_F \equiv \Delta_F \Sigma^* \Delta_F \,, \tag{2}$$

eq. (1) becomes

$$\Delta'_F = \Delta_F/(1 - \Delta_F^{-1}\Delta^*_F) \,. \tag{3}$$

Now we define the renormalization by $\Delta'_{F_1} = Z^{-1}\Delta'_F$, and further introduce a renormalized propagator $\Delta^*_{F_1}$ corresponding to Δ^*_F so that

$$\Delta'_{F_1} = \Delta_F/(1 - \Delta_F^{-1}\Delta^*_{F_1}) \,. \tag{4}$$

Then we obtain from (3) and (4)

$$\Delta^*_{F_1} = (1 - Z^{-1})\Delta_F + Z^{-1}\Delta^*_{F_1} \,. \tag{5}$$

From Lehmann's conclusion [1]

$$\Delta'_{F_1} = \int \frac{\varrho(u)}{k^2 - u - i\varepsilon}\, \mathrm{d}u \,, \tag{6}$$

with

$$\varrho(u) \geqslant 0 \,, \tag{7}$$

(1) H. Lehmann: *Nuovo Cimento*, **11**, 342 (1954).

(2) Y. Nambu: *Phys. Rev.*, **100**, 394 (1955).

(3) K. Hiida and M. Sawamura: *Prog. Theor. Phys.*, **14**, 167 (1955).

(4) F. J. Dyson: *Phys. Rev.*, **75**, 1736 (1949).

(5) H. Araki, Y. Munakata, M. Kawaguchi and T. Goto: *Prog. Theor. Phys.*, to be published.

and likewise, by means of the general integral formula of the perturbation term [6] we can prove

$$(8) \qquad \Delta_F^* = \int \frac{\tilde{\varrho}^*(u)}{k^2 + u - i\varepsilon}\,\mathrm{d}u\,,$$

where $\tilde{\varrho}^*(u)$ is some real function. Hence also we can write

$$(9) \qquad \Delta_{F_1}^* = \int \frac{\varrho^*(u)}{k^2 + u - i\varepsilon}\,\mathrm{d}u\,.$$

At the performance of renormalization we require the following two conditions:

1) $\varrho^*(u)$ is real.

2) $\varrho^*(u)$ has no δ-singularity.

Substituting (8) and (9) into (5) and taking the imaginary part, we obtain

$$(10) \qquad \tilde{\varrho}^*(u) = (1 - Z^{-1})\,\delta(u - m^2) + Z^{-1}\varrho^*(u)\,.$$

On the other hand, the substitution of (8) into (2) yields

$$(11) \qquad \int \frac{\tilde{\varrho}^*(u)}{k^2 + u - i\varepsilon}\,\mathrm{d}u = \frac{\Sigma^*(-k^2) - \delta m^2}{(k^2 + m^2 - i\varepsilon)^2}\,,$$

where the mass renormalization is explicitly written. If we make use of the formula

$$(12) \qquad \frac{1}{(x - i\varepsilon)^2} = Pf\frac{1}{x^2} + i\pi\cdot\delta'(-x)\,,$$

where Pf is a symbol of pseudo-function which denotes Hadamard's finite part [7], the imaginary part of (11) is

$$(13) \qquad \tilde{\varrho}^*(u) = \delta'(u - m^2)[\mathrm{Re}\;\Sigma^*(u) - \delta m^2] + \frac{1}{\pi}\,Pf\frac{1}{(u - m^2)^2}\cdot\mathrm{Im}\,\Sigma^*(u)\,.$$

Comparing (13) with (10), since the δ-singularities of both must coincide, by means of the formula $x\,\delta'(x) = -\delta(x)$ we obtain

$$(14) \qquad \delta m^2 = -\,\mathrm{Re}\;\Sigma^*(m^2)\,,$$

$$(15) \qquad Z^{-1} = 1 + \mathrm{Re}\left[\frac{\mathrm{d}}{\mathrm{d}u}\,\Sigma^*(u)\right]_{u = m^2}$$

and at the same time

$$(16) \qquad \varrho^*(u) = \frac{1}{\pi}\cdot Z\cdot Pf\frac{1}{(u - m^2)^2}\cdot\mathrm{Im}\,\Sigma^*(u)\,.$$

Since for a stable particle $\mathrm{Im}\,\Sigma^*(m^2) = 0$, the symbols Re in (14) and (15) and Pf in (16) are unnecessary, thus the above renormalization procedure coincides with DYSON's prescription. For an unstable particle this coincides with the K-matrix method [5].

Finally, we investigate the physical meaning of the function $\varrho^*(u)$. Substituting (6) and (9) into (4),

$$(17) \qquad \int \frac{\varrho(u)}{k^2 + u - i\varepsilon}\,\mathrm{d}u = \frac{1}{k^2 + m^2 - i\varepsilon}\cdot\left[1 - (k^2 + m^2)\int \frac{\varrho^*(u)}{k^2 + u - i\varepsilon}\,\mathrm{d}u\right]^{-1}.$$

If we take the imaginary part of (17), $\varrho(u)$ is expressed by $\varrho^*(u)$. Then referring to (7) we find

$$(18) \qquad \varrho^*(u) \geqq 0 \quad (*).$$

For an unstable particle, $\varrho^*(u)$ is a pseudo-function given by (16), while $\varrho(u)$ is an usual continuous function (the so-called resonance curve near $u = m^2$).

Next, multiplying (17) by $k^2 + m^2$, taking the limit $-k^2 \to \infty$ and exchanging the order of the limit and the integration, we obtain

$$(19) \qquad \int \varrho^*(u)\,\mathrm{d}u = 1 - Z\,.$$

(5) N. NAKANISHI: *Prog. Theor. Phys.*, to be published.

(7) L. SCHWARTZ: *Théorie des Distributions* (Paris, 1950).

(*) Strictly speaking, one point $u = m^2$ should be excluded for an unstable particle.

This relation is valid even in the case that $\int\varrho(u)\,\mathrm{d}u$ is divergent, if the theory is consistent. From (19) and (18) it proves that for a stable particle $\varrho^*(u)$ is a probability density of clothing at energy $\sqrt{u}$. Hence the two requirements for $\varrho^*(u)$ are physically reasonable. For an unstable particle, however, since $\varrho^*(u)$ is a pseudo-function, the left hand side of (19) is not positive definite, and therefore the interpretation as probability is not allowed; thus the requirements lose their physical meaning (but are of course still natural).

Though in the argument above we have made use of the perturbation expansion to introduce $\varrho^*(u)$, the existence of such a function has been directly proved (for a stable particle) by H. Lehmann, K. Symanzik and W. Zimmermann ([8]). Hence their function $F(\varkappa^2)$ should coincide with $2Z\cdot\mathrm{Im}\,\Sigma^*(\varkappa^2)$.

* * *

The author would like to thank Mr. H. Araki and Dr. H. Kita for their discussions.

([8]) H. Lehmann, K. Symanzik and W. Zimmermann: *Nuovo Cimento*, **2**, 425 (1955).

Effective Nuclear Potentials.

W. E. Frahn and R. H. Lemmer

Nuclear Physics Division, National Physical Research Laboratory, C.S.I.R. Pretoria, South Africa

(ricevuto il 20 Novembre 1956)

In a previous paper [1] the effective non-local nucleon-nucleus potential following from the statistical nuclear model with Majorana exchange forces between the nucleons has been reconsidered. For a Gaussian spatial dependence of the nucleon-nucleon interaction the resulting effective potential is known as «Van Vleck's potential» [2,3]. In the present note we summarize the results obtained by the same procedure using the following conventional potential types of the two-nucleon problem:

Square well:

$$J_1(r) = \begin{cases} V_0\,, & r < a \\ 0\,, & r > a \end{cases} \tag{1a}$$

Exponential well:

$$J_2(r) = -V_0 \exp\left[-\frac{2r}{a}\right] \tag{1b}$$

Yukawa well:

$$J_3(r) = -V_0 \frac{\exp[-2r/a]}{2r/a}\,. \tag{1c}$$

The resulting effective potentials $V(k)$ are given by:

$$V_1(k) = -\frac{2V_0}{\pi}\left[\mathrm{Si}\,(2x+2y) + \mathrm{Si}\,(2x-2y) - \frac{1}{y}\sin 2x \sin 2y\right], \tag{2a}$$

$$V_2(k) = -\frac{2V_0}{\pi}\left[-\frac{1}{2y}\log\frac{1+(x+y)^2}{1+(x-y)^2} + \mathrm{tg}^{-1}(x+y) + \mathrm{tg}^{-1}(x-y)\right]. \tag{2b}$$

$$V_3(k) = -\frac{2V_0}{\pi}\left[x + \frac{1+(x+y)(x-y)}{4y}\log\frac{1+(x+y)^2}{1+(x-y)^2} - \mathrm{tg}^{-1}(x+y) - \mathrm{tg}^{-1}(x-y)\right], \tag{2c}$$ [4]

$$(x = \tfrac{1}{2}k_F a,\quad y = \tfrac{1}{2}ka;\quad \mathrm{Si} = \text{sine-integral}).$$

---

(1) W. E. Frahn: *Nuovo Cimento*, **5**, 393 (1957).
(2) J. H. Van Vleck: *Phys. Rev.*, **48**, 367 (1935).
(3) C. Fay: *Phys. Rev.*, **50**, 560 (1936).
(4) Cf. also A. Kind and C. Villi: *Nuovo Cimento*, **1**, 749 (1955).

The development for $y \ll 1$,

$$V(k) \approx -\alpha(x) + \beta(x)\frac{k^2}{k_F^2}, \tag{3}$$

yields

$$\alpha_1(x) = \frac{4}{\pi} V_0(\mathrm{Si}\,(2x) - \sin 2x)\,, \tag{4a}$$

$$\alpha_2(x) = \frac{4}{\pi} V_0\left(\mathrm{tg}^{-1} x - \frac{x}{1+x^2}\right), \tag{4b}$$

$$\alpha_3(x) = \frac{4}{\pi} V_0(x - \mathrm{tg}^{-1} x)\,. \tag{4c}$$

$$\beta_1(x) = \frac{8}{3\sqrt{\pi}} V_0 x^{\frac{5}{2}} J_{\frac{5}{2}}(2x)\,. \tag{5a}$$

$$\beta_2(x) = \frac{16}{3\pi} V_0 \frac{x^5}{(1+x^2)^3}\,. \tag{5b}$$

$$\beta_3(x) = \frac{4}{3\pi} V_0 \frac{x^5}{(1+x^2)^2}\,. \tag{5c}$$

These functions, together with those obtained for the Gaussian well [1], $J_4(r) = -V_0 \exp[-r^2/a^2]$, are shown in Figs. 1 and 2.

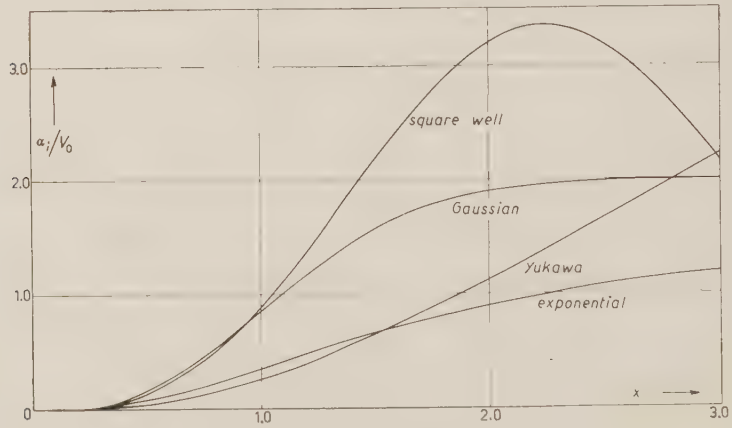

Fig. 1. – α_i/V_0 as functions of x.

The modified nucleon mass, M^*, following from (3), is given by

$$\frac{M^*}{M} = \left(1 + \frac{\beta}{E_F}\right)^{-1} \tag{6}$$

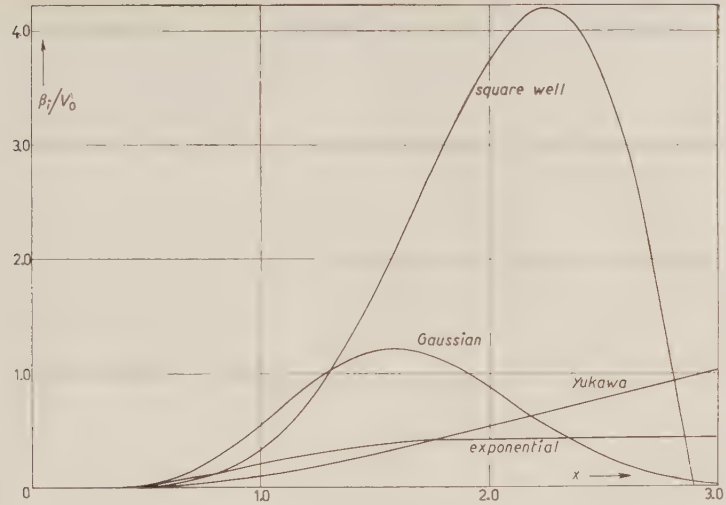

Fig. 2. – β_i/Γ_0 as functions of x.

and thus depends on the range parameter a. In order to make the nucleon-nucleon parameters comparable, we use the intrinsic ranges [5] $b = (a_1; 1.77a_2; 1.06a_3; 1.44a_4)$ and the well depth parameters [6] $(\hbar^2/MV_0)s = (0.405a_1^2; 0.173a_2^2; 0.149a_3^2; 0.373a_4^2)$. For $s = 1$, b equals the effective range. With the assumption $b = 2.6 \cdot 10^{-13}$ cm we obtain the values in Table I.

TABLE I.

	M^*/M	$-V(0)$ (MeV)
Square well	0.55	28.8
Exponential well	0.64	26.2
Yukawa well	0.69	23.3
Gaussian well	0.59	27.6

* * *

The authors are indebted to the South African Council for Scientific and Industrial Research for permission of publication.

([5]) J. M. BLATT and J. D. JACKSON: *Phys. Rev.*, **76**, 18 (1949).
([6]) J. M. BLATT and V. F. WEISSKOPF: *Theoretical Nuclear Physics* (New York, 1952).

The Effect of Ultra-Violet Converters on the Efficiency of Liquid Čerencov Counters.

N. A. Porter

A.E.R.E., Harwell, Berks., England

(ricevuto il 10 Dicembre 1956)

Large liquid Čerenkov counters have been used in cosmic ray experiments by several authors [1,2]. Their application in this field is limited, since detectors of large sensitive area are usually required, and the intensity of light emission in the visible and near ultra-violet is small compared with that from liquid scintillators. Most of the energy in the Čerenkov spectrum is released in the ultra-violet, since the number of photons emitted-unit path in the wavelength range λ, $\lambda - \mathrm{d}\lambda$, (where λ is the wavelength in vacuo) is:

$$\frac{\mathrm{d}N}{\mathrm{d}l} = \frac{4\pi^2 e^2}{hc}\left(1 - \frac{1}{\beta^2 n^2}\right)\frac{\mathrm{d}\lambda}{\lambda^2} \quad [3].$$

In water most of this light is transmitted, down to wavelengths of about 2000 Å, but the far ultra-violet component is absorbed at the walls of the counter or in the glass of the photomultiplier. Tests have therefore been made on the effects of ultra-violet converters, in solution in a water-filled Čerenkov counter [4]. The water was contained in a rectangular box, 15 cm × 30 cm in horizontal section, and 15 cm deep. A single E.M.I. photomultiplier, type 6260, with a 5 cm photocathode, was mounted on top of the box, in contact with the liquid. The walls were lined with a white diffusive reflector, of polyvinyl chloride loaded with magnesium oxide and titanium dioxide. The theoretical efficiency of the counter for light collection [5] was very low, about 0.015, and a relativistic particle traversing the counter vertically produced 3-4 photoelectrons on average at the photocathode. Provision was made for removing the liquid from the counter, and refilling, without exposing the photocathode to light. Relativistic μ-mesons traversing the counter were

---

[1] T. Duerden and B. D. Hyams: *Phil. Mag.*, **43**, 717 (1952).

[2] K. W. Ogilvie: *Can. Journ. Phys.*, **33**, 555 (1955).

[3] J. V. Jelley: *Progress in Nuclear Physics*, **3**, 84 (1953).

[4] Somewhat similar experiments have recently been reported by Heiberg and Marshall, (*Rev. Sci. Instr.*, **27**, 618 (1956)) who have studied a number of fluorescent materials in solution, and found increases in pulse-height by a factor varying from 1 to 1.3.

[5] M. Mandò: *Nuovo Cimento*, **12**, 5 (1954).

selected with a Geiger counter telescope, and the pulse-heights from the counter were measured, after amplification, with a recording oscilloscope, which was triggered by the telescope.

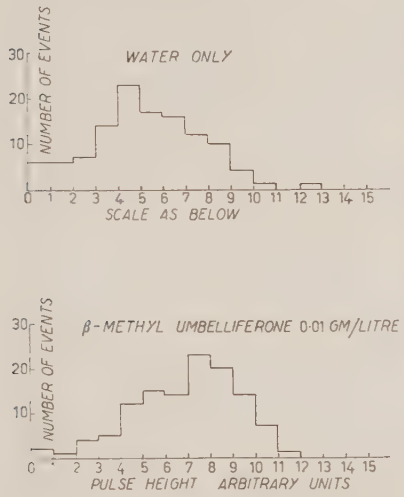

Fig. 1.

Three water-soluble fluorescent materials were examined, Fluorescein, β-Methyl Umbelliferone [6], and the commercial product Uvitex. No increase in pulse-height was found for Fluorescein or Uvitex. An increase in mean pulse-height of approximately 100% was observed with slightly alkaline solutions of β-Methyl Umbelliferone. The effect was almost independent of concentration between 0.005 g/litre and 0.1 g/litre. At concentrations higher than the latter, the mean pulse height decreased steadily with increased concentration. Typical pulse-height distributions for pure water and a solution of Umbelliferone are shown in the figure. The concentration in the example was 0.01 g/litre, in ammoniacal solution at pH 9. The distribution for water is the sum of two very similar distributions taken before and after the test on the solution. The width of the pulse-height distribution corresponds to a mean of about 4 photoelectrons, and that for the solution to about 10 photoelectrons, released at the cathode. The distributions shown were obtained with a differentiation time constant of 250 μs in the amplifier, but corresponding improvements in the pulse-height were observed at differentiation time constants down to 0.08 μs. This implies that much of the converted radiation is re-emitted within about 10^{-7} s of absorption. Some work has also been done on the effect of incorporating fluorescent materials into the reflecting walls of the counter. There appears to be some improvement in the pulse-height distribution, but the effects are not so marked as those obtained with the converter in solution.

The increase in pulse height is believed to be a true conversion of ultra-violet Čerenkov radiation, and not a scintillation effect, since the response of the counter to Compton electrons produced by low-energy γ-rays is similar for water and for solutions of the converter [7].

* * *

The author would like to thank Dr. J. V. Jelley, who suggested the experiment.

[6] J. de Ment: *Fluorescent chemicals and their applications* (New York, 1942).

[7] The γ rays were produced by a ^{60}Co source, mounted outside the counter in a standard position. Counting rates due to Compton electrons were measured with water and with the solution of Umbelliferone. These were the same within small statistical errors, a result consistent with the whole of the effect being due to conversion of Čerenkov radiation. It was not possible by this method to establish a reliable upper limit for the contribution from scintillation, and further tests have therefore been carried out in a smaller counter, using a ^{210}Po α-particle source in contact with the medium. These indicate that a feeble scintillation does occur in solutions of Umbelliferone, but that less than 1% of the increase in light output observed with relativistic μ-mesons can be ascribed to scintillation.

C and Al Photoproton Angular and Energy Distribution.

C. Milone, R. Ricamo and A. Rubbino

Istituto di Fisica dell'Università - Catania
Centro Siciliano di Fisica Nucleare - Catania

(ricevuto il 19 Dicembre 1956)

1. – Introduction.

The abnormally high photoproton yields observed for elements of high atomic number (Weinstock and Halpern [1], Toms and Stephens [2,3]) indicate that the simple evaporation model is inadequate. A better fit with experimental results is given by the direct interaction model (Courant [4]). However the compound nucleus theory can in some cases account for the experimental (γ, p) cross-sections if a lower proton barrier is assumed (Spicer [5]) or some « ad hoc » assumptions are made on the level density of the residual nucleus (Spicer [5], Butler and Almy [6]).

No consistent and unique theory of the nuclear photoeffect seems at present to be generally satisfactory (for instance photoprotons are emitted according to the statistical theory from ^{92}Mo and according to the direct process for ^{100}Mo) (Butler and Almy [6]) and more detailed informations are then necessary about the photoeffect in a single nucleus.

We decided therefore to measure energy spectra and angular distributions of photoprotons in ^{12}C and ^{27}Al, firstly because these natural elements are practically pure isotopes and secondly because their (γ, p) cross-sections are well known (Halpern and Mann [7]). Also the (γ, n) cross-sections for carbon (Montalbetti *et al.* [8]) have been measured.

Comparison between (γ, p) and (γ, n) cross-sections for these nuclei shows that they are very similar in the region around the giant resonance. This behaviour which might be due mainly to a resonance in the absorption cross-section for photons, justifies further investigation of the photoeffect in these nuclei.

(1) E. V. Weinstock and J. Halpern: *Phys. Rev.*, **94**, 1651 (1954).
(2) M. E. Toms and W. E. Stephens: *Phys. Rev.*, **92** 362 (1953).
(3) M. E. Toms and W. E. Stephens: *Phys. Rev.*, **98**, 626 (1955).
(4) E. D. Courant: *Phys. Rev.*, **82**, 703 (1591).
(5) B. M. Spicer: *Phys. Rev.*, **100**, 791 (1955).
(6) W. A. Butler and G. M. Almy: *Phys. Rev.*, **91**, 58 (1953).
(7) J. Halpern and A. K. Mann: *Phys. Rev.*, **83**, 370 (1951).
(8) R. Montalbetti, L. Katz and J. Goldemberg: *Phys. Rev.*, **91**, 659 (1953).

2. – Experimental Procedure.

Aluminium and carbon targets in form of 4 mm diameter disks were exposed to the collimated 31 MeV bremsstrahlung beam from the Brown-Boveri betatron of the University of Turin (Fig. 1). The aluminium disk was 66 μm thick and the carbon disk 200 μm. Photoprotons were detected in 200 μm C_2 Ilford $3'' \times 3''$ plates, placed together with the target T in an evacuated camera.

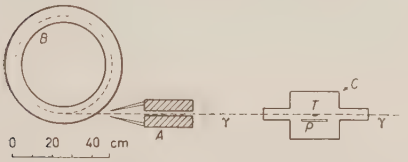

Fig. 1. – Experimental arrangement for photoprotons angular distribution measurements. A = lead collimator; C = exposure chamber; T = target; P = photoplate; B = betatron doughnut.

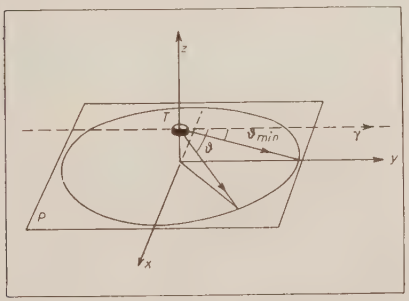

Fig. 2. – Geometry of the experimental arrangement for photoprotons angular distribution measurements. P – photoplate; T = target.

To measure the angular distribution of the photoprotons, photoplates were exposed parallel to the beam and 1 cm apart (Fig. 2). Targets were fixed in the center of the beam and parallel to it. Only photoprotons ejected from the target with an angle $16° < \vartheta < 164°$ from the beam axis entered the scanned area of the emulsion and from the geometry of the experiment it was easy to control if the protons were originated in the target. Very few protons were observed when the target was removed from the chamber.

In order to measure the energy distributions, targets and photoplates were exposed normally to the beam; targets, 0.5 mm thick, were placed 6 mm apart from the plates.

Angular distributions were obtained by grouping protons into angular intervals on the plates corresponding to equal solid angles seen from the target.

Energy distributions of photoprotons emitted from thick targets were obtained by deriving with respect to the range the observed proton spectra and converting them afterwards in energy spectra.

3. – Results and Discussion.

3·1. *Carbon.* – Photoprotons ejected from carbon with energy greater than 5.5 MeV show a pronounced forward asymmetry peaked at 60° (Fig. 3). The

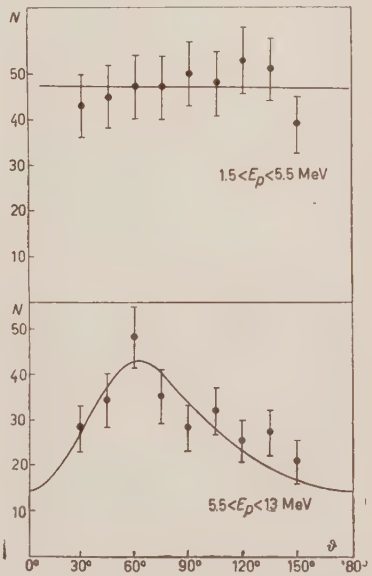

Fig. 3. – Angular distribution of photoprotons from Carbon. N – number of photoprotons observed with energy E_p for unit solid angle in arbitrary scale.

lower energy proton component has a practically isotropic distribution.

The differential cross-section for the former group of protons can be fitted by a function $0.6+(\sin\vartheta+0.6\sin\vartheta\cos\vartheta)^2$. This is to be compared with the distribution given by HALPERN, MANN and ROTHMAN [9] who found a less pronounced forward asymmetry using a bremsstrahlung beam with maximum energy 23 MeV.

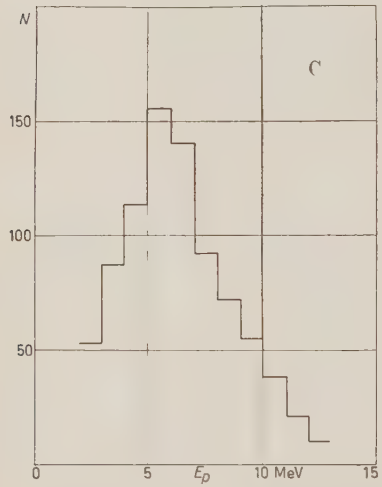

Fig. 4. – Photoproton energy distribution from Carbon irradiated at 31 MeV photon max energy. N = number of protons observed into 1 MeV interval.

JOHANSSON [10] using a 65 MeV bremsstrahlung beam observed a strong maximum at 60° for proton energy greater then 14 MeV. HENDEL [11] found a maximum at $\vartheta = 45°$ with a 150 MeV bremsstrahlung beam.

It is evident that the high energy protons are emitted with high orbital momentum, presumably corresponding to high multipole orders of photon interaction.

The proton energy spectrum shows a maximum between 5 and 6 MeV. This proton energy, taking into account the threshold value of 15.9 MeV, corresponds to the maximum of the (γ, p) cross-section as given by HALPERN and MANN [7] at 21.5 MeV photon energy. This fact strongly suggests that direct photoeffect takes place; such interpretation is supported also by the observation of the pronounced anisotropy in the angular distribution.

3·2. *Aluminium.* – The anisotropy of the angular distribution of photoprotons emitted from aluminium depends on the proton energy as shown in Fig. 5. Experimental points can be fitted by a curve $N=a+b\sin^2\vartheta$, the ratio b/a increasing with the energy of photoprotons.

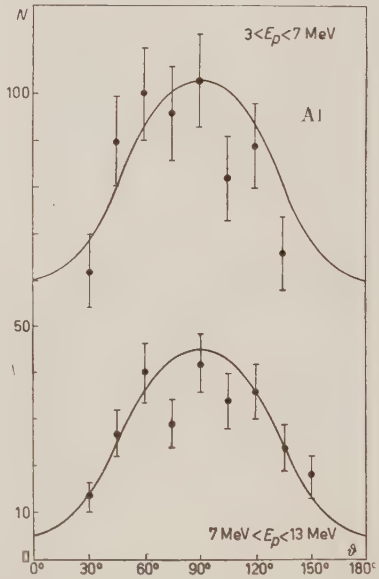

Fig. 5. – Angular distribution of photoprotons from Aluminium. N = number of photoprotons observed with energy E_p for unit solid angle in arbitrary scale.

[9] J. HALPERN, A. K. MANN and M. ROTHMAN: *Phys. Rev.*, **87**, 164 (1952).

[10] S. A. E. JOHANSSON: *Phys. Rev.*, **97**, 434 (1955).

[11] H. HENDEL: *Zeitsch. f. Phys.*, **135**, 168 (1953).

DIVEN and ALMY [12], HOFFMANN and CAMERON [13], with respectively 22 and 25 MeV bremsstrahlung beams found almost isotropic distributions. This probability is due to the lower photon energy used and to the absence of proton energy selection.

Fig. 6. – Photoproton energy distribution from Aluminium irradiated at 31 MeV photon max energy. N = number of protons observed into 1 MeV interval.

At higher $E_{\gamma\,max}$ energies, 40 and 65 MeV, HOFFMANN and CAMERON [13] observed a pronounced maximum at 60° for proton energy between 16 and 28 MeV and between 27 and 43 MeV respectively. Also JOHANSSON with $E_{\gamma\,max} = 65$ MeV and selecting protons with energy greater than 14 MeV found a maximum at 60°.

The proton energy spectrum from Al was measured by DIVEN and ALMY [12] with $E_{\gamma\,max} = 20.8$ MeV and found to be peaked at 4 MeV. HOFFMANN and CAMERON [14] with an $E_{\gamma\,max} = 25$ MeV found a maximum at 5 MeV.

Our results give a maximum at 5 MeV with a distribution similar to that measured by other authors. The (γ, pn) threshold from mass differences (MATTAUCH, FLAMMERSFELD [15]) is 19.5 MeV and therefore in present experiments the (γ, pn) reaction could have contributed to shift the maximum to lower proton energies.

[12] B. C. DIVEN and A. K. ALMY: *Phys. Rev.*, **80**, 407 (1950).

[13] M. M. HOFFMANN and A. G. W. CAMERON: *Phys. Rer.*, **92**, 1184 (1953).

[14] L. KATZ and A. G. W. CAMERON: *Phys. Rev.*, **84**, 1115 (1951).

[15] J. MATTAUCH and A. FLAMMERSFELD: *Isotopic Report* 1949.

Photoprotons from Oxygen up to 30 MeV.

C. Milone, R. Ricamo and R. Rinzivillo

Istituto di Fisica dell'Università - Catania
Centro Siciliano di Fisica Nucleare - Catania

(ricevuto il 2 Gennaio 1957)

1. – Introduction.

The predicted value of the integrated cross-section for photonuclear reactions resulting from dipole photon absorption in oxygen, according to Levinger and Bethe [1], is 337 MeV·mb, allowing for 0.5 exchange forces. The measured (γ, p) cross-section between 13.5 MeV photon energy (threshold at 12 MeV) and 18.7 MeV (Spicer [2]) gives a contribution of only 10 MeV·mb to the integrated cross-section. From the measured (γ, n) cross-section (Montalbetti and Katz [3], Montalbetti, Katz and Goldemberg [4]) from threshold to 23 MeV one can calculate a contribution of about 30 MeV·mb. It is to be expected therefore that the (γ, p) cross-section rises once more at photon energies higher than 19 MeV.

Furthermore the presence of a maximum around 22 MeV in the $^{16}O(\gamma, n)$ cross-section leads to the prediction of a maximum at about the same energy also for the (γ, p) cross-section. This prediction is supported by the observation that the giant resonances for protons and neutrons occur at the same energy at least in nuclei as ^{12}C, ^{27}Al, and Ni for which both cross-sections are known. The situation for C, O and Al is summarized in Fig. 1, as given by measurements of Montalbetti, Katz and Goldemberg [4] for $\sigma(\gamma, n)$, by Halpern and Mann [5] for $\sigma(\gamma, p)$ in C and Al, and by Spicer [2] for $\sigma(\gamma, p)$ in O.

We decided then to measure the photoproton yield for oxygen up to 30 MeV photon energy. (First results were presented at the Turin meeting of the « Società Italiana di Fisica » in September 1956).

2. – Experimental Procedure and Results.

Ilford C_2 200 μm (1″ × 3″) plates both loaded with water or dry, were exposed to the beam at 2 m from the target of the Brown-Boveri betatron of the University of Turin. No special collimation was used.

(1) J. S. Levinger and H. A. Bethe: *Phys. Rev.*, **78**, 115 (1950).

(2) B. M. Spicer: *Phys. Rev.*, **99**, 33 (1955).

(3) R. Montalbetti and L. Katz: *Can. Journ. Phys.*, **31**, 798 (1953).

(4) R. Montalbetti, L. Katz and J. Goldemberg: *Phys. Rev.*, **91**, 659 (1953).

(5) J. Halpern and A. K. Mann: *Phys. Rev.*, **83**, 370 (1951).

Exposures were made at 12, 18, 22, 26, 30 MeV betatron maximum energy. The amount of radiation in each exposure

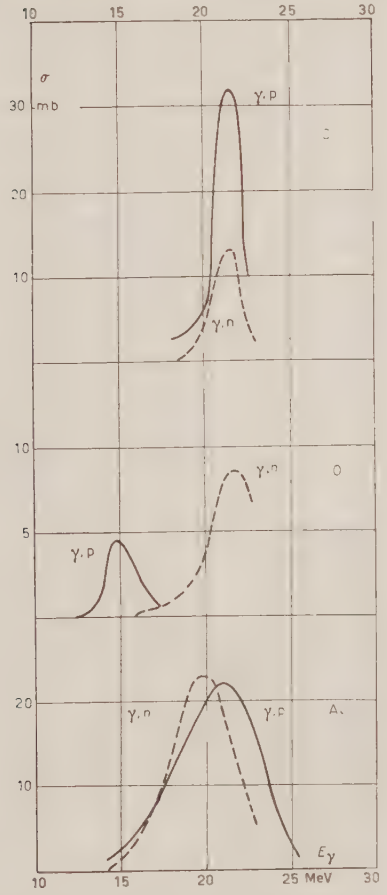

Fig. 1.—Cross-section for (γ, p) (continuous curve), and (γ, n) (dotted curve) for C, O, Al. For references see text.

was kept constant and monitored by means of a Philips ionization chamber placed in a 7 cm lucite block behind the photoplates.

In each exposure two plates, one dry and the other loaded with water, were placed perpendicularly to the horizontal betatron beam. For test purposes the dry plates were covered alternatively with an aluminium foil 1 mm thick, 1 × 1 cm, and with a 2 mm thick 1 × 1 cm carbon target. Plates were processed with D19b soon after the exposition to reduce the fading (WÄFFLER and YOUNIS [6]).

Observations on proton tracks were made with binocular microscopes using × 55 objectives and × 7.8 oculars giving a field of view that was approximately 250 μm in diameter.

After development 10 to 30 mm² of each plate were scanned and proton tracks counted. To be accepted tracks were required to have an horizontal projection longer than 25 μm ($E_p > > 1.5$ MeV) and to start in emulsion in the area not covered by aluminium or carbon. In the covered area tracks were required to start at the surface of the emulsion.

Results are shown in Fig. 2 for dry emulsion (Em), for the water loaded emulsions (H), and for C and Al. The number of proton tracks per mm² is plotted as a function of the maximum

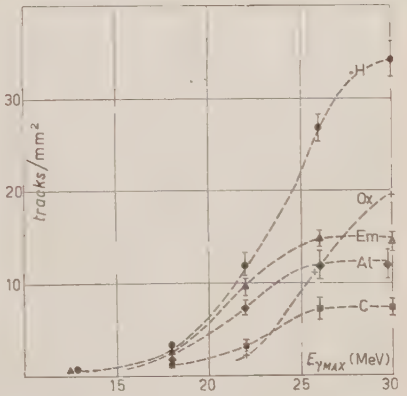

Fig. 2. – Yield curves for photoprotons from C, Al, dry emulsion Em, water loaded emulsion H, and oxygen Ox = H – Em.

(6) H. WÄFFLER and S. YOUNIS: *Helv. Phys. Acta*, **22**, 414 (1949).

photon energy for each exposure. Statistical errors are indicated.

The difference H — Em = Ox gives the number of protons emitted by oxygen in the water loaded emulsions.

The higher number of recoil protons in water loaded emulsions, due to higher hydrogen content, is negligible. The number of recoil protons has been calculated by taking into account the spectrum intensity of the neutron background of the betatron (WÄFFLER [7]) and the known (n, p) elastic scattering cross-section. This number results to be 10^{-3} times the number of the observed protons. Furthermore the 80% of the latter has energy greater than 3 MeV, while only 5% of the background neutrons has energy greater than 3 MeV, and so recoil protons can be neglected. Also the $^{16}O(n, p)$ process cannot contribute appreciably since its threshold is 10.2 MeV.

3. – Discussion and Conclusions.

The standing rise of the oxygen excitation curve up to 30 MeV betatron energy clearly indicates a remarkable contribution of the high energy photons to the proton yield.

The carbon and aluminium curves are consistent with the known maxima in the (γ, p) cross-sections around 22 MeV and the oxygen curve indicates a maximum for the (γ, p) cross-section well above the known resonance at $E_\gamma =$ = 15 MeV (Fig. 1).

SPICER [2] refers to electric quadrupole and magnetic dipole photon absorption the observed resonance in the (γ, p) cross-section of oxygen at $E_\gamma =$ = 15 MeV. According to the LEVINGER and BETHE [1] α-particle tentative model for photon reactions, electric dipole interaction is possible only at $E_\gamma > 20$ MeV. This fact is confirmed by the study on the fine structure the of (γ, n) cross-section in oxygen made by PENFOLD and SPICER [8] who concluded that only between 22 and 23 MeV the reaction can proceed principally by absorption of $E1$ radiation.

We conclude therefore that we have given evidence for the giant resonance for the (γ, p) reaction via $E1$ absorption in the region between 20 and 25 MeV photon energy.

We can give a rough estimate of the contribution of this resonance to the integrated cross-section for the (γ, p) reaction. The expected number of photoproton tracks at 30 MeV irradiation in our water loaded emulsions due to the $^{16}O(\gamma, p)$ process was $n_0 = 5$ tracks/mm^2 of emulsion, according to: *a*) SPICER's [2] values for the cross-section between 13 and 19 MeV; *b*) the number of photons with energies between 13 and 19 MeV for a 5 roentgen irradiation with a bremsstrahlung beam from the betatron working at 30 MeV maximum energy; *c*) the number of oxygen atoms introduced in the emulsions loaded with (1 ± 0.1) g of water for each $1'' \times 3''$ plate.

The observed proton number was $n = 20$ tracks/mm^2 of emulsion. This fact allows us to affirm that the new found resonance around $E_\gamma = 25$ MeV contributes to the (γ, p) integrated cross-section three times more than the previously known resonance at 15 MeV.

* * *

The Authors are grateful to Prof. M. CINI and G. CORTINI for many helpful discussions, to Prof. G. WATAGHIN and Prof. P. BASTAI who allowed the use of the betatron, to Dr. V. EMMA for the assistance and the work done by the microscopes laboratory.

(7) H. WÄFFLER: *Das Brown-Boveri Betatron*, (Zürich 1953), p. 17.

(8) A. S. PENFOLD and B. M. SPICER: *Phys. Rev.*, **100**, 1377 (1955).

LIBRI RICEVUTI E RECENSIONI

Handbuch der Physik - Herausgegeben von S. Flügge, Band I - *Mathematische Methoden* I, Springer-Verlag, Berlin-Göttingen-Heidelberg, 1956, pag. VII+364.

Due volumi dell'*Handbuch der Physik* sono dedicati ai metodi matematici. Il primo volume dedicato all'analisi, il secondo all'algebra, alla geometria, all'analisi funzionale ed ai metodi numerici. Il primo volume, che qui recensiamo, comprende cinque articoli dovuti a Lense, a Meixner ed a Schlögl.

Il primo articolo, di Lense, contiene l'esposizione dell'analisi classica, delle equazioni differenziali ordinarie e della teoria delle funzioni. Dei teoremi è dato generalmente solo l'enunciato e la trattazione è di tipo tradizionale. Riteniamo però che questa sia proprio la fisionomia adatta ad un testo che si propone di servire anche per consultazione. Riportare le dimostrazioni porterebbe a rendere più dispersi i risultati, ed una trattazione non di tipo tradizionale richiederebbe una lettura dettagliata dell'articolo prima di potersene servire per consultazione. Meno tradizionale l'appendice dell'articolo, dedicata all'integrale di Lebesgue, dove si trovano enunciati i teoremi di convergenza sotto il segno d'integrale, che piacerebbe vedere più spesso adoperati dai fisici teorici.

Il secondo articolo di Lense, sulle equazioni differenziali a derivate parziali, contiene gli aspetti generali della teoria (trasformazioni di contatto, sistemi di Pfaff e di Monge, parentesi di Jacobi e di Lagrange). Pochi cenni sulle classiche equazioni lineari del secondo ordine a derivate parziali. Queste vengono, più opportunamente, discusse più avanti nell'articolo sui problemi ai limiti.

Ancora di Lense è l'articolo sulle funzioni e sugli integrali ellittici. A differenza di molte altre trattazioni, non si tratta del solito formulario. La teoria viene svolta ordinatamente partendo dal concetto di funzione analitica doppiamente periodica e ne vengono ampiamente illustrati gli aspetti geometrici sulla superficie di Riemann.

Non è difficile prevedere il favore che incontrerà presso i fisici l'articolo sulle funzioni speciali della fisica matematica, dovuto a Meixner. Vengono prima esaminate le varie funzioni ipergeometriche ed i loro casi limite. Queste sono le funzioni speciali più semplici. Successivamente vengono trattate le funzioni di Mathieu e le funzioni sferoidali. L'autore si sforza di mettere in evidenza la comune parentela, che segue, in molti casi, dalla comune discendenza dalla equazione delle onde tridimensionali. Per le funzioni speciali semplici Meixner espone dei punti di vista moderni che difficilmente si trovano illustrati in altre trattazioni. Per esempio, oltre alla classica discussione delle funzioni speciali come soluzioni di particolari equazioni differenziali del secondo ordine, ben nota ai fisici teorici, viene esposta una teoria unitaria di tali funzioni come soluzioni di una classe di equazioni funzionali.

L'ultimo articolo, dovuto a Schlögl, è dedicato ai problemi ai limiti. L'autore espone la teoria dei sistemi di funzioni ortogonali e delle trasformazioni lineari

nello spazio delle funzioni e discute le equazioni integrali lineari ed i loro metodi di soluzione. Dopo pochi cenni di calcolo delle variazioni, si trova la discussione dei problemi ai limiti per equazioni differenziali. La discussione è svolta sostanzialmente secondo la linea tradizionale, va però notato il largo uso delle funzioni di Green e di quelle che l'autore chiama, seguendo l'uso in fisica toerica, funzioni di propagazione. Questo articolo è il più vasto del volume. Non diremo che la sua vastità derivi dalla maggiore abbondanza di dettagli. Al contrario è un articolo che abbraccia moltissime cose senza approfondirne molto la discussione. Tutti argomenti importantissimi per il fisico, che fanno parte della sua normale preparazione matematica.

L'indice bilingue tedesco-inglese è molto accurato.

I singoli capitoli sono svolti con maestria, in molti punti con originalità, e sempre curata è la chiarezza dell'esposizione. Un libro che può servire non solo per consultazione ma anche per lo studio di taluni argomenti. Vorremmo anzi aggiungere che forse è più adatto per questo secondo scopo che non per il primo. Un libro per sola consultazione avrebbe dovuto contenere più tabelle di limiti, di serie, di integrali, di funzioni speciali, più casi particolari di equazioni differenziali, e gli enunciati di molti teoremi che qui invece sono omessi per non appesantire la lettura.

R. Gatto

K. Hauffe – *Oxydation von Metallen und Metallegierungen*, Springer-Verlag, 1956; pag. VII+389, 212 figure.

Il quindicesimo volume della serie di monografie di Metallurgia pura ed applicata, curata da W. Koester, è stato affidato ad una delle maggiori autorità nel campo della chimica-fisica delle strutture solide difettive, che i lettori di questa rivista conoscono anche attraverso la sua recente pubblicazione: *Reaktionen in und an festen Stoffen*, recensita nell'agosto del 1955.

La presente monografia non vuole essere una rassegna della grande mole di lavori scientifici e tecnici pubblicati in questo campo, ma intende costituire un esame critico dei fenomeni di ossidazione e di corrosione, basato sulla natura dei processi di diffusione e di trasporto. Poichè le caratteristiche di questi processi vengono determinate dalla struttura difettiva dello strato che si viene formando durante l'ossidazione, si può dire che lo sforzo principale dell'autore è stato quello di inquadrare organicamente i fenomeni di ossidazione dei metalli e delle leghe nelle teorie attuali delle strutture difettive, così da poter presentare tutta la complessa materia da un punto di vista unitario.

La trattazione dei fenomeni di ossidazione è preceduta da un capitolo introduttivo in cui vengono tratteggiati i principi essenziali della chimica fisica delle strutture solide difettive, e dei fenomeni di diffusione nei metalli e nei cristalli ionici.

Il meccanismo di ossidazione, sia per la formazione di strati sottili che per la formazione di strati spessi viene trattato da un punto di vista generale nel 3° capitolo, ed il 4° capitolo costituisce un esame dettagliato dei processi di ossidazione con formazione di strati spessi. Il 5° ed il 6° capitolo riguardano rispettivamente i fenomeni di solforazione e quelli di ossidazione di leghe metallo-carbonio e dei carburi. Il settimo capitolo è dedicato ai fenomeni di ossidazione in soluzione acquosa con particolare riguardo ai fenomeni di passività. L'ultimo capitolo è una brevissima rassegna di alcune tecniche sperimentali.

È indubbio che il punto di vista adottato dall'Autore, malgrado porti a inevitabili esclusioni, riesce a dare una note-

vole organicità a tutta la trattazione, svolta con ricchezza di illustrazioni e di tabelle e corredata di una vasta bibliografia.

Questa monografia costituisce per coloro che si occupano di problemi di ossidazione e di corrosione, sia da un punto di vista scientifico che da un punto di vista tecnico, una base teorica di interpretazione e di discussione di importanza fondamentale che, nell'attuale rapido sviluppo di questo campo di ricerche, è di grande utilità trovare organicamente esposta ed applicata.

E. Molinari

F. Conforto – *Abelsche Funktionen und algebraische Geometrie* aus dem Nachlaß bearbeitet und herausgegeben von W. Gröbner, A. Andreotti und M. Rosati, con 8 illustrazioni nel testo, Springer-Verlag, Berlin-Göttingen-Heidelberg, 1956, 1 vol. XII+276 pagg.

È il volume LXXXIV dei *Grundlehren der mathematischen Wissenschaften*.

I cultori della teoria delle funzioni abeliane sanno come sia rapidamente divenuto un rarità il volume *Funzioni abeliane e matrici di Riemann* di F. Conforto (Roma, 1942; lo citeremo nel seguito con F.A.), nel quale sono raccolte le lezioni tenute da Conforto nell'anno precedente in un corso presso l'Istituto Nazionale di Alta Matematica in Roma; tale volume ha avuto tiratura limitata, ben inferiore alle successive richieste, e una veste litografica alquanto modesta, per le difficoltà del momento; esso è un'originale esposizione di svariati risultati sull'argomento, fusi in un tutto organico, completato da risultati nuovi, sì da fare il punto della situazione di allora nella teoria classica delle funzioni abeliane, soprattutto per quanto riguarda il suo collegamento con la geometria algebrica.

L'opera che qui recensiamo è da parecchi anni in forma di progetto, come lavoro in collaborazione tra F. Conforto e W. Gröbner; tale progetto aveva lo scopo di ovviare agli inconvenienti di F.A., cioè di fornire un'edizione limpida, integrata con i nuovi risultati sull'argomento (dovuti principalmente a F. Conforto e a C. L. Siegel) e resa più completa, soprattutto per quanto riguarda la parte nella quale si espongono i collegamenti tra funzioni abeliane e geometria algebrica. Il lavoro, interrotto al suo inizio dalla tragica morte di Conforto, è stato continuato da Gröbner, che, con l'aiuto di Andreotti e Rosati, allievi di Conforto, l'ha portato brillantemente a termine, raggiungendo in pieno i risultati prefissi. Lo schema del volume F.A. è stato rispettato, come pure il suo spirito. Il primo capitolo tratta della definizione di funzione abeliana, intesa come una funzione meromorfa di p effettive variabili complesse e dotata di $2p$ periodi indipendenti, e dimostra le condizioni necessarie e sufficienti perchè una matrice $(p, 2p)$ sia matrice di periodi primitivi per una funzione abeliana, o, per meglio dire, di un corpo di funzioni abeliane; in altre parole, perchè sia una matrice di Riemann; si mette quindi in luce l'equivalenza tra il concetto analitico-funzionale di corpo di funzioni abeliane (a meno di una sostituzione lineare non degenere sulle variabili) con quello algebrico-aritmetico di matrice di Riemann, cioè di matrice soddisfacente con i suoi elementi a certe relazioni di uguaglianza e di disuguaglianza; particolare risalto merita il modo del tutto naturale di introdurre le serie theta. Questo primo capitolo coincide sostanzialmente con la prima parte di F.A.; abbiamo notato un certo snellimento delle dimostrazioni e un notevole snellimento delle notazioni; da osservare anche taluni complementi nella teoria delle serie theta. Nel secondo

capitolo, corrispondente come argomenti alla seconda parte di F.A., si dà la definizione di varietà di Picard di un corpo di funzioni abeliane, come una varietà algebrica a p dimensioni, rappresentabile parametricamente, in maniera opportuna, mediante funzioni abeliane del corpo; si espongono le più notevoli proprietà di tale varietà, soprattutto quelle che permettono di tradurre le proprietà analitico-funzionali dei corpi di funzioni abeliane in proprietà algebrico-geometriche della varietà di Picard, intesa in senso invariantivo. In questa seconda parte, che si spinge fino ad argomenti che sono tuttora oggetto di ricerche originali, notiamo, rispetto all'opera precedente, radicali modifiche nelle dimostrazioni e nelle stesse tecniche dimostrative, atte a snellire l'esposizione precedente e a conferirle un maggior rigore; allo scopo si è fatto uso delle nozioni fondamentali dell'algebra astratta e degli ultimi risultati negli argomenti trattati. È aggiunta un'appendice, oltremodo opportuna, sulle nozioni fondamentali della teoria delle funzioni meromorfe di più variabili complesse.

Il volume è praticamente autosufficiente, richiedendo come preliminari solo le nozioni fondamentali di geometria proiettiva e di calcolo matriciale; le poche nozioni presupposte nel campo delle funzioni analitiche di più variabili complesse sono rapidamente richiamate. I capitoli e paragrafi sono i seguenti: Capitolo I: 1. Die Perioden meromorpher Funktionen. Riemannsche Matrizen. 2. Die intermediären Funktionen. 3. Das Existenztheorem der Abelschen Funktionen. Capitolo II: 1. Die Picardsche Mannigfaltigkeit. 2. Algebraische Korrespondenzen zwischen Picardschen Mannigfaltigkeiten. 3. Anhang über analytische und meromorphe Funktionen von mehreren komplexen Variablen. Segue una bibliografia, relativa alla sola appendice, ed un indice analitico.

MARIO BENEDICTY

F. BITTER – *Currents, Fields, and Particles*; Technology Press of Massachusetts Institute of Technology and John Wiley and Sons, New York, 1956), XIV+600 pagg.

Questo volume, a carattere didattico, è indubbiamente nuovo come impostazione; esso è il risultato di un notevole sforzo, da parte dell'autore, per collegare in un tutto armonico i campi più disparati della fisica.

Pur riconoscendo originalità a tale tentativo, esprimiamo però il dubbio che si possa nello stesso volume di 570 pagine, introdurre la legge di Coulomb, la legge di Ohm, l'equazione di Schrödinger.

La mole della materia trattata è enorme, e questo rende necessario sorvolare su molte questioni, affrontarne altre con un tono estremamente elementare ed incompleto, mentre in altri capitoli riguardanti l'elettromagnetismo, la trattazione assume talvolta un livello piuttosto elevato.

Il volume può essere diviso in due parti.

La I parte corrisponde, grosso modo, alla seconda parte del corso di fisica sperimentale del 1° biennio delle nostre Università. Vengono trattati i principi fondamentali dell'elettricità e del magnetismo; un capitolo è dedicato alle onde elettromagnetiche e due capitoli all'ottica.

La II parte del volume (in tutto quattro capitoli) tende a dare i primi rudimenti di fisica atomica e nucleare; un capitolo è dedicato alle basi sperimentali della fisica atomica, un secondo alla introduzione dei concetti basilari della meccanica quantistica, un terzo agli atomi, un quarto ai nuclei ed alle radiazioni nucleari.

Un simile volume è di scarsa utilità per gli studenti di fisica perchè troppo superficiale e poco critico, ma invece può essere di grande utilità per studenti di altre specialità (chimica, ingegneria, ma-

tematica e fisica, ecc.) perchè ad essi può offrire una adeguata base per destare interesse nella fisica moderna e per spingerli ad approfondire gli argomenti trattati in questo volume.

B. RISPOLI

E. J. DIJKSTERHUIS – *Die Mechanisierung des Weltbildes*; 1 vol. in-8° di pp. VII+594; Springer-Verlag, Berlin - Göttingen - Heidelberg, 1956.

Questo volume è apparso la prima volta in lingua olandese nel 1950 e, quantunque non sia stato concepito come un contributo originale alla storia della scienza, è stato apprezzato dagli specialisti in misura tale da farne prevedere prossima l'edizione in altre lingue oltre che in tedesco. Il titolo vuole indicare genericamente lo spirito meccanicistico impresso dalla nascita della fisica newtoniana all'interpretazione dei fenomeni naturali. In realtà si tratta di un'erudita sintesi storica, non richiedente nel lettore particolari nozioni di fisica e di matematica, dei contributi offerti allo studio della natura inorganica dai pensatori compresi fra PITAGORA e NEWTON. Prima dei grandi fisici, astronomi e chimici del Seicento, vengono accuratamente presentati non solo i « precursori » più noti, da DEMOCRITO a LEONARDO, ma molti di quegli autori medioevali ai cui pazienti sforzi critici e costruttivi sembra dovuto il graduale trasferimento dell'esperienza greca nel nuovo mondo delle ricerche rinascimentali. L'Autore ha tenuto conto di quasi tutti gli studi più importanti in questo campo, in particolare di quelli di PIERRE DUHEM e di ANNELIESE MAIER sui teorici scolastici dell'« impetus » e su NICOLA ORESME, ideatore della rappresentazione grafica dei fenomeni dinamici che ha permesso lo sviluppo del concetto di accelerazione. Ma il peso della bibliografia cui egli ha fatto ricorso, e di cui è traccia nelle numerose appendici dedicate alle relative indicazioni, non influisce sulla chiarezza della sua esposizione; come le tendenze filosofiche personali e le difficoltà linguistiche non gli impediscono di raggiungere una notevole obbiettività e fedeltà nei riferimenti agli scienziati e storici della scienza di altre tendenze ed altri paesi, in particolare l'Italia.

V. SOMENZI

W. HEITLER – *Elementary Wave Mechanics with Applications to quantum Chemistry*, 2nd ed., Oxford, 1956; pag. 190.

Si tratta della seconda edizione, con poche aggiunte e varianti, di un volumetto di formato tascabile, pubblicato la prima volta nel 1945. Pur diretto a lettori « non matematici », il libro fa abbondante uso di matematica, rendendola però facilmente accessibile a chiunque non sia completamente digiuno di calcolo infinitesimale.

Consiglieremmo specialmente gli ultimi capitoli sulla teoria della valenza allo studente che si accinge a imparare la meccanica quantistica, perchè non segua un malvezzo abbastanza diffuso che tende a liquidare con i soliti tre o quattro esempi (buche di potenziale, oscillatore armonico, atomo di idrogeno) l'equazione di Schrödinger, per arrivare quanto più rapidamente possibile alla equazione di Dirac.

Il libro ha molti pregi, non ultimo quello di aver messo in forma piana una così notevole mole di materiale in un numero di pagine tanto ridotto (meno di 100 pagine di formato normale).

Vale la pena di segnalare in un così bel libro — a sollazzo dei collezionisti di curiosità — un incredibile svarione del fondatore della teoria della valenza, proprio nella discussione di questa teoria. A pag. 135 — laddove l'autore tenta di

dare un'interpretazione alla frequenza corrispondente all'energia di scambio — si trova scritto che l'interpretazione che si tratti della frequenza di *scambio delle posizioni* dei due elettroni è errata, questa è invece la frequenza di *scambio degli spin*. Chiunque abbia un minimo di familiarità con la meccanica quantistica sa benissimo che scambiare le posizioni di una coppia di elettroni o scambiare i loro spin sono operazioni matematicamente e operativamente equivalenti. Pertanto le alternative sono due: le due interpretazioni (frequenza di scambio delle posizioni e frequenza di scambio degli spin) sono o entrambe valide o entrambe errate. Non ha senso la terza alternativa proposta da HEITLER.

Naturalmente queste sono cose che possono succedere in un libro che fa ricorso a ragionamenti di carattere intuitivo, e dimostrano, se ce ne fosse ancora bisogno, come sia assai più semplice scrivere un libro « difficile » che non un libro « facile ». Proprio per questo il libro di HEITLER ci pare ancora più meritevole di segnalazione.

A. GAMBA

PROPRIETÀ LETTERARIA RISERVATA

Direttore responsabile: G. POLVANI Tipografia Compositori - Bologna

Questo fascicolo è stato licenziato dai torchi il 27-I-1957